

VIBRATION SPECTRA OF CHARGE-TRANSFER COMPLEXES  
AND SOME RELATED COMPOUNDS

by

INAMUL HAQUE

A thesis submitted for the  
DEGREE OF DOCTOR OF PHILOSOPHY IN THE  
UNIVERSITY OF LONDON

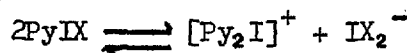
Department of Chemistry  
Imperial College of Science and Technology  
London S.W.7.

July 1968.

ABSTRACT

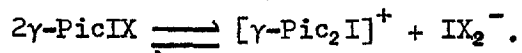
Following a brief introduction to charge-transfer complexes, the far-infrared vacuum grating spectrometer used in this research is briefly discussed.

The infrared spectra of the  $\text{PyI}_2$ ,  $\text{PyIBr}$ ,  $\text{PyICl}$  and  $\text{PyICN}$  charge-transfer have been examined in a range of environments. The Raman spectra of  $\text{PyIBr}$  and  $\text{PyICl}$  have also been examined. In polar solvents the ionization



takes place. The vibration spectra of the complexes are assigned.

The infrared spectra of the complexes  $\gamma\text{-PicI}_2$ ,  $\gamma\text{-PicIBr}$ ,  $\gamma\text{-PicICl}$  and  $\gamma\text{-PicICN}$  have been recorded in a range of environments. In polar solvents the first three complexes ionize



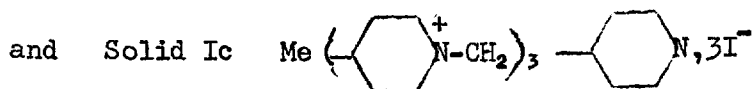
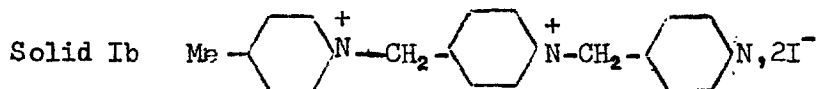
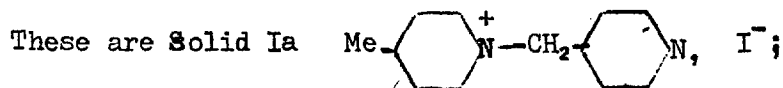
The vibrations of the complexes are assigned on the basis of  $C_{2v}$  symmetry.

The infrared and Raman spectra of complexes formed by pyridine with bromine, and bromine chloride have also been examined. In non-polar solvents these complexes are predominantly un-ionized. In polar solvents the additional bands are assigned to the cation  $[\text{Py}_2\text{A}]^+$ , and the anions  $\text{Br}_3^-$  or  $\text{BrCl}_2^-$ . The spectra of the solid complexes are quite different from those in solution.

Infrared and Raman spectra of salts of the cations bis-pyridine iodine(I), bis-pyridine bromine(I), bis- $\gamma$ -picoline iodine(I) and bis- $\gamma$ -picoline bromine(I) have been examined. The spectra of these cations are correlated with the vibrations of their respective bases, pyridine and  $\gamma$ -picoline. The linearity of the N-X-N atoms, and the presence of a centre of symmetry are definitely indicated for the first three cations.

The force constants for halogen-halogen and donor-acceptor intermolecular stretching vibrations have been calculated using a simple triatomic model. The frequency shifts and environmental effects are discussed. These may be explained in terms of the degree of charge transfer.

The structures of the products from the reaction of  $\gamma$ -picoline with iodine are established by infrared, N.M.R. and mass spectra.



ACKNOWLEDGEMENTS

The author wishes to express his sincere thanks to his supervisor, Dr J.L. Wood, for his help, encouragement and advice throughout the course of this work.

Thanks are also due to his colleagues in the laboratory for innumerable stimulating and helpful discussions.

Grateful acknowledgement is made of the award of an Overseas Scholarship by the Education Department, Government of Assam.

CONTENTS

	<u>Page</u>
ABSTRACT	2
ACKNOWLEDGEMENTS	4
1. INTRODUCTION	8
1.1. Types of donors	8
1.2. Types of acceptors	9
1.3. Theory	11
1.4. Properties of charge-transfer complexes	17
1.4.1. Electronic spectra	17
1.4.2. Infrared spectra	22
1.4.21. The donor spectrum	22
1.4.22. The acceptor spectrum	24
1.4.23. Intermolecular vibrations	26
1.4.3. Dipole moment	26
1.4.4. Crystal structure	27
1.4.5. Equilibrium constant	29
1.4.6. Thermodynamic constant	32
1.5. Solvent Effects	33
2. INSTRUMENTAL	36
2.1. Filtering	38
2.1.1. Potassiumbromide Chopper	38
2.1.2. Black Polythene	38
2.1.3. Manley filter	38
2.1.4. Reststrahlem	39
2.2. Sample cells	39
2.3. Raman Spectra	40
3. CHARGE-TRANSFER STUDIES	41
3.1. The spectra of pyridine-iodine, pyridine-iodine bromide, pyridine-iodine chloride and pyridine- iodine cyanide complexes	41
3.1.1. Introduction	42
3.1.2. Experimental	43
3.1.21. Purity of materials	43

3.1.22. Preparation of complexes	44
3.1.23. Spectra	45
3.1.3. Results	45
3.1.4. Nature of species present	60
3.1.5. Classification of modes and assignments	64
3.2. $\gamma$ -picoline-halogen Complexes	70
3.2.1. Introduction	70
3.2.2. Experimental	73
3.2.21. Purity of materials	73
3.2.22. Preparation of complexes	73
3.2.3. Spectra	74
3.2.4. Results	75
3.2.5. Nature of the species	75
3.2.51. $\gamma$ -picoline-iodine	75
3.2.52. $\gamma$ -picoline-iodine bromide	87
3.2.53. $\gamma$ -picoline-iodine chloride	88
3.2.54. $\gamma$ -picoline-iodine cyanide	90
3.2.6. Assignments	90
3.3. Pyridine-bromine and Pyridine-bromine chloride complexes	94
3.3.1. Introduction	94
3.3.2. Experimental	95
3.3.21. Purity of materials	95
3.3.22. Preparation of complexes	95
3.3.3. Spectra	96
3.3.4. Results	97
3.3.5. Interpretation of spectra	97
3.3.51. Pyridine-bromine system	97
3.3.52. Pyridine-bromine chloride	111
3.3.6. Assignments	119
4. The vibration spectra and structure of the bis-pyridine iodine(I), bis-pyridine-bromine(I), bis- $\gamma$ -picoline iodine(I) and bis- $\gamma$ -picoline-bromine(I) cations	121
4.1. Introduction	122
4.2. Experimental	123

4.2.1. Purity of materials	123
4.2.2. Preparations	123
4.2.3. Spectra	125
4.3. Results	127
4.4. Discussion	127
4.5. Classification of modes	155
5. GENERAL DISCUSSIONS	156
5.1. Force constants	156
5.2. Effect of environment	167
5.3. Frequency shift	179
5.4. Change in intensity	187
5.5. Conclusions	188
6. THE REACTION PRODUCTS OF $\gamma$ -PICOLINE AND IODINE	189
6.1. Introduction	189
6.2. Discussion	190
REFERENCES	192

PUBLISHED PAPERS:-

- No.1 The iododipyridinium ion
- No.2 The Infrared spectra of Pyridine-halogen Complexes
- No.3 The Infrared spectra of  $\gamma$ -Picoline-halogen Complexes
- No.4 The vibration spectra of the complexes Pyridine-bromine and Pyridine-bromine chloride
- No.5 The vibrational spectra and structure of the bis-Pyridine iodine(I), bis-Pyridine-bromine(I), bis- $\gamma$ -Picoline iodine(I) and bis- $\gamma$ -Picoline bromine(I) cation
- No.6 The Reaction products of  $\gamma$ -Picoline and iodine.

## 1. INTRODUCTION

Charge-transfer complexes or donor-acceptor complexes are formed by molecules or ions or both, without a covalent bond participating in the complex formation. These complexes are generally very weak; heats of formation are less than 20 kcal/mole. In many cases they are so unstable at ordinary temperatures that they cannot be isolated in the pure state but exist only in solution in equilibrium with their components. A feature of such complexes is the transfer of an electron from one component (donor) to the other (acceptor). These complexes can usually be detected by a change of colour from the parent components and a characteristic absorption band which is absent in both the components.

Besides three excellent books<sup>(1)</sup>, several reviews (2-10) of charge-transfer complexes have been published during the last three decades. However, a short review will not be out of place.

1.1. Types of donors. Donors in charge-transfer complexes may be divided into three groups, according to the nature of donation<sup>(10)</sup>.

Increvalent or 'n' donors are lone-pair donors; the donation taking place from the non-bonding lone-pair of electrons, located on a key atom such as nitrogen, sulphur, etc. A large variety of nitrogen containing organic bases including aliphatic amines, pyridine and



substituted pyridines, piperidine, etc. are 'n' donors. These donors usually form comparatively strong charge-transfer complexes with halogens and are the most studied class of 'n' donors. Alcohols, organic sulphides, organic iodides are also 'n' donors.

$\pi$  donors, where the donation takes place from a bonding molecular  $\pi$  orbital, are also known as "sacrificial" donors, because as a result of donation, the bonding within the donor molecule is weakened. A large class of organic compounds including unsaturated and aromatic hydrocarbons and their substituted analogues are  $\pi$  donors. This class of  $\pi$  donors generally forms weaker complexes than 'n' donors.

The final class is the  $\sigma$  donor, and is also a "sacrificial" type. In this case the donation takes place from the bonding molecular orbital. Aliphatic hydrocarbons, especially if cyclic, are  $\sigma$  donors. This class of donor generally form very weak complexes and is not often encountered.

1.2. Types of Acceptors: Many inorganic and organic substances are known as acceptors in charge-transfer complexes. Broadly, they may be divided into three classes according to the nature of acceptance of electrons<sup>(10)</sup>.

Increvalent acceptors which accept electrons into a vacant orbital of a key atom, so that this atom can form an additional valency bond. This class of acceptors includes  $BR_3$ ,  $AlR_3$ ,  $AlX_3$ ,  $SnCl_4$ , etc., (R=alkyl group, X=halogens).

Halogens, sulphurdioxide, oxygen, hydrogenhalide, etc., are  $\sigma$  acceptors. Halogens accept electrons into their  $\sigma$  antibonding molecular orbitals, and as a result bonding within the halogen molecule is weakened. This class of acceptor is also known as a "sacrificial acceptor". The relative acceptor strength or acid strength of halogens, has been measured by Scott<sup>(11)</sup> from thermodynamic data. The relative acceptor strength depends upon their electron affinities, and it follows the series  $ICl \gg BrCl \gg Br \gg I_2 \gg Br_2 \gg Cl_2$ . The fact that interhalogens are stronger acids than the elemental substances must be ascribed to the polar nature of the mixed halogens<sup>(8)</sup>. In the case of interhalogens the less electronegative atom, such as iodine in  $ICl$ , is the co-ordination centre.

A large group of organic compounds accept electrons into their antibonding  $\pi$  orbitals. These are known as " $\pi$ " or "sacrificial" acceptors. Many of the  $\pi$  acceptors are ethylenes, substituted with highly electronegative substituents. The acceptor strength is related to the capacity of these substituents to withdraw electrons from the ethylenic groups. One of the strongest  $\pi$  acceptors is tetracyanoethylene,  $(NC)_2C=C(CN)_2$ ; which gives brilliantly coloured complexes

with aromatic hydrocarbons and other donors. Benzene is a  $\pi$  donor, but when it is substituted with electronegative groups it becomes a  $\pi$  acceptor. A great many coloured solid adducts of polynitroaromatic compounds with organic donors have been prepared. Some of these molecular compounds are sufficiently stable to have a characteristic melting-point<sup>(2)</sup>.

1.3. Theory: Donor-acceptor complexes have attracted the interest of chemists for a long time and a number of theories have been put forward, to explain the bonding forces between the components of the complexes.

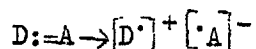
Pfeiffer<sup>(2,12)</sup> first tried to explain the bonding of organic complexes by residual valency theory. According to this theory, the residual valency forces were saturated by the complex formation. Barnett and Wills<sup>(13)</sup> discarded this theory on the ground that it failed to explain the occurrence of simple stoichiometric ratios. They, in order to explain some complexes of aromatic substances with nitrocompounds, put forward the theory of co-valent bonding. However, it became untenable when it was discovered that the separation distances between components in solid complexes were much longer than normal co-valent bond lengths<sup>(14)</sup>.

Briegleb<sup>(2,3,15)</sup> explained the interaction of nitrocompounds with aromatic hydrocarbons, in terms of dipole-induced dipole electrostatic

attraction. The molecules with permanent dipoles, induces a dipole in the polarizable hydrocarbon and they are held together by electrostatic forces. This theory is supported by the fact that heats of formation of a series of complexes with S-trinitrobenzene decreases with the decrease of polarizability of the hydrocarbon in the order, anthracene > phenanthrene > naphthalene > benzene. He was able to estimate gram molecular heats of interaction of the order of 2 kcal for assumed intermolecular distances of the order of  $3A^{\circ}$ . The experimentally determined heats of formation of some complexes of S-trinitrobenzene with naphthalene, anthracene, etc., in carbontetrachloride are of this order of magnitude. The attractive force between the polarizing and polarized molecules varies according to the inverse sixth power and the inference is that the interacting molecules cannot possibly get as close together as is required for ordinary chemical bond formation. This conclusion is supported by crystallographic evidence. However, it is difficult to conceive that the formation of colour is only the result of interaction between inducing and induced dipoles. Briegleb's theory is also unable to explain the formation of complexes between iodine and hydrocarbons such as benzene.

Gibson and Loeffler<sup>(16)</sup> and Hammick and Yule<sup>(17)</sup> presumed that the colour phenomena are associated with the drift of electrons from one component to the other when the reactive centres are appropriately located during normal collisions.

Weiss<sup>(18)</sup> described the formation of deeply coloured molecular compounds from quinones and nitroquinones; and certain unsaturated hydrocarbons on their derivatives, in terms of an electron transfer from one component (D) to the other component (A), according to the net reaction,



The ions composing the compound, have each an odd number of electrons. As a result transitions to excited states require less energy and can be effected by the visible light. He also suggested that acceptor molecules must have positive electron affinities and the donor molecules, low ionization potentials in order for complex formation.

The mechanism of the Diels Alder reaction has also been explained in terms of an electron transfer from the diene to the dienophile with the formation of an ion pair intermediate<sup>(19)</sup>. The term 'intermolecular semipolar bond' has been used to describe the intermolecular overlapping of the orbitals of the non bonded electrons in each half.

Brackman<sup>(20)</sup> has discussed 'complex resonance' as the source of the stabilization of the complexes. His concept, which requires only partial ionic character in the complex is more realistic than those theories previously described. According to this theory the donor compound can also share an electron pair with the acceptor by a process comparable to Lewis-acid-base interactions. The complex structure is regarded as a resonance hybrid  $D:A \leftrightarrow D^+ : A^-$  to which no bond and dative structures

contribute. The physical properties of such complexes cannot be interpreted in terms of those of the separate components. The pronounced ultraviolet absorption band is not the modification of a band present in one of the components, but a new characteristic band of the complex.

The generally accepted, present form of the theory is that presented by R.S. Mulliken<sup>(21,22)</sup>. He has explained the bonding in charge transfer complexes in terms of a general quantum mechanical theory. The wave function of the ground state charge-transfer containing one donor (D) and one acceptor molecule (A) is described by the equation.

$$\Psi_N = a \Psi_0(DA) + b \Psi_1(D^+A^-)$$

The  $\Psi_0$  is the no bond wave function and  $\Psi_1$  is the dative bond wave function, a and b are the co-efficients of no-bond and dative bond states. In the no-bond state D and A are held together by classical intermolecular forces such as dipole-dipole, ion-dipole, dipole-induced dipole, etc., or Heitler-London dispersion forces. The dative bond state is formed as a result of transfer of an electron from the donor to the acceptor molecule  $D^+$  and  $A^-$ , besides all the forces mentioned above are also held together by electrostatic force. For weak complexes  $a^2 \gg b^2$ , but for strong complexes such as  $BX_3 \cdot NR_3$ , a and b are more nearly equal.

If D and A are weak donors and acceptors then a third term, representing electron transfer from the acceptor to the donor, may be important. In this case,  $\psi_N = a\psi_0(DA) + b\psi_1(D^+A^-) + c\psi_2(D^-A^+)$  where  $b^2 \gg c^2$ . For self complexes such as benzene-benzene, b and c are equal.

If  $\psi_N$ ,  $\psi_0$  and  $\psi_1$  are all normalized then the equation relating a and b is:-

$$\int \psi_N^2 d\tau = 1 = a^2 + 2abS + b^2$$

where S is the overlap integral given by  $S = \int \psi_0 \psi_1 d\tau$ . The energy E of the ground state is given by the relation

$$(W_0 - E)(W_1 - E) = (H_{01} - ES)^2$$

where  $W_0 = \int \psi_0 H \psi_0 d\tau$ : the energy associated with the no bond structure DA.

$W_1 = \int \psi_1 H \psi_1 d\tau$ : the energy associated with the structure  $D^+A^-$ .

$H_{01} = \int \psi_0 H \psi_1 d\tau$ : the interaction energy of structures DA and  $D^+A^-$ .

H is the exact Hamiltonian operator for the entire set of nuclei and electrons, which comprise the complex. Since the ground state energy  $E \approx W_N$  is not much less than  $W_0$  for weak complexes,  $W_0$  may be substituted for E for all terms except  $(W_0 - E)$ . Using these approximations the energy of the ground state may be written as

$$W_N \approx W_0 - \frac{(H_{01} - SW_0)^2}{(W_1 - W_0)}$$

The energy difference ( $W_0 - W_N$ ) represents the resonance energy arising from the dative bond contribution to the ground state and can be thought of as the charge-transfer stabilization energy.

It can also be shown that -

$$\frac{b}{a} = - \frac{H_{01} - W_0 S}{W_1 - W_0}$$

There also exists an excited state whose energy should be approximately the energy of the dative resonance form. The excited state wavefunction is given by

$$\psi_E = a^* \psi_1 (D^{\pm}A^{\mp}) - b^* \psi_0 (DA)$$

The following relations may be established for the excited state

$$W_E = W_1 + \frac{(H_{01} - SW_1)^2}{(W_1 - W_0)} \quad \text{the energy of the excited state.}$$

$$\text{and } \frac{b^*}{a^*} = - (H_{01} - SW_1) / (W_1 - W_0)$$

Here  $a^{*2} \gg b^{*2}$  and if overlap  $S$  is small  $a^* \approx a$  and  $b^* \approx b$ . The excited state is largely ionic in character. The transition from the ground to the excited state, which accompanies the absorption of light corresponds to the transfer of an electron from the donor to the acceptor. The spectrum associated with the transition is called an intermolecular charge-transfer spectrum.



If the donor and acceptor species are in their singlet ground state, i.e. they have closed-shell atomic orbitals, then

$$S = \sqrt{2} S_{DA} / (1 + S_{DA}^2)^{\frac{1}{2}}$$

where

$$S_{DA} = \int \psi_D \psi_A d\tau$$

and is the overlap integral between the highest energy filled orbital of the donor,  $\psi_D$ , and the lowest energy unfilled orbital of the acceptor,  $\psi_A$ . The partners in a donor-acceptor complex tend to assume a relative orientation so as to make  $S$  and  $S_{DA}$  a maximum. For an orientation of the partners such that  $S_{DA}$  is zero,  $b$  also is zero, and the charge-transfer interaction disappears.

1.4. Properties of charge-transfer Complexes: The properties of charge transfer complexes can be divided into two classes, depending on whether they are determined only by the structure of the ground state of the complex or whether they depend on both the ground and excited state structures. Properties of the complex such as geometry, dipole moment, enhanced intensity and frequency shift of ~~the~~ the infrared and Raman spectra, formation constant, enthalpy of formation and magnetic properties fall in the first class. The electronic spectra of the complexes fall into the second class.

1.4.1. Electronic Spectra: Detailed study of charge-transfer spectra has strengthened the Mulliken's charge-transfer theory. Since an electron moves from the donor to the acceptor in a charge-transfer

process, the energy of the complex and the process of complex formation depend on the ionization potential of the donor molecule and the electron affinity of the acceptor molecule. A linear relationship has been found between the ionization potentials of several alkyl benzenes and the charge-transfer frequencies of the corresponding iodine complexes.<sup>(23)</sup> (Fig.1) The charge-transfer band shifts towards the visible region as the donor ionization potential increases.

The energy required for optically induced intermolecular charge-transfer may be expressed as (9)

$$h\nu_{CT} = W_1 - W_0 + X_1 - X_0$$

$W_0$  is defined as  $W_{\infty} + G_0$ , where  $W_{\infty}$  is the energy of the separated molecules and  $G_0$  is the sum of several terms including - electrostatic energy and van der Waals energy.  $X_0$  is the resonance energy of interactions between the 'no-bond' and dative states in the ground state. Similarly  $W_1$  is defined as  $W_{\infty} + I_D^V - E_A^V - G_1$ , where  $I_D^V$  is the vertical ionization potential of the donor,  $E_A^V$  is the vertical electron affinity of the acceptor and  $G_1$  is the term involving all  $D^+ - A^-$  interactions.  $X_1$  is the resonance energy due to interaction with the no-bond state.

The authors derived the following equation

$$h\nu_{CT} = I_D^V - C_1 + \frac{C_2}{I_D^V - C_1}$$

where  $C_1$  and  $C_2$  are constants for a given acceptor. It follows that when the energy  $h\nu_{CT}$  is plotted against  $I_D^V$ , a curve results, and  $C_1$  and  $C_2$  can then be evaluated.

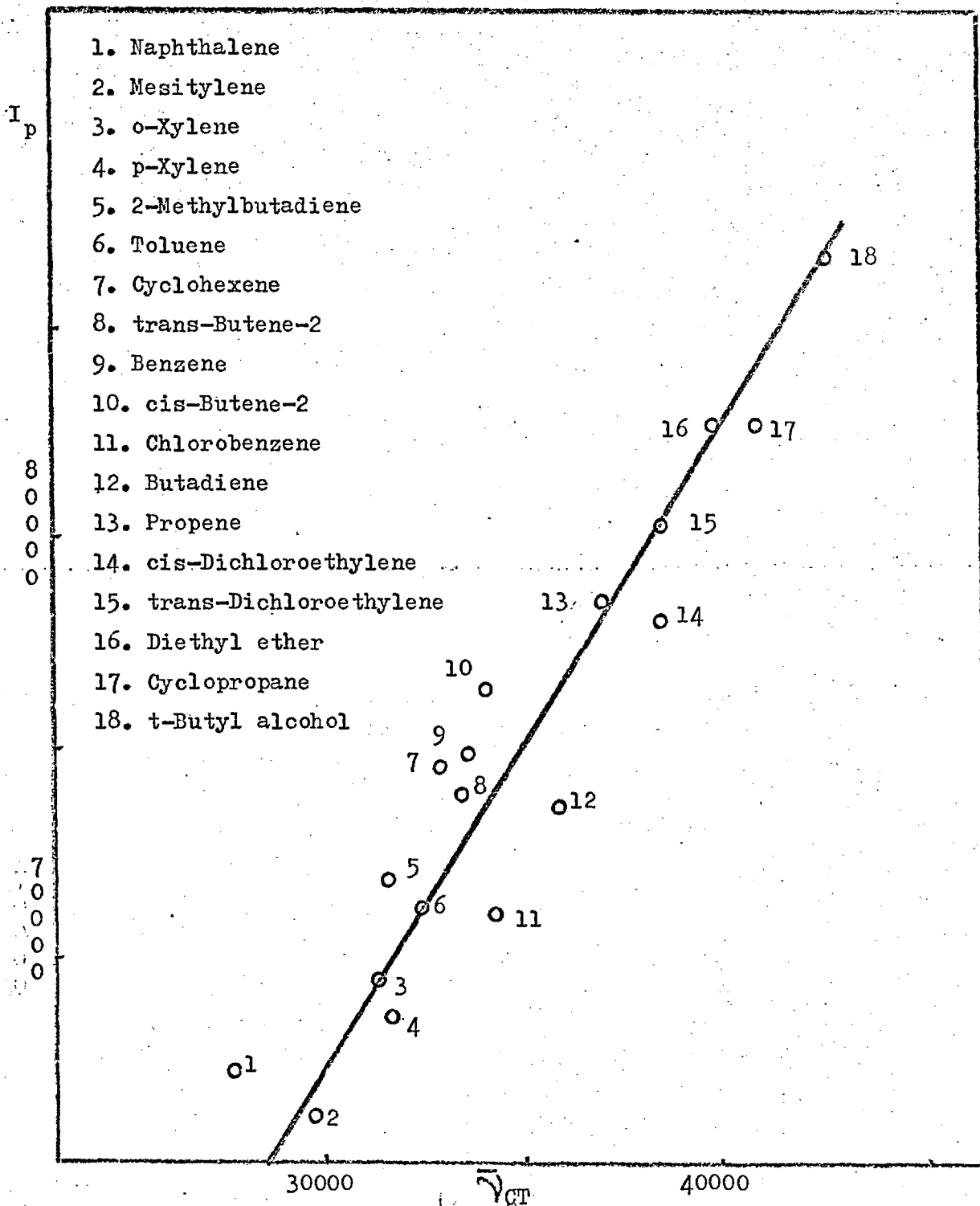


Fig. 1. Ionization potential of the donor molecules versus the frequency of the charge-transfer transition maximum of its complex with iodine. (McConnel, Ham, and Platt, loc. cit.)

In most cases where  $C_1$  and  $C_2$  have been determined; these values are such that the last term is small for fairly high ionization potentials<sup>(24)</sup>.

(>7.5ev) and a linear relation between charge-transfer frequency and vertical ionization potential may result e.g.

$$h\nu_{CT} = 0.92I_D^V - 5.12 \quad (24)$$

Although a linear relationship has been demonstrated experimentally many times, there are a few misfits which may be due to changing intermolecular distance, steric or inductive effect of substituents groups, etc.<sup>(24)</sup>

For amine halogen complexes, as  $W_1$  is approximately equal to  $W_0$ , a different relation has been suggested<sup>(9)</sup>

$$(h\nu_{CT})^2 = \left[ \frac{W_1 - W_0}{1 - S^2} \right]^2 \left[ 1 + \frac{4B_1 B_0}{(W_1 - W_0)^2} \right]$$

where  $S$  is the overlap integral,  $B_0 = H_{01} - W_0 S$  and  $B_1 = H_{01} - W_1 S$ .

The intensity of a charge-transfer band, or oscillator strength, is given theoretically<sup>(6)</sup> by

$$f_t = (1.085 \times 10^{11}) M_{01}^2 \nu_{01}$$

where  $\nu_{01}$  is the frequency in  $\text{CM}^{-1}$ , and  $M_{01}$  is the transition moment.

Oscillator strength  $f$  may also be determined experimentally, using the relations<sup>(5)</sup>.

$$f_{ex} = 4.32 \times 10^{-4} \int \epsilon d\nu$$

or

$$f_{ex} = 1.35 \times 10^{-8} \left( \max(\nu) \max(\epsilon) - \bar{\nu} \bar{\epsilon} \right) \frac{1}{2}$$

where  $\nu$  is the frequency,  $\epsilon$  is the molar extinction co-efficient.

$\nu_{\max}^x$  and  $\epsilon_{\max}^x$  are the frequency and molar extinction coefficient respectively at peak absorption;  $\nu_{1/2}$  is the half-width of the absorption band. There is satisfactory agreement between the values of  $f_t$  and  $f_{ex}$  in some cases<sup>(1,21)</sup>. The various aspects of charge-transfer intensity has been discussed by Murrell<sup>(6)</sup>. According to him, the charge-transfer band borrows some intensity from the excited state of the donor. Mulliken<sup>(10)</sup> has pointed out that for amine halogen complexes the oscillator strength cannot be accurately gauged by  $\epsilon_{\max}$  alone, since  $\nu_{1/2}$  shows considerable variations.

Mulliken's idea has been strongly supported by Nakamoto's<sup>(25)</sup> study of the optical dichromism of single crystals of a number of molecular complexes, such as quinhydrone and hexamethyl benzene, which have typical intense new absorption bands. The spectra of these complexes are polarised with the large component perpendicular to, and the small component parallel to the planes of the two interacting molecules. These results are in marked contrast to those obtained by Nakamoto for ordinary aromatic compounds. The difference is to be expected from Mulliken's theory, since electron transport between the rings can only be brought about by that component of the incident light which is oscillating perpendicular to the ring plane. In transitions of aromatic systems on the otherhand only the component in the plane of the ring system is effective<sup>(3)</sup>.

1.4.2. Infrared Spectra: Infrared absorption and to a limited extent Raman spectra have also been used to study a variety of molecular complexes, though not as extensively as the ultraviolet or visible spectra. On complex formation, the spectra of both donor and acceptor changes. Three types of changes are found to occur: (1) the vibrational frequencies in donor and acceptor may be shifted, (2) the intensity of bands may be changed, and (3) new low frequency bands appear due to the vibration of one molecule of the complex against the other. Furthermore a decrease in total symmetry is usually associated with complexing, causing some new infrared bands to appear which are inactive in the isolated molecules due to symmetry requirements.

1.4.21 The donor Spectrum: The changes of the spectra of donor molecules are not very obvious. There are so many things which can cause frequency shifts without any very large change in electronic structure. For example, the change in symmetry on complexing can cause vibrations which are isolated in the free molecule to mix in the complexed molecule, resulting in large changes in the appearance of the spectrum. However, some changes in the donor spectra can be accounted for.

The most intensely studied donor molecule is benzene<sup>(26-32)</sup>.

The vibration frequencies of the benzene molecule do not shift on complex formation. However, the intensity of some bands change. The 850 and 992 $\text{cm}^{-1}$  peaks of benzene are enhanced both by bromine and iodine. These intensity changes are presumed to be due to changes in symmetric ring breathing modes<sup>(1b)</sup>.

The infrared spectra of trimethylamine, on complex formation with iodine has been found to change remarkably<sup>(33)</sup>. The C-N stretching vibration frequency decreases; the degenerate C-H deformation splits into three lines, and the C-N deformation vibration shifts towards higher frequencies. These changes are attributed to the weakening of C-N band and repulsions between the iodine and nitrogen atoms.

Interaction of pyridine with halogens are accompanied by changes of intensity and shifts of certain infrared bands<sup>(34-39)</sup>. The totally symmetric  $990\text{cm}^{-1}$  band of pyridine, shifts to higher frequency upon addition of iodine and appears as a sharp intense band at  $1005\text{cm}^{-1}$ . The  $1027\text{cm}^{-1}$  band shifts to  $1031\text{cm}^{-1}$  and markedly diminishes in intensity. There is a  $\sim 10\text{cm}^{-1}$  shift of the  $1070\text{cm}^{-1}$  pyridine band to a lower frequency upon the addition of iodine. This band is extremely well defined and its intensity is almost equal to that of the  $1005\text{cm}^{-1}$  band. The  $605$  and  $405\text{cm}^{-1}$  (40) bands of pyridine are also observed to shift to higher frequency on addition of halogens by  $10-30\text{cm}^{-1}$  depending upon the electron affinity of the halogen. These effects are noted for all the pyridine halogens or interhalogens complexes that have been studied. It has also been observed that when pyridine forms complexes with  $1-X$  ( $X=F, Cl, Br$  and  $I$ ) the shift in the  $990\text{cm}^{-1}$  band is directly related to the electronegativity of the X-atom. This band of pyridine has been observed at a maximum frequency of  $1014\text{cm}^{-1}$  for  $IF$ , shifting gradually to slightly lower frequencies of  $1012$  and  $1011\text{cm}^{-1}$  for  $ICl$  and  $IBr$  and finally to  $1005\text{cm}^{-1}$  for the iodine pyridine system.

It is obvious that for all the pyridine halogen complexes there is a remarkable consistency in frequency changes. The complexes between Picolines and halogens behave similarly.

The changes in intensity of the infra-red spectrum of pyridine on complex formation with halogens have been discussed by Person et al.<sup>(38)</sup> The redistribution of charge which results on complexing is not symmetrical over the pyridine molecule. Thus, vibrations with no resulting dipolemoment change in pyridine suddenly appear with rather large moment changes in pyridine complexes. This gives rise to the very great changes in the appearance of the spectrum.

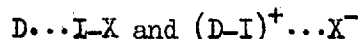
1.4.22 The Acceptor Spectrum: Halogens accept electrons to an antibonding molecular orbital when forming charge-transfer complexes; as a result the halogen-halogen bond weakens with an accompanying decrease in the vibration frequency of the halogen fundamental.

The fundamental vibrational frequency of chlorine, at  $557\text{cm}^{-1}$  in the isolated halogen is reduced to  $530\text{cm}^{-1}$  when chlorine is dissolved in benzene.<sup>(41-43)</sup> Similarly, the  $217\text{cm}^{-1}$  frequency of iodine is reduced to  $207\text{cm}^{-1}$  in benzene and to  $174\text{cm}^{-1}$  in the pyridine iodine complex.<sup>(44)</sup> The frequency of these bands is lowered and absorption intensity increases as the ionization potential of the donor decreases. Furthermore these bands, normally only Raman active, are now observed in the infra-red.



This is what is expected if the halogen molecules are bound in a charge-transfer complex. Similar changes in position and intensity of the fundamental frequencies of  $\text{ICl}$ ,  $\text{IBr}$ ,  $\text{ICN}$  and  $\text{Br}_2$  take place when they form complexes. (43,45-50)

The frequency change in the acceptor spectrum has been explained by Person et al. (46) The structure of the complex between donor molecule D, and the halogen,  $\text{I-X}$  may be described in terms of resonance structures.



For weak complexes the no-bond structure is most important. As the strength of the complex increases the ionic structure becomes more and more important. From this model it is obvious that the  $\text{I-X}$  force constant will decrease as the ionic structure becomes more and more important.

The enhancement of the infra-red intensity of the halogen-halogen stretching vibration has been explained by Ferguson and Matsen. (29) According to them, the electron affinity of the halogen changes during the vibration and as a result the energy difference between the no-bond and dative bond states changes, so that the extent of mixing of these two wave functions changes during the vibration. As the halogen-halogen bond vibrates, there is an oscillating flow of electrons from donor to acceptor; the resulting large change in dipole moment causes the intensity enhancement.

Frederic and Person <sup>(51)</sup> have also explained the intensity enhancement with emphasis on electron reorientation during the vibration.

1.4.23 Intermolecular Vibrations: The intermolecular vibration bands for charge-transfer complexes is due to the vibration of one molecule in the complex against the other, i.e. the D-A stretching vibration. Only a very few examples of such bands have been observed and they are all for the complexes of 'n' donors and halogen acceptors. As the interaction forces of charge-transfer complexes are very weak, they generally appear in the low frequency region. For example,  $(\text{CH}_3)_3\text{N-I}_2$  gives a new band at  $135\text{cm}^{-1}$  which has been identified as N-I stretching frequency. <sup>(33)</sup> For the pyridine 1-X complexes the N-I stretching bands have been found to be at  $94\text{cm}^{-1}$  for  $\text{PyI}_2$ ; <sup>(52)</sup>  $134\text{cm}^{-1}$  for  $\text{PyIBr}$  and  $147$  for  $\text{PyICl}$ . <sup>(48)</sup> It is obvious that the stronger is the complex the higher is the N-I stretching vibration. However, the N-I vibration band is a function of the mass of the donor <sup>(52)</sup> and also depends on the nature of the solvent. <sup>(48)</sup>

1.4.3. Dipole Moment: In complexes such as benzene and iodine, in which both components are nonpolar, the dipolemoment of the no-bond structure will be almost zero; and the observed dipolemoment must result entirely from a dative bond structure. For the case where one of the components is initially dipolar, the situation becomes more complicated and the dipolemoment of the complex may be either greater or less than that of the dipolar component. <sup>(5)</sup>

The dipole moment of the complex, if both donor and acceptor are non-polar is given by (21)

$$\mu_N = \mu_1(b^2 + abS)$$

where S is the overlap integral between  $\psi_0$  and  $\psi_1$ ;  $\mu_1$  is the dipole moment of the dative structure and can be estimated from a knowledge of the geometry of the complex. If the value of S and  $\mu_1$  are known, one can evaluate a, b and the percentage ionic character of the ground state,  $\frac{100b^2}{a^2+b^2}$ , from the observed dipole moment. For weak complexes, as the value of overlap integral S is very small,  $\mu_N \approx b^2 \mu_1$ .

The dipole moment of charge-transfer complexes should increase with an increase in the contribution of the dative state to the ground state. As expected the iodine complex of pyridine is considerably more polar than the benzene complex, but less polar than the trimethyl amine complex. The dipole moment and percentage ionic character of pyridine-iodine, (53,54) benzene-iodine (5,55) and tri-ethylamine-iodine (56,57,58) complexes are 4.5D; 25%; 1.8D; 8.2% and 11.3D; 59% respectively.

1.4.4. Crystal Structure: During the last 15 years the crystal structures of several 1:1 donor-acceptor complexes have been determined. (59)

The most interesting are the  $\pi$  and n donors-halogen complexes. As the halogen accepts electrons into its antibonding molecular orbital, the bonding within the halogen molecule weakens. This weakening of the bond should be accompanied by increase in bond length. The stronger is the complex the longer should be the halogen-halogen bond length in the complex.

On the other hand the D-X (donor-halogen) bond should lie between the sum of Van der Waals radii and the co-valent bond length. The difference between the length of the co-valent D-X bond and the observed D-X distance should diminish as the strength of the interaction increases.

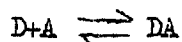
The study of several n donor halogen complexes has proven the above predictions. In the case of amine halogen complexes, it is generally found that the donor atom-halogen-halogen linkage is linear, and that the more electropositive of the two halogen atoms is the acceptor co-ordination centre. (59) Taking crystalline Py-I<sub>2</sub> as an example, Hassel et al have found that the nitrogen atom of Pyridine is linked to the iodine atom of I-Br; the N...I-Br arrangement is nearly linear with a I-Br distance of 2.66Å<sup>0</sup> as compared with 2.417Å<sup>0</sup> in free I-Br. The N-I distance is 2.26Å<sup>0</sup> which is less than sum of the Van der Waals radii (3.65Å<sup>0</sup>) and slightly larger than the value of the co-valent bond (2.03Å<sup>0</sup>). (60) This indicates a very strong interaction between the nitrogen atom and the iodine atom directly attached to it. For weak 'n' donors like the oxygen atoms of ethers or Ketones, both halogen atoms of a particular halogen molecule are simultaneously involved and an intermolecular halogen molecule bridge between the oxygen atoms of two donor molecules results. (61,62)

The most interesting structure found in n donor-σ acceptor complexes is the benzene-bromine complex. The study of a single crystal of the 1:1 benzene-bromine complex at -40<sup>0</sup> to -50<sup>0</sup>c, has shown that the

benzene and bromine molecules are alternately arranged and that the axes of the bromine molecules are nearly perpendicular to the planes of the benzene rings and pass through the symmetry centres of adjacent rings; (63) however, this structure is not supported by Muliken's charge-transfer theory. The distance between the bromine atoms and the nearest benzene plane is  $3.36\text{\AA}$  as compared with  $3.65\text{\AA}$  for the Van der Waals separation and the bromine-bromine distance is almost the same as in free bromine.

A number of complexes of aromatic  $\pi$  donors with aromatic or aliphatic  $\pi$  acceptors have been studied. In all cases the nearest distance between the two components is slightly smaller than the sum of the Van der Waals radii. (1)

1.4.5. Equilibrium Constant: Most of the equilibrium constants of donor-acceptor complexes reported in the literature have been determined by the spectrophotometric method. The absorption spectrum of a solution containing a donor-acceptor complex (DA) differs markedly from the spectrum of either component. Benesi and Hildebrand (64) were the first to use the new strong peak in the U.V. region to calculate the equilibrium constant and the extinction co-efficient. Applying the law of mass action to the donor acceptor reaction



the equilibrium constant K may be written as

$$K = \frac{[DA]}{([D] - [DA])([A] - [DA])}$$

where  $[D]$  and  $[A]$  are the total concentrations of donor and acceptor, both complexed and uncomplexed and  $[DA]$  is the concentration of the complex. The optical density is related to the concentration of the complex and the cell path-length by the equation

$$d = [DA] l \epsilon_{DA}$$

where  $l$  is the path length of the cell and  $\epsilon_{DA}$  is the extinction co-efficient of the complex at some wave length where neither D nor A absorb. Using the above equations Benasi and Hilderbrand derived the relationship, valid under the condition  $[D] \gg [A]$ .

$$\frac{[A]l}{d} = \frac{1}{\epsilon_{DA}} + \frac{1}{K \epsilon_{DA}} \cdot \frac{1}{[D]}$$

If values of  $[A]l/d$  are plotted against  $1/[D]$  for solutions of 1:1 complexes a straight line should be obtained. The values of  $\epsilon_{DA}$  and of  $K$  may be calculated from the intercept and the slope of the line.

Where absorption due to the acceptor molecule cannot be neglected Ketelaar et al.<sup>(65)</sup> have proposed the following relation

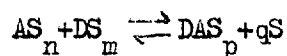
$$\frac{1}{\epsilon_a - \epsilon_A} = \frac{1}{K[D] (\epsilon_{DA} - \epsilon_A)} + \frac{1}{\epsilon_{DA} - \epsilon_A}$$

where  $\epsilon_a$  is the apparent extinction co-efficient of the acceptor in the donor solution.

The B-H equation cannot be applied to weak donor-acceptor complexes. Mulliken and Orgel<sup>(66)</sup> suggested that there are two types of charge-transfer absorption, one associated with real complexes which satisfy the law of mass action, and the other with DA pairs, which happen to be

together just through chance collisions. However, there is little justification for assuming two kinds of complexes. (71,72)

Recently a new theory for weak charge-transfer complexes has been proposed by Carter, Murrell and Rosh.<sup>e</sup> (67) According to them solvation competes with complexation in weak complexes, and the effect of neglecting the solvation in treating the data is to decrease K and to increase the extinction co-efficient. Assuming the free donor, free acceptor and complex occur in solution each with a well-defined solvation shell the equilibrium is given by



where  $q=n+m-p$ .

The equilibrium constant for this equation is determined by

$$\frac{(A)}{d} \frac{1}{D} = \frac{1}{D} \cdot \frac{1}{K K_{DA}} + \frac{1}{\epsilon_{DA}} \left( 1 - \frac{q(m+1)}{K [S]} \right)$$

where  $[S]$  is the total concentration of solvent when  $[D]=0$ . It may also be shown that B-H equation underestimates K by an amount  $q(m+1)/[S]$  and overestimates  $\epsilon_{DA}$  by the ratio  $(K/K_{B-H})$ . For strong complexes  $K \gg q(m+1)/[S]$ , the B-H equation may be applied.

Infra-red spectroscopy has also been used for the determination of the formation constant of charge-transfer complexes. (52,69,70)

The value of K is calculated from the known initial concentrations of donor and acceptor and the concentrations of the complex. The concentration of the complex in a particular solution is determined from

the intensity of a characteristic vibration band. The integrated intensity of an absorption band is given by

$$A = \frac{l}{C} \int \log \frac{I_0}{I} d\tilde{\nu}$$

where  $C$  is the concentration in moles per litre of solution,  $l$  is the path length in cm, and  $\tilde{\nu}$  is the frequency in  $\text{cm}^{-1}$ . By using a large excess of donor and an amount of acceptor sufficient to yield a concentration of complex which gives a band of same intensity of that found in the particular solution,  $A$  can be calculated. In determining  $A$  a correlation is made for the non-infinite concentration of donor. For this purpose a guessed value for the formation constant is used.

The equilibrium constant serves as a basis for a discussion by changes in the acceptor, the donor and the solvent. The equilibrium constant increases as the ionization potential of the donor decreases for a particular acceptor or donor. For example, the equilibrium constant of  $\text{PyI}_2$  in cyclohexane is  $131 \pm 30^1/\text{mole}$ , and of  $\text{PicI}_2$  in the same solvent is  $478 \pm 120^1/\text{mole}$ .<sup>(52)</sup> The best value of the equilibrium constant for  $\text{PyI}_2$  in cyclohexane has been reported to be  $317 \pm 5^1/\text{mole}$ .<sup>(71)</sup>

1.4.6. Thermodynamic Constants: Most of the thermodynamic constants of charge-transfer complexes have been obtained by spectrophotometric study of solutions of the complex components at several different temperatures. Values of heats of formation are generally evaluated from a graph of data taken at any wave length and temperatures  $T_1$  and  $T_2$  using the equation.<sup>(72)</sup>

$$2.303 \log \frac{(\text{Slope})_{T_1}}{(\text{Slope})_{T_2}} = - \frac{\Delta H^\circ}{R} \left( \frac{1}{T_2} - \frac{1}{T_1} \right)$$



The slopes of these graphs are the reciprocals of the products of equilibrium constants and extinction co-efficient of the complex. The entropy change is calculated from the complex equilibrium constant and the enthalpy change in the usual way.

Heats of formation of many charge-transfer complexes are reported in the literature, but very little data is available for amine halogen complexes. The heat of formation of trimethylamine<sup>(73)</sup>-iodine is very high,  $H_f = -12.3 \text{ Kcal/mole}$  in heptane solution; the value for the pyridine-iodine complex is  $H_f = -7.8 \text{ Kcal/mole}$ .<sup>(54)</sup> On the otherhand the heat of formation of  $\pi$  donor-halogen complexes are very low, generally of the order of 2 or 3 Kcal/mole.<sup>(61)</sup>

1.5. Solvent Effects: The solvent plays a great part in the stability and strength of a charge-transfer complex. For a complex DA, whose excited state resembles  $D^+A^-$ , the effect of increasing the polarity or dielectric constant of the medium should be to stabilize the excited state, despite the restriction of the Frank-Condon principle.<sup>(6,74)</sup> Therefore, the charge-transfer band should shift to lower energies in polar solvents. However, experimentally it has been shown that on increasing the solvent polarity, the charge-transfer band shifts to higher energies.

(75,76)

Davis et al have explained the solvent effect by giving more emphasis to the 'dative bond' structure of the ground state. In solution the complex is surrounded by a shell of solvent molecules whose dipoles define

the ground state. A polar solvent favours the 'dative bond' structure and so this makes a larger contribution to the ground state of the complex than it would in non-polar solvents. However, the excited state of the complex in polar solvents is stabilised much less than the ground state. This is because the time interval for an electronic transition to a Franck-Condon state is not sufficient for effective reorientation of the permanent dipoles of the solvent to their most stable arrangement around the polar excited state of the complex. Hence, the energy of the charge-transfer transition is raised on increasing the polarity of the solvent.

Rosenberg et al<sup>(77)</sup> have found that transition energies of complexes decrease with increasing solvent refractive index. Charge-transfer transition energies for a given complex show a linear dependence on  $(n^2-1)/(2n^2+1)$  for varying solvents of refractive index. The magnitude of the decrease is a function of the donor strength. It has been inferred that the excited state dipole moment decreases with increasing donor strength.

A few authors<sup>(48,49)</sup> have observed that the halogen-halogen stretching frequency has a lower value in more polar media, which reflects the stronger donor-acceptor bond in polar media. The iodine-iodine stretching frequency for the pyridine-iodine complex in benzene solution is at  $171\text{cm}^{-1}$ , and in pyridine solution it appears at  $167\text{cm}^{-1}$ .

Kobinta and Nagakura<sup>(78)</sup> have also explained the increase in dipole moment of charge-transfer complexes in polar media by considering that the contribution of the charge-transfer configurations in the ground state of the complex increases with increasing dielectric constant of the environment.

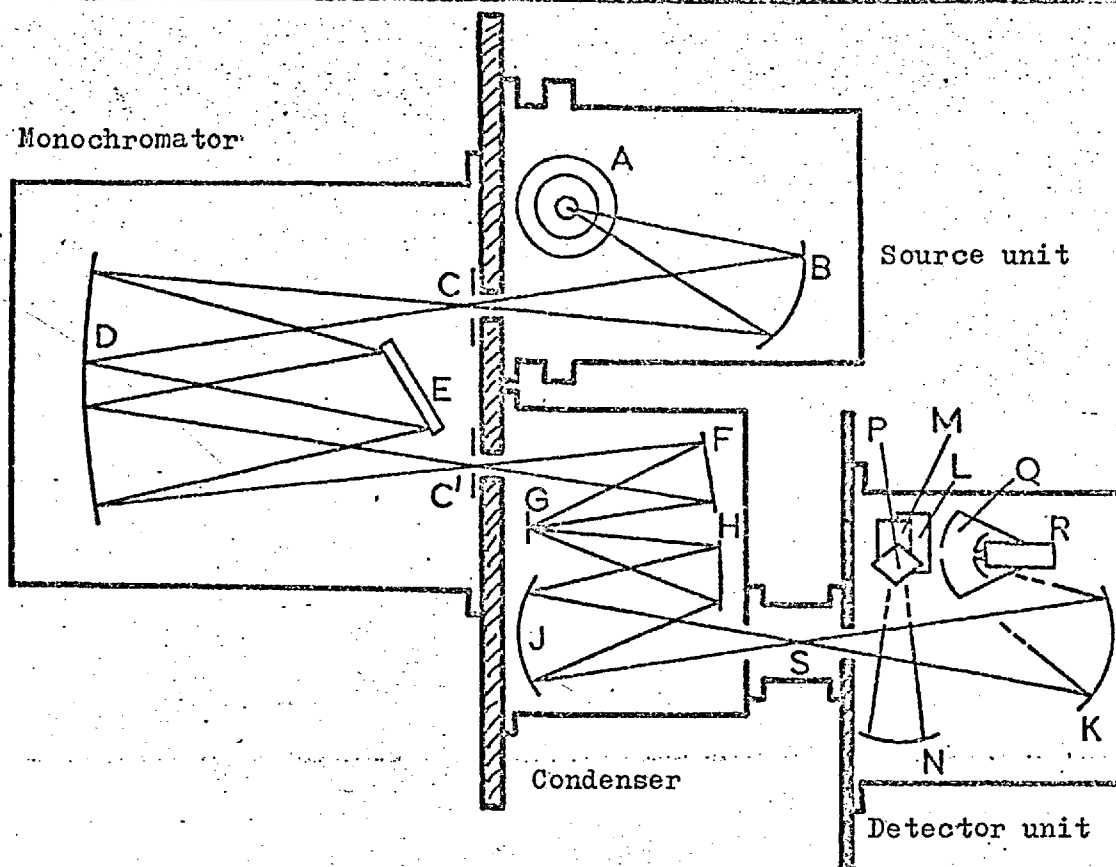
2. INSTRUMENTAL

Two instruments were used to obtain infra-red spectra.

A Grubb-Parson's spectromaster was used for measurements from  $4000-400\text{cm}^{-1}$

A single beam vacuum grating spectrometer designed and constructed in the department was used for measurements from  $400$  to  $60\text{cm}^{-1}$ . The instrument has been described in detail <sup>(79-82)</sup> and only a brief outline will be given here.

Figure I shows the optical path of the spectrometre. (The description of the figure is based upon that given in references 79,80). Radiation from the source A, a Phillips 125 watt fused quartz mercury lamp, is reflected from the mirror B to illuminate the entrance slit C. It passes to the Ebert Spherical mirror D for collimation, then to the reflection grating E. The diffracted beam is focussed on the exit slit C by the other side of the mirror D. After leaving the exit slit, the beam passes to a five part image slicer F which focusses the beam on to the five narrow, plane 'matchstick' mirrors assembled side by side. The beam, after reflection from other plane mirror G is brought to a focus in the middle of the sample area S by a concave mirror J, the height of the slit image in the process being reduced from 3" to  $\frac{3}{4}$ ". The beam is then focussed by a spherical mirror K in the detector unit on to a reststrahlen reflector M, from which it passes to a spherical mirror N and is reflected on to a second reststrahlen plate P crossed with respect to M. This directs the beam through a 4 to 1 Greenler image reducer Q.



- A Hg source, Cu cooling jacket & KBr chopper blades.
- B Spherical mirror.
- C Entrance slit.      C' Exit slit.
- D Spherical Ebert mirror.
- E Echelette grating (80 or 200 lines/cm).
- F "Sliced" spherical mirrors.
- G Plane "matchstick" mirrors.
- H Plane mirror.
- J Spherical mirror.
- S Sample cell.
- K Spherical mirror.
- L Plane mirror.
- M First reststrahlen "windmill".
- N Spherical mirror.
- P Second reststrahlen "windmill".
- Q Greenler image reducer.
- R Golay pneumatic detector.

Fig.2. Optical path of the spectrometer.

into the diamond window of the Golay detector R. The resulting AC electronic signal is amplified, rectified and fed to a Honeywell-Brouen 'Electronk' strip chart recorder.

2.1. Filtering: The removal of unwanted higher frequency radiation is extremely difficult. It has been discussed by Oetjen et al<sup>(82)</sup>.

The problem is solved by using the combination of filtering aids given below.

2.1.1. Potassiumbromide chopper: This modulates the radiation emitted by the mercury lamp of frequency less than about  $400 \text{ cm}^{-1}$  at 10 cycles/second. The AC electronic amplifier is tuned to the modulated frequency.

2.1.2. Black Polythene: A sheet of 500 gauge (0.125mm) black polythene absorbs u.v., visible and near infra-red radiation and transmits radiation of frequency less than  $600 \text{ cm}^{-1}$ . With the combination of KBr chopper and black polythene, very little radiation of frequency greater than  $\sim 450 \text{ cm}^{-1}$  is detected.

2.1.3. Manley filter: A single sheet of polythene (thickness 250 ) embedded  $\text{Cu}_2\text{O}$ (18%) and  $\text{W}_3\text{O}_3$ (18%) greatly attenuates the near and middle infra-red radiation and transmits radiation of frequency less than  $\sim 140 \text{ cm}^{-1}$ .

2.1.4. Reststrahlen<sup>m</sup>: Many crystalline materials are almost perfect reflectors of a band of radiation in the far infra-red spectral region. This isolation of a range of frequencies is based on the fact that crystals reflect radiation at the frequency of their fundamental crystal lattice vibrations. This property may be used to isolate far infra-red radiation of narrow band-width. In order to improve spectral purity two reststrahlen reflectors are used. In Table I, the frequency range covered by the reststrahlen crystals are given.

Table I

Grating.	Reststrahlen	Other filter useful frequency range.
	2LiF	Black Polythene 4-340cm <sup>-1</sup>
80 lines/cm	2NaF	Black Polythene 380-240cm <sup>-1</sup>
	2NaCl	Black Polythene 265-160cm <sup>-1</sup>
	2KCl	Black Polythene 190-120cm <sup>-1</sup>
200 lines/cm	2KBr	Black Polythene 150-105cm <sup>-1</sup>
	2CsBr	Manley 120-75cm <sup>-1</sup>
	2CsI	Manley 90-60cm <sup>-1</sup>

2.2. Sample Cells: The sample compartment is fitted with windows made of 1,000 gauge polythene, a material which is transparent to far infra-red radiation. Liquid samples were contained either in a variable path length cell fitted with rigid polythene windows or in sealed polythene bags. Solid samples were examined in Nujol Mulls

in a polythene bag. The cell compartment was dried with  $P_2O_5$  and by passing dry nitrogen. The dry nitrogen was obtained from liquid nitrogen held in a dewar. A heating element evaporates the nitrogen and any water is left behind in the form of ice as long as some liquid nitrogen remains in the flask. On carefully drying in this way no background absorption due to water vapour was observed.

In the normal infra-red range ( $4000-400\text{cm}^{-1}$ ) samples were usually examined in cells with KBr or AgCl windows.

The Grubb-Paron's spectrometer GM3 were also used for running some of the spectra in Mulls.

2.3. Raman Spectra: Raman spectra were recorded with a Cary 81 spectromaster equipped with a 'Spectraphysics' model 125 He-Ne laser, giving  $6328\text{\AA}$  radiation. The solutions were contained in a 10cm long capillary glass tube of approximately 1mm internal diameter sealed in one end. The sealed end was flattened with a fine file. After filling the tube with solution it was sealed with plasticine, leaving a small gap of about 2mm between the solution and plasticine. Glycerol was employed between the flat end of the capillary cell and the spectrometer lens to assure good contact and thereby reduce reflection losses. Solid samples were run in a sample tube.



### 3. CHARGE-TRANSFER STUDIES

- 3.1. The spectra of pyridine-iodine, pyridine-iodine-bromide, pyridine-iodine chloride and pyridine-iodine-cyanide complexes.

3.1.1. INTRODUCTION

Pyridine-halogen charge-transfer complexes have been the subject of much discussion during the last two decades. Most of the investigations have been made by u.v. and conventional infra-red spectroscopy, to a lesser extent by conductivity measurements and more recently by the widely used technique of far infra-red spectroscopy.<sup>(1)</sup> It is now generally accepted that pyridine forms relatively strong complexes with iodine, iodinechloride, iodine-bromide and iodinecyanide. Their heats of formation vary from 5-10Kcal/mole.<sup>(1)</sup>

The geometries of PyIBr, PyICl and PyICN in the crystalline state have been established by X-ray diffraction.<sup>(59,60)</sup> In all these three complexes a linear arrangement N-I-X has been established. Hassel was unable to prepare the 1:1PyI<sub>2</sub> complex, isolating instead the compound (Py<sub>2</sub>I)<sup>+</sup>I<sub>7</sub><sup>-</sup>.<sup>(83)</sup> It seems that the PyI<sub>2</sub> complex does not exist in the pure solid state.

When iodine is dissolved in excess of pyridine or solutions of pyridine in polar solvents, the I<sub>3</sub><sup>-</sup> ion is found to be present.<sup>(48,54)</sup> However, the nature of the other ion is a matter of some controversy. In order to know the origin of every band one has to study the entire range of spectra. The purpose of the present study is to account for the molecular origin of all the observed bands, to provide an assignment of the vibrational fundamentals and to see the environmental effects on some sensitive bands.

In this section results are reported for the PyIX complexes, frequencies assigned and the nature of the species present discussed. Consideration of the frequency shifts of the pyridine ring vibrations, solvent effects and force constants is deferred until a later section where a general comparison with the other complexes studied is possible.

### 3.1.2. Experimental.

3.1.21. Purity of Materials: 'Analar' pyridine was dried over sodium hydroxide and bariumoxide for several days. The dried liquid was then distilled from fresh bariumoxide. The infra-red spectrum of purified pyridine obtained in this way did not show any bands of picolines which are the most likely contaminants.

'Analar' benzene and carbontetrachloride were dried over  $P_2O_5$  and distilled. General purpose reagent grade (G.P.R.) Cyclohexane and n-hexane were dried over  $P_2O_5$  for a few days and distilled. Acetonitrile and nitromethane (G.P.R.) were dried over potassium carbonate and distilled. Methylene chloride (G.P.R.) was first dried over anhydrous calcium-chloride and then over  $P_2O_5$  and distilled. 'Spectrograde' carbondisulphide (B.D.H), analar iodine, analar methanol, analar nitrobenzene, iodinechloride (B.D.H.) and iodine bromide (B.D.H) were used without further purification. Nujol (liquid paraffin) was kept over molecular sieves 'type 4A' for several days prior to use and 'spectrosol' hexachlorobuta-1,3-diene supplied by Hopkins and Williams Ltd., was used without further purification.

### 3.1.22 Preparation of Complexes:

Pyridine-iodine: Measured equimolar quantities of pyridine and iodine dissolved in appropriate solvents were mixed together just before running the spectrum.

Pyridine-iodinechloride: The preparation of this complex has been discussed by Willams and others.<sup>(84)</sup> It was prepared by adding a solution of pyridine in carbontetrachloride to a solution of iodinechloride in the same solvent. The yellow solid obtained thus was washed thoroughly with carbontetrachloride and recrystallised from methanol. The crystalline yellow compound was washed with sodium dried ether and dried in a vacuum desiccator over  $P_2O_5$ . The melting point was found to be  $133^{\circ}C$  (lit.  $134-135^{\circ}C$ ).

Pyridine-iodinebromide: This was prepared by mixing pyridine and iodinebromide dissolved in carbontetrachloride<sup>(84)</sup> and was purified and dried as  $PyI_2Br$ , m.pt.  $116^{\circ}C$  (lit  $116-117^{\circ}C$ ).

Pyridine-iodinecyanide: The preparation and isolation of the solid pyridine-iodinecyanide has been reported by Zingaro and Tolberg.<sup>(36)</sup> As the complex is unstable no attempt was made to prepare the solid compound. Spectra were examined by mixing appropriate quantities of pyridine and cyanogen iodide, and diluting with another solvent where required.

Cyanogen iodide was prepared by slowly adding powdered iodine to an aqueous solution of NaCN. (85) The ICN thus formed was obtained by extracting with ether and evaporating to dryness. The solid compound was then dissolved in water and heated at 50°C under reduced pressure. The mixture was cooled to 0°C and a light yellow solid was filtered out and dried. It was further purified by recrystallisation from chloroform, m.p. 146°C (lit. 146-147°C).

3.1.23. Spectra: All the solution spectra refer to freshly made up solutions. Some attack on the KBr windows was observed in all runs in which pyridine was used as a solvent. However, no appreciable differences in the spectra were found when polythene bags, or AgCl windows were used. On standing for some hours, changes in all the spectra occurred. For the example, PyICN changes were more marked, and some new bands developed. To get a reliable spectra of PyICN several spectra were run, each time using freshly made solutions.

No decomposition of any kind were observed while running the Raman spectra or far infra-red spectra in mulls or in solution.

3.1.3. Results: All the four complexes were examined over the frequency range 3500 to 400 $\text{cm}^{-1}$  in a range of solvents and some of the earlier low frequency (below 100 $\text{cm}^{-1}$ ) work was repeated in mulls. Many of the bands of solvents and mulling agents overlies those of the complexes. In all cases only bands that can be clearly distinguished

TABLE 2

Infra-red Spectra of the Pyridine-iodine System in various media.

Iodine in excess of Pyridine	Equimolar Pyridine and iodine in CS <sub>2</sub>	Equimolar Pyridine and iodine in benzene	Equimolar Pyridine and iodine in n-heptane	Equimolar Pyridine and iodine in Cyclohexane	Interpretation
	3149w				1594 x 2
	3085m				b <sub>1</sub> fundamental
	3065s				a <sub>1</sub> fundamental
	3042w				a <sub>1</sub> fundamental
	3032w				1445 + 1594
	2999½m				
	2952w				1351 + 1594
	1990w				746 + 1236
	1911m				694 + 1209
	1868w				694 + 1151
		1594s			a <sub>1</sub> fundamental
1445s		1445m			b <sub>1</sub> fundamental
	1351w	1351w			b <sub>1</sub> fundamental 620 + 746
	1295vw				420 + 746
1240w	1236m				b <sub>1</sub> fundamental
	1209s	1209s		1212w	a <sub>1</sub> fundamental
	1151s				b <sub>1</sub> fundamental

TABLE 2 (Cont'd)

Iodine in excess of Pyridine	Equimolar Pyridine and iodine in CS <sub>2</sub>	Equimolar Pyridine and iodine in benzene	Equimolar Pyridine and iodine in n-heptane	Equimolar Pyridine and iodine in Cyclohexane	Interpretation
	1067s	1067s		1067w	a <sub>1</sub> fundamental
1038vw	1038vw				(Py <sub>2</sub> I) <sup>+</sup>
	1030m				a <sub>1</sub> fundamental
1007s	1005vs	1006vs	1003w		a <sub>1</sub> fundamental
	939w	944w			b <sub>2</sub> fundamental
	746vs	748s		746s	b <sub>2</sub> fundamental
	694vs				b <sub>2</sub> fundamental
	677w				
	653w				b <sub>1</sub> fundamental
636m	639vw				(Py <sub>2</sub> I) <sup>+</sup>
625s	620vs		617s	617s	a <sub>1</sub> fundamental
436w					(Py <sub>2</sub> I) <sup>+</sup>
421	420w			420s	b <sub>2</sub> fundamental

TABLE 3

Infra-red Spectra of the Pyridine-iodinebromide in various media

Saturated Solution of PylBr in Pyridine	Saturated Solution of PylBr in CS <sub>2</sub>	Saturated Solution of PylBr in C <sub>6</sub> H <sub>6</sub>	PylBr in Nujol Mull	PylBr in Hexachlorobutadiene mull	Interpretation
	3159w				1597 x 2
	3089w			3093w	b <sub>1</sub> fundamental
	3067m			3065s	a <sub>1</sub> fundamental
	3034w			3034w	a <sub>1</sub> fundamental
	3021w			3020w	1449 + 1572
				2909w	1346 + 1572
	1914m				693 + 1210
	1848w				693 + 1152
		1597w	1597s		a <sub>1</sub> fundamental
			1572w		b <sub>1</sub> fundamental
1445s		1449s	1447s	1449s	b <sub>1</sub> fundamental
	1353w	1351w	1346w	1348m	b <sub>1</sub> fundamental 625 + 747
	1242m		1245m	1250m	b <sub>1</sub> fundamental
1210s	1210s	1209s	1209w 1194w	1212w 1202m	a <sub>1</sub> fundamental
	1152s		1153w	1156w	b <sub>1</sub> fundamental
	1067s	1066s	1057s	1058s	a <sub>1</sub> fundamental
	1031ms		1032m	1034w	a <sub>1</sub> fundamental



TABLE 3 (Cont'd)

Saturated Solution of PylBr in Pyridine	Saturated Solution of PylBr in CS <sub>2</sub>	Saturated Solution of PylBr in C <sub>6</sub> H <sub>6</sub>	PylBr in Nujol Mull	PylBr in Hexachlorobutadiene mull	Interpretation
1010s	1009s	1010s	1012s	1013s	a <sub>1</sub> fundamental
	490w	944w			b <sub>2</sub> fundamental
	747s	749s	751s	751s	} b <sub>2</sub> fundamental
	701sh		704vw		
	693s		689s	689s	b <sub>2</sub> fundamental
	675vw		676vw		
			670vw		
	655w				b <sub>1</sub> fundamental
637s					(Py <sub>2</sub> I) <sup>+</sup>
629vs	625s	627s	632s	635s	a <sub>1</sub> fundamental
436w					(Py <sub>2</sub> I) <sup>+</sup>
420s	420s	420s	420m	420m	b <sub>2</sub> fundamental
			200s		l-Br stretching
			160s		N-I stretching
			94w		N-I-Br bending
			68s		N-I-Br bending

TABLE 4

Infra-red Spectra of the Pyridine iodine-chloride system in various media

Saturated solution of PylCl in Pyridine	Saturated solution of PylCl in CS <sub>2</sub>	Saturated solution of PylCl in C <sub>6</sub> H <sub>6</sub>	PylCl in Nujol Mull	PylCl in Hexachlorobutadiene mull (4000-2000cm <sup>-1</sup> )	Interpretation
	3149w			3099m	
	3085w			3089m	b <sub>1</sub> fundamental
	3068m			3065m	a <sub>1</sub> fundamental
				3053s	1449 + 1597
	3039w			3039w	a <sub>1</sub> fundamental
	2999w			2999w	
				2952w	1347 + 1597
				2928m	1347 + 1592
			1980vw		748 + 1239
	1910w		1915w		692 + 1209
			1838vw		692 + 1150
			1647w		627 + 1011
		1597s	1597s		a <sub>1</sub> fundamental
			1569m		b <sub>1</sub> fundamental
1449s		1449s	1449s		b <sub>1</sub> fundamental
			1390w		630 + 749
	1347m	1350w	1344w		b <sub>1</sub> fundamental
1244w	1239m		1247s		b <sub>1</sub> fundamental
1209s	1209s	1209s	1209s	}	a <sub>1</sub> fundamental
			1197s		

TABLE 4 (Cont'd)

Saturated solution of PylCl in Pyridine	Saturated solution of PylCl in CS <sub>2</sub>	Saturated solution of PylCl in C <sub>6</sub> H <sub>6</sub>	PylCl in Nujol Mull	PylCl in Hexachlorobutadiene mull (4000-2000cm <sup>-1</sup> )	Interpretation
	1150s		1154w		b <sub>1</sub> fundamental
			1087w		b <sub>1</sub> fundamental
	1067s	1064s	1056vs		a <sub>1</sub> fundamental
	1030ms		1035m		a <sub>1</sub> fundamental
1011s	1009s	1011s	1013s		a <sub>1</sub> fundamental
	941vw		948w		b <sub>2</sub> fundamental
			869vw		b <sub>2</sub> fundamental
			851vw		
	748s	749s	752va		b <sub>2</sub> fundamental
	702w		704w		
	692s		689vs		b <sub>2</sub> fundamental
	675w				
	655w		649w		b <sub>1</sub> fundamental
632s	627s	630s	636vs		a <sub>1</sub> fundamental
434w					(Py <sub>2</sub> I) <sup>+</sup>
424s	421s	421s	426s		b <sub>2</sub> fundamental
			265s		1-Cl stretching
			170s		N-I stretching
			92s		N-I-Cl bending

TABLE 5

Infra-red Spectra of the Pyridine iodinecyanide in  
various media

Iodine cyanide in excess of Pyridine	Iodine cyanide in excess of Pyridine after 2 days	Equimolar solution of Pyridine and iodinecyanide in CS <sub>2</sub>	Equimolar solution of Pyridine and iodinecyanide in C <sub>6</sub> H <sub>6</sub>	Interpretation
		3150w		1597 + 1557
		3085s		b <sub>1</sub> fundamental
		3065m		a <sub>1</sub> fundamental
		3048m		a <sub>1</sub> & b <sub>1</sub> fundamental
		3015m		1445 + 1597
		3001w		1445 + 1557
2155s				C-N stretching
		1914m		698 + 1213
		1856m		617 + 1235
			1597s	a <sub>1</sub> fundamental
			1557vw	b <sub>1</sub> fundamental
	1488s			
1445s			1445s	b <sub>1</sub> fundamental
	1371w			617 + 748
	1350w	1357w		b <sub>1</sub> fundamental
	1290w			

TABLE 5 (Cont'd)

Iodine cyanide in excess of Pyridine	Iodine cyanide in excess of Pyridine after 2 days	Equimolar solution of Pyridine and iodinecyanide in CS <sub>2</sub>	Equimolar solution of Pyridine and Iodinecyanide in C <sub>6</sub> H <sub>6</sub>	Interpretation
1238w	1250w	1235m		b <sub>1</sub> fundamental
		1213s	1216s	a <sub>1</sub> fundamental
		1149s		b <sub>1</sub> fundamental
		1068s	1068s	a <sub>1</sub> fundamental
	1039w	1032s		a <sub>1</sub> fundamental
1003s	1006s	1003s	1004s	a <sub>1</sub> fundamental
	778w			
		748vs		b <sub>2</sub> fundamental
		698vs		b <sub>2</sub> fundamental
		677w		
636sh		656w		b <sub>1</sub> fundamental (Py <sub>2</sub> I) <sup>+</sup>
623s	628s	617s	617s	a <sub>1</sub> fundamental
	564w			
	551m			
430m	429w		423s	l-C stretching
420m	420w		413s	b <sub>2</sub> fundamental

TABLE 6

Raman Spectra of the Pyridine-iodine chloride.

Solid	Solution in CH <sub>2</sub> Cl <sub>2</sub> , Pyridine, or CH <sub>3</sub> CN	
1598s	1600w(P?)	a <sub>1</sub> fundamental
1576m	1567w	b <sub>1</sub> fundamental
1474w		a <sub>1</sub> fundamental
1248w		} b <sub>1</sub> fundamental
1238w		
1202s	1208m (P)	} a <sub>1</sub> fundamental
1192w		
1156m	1156m (dp)	b <sub>1</sub> fundamental
1034s	1039s (P)	a <sub>1</sub> fundamental
1013s	1012s (P)	a <sub>1</sub> fundamental
980vw		a <sub>2</sub> fundamental
948w		b <sub>2</sub> fundamental
872w		a <sub>2</sub> fundamental
754w		b <sub>2</sub> fundamental
688w		b <sub>2</sub> fundamental
648m	646m (dp)	b <sub>1</sub> fundamental
636s	633s (P)	a <sub>1</sub> fundamental
425w		b <sub>2</sub> fundamental
388		a <sub>2</sub> fundamental

TABLE 6 (Cont'd)

Solid	Solution in CH <sub>2</sub> Cl <sub>2</sub> ; pyridine, or CH <sub>3</sub> CN	
272	275s (P)	I-OI stretching
254		
	264sh	1Cl <sub>2</sub> <sup>-</sup> symmetric stretch
	178	(Py <sub>2</sub> I) <sup>+</sup> skeletal
174m	160w	N-I stretching
164m		
92s		bending
72s		bending

TABLE 8

Low frequency Raman Spectra of the Pyridine-iodinebromide and the Pyridine-iodinechloride in different media.

Solvents	PyICl			PyIBr		
	1-Cl Stretch- ing	$1\text{Cl}_2^- (\text{Py}_2\text{I})^+$	N-I Stretch- ing	1 Br Stretch- ing	$1\text{Br}_2^- (\text{Py}_2\text{I})^+$	N-I Stretch- ing
Benzene	292s			204s		
1:4 Dioxane	290s	270w		202s		146w
Acetone	280s	270w		197s	159m 179vw	146w
$\text{CH}_2\text{Cl}_2$		178w	160w	199s	160m 180w	144w
Pyridine	275s			196s	159m 180w	
$\text{C}_6\text{H}_5\text{NO}_2$	276s	264sh		195s	158m	
$\text{CH}_3\text{CN}$	274s	262sh 178w	162w	194s	158m 176w	
$\text{CH}_3\text{NO}_2$	272s	264sh 178w	162w	193s	160m 180w	



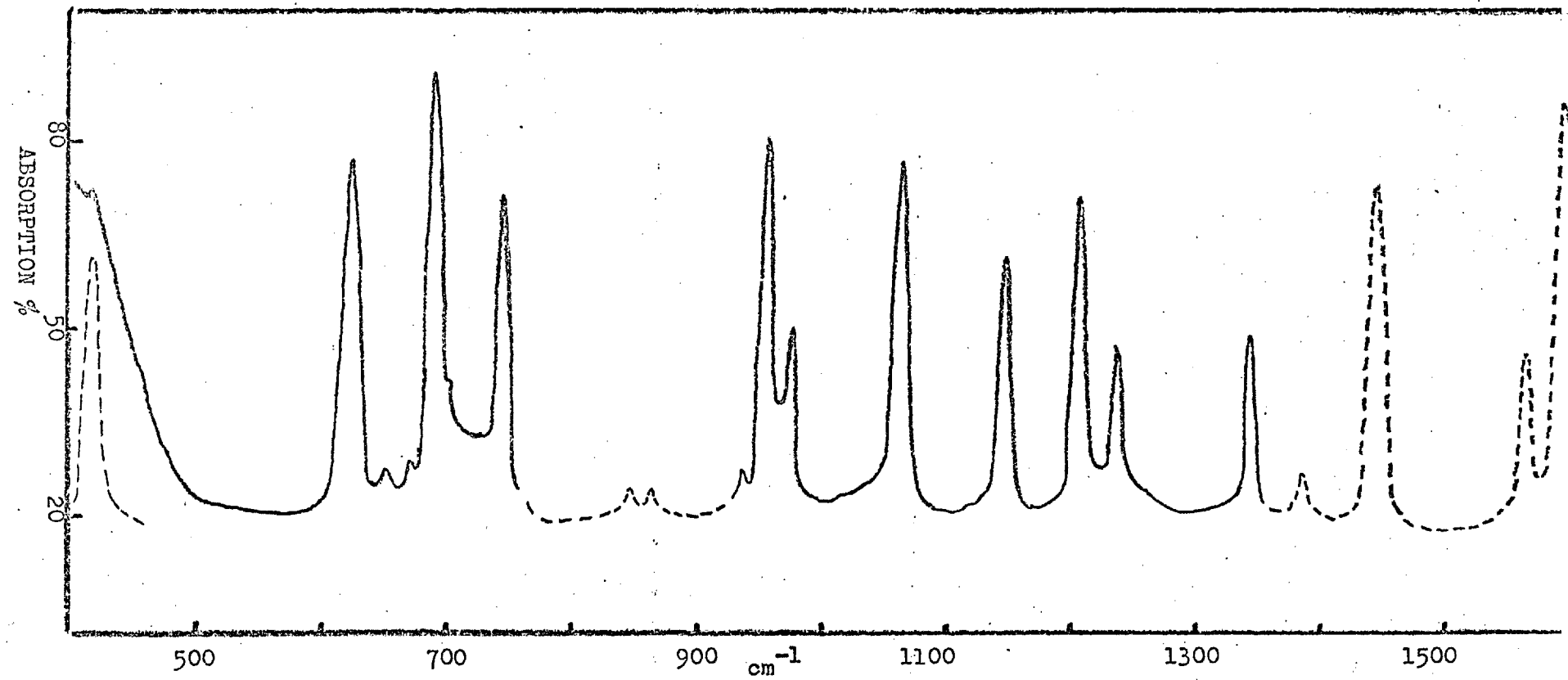


Fig. 3 Composite spectra of PyICl. — CS<sub>2</sub> solution; - - - Mull

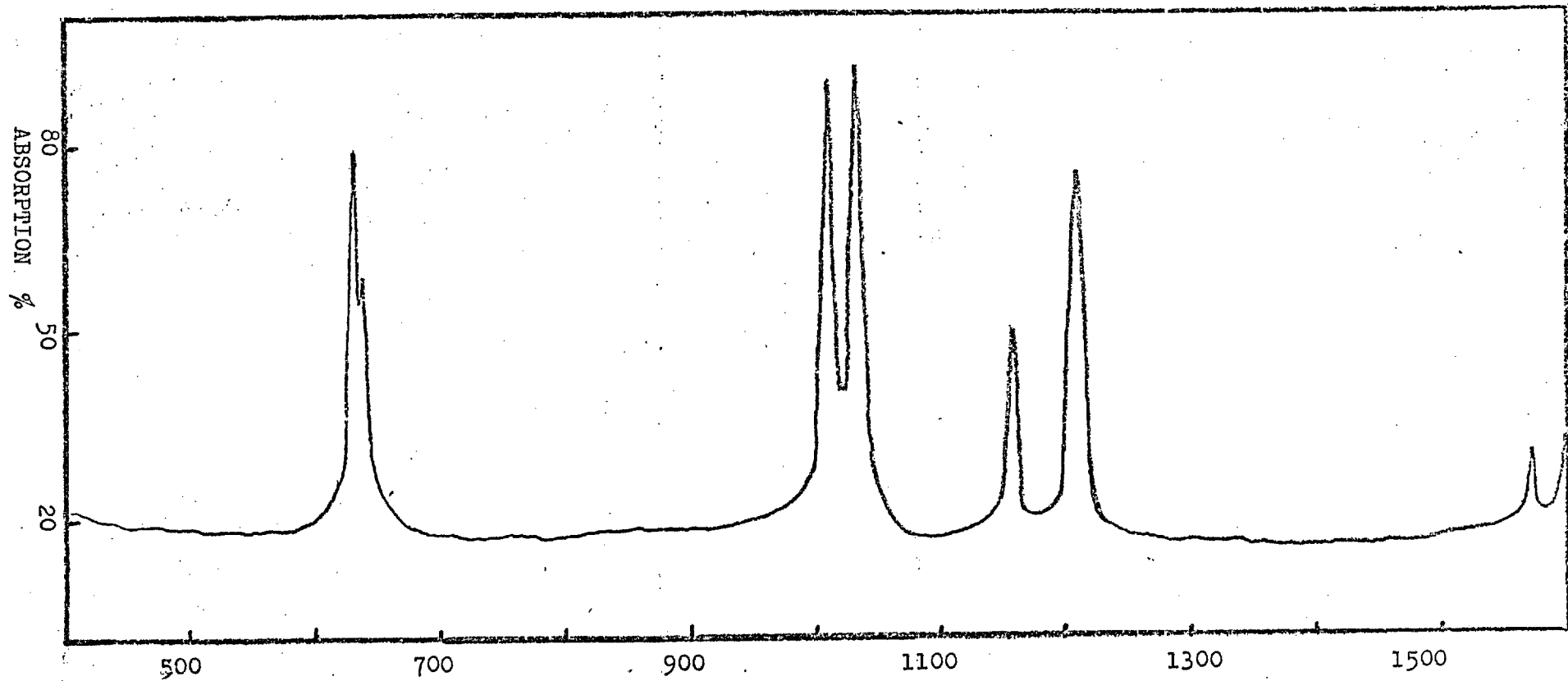


Fig. 4 Composite Raman spectra of PyICl.

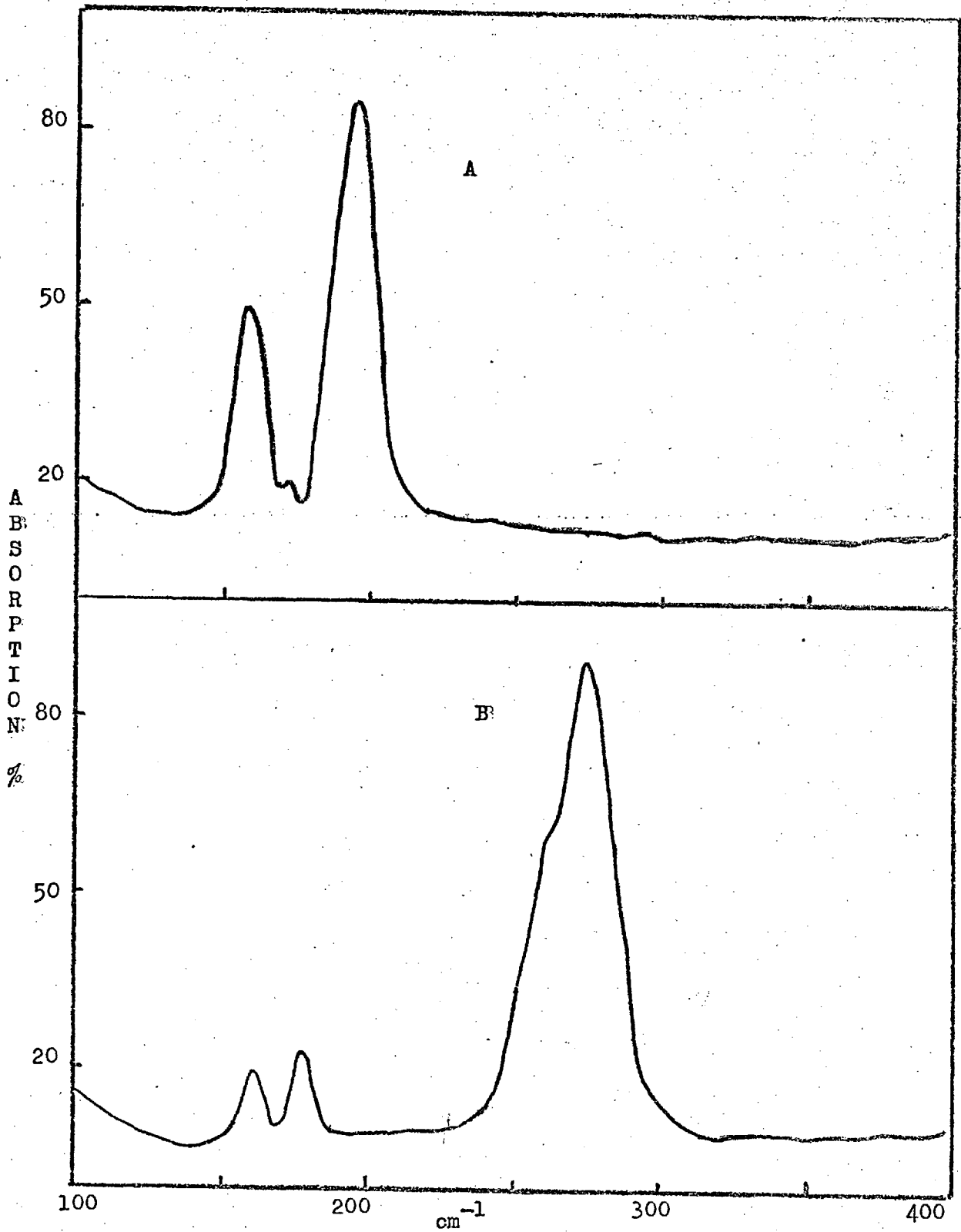
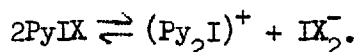


Fig. 5. Raman spectra of (A) PyIBr in acetonitrile solution,  
(B) PyICl in acetonitrile solution.

from the solvent background are noted in tables 2 to 5. Table 6 shows the Raman bands of pyridine-iodinechloride. Figures 3 and 4 show the higher frequency infra-red and Raman spectra of PyICl and figure 5 shows the low frequency Raman spectra of PyICl and PyIBr.

3.1.4. Nature of Species Present: The low frequency range is the most useful for identifying the species present. In this section only low frequency Raman spectra is discussed in detail while mentioning only briefly the infra-red spectra, as the latter has been discussed elsewhere.<sup>(48)</sup> Detail discussion of higher frequency spectra is also given here.

The low frequency infra-red spectra of PyI<sub>2</sub>, PyIBr or PyICl in non polar solvents like benzene, cyclohexane, etc., show only two bands. These bands are assigned to the I-X (X=I, Br or Cl) and N-I stretching vibrations of unionised charge-transfer complexes. The presence of additional low frequency bands of PyI<sub>2</sub>, PyICl and PyIBr in polar solvents, such as pyridine, nitrobenzene, etc., at 137, 174 and 223cm<sup>-1</sup> respectively have been assigned to the antisymmetric stretching vibration of I<sub>3</sub><sup>-</sup>, IC1<sub>2</sub><sup>-</sup> and IBr<sub>2</sub><sup>-</sup> respectively.<sup>(48)</sup> The formation of these polyhalide ions has been explained in terms of the reaction



This scheme suggests the formation of the ion (py<sub>2</sub>I)<sup>+</sup>. The vibration spectra of salts of this ion have been examined (ref.sec.4) and show

two stretching bands occur in the low frequency range,  $172\text{cm}^{-1}$  (infra-red) and  $180\text{cm}^{-1}$  (Raman). However, for solutions of the complex in polar solvents the infra-red band at  $172\text{cm}^{-1}$  is expected to be weaker. It also lies very close to the I-I stretching vibration of  $\text{PyI}_2$  and  $167\text{cm}^{-1}$ , the  $\text{IBr}_2^-$  antisymmetric stretching vibration at  $174\text{cm}^{-1}$ , and the N-I stretching vibration of  $\text{PyICl}$  at  $160\text{cm}^{-1}$ . Thus it is not possible to distinguish this N-I-N antisymmetric stretching vibration at  $172\text{cm}^{-1}$  from the above bands.

However, the symmetric  $\text{IBr}_2^-$  stretching frequency at  $\sim 158\text{cm}^{-1}$ ,<sup>(91)</sup> and the N-I stretching frequency, at  $160\text{cm}^{-1}$  for the  $\text{PyICl}$  complex in pyridine solution, do not interfere with the symmetric stretching frequency for the  $(\text{py}_2\text{I})^+$  ion observed at  $180\text{cm}^{-1}$  in the Raman spectra. To take advantage of this, low frequency Raman spectra of the  $\text{pyICl}$  and  $\text{pyIBr}$  were run (Table 8). A further advantage of the Raman spectra is that a wide variety of solvents can be used. In polar solvents such as  $\text{CH}_3\text{CN}$ ,  $\text{CH}_3\text{NO}_2$ ,  $\text{C}_6\text{H}_5\text{NO}_2$  etc., the Raman spectra of  $\text{pyICl}$  show four bands in the frequency range  $400-100\text{cm}^{-1}$ . By comparison with the infra-red spectra of  $\text{pyICl}$  in pyridine solution,<sup>(48)</sup> the strong polarised band at  $\sim 274\text{cm}^{-1}$  and the weak band at  $160\text{cm}^{-1}$  may be assigned respectively to the I-Cl and N-I stretching frequencies of the unionised  $\text{pyICl}$  complex.<sup>(48)</sup> Similarly by comparison with the Raman band at  $182\text{cm}^{-1}$  for the  $(\text{py}_2\text{I})^+\text{PF}_4^-$  (ref.sec.4), the weak band at  $178\text{cm}^{-1}$  may be assigned to the NIN symmetric stretching frequency

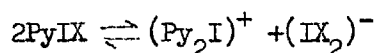
of the  $(\text{Py}_2\text{I})^+$  ion. Also by comparison with the Raman band at  $254\text{cm}^{-1}$  of the  $(\text{CH}_3)_4\text{N}^+(\text{ICl}_2)^-(91)$  the band at  $\sim 264\text{cm}^{-1}$  which appears as a shoulder may be assigned to the symmetric stretching frequency of the  $\text{ICl}_2^-$  ion. In benzene solution, only the I-Cl stretching band of  $\text{PyICl}$  at  $292\text{cm}^{-1}$  is observed.

The Raman spectra of the  $\text{PyIBr}$  complex also show four bands in polar solvents in the region  $400-100\text{cm}^{-1}$ . By comparison with infra-red spectra of  $\text{PyIBr}$  in pyridine solution<sup>(48)</sup> the strong polarised band at  $\sim 192\text{cm}^{-1}$  and the weak band at  $146\text{cm}^{-1}$  may be assigned respectively to the I-Br and N-I stretching vibrations of un-ionised  $\text{PyIBr}$  complex. The other two bands at  $\sim 160$  and  $\sim 180\text{cm}^{-1}$  may be assigned to the  $\text{IBr}_2^-(91)$  symmetric stretching and the NIN symmetric stretching of the  $(\text{Py}_2\text{I})^+$  ion. Again in benzene solution only the I-Br stretching band of  $\text{PyIBr}$  at  $205\text{cm}^{-1}$  is observed.

In the frequency range  $3500-400\text{cm}^{-1}$  all the observed bands of  $\text{PyIX}$  ( $X=\text{Cl}, \text{Br}$  or  $\text{I}$ ) in non polar solvents can be assigned to the unionised complex. However, solutions of iodine in excess of pyridine show some additional bands. In the  $600\text{cm}^{-1}$  region two new bands are observed; a strong band at  $625\text{cm}^{-1}$  and a medium band at  $636\text{cm}^{-1}$  (Table 2). In the  $400\text{cm}^{-1}$  region also, two new bands are observed; a strong band at  $420\text{cm}^{-1}$  and a weaker band at  $436\text{cm}^{-1}$ . With equimolar solutions of pyridine and iodine in n-hexane, cyclohexane or benzene the bands at  $636$  and  $436\text{cm}^{-1}$  disappear and

only bands at  $\sim 417$  and  $\sim 617\text{cm}^{-1}$  are observed. Sharp et al have <sup>(90)</sup> noted only one band in the  $600\text{cm}^{-1}$  region and a single band in the  $400\text{cm}^{-1}$  region for a series of pyridine metal co-ordinated complexes, where there is only one species present. To establish the origin of the bands at  $636$  and  $436\text{cm}^{-1}$ , which appear in polar pyridine solution, the vibration spectra of the salts of the ion  $(\text{py}_2\text{I})^+$  which is the most likely ionised product, has been independently examined (see 4). The additional bands ( $436$  and  $636\text{cm}^{-1}$ ) that are observed in excess of pyridine are also found in the spectra of  $(\text{py}_2\text{I})^+$  salts. The other complexes  $\text{PyICl}$  and  $\text{PyI}Br$  behave similarly.

From the above discussions it may be concluded that the bands present in non polar solvents can all be assigned to species  $\text{PyIX}$ . The spectra of freshly prepared solutions in polar solvents can be entirely accounted for by the equilibria



However, the possibility of formation of small amounts of species like  $\text{PyI}^+$  cannot be eliminated.

The presence of a weak band at  $636\text{cm}^{-1}$  in a freshly made up solution of  $\text{ICN}$  in pyridine indicates the presence of  $(\text{Py}_2\text{I})^+$ . However, no bands which could be attributed to the  $(\text{I}(\text{CN})_2)^-$  ion corresponding to the  $\text{IX}_2^-$  ion were observed. In every respect the  $\text{PyICN}$  complex appears to be less stable than the other pyridine-halogen complexes. After some hours the band at  $636\text{cm}^{-1}$  completely disappears

and the bands due to the complex become weaker, new bands appearing e.g. at 551, 564 and  $1488\text{cm}^{-1}$ . These new bands are considered to arise from the products of a slow reaction, probably that of substitution in the pyridine ring.

3.1.5. Classification of modes and assignments: In the crystalline state the symmetry point group of the PyIX units is  $C_{2v}$ . (59,60).

In solution it is not theoretically impossible for the same structure to be retained. The infra-red data also supports the  $C_{2v}$  symmetry in solution. The presence of a bent N-I-X in the complex would reduce the symmetry to  $C_2$ , and allow the vibrations derived from the  $a_2$  class, which is infra-red inactive for  $C_{2v}$  point group, to become infra-red active. The absence in most of the observed spectra of any bands near to the  $a_2$  class frequencies of pyridine ( $986, 891$  and  $375\text{cm}^{-1}$ ) supports a  $C_{2v}$  structure of the complex.

For  $C_{2v}$  symmetry the vibrations fall into four classes  $a_1, b_1$  (in-plane) and  $a_2, b_2$  (out of-plane). For pyridine-IX the 33 fundamental vibrations are distributed among the classes as follows.

In plane vibrations:

Class  $a_1$ : twelve vibrations Raman (polarised) and infra-red active.

Class  $b_1$ : eleven vibrations Raman (depolarised) and infra-red active.



Out of-plane vibrations:

Class  $a_2$ : three vibrations Raman active  
(depolarised) only.

Class  $b_2$ : seven vibrations Raman (depolarised)  
and infra-red active.

Most of the vibrations will be similar to those in pyridine which has  $10a_1+9b_1+3a_2+5b_2$  normal vibrations. Since the interaction between pyridine and halogen is relatively weak, these vibrations will have frequencies close to their counterparts in pyridine.

Going from pyridine to Py-IX (X=Cl, Br or I) results in the appearance of six new modes. These six vibrations  $2a_1+2b_1+2b_2$  comprise five intermolecular modes and the  $a_1$  IX stretching vibration, all lying below  $400\text{cm}^{-1}$ . Adopting a  $C_{2v}$  structure the vibrations of PyICN classify as  $13a_1+3a_2+12b_1+8b_2$ . The nine additional vibrations comprise five intermolecular vibrations ( $a_1+2b_1+2b_2$ ) and four vibrations derived from internal modes of ICN ( $2a_1+b_1+b_2$ ).

The normal vibrations of pyridine have been assigned by several authors<sup>(86)</sup> and recently by Long et al.<sup>(87)</sup> We have followed the assignment of the latter authors since this assignment is supported by a force constant calculation. The notation of Green et al.,<sup>(88)</sup> however, is used partial assignments of the complexes PyIX vibrations have been given by Watari et al.<sup>(39)</sup>

Comparison with pyridine enables one to make an almost complete assignment of the infra-red and Raman active fundamentals of the PyIX complexes. Table 7 shows the assignments for the complexes and also includes that for the pyridinium ion, given by Cook.<sup>(89)</sup> The Raman polarised data of the PyICl confirms this assignment. (Table 6). Most of the infra-red frequencies in this table refer to solution in CS<sub>2</sub>. In regions where CS<sub>2</sub> bands occur other solvents are utilised.

The band at 1219cm<sup>-1</sup> was assigned to  $\nu_{9a}$ <sup>(39)</sup> and is possibly due to pure pyridine, the solvent used. This band was not observed in other solvents such as CS<sub>2</sub> (Table 2-5). Therefore despite the arguments put forward by Wateri et al<sup>(39)</sup> the 1210cm<sup>-1</sup> band has been assigned to  $\nu_{9a}(a_1)$  and 1240cm<sup>-1</sup> to  $\nu_3(b_1)$ . This assignment has been confirmed by the fact the band at 1210cm<sup>-1</sup> of PyICl is found to be polarised.

The two very low frequency bands of crystalline PyICl and PyIBr at 92 and 94cm<sup>-1</sup> respectively, which have not been previously reported, may be assigned to the N-I-X in-plane bending mode. The expected positions of the bending frequencies of PyICl and PyIBr may be roughly estimated from known stretching force constants and interatomic distances, using the relation

$$\lambda = 4\pi^2 \nu^2 = \frac{1}{b_1^2 b_2^2} \left\{ \frac{b_1^2}{m_x} + \frac{b_2^2}{m_I} + \frac{(b_1 + b_2)^2}{m_{py}} \right\} K_S$$

TABLE 7

Assignment of fundamental vibrational frequencies of  
 Pyridine complexes, and comparison with Pyridine and  
 Pyridinium ion.

Designation		Pyridine	Pyridine 1CN	Pyridine I <sub>2</sub>	Pyridine 1Br	Pyridine 1Cl	Pyridinium <sup>+</sup> (I <sup>-</sup> )
a <sub>1</sub> ∇(CH)	2	3054	3065	3065	3067	3067	3060
∇(CH)	20a	3054	3065	3065	3067	3068	
∇(CC)	8a	1583	1597	1594	1597	1597	1638
∇(CC,CN)19a		1482				1474	1484
β(CH)	9a	1218	1213	1209	1210	1209	1194
β(CH)	18a	1068	1068	1067	1067	1067	1030
Ring	1	992	1003	1005	1009	1009	1010
X sens	13	3036	3048	3042	3034	3039	
X sens	12	1030	1032	1030	1031	1030	
X sens	6a	605	617	620	625	627	633
N-I stretching				94	134	147	
I-X Stretching			423	171	204	290	
C-N stretching			2155				
b <sub>1</sub> ∇(CH)	20b	3083	3085	3085	3089	3085	
∇(CH)	7b	3036	3048	3042	3034	3039	3045
∇(CC)	8b	1572	1557		1572	1569	1608
∇(CC,CN)19b		1439	1445	1445	1449	1449	1535

TABLE 7 (Cont'd)

Designation		Pyridine	Pyridine	Pyridine	Pyridine	Pyridine	Pyridinium <sup>+</sup>
		1CN	I <sub>2</sub>	1Br	1Cl	(I <sup>-</sup> )	
$\nu$ (CC,CN) 14		1375					
$\rho$ (CH) 3		1218	1235	1236	1242	1239	1326
$\beta$ (CH) 18b		1085				1087	1050
$\alpha$ (CCC) 6b		652	656	653	655	649	
X sens 15		1148	1149	1151	1152	1150	1161
Py-I-X bending					94	92	
1CN bending			336				
$a_2\gamma$ (CH) 17a		981				980	
$\gamma$ (CH) 10a		886				872	
$\phi$ (CC) 16a		374				388	
$b_2\gamma$ (CH) 5		942		939	940	941	
$\gamma$ (CH) 10b		886				869	855
$\phi$ (CC) 4		749	748	746	749	748	738
$\phi$ (CC) 11		700	698	694	693	692	671
X sens 16b		405	413	420	420	421	
PyIX bending					68	72	

where  $b_1$  and  $b_2$  are the distances of N (of pyridine) and X respectively from I. The bending force constant,  $K_\xi$ , is taken to be one tenth of the stretching force constant,  $K_{NI}$ . Using  $K_{NI}$  force constant value of Watari<sup>(40)</sup> and the NI and I-X distances of Hassel et al,<sup>(59,60)</sup> the bending frequencies of PyICl and PyIBr are calculated at 98 and  $83\text{cm}^{-1}$ . These may be compared with the observed values of 92 and  $94\text{cm}^{-1}$  respectively. The infra-red band at  $68\text{cm}^{-1}$  of the PyIBr and the Raman band at  $72\text{cm}^{-1}$  may be assigned to bending or crystal lattice vibrations.

### 3.2. $\gamma$ -Picoline-halogen complexes.

#### 3.2.1. INTRODUCTION

$\gamma$ -Picoline-halogen complexes have not been as extensively studied as pyridine-halogen complexes.  $\gamma$ -Picoline forms stronger complexes than pyridine. The stability constant and heat of formation of the  $\gamma$ -picoline-iodine complex in *n*-heptane solution have been reported to be  $368^1/\text{mole}$  and  $8.93 \text{ KCal/mole}$  respectively, compared with  $160.5^1/\text{mole}$  and  $7.47 \text{ KCal/mole}$  for the pyridine-iodine complex in the same solvent and at the same temperature<sup>(93)</sup>. This increase in strength is due to the fact that the methyl substituent of  $\gamma$ -picoline increases the electron density through induction and hyperconjugation and as a result the ionization potential drops.

Glusker and Thompson<sup>(35)</sup> observed changes in the frequencies of a number of  $\gamma$ -picoline bands on addition of iodine providing evidence of complex formation. Recently Lorenzelli<sup>(92)</sup>, and Lake and Thompson<sup>(52)</sup> have observed the I-I stretching and N-I stretching vibrations of the  $\gamma$ -picoline-iodine complex in cyclohexane solution.

Glusker and Miller<sup>(94)</sup> have reported the formation of two distinct solid compounds when iodine is dissolved in excess of  $\gamma$ -picoline. One compound (I),  $(\text{C}_6\text{H}_7\text{N})_2\text{I}_2$ , is water-soluble, alcohol-insoluble, and contains no I-I covalent bond. The second compound (II),  $\text{C}_6\text{H}_7\text{N}\cdot\text{I}_2$ , is insoluble in water but soluble in organic solvents, and was found to contain a pair of iodine atoms separated by a distance close to the covalent bond length. The structure of the compound II has been

examined in more detail by Hassel et al,<sup>(94)</sup> confirming Glusker and Miller's conclusion. In addition, he found that the N-I-I arrangement is linear with the I-I distance  $2.83\text{\AA}$  and the N-I distance  $2.3\text{\AA}$ . Compound II, which is the charge-transfer complex is discussed in this section and the compound I will be discussed in detail in a later section.

As an electron acceptor ICN is weaker than  $\text{I}_2$ . The vertical electron affinity of ICN has been predicted to be about 0.9ev which is about 0.8ev less than iodine.<sup>(97)</sup> The u.v. spectra of a number of ICN complexes with 'n' donors have been reported.<sup>(97)</sup> The infra-red spectra of  $\gamma$ -piclCN complex has been discussed by Glusker and Thompson<sup>(35)</sup> and a number of ICN complexes have been reported by Person et al<sup>(46)</sup> who extended observations of the infra-red spectra up to CsBr region ( $280\text{cm}^{-1}$ ). The two ICN stretching modes were found to shift to lower frequencies and the bending mode to higher frequency on complex formation. The IC stretching mode appears at  $486\text{cm}^{-1}$  in chloroform solution, and shifts to 430 and  $398\text{cm}^{-1}$  on complex formation with pyridine and trimethylamine respectively. The ICN bending mode which appears at  $320\text{cm}^{-1}$  in chloroform solution shifts to  $336\text{cm}^{-1}$  on complex formation with pyridine. The CN stretching mode becomes weaker and shifts to a slightly lower frequency on complex formation.

In this section results are reported for a series of  $\gamma$ -picIX complexes (X=Cl, Br or I). The nature of the species present is

discussed and the frequencies assigned. Consideration of frequency shifts of the \-picoline ring vibrations, intensity changes, solvent effects, and force constants is deferred until a later section.



### 3.2.2. EXPERIMENTAL

3.2.21. Purity of Materials:  $\gamma$ -Picoline(GPR) was dried over KOH and  $B_2O_3$  and finally distilled under reduced pressure. The purity of  $\gamma$ -picoline was found to be 99% by V.P.C. Purification of other chemicals has already been discussed in section 3.1.21.

#### 3.2.22. Preparation of Complexes

$\gamma$ -picoline-iodine:  $\gamma$ -picoline iodine solutions were prepared by mixing the components in suitable solvents immediately before use. Solid  $\gamma$ -picoline- $I_2$  was prepared as described by Glusker and Miller.<sup>(94)</sup> A saturated ethanolic solution of iodine was added to excess of  $\gamma$ -picoline. Water was immediately added and the resulting precipitate filtered and washed with water containing a little  $\gamma$ -picoline. After drying in a stream of nitrogen the product was recrystallised from sodium dried anhydrous ether by evaporating slowly at a low temperature. The melting point of the compound was found to be  $83^\circ\text{C}$ (lit.  $83.2-83.4^\circ\text{C}$ ).

$\gamma$ -Picoline-iodinechloride: Preparation of this complex has been discussed by Whittaker<sup>(96)</sup> et al. It was prepared by adding a solution of  $\gamma$ -picoline in carbontetrachloride to a solution of iodinechloride in the same solvent. The yellow crystalline solid was washed with carbontetrachloride and recrystallised from methanol. Washing finally with anhydrous ether and then dried in a stream of nitrogen. The melting point was found to be  $106^\circ\text{C}$ (lit.  $107-108^\circ\text{C}$ ).

$\gamma$ -Picoline-iodine bromide: This compound was prepared by adding a solution of  $\gamma$ -picoline in carbontetrachloride to a solution of iodine bromide in carbontetrachloride. The orange yellow crystalline substance thus obtained was washed with carbontetrachloride and recrystallised from methanol, washing finally with sodium-dried ether, and then dried. The melting point was found to be 79-80<sup>o</sup>c; calculated from  $\gamma$ -piclBr:Iodine, 42.3% found 41.9%.

$\gamma$ -Picoline-iodinecyanide: This compound was prepared immediately before use by mixing equivalent amounts of  $\gamma$ -picoline and cyanogeniodide and diluting with another solvent where required. The preparation of ICl has already been discussed in section 3.1.22.

3.2.3. Spectra: No decomposition was observed while running the spectra in Mulls. All the complexes were found to be stable for at least 30 minutes in polar or non-polar solvents provided there was no excess of  $\gamma$ -picoline present. Nevertheless the spectra usually showed some change after the solution were left to stand for several hours. Consequently, all measurements were made on freshly prepared solutions. However, when  $\gamma$ -piclBr or  $\gamma$ -piclCl were dissolved in  $\gamma$ -picoline or when iodine or cyanogeniodide were dissolved in excess of  $\gamma$ -picoline, noticeable changes occurred within 15 minutes. All the spectra for which  $\gamma$ -picoline was used as a solvent were carefully repeated, using freshly made up solutions every time for each section of spectrum. In this way it was possible to get reproducible spectra.

3.2.4. Results: The general features of the infra-red absorption of  $\gamma$ -picoline-halogen complexes are shown in Figures 6 and 7.

All the bands ascribed to the complexes are summarized in Tables 9-12.

In all cases, only bands clearly distinguished from the solvent background have been included in the tables.

3.2.5. Nature of the Species Present: The most notable solvent effects of the spectra occur in the far-infra-red region, which thus is most usefully considered in discussing the species present.

3.2.5.1.  $\gamma$ -Picoline-iodine: An equimolar solution of iodine and  $\gamma$ -picoline in non polar solvents such as benzene show only one single strong band at  $169\text{cm}^{-1}$  in the  $100\text{-}200\text{cm}^{-1}$  range compared with the band found at  $175\text{cm}^{-1}$  by Loranzelli<sup>(93)</sup> and at  $181\text{cm}^{-1}$  by Lake and Thompson<sup>(52)</sup> in cyclohexane solution. This band at  $169\text{cm}^{-1}$  can be confidently assigned to the I-I stretching frequency of the unchanged  $\gamma$ -picI<sub>2</sub> charge-transfer complex. In contrast freshly made up solutions of iodine in excess of  $\gamma$ -picoline show two absorption bands in the  $100\text{-}200\text{cm}^{-1}$  region; a strong band at  $162\text{cm}^{-1}$  and a medium band at  $137\text{cm}^{-1}$ . Spectra in a second polar solvent, nitrobenzene, also show the additional band at  $137\text{cm}^{-1}$ . The band at  $162\text{cm}^{-1}$  is assigned to the I-I stretching frequency of the ionised complex, and can be compared with the I-I stretching frequency at  $167\text{cm}^{-1}$  of PyI<sub>2</sub> in pyridine solution.<sup>(48)</sup> The new medium intensity band at  $137\text{cm}^{-1}$  is assigned to the antisymmetric stretching vibration of the I<sub>3</sub><sup>-</sup> ion.<sup>(48,91)</sup>

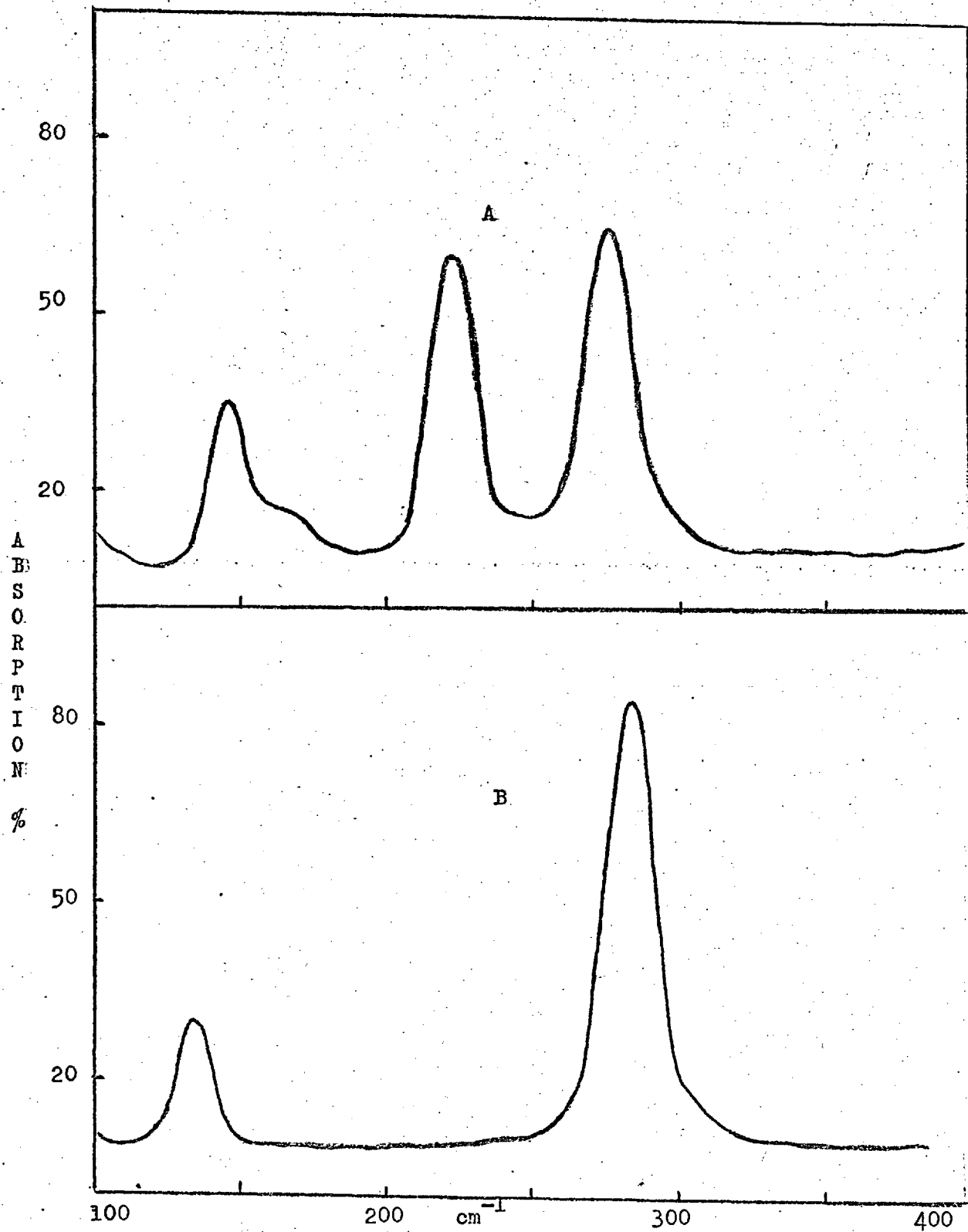


Fig. 6. A.  $\gamma$ -Picoline-ICl in  $\gamma$ -picoline. B.  $\gamma$ -Picoline-ICl in benzene solution.

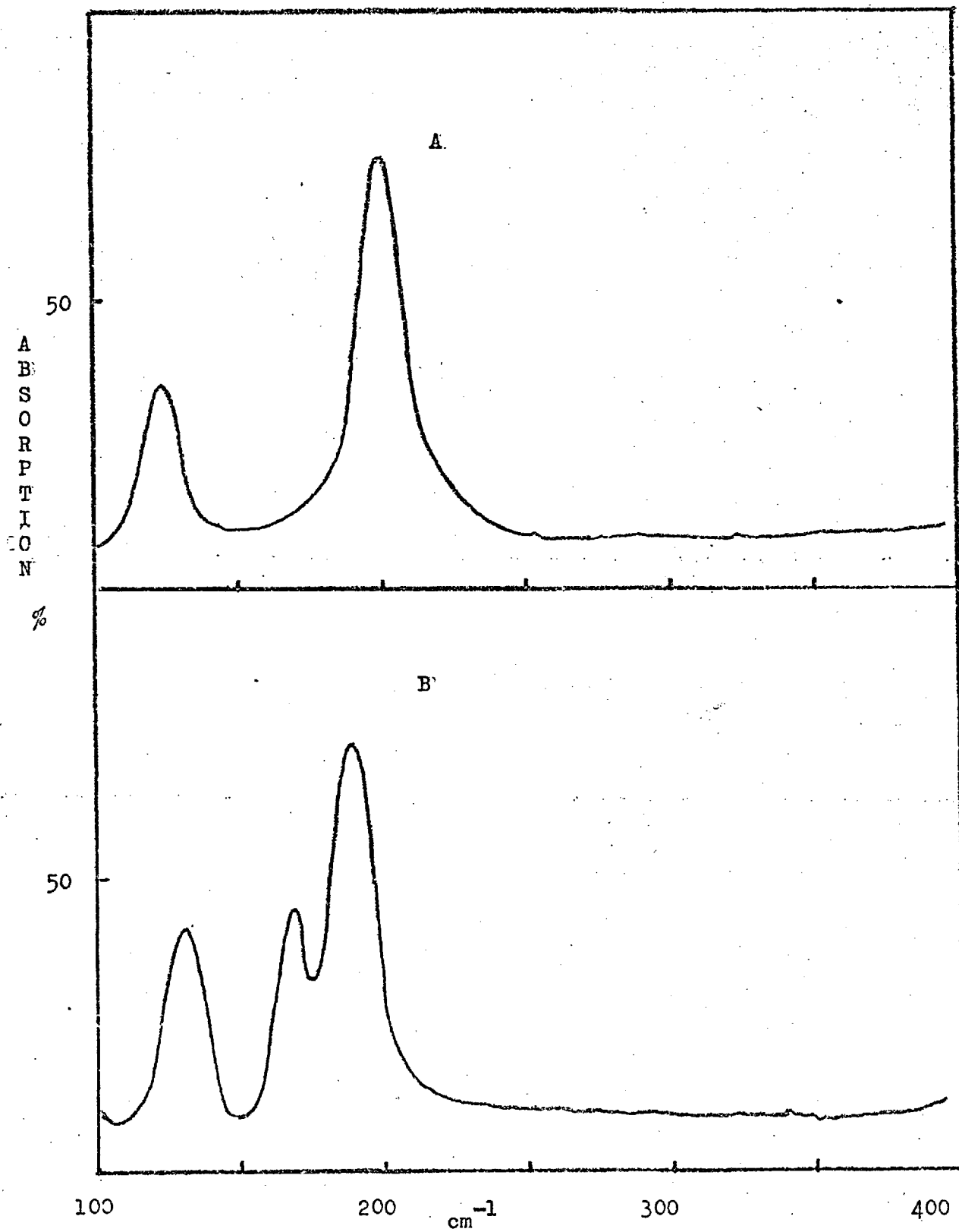


Fig. 6a. The infrared spectra of  $\gamma$ -PicI Br (A) in benzene solution; (B) in  $\gamma$ -picoline solution.

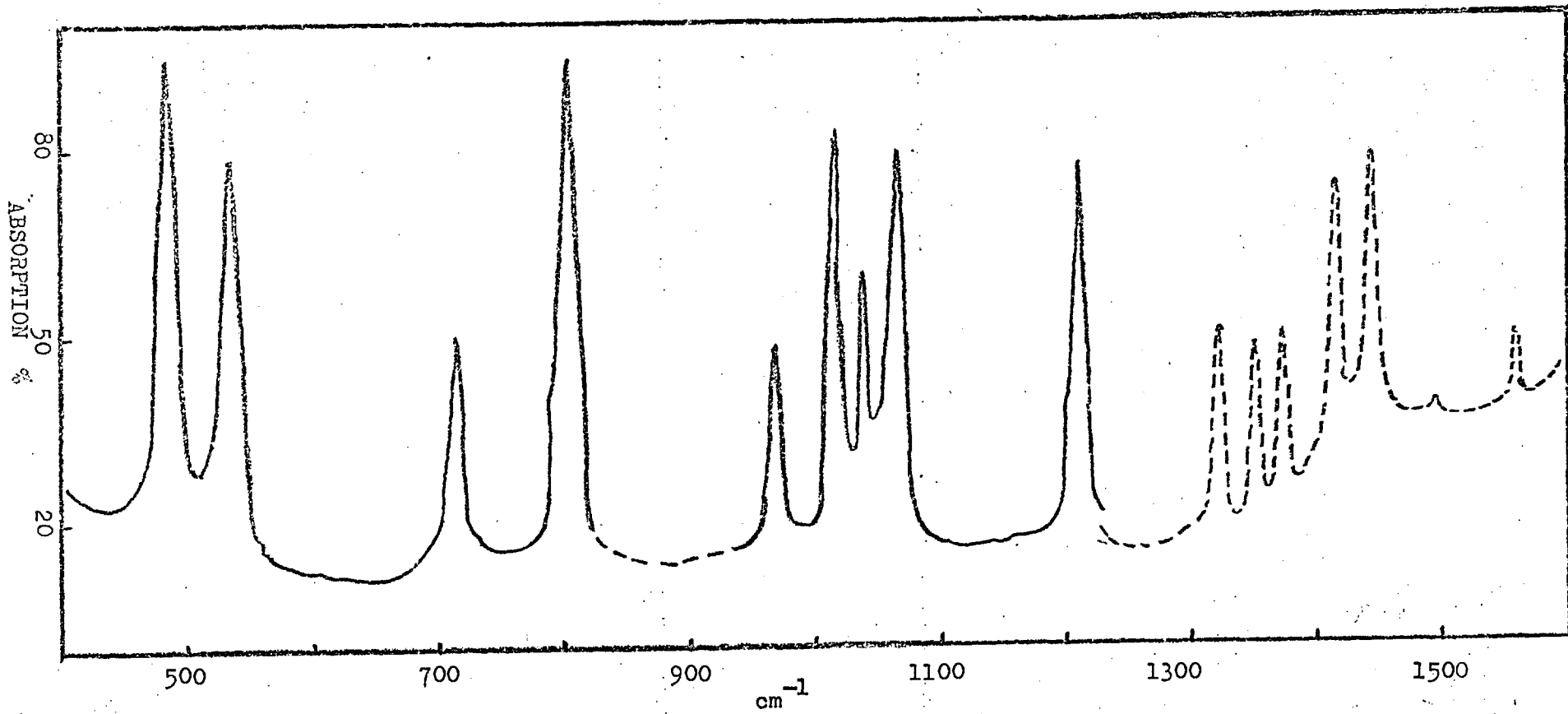


Fig. 7 Composite spectra of  $\gamma$ -PicI Cl. — CS<sub>2</sub> solution; - - - Mull.

Table 9

Infrared spectra of the  $\gamma$ -picoline-iodine system in various media

Equimolar $\gamma$ -picoline and iodine in					Iodine in excess of $\gamma$ -picoline	Interpretation
CS <sub>2</sub>	benzene	CHCl <sub>3</sub>	hexane	CH <sub>2</sub> Cl <sub>2</sub>		
3060m						a <sub>1</sub> and b <sub>1</sub> fundamental
3042vww						a <sub>1</sub> fundamental
3025w						b <sub>1</sub> fundamental
2992w						1499 x 2
1927m				1938w		968 x 2
1835w				1841w		802 + 1039
1667m				1667w		
		1615s	1613w	1616s		a <sub>1</sub> fundamental
				1562w		b <sub>1</sub> fundamental
				1499w		a <sub>1</sub> fundamental
		1382w				a <sub>1</sub> fundamental
				1353w		545 + 802
				1332w		531 + 802
1286w						485 + 802
1249m					1243w	b <sub>1</sub> fundamental
1212s	1212m		1213w	1212s		a <sub>1</sub> fundamental
1202sh						485 + 714
1067s	1067s	1067s	1069w	1067s		b <sub>1</sub> fundamental
1039m				1040w		a <sub>1</sub> fundamental
1026m				1027s	1025w	[ $\gamma$ -pic <sub>2</sub> I] <sup>†</sup>
1012s	1010m	1012s		1013s	1012m	a <sub>1</sub> fundamental
968m		970w		970w		b <sub>2</sub> fundamental
952w						a <sub>2</sub> fundamental
802vs	802m			805vs		a <sub>1</sub> and b <sub>1</sub> fundamental
775sh						

Table 9 (continued)

Equimolar $\gamma$ -picoline and iodine in					Iodine in excess of $\gamma$ -picoline	Interpretation
CS <sub>2</sub>	benzene	CHCl <sub>3</sub>	hexane	CH <sub>2</sub> Cl <sub>2</sub>		
740vw						) b <sub>2</sub> fundamental
714w						
709w						
544w				545ms	544sh	[ $\gamma$ -pic <sub>2</sub> I] <sup>+</sup>
531s		533s		533s	536s	e <sub>1</sub> fundamental
485s	485s	485s	485s	485s		b <sub>2</sub> fundamental
	169s				162s	I-I stretching
					137ms	I <sub>3</sub> <sup>-</sup>



Table 10

Infrared spectra of the  $\gamma$ -picoline-iodine bromide system in  
various media

Saturated solution in				In hexa- chloro- butadiene mull	In Nujol mull	Interpretations
CS <sub>2</sub>	benzene	CH <sub>2</sub> Cl <sub>2</sub>	$\gamma$ -pico- line			
3150w						1560 + 1613
3080w				3082m		1445 + 1620
3063s				3057m		a <sub>1</sub> and b <sub>1</sub> fundamental
3042vww						a <sub>1</sub> fundamental
3028vww						b <sub>1</sub> fundamental
2980w (broad)						1498 x 2
1930w		1937w		1923w	1927w	973 x 2
1838w		1845w				808 + 1039
1667w		1667w		1674w	1673w	540 + 1115
		1620s			1613s	a <sub>1</sub> fundamental
					1602sh	
		1498vw			1560w	b <sub>1</sub> fundamental
				1445sh		a <sub>1</sub> fundamental
				1418s	1420s	b <sub>1</sub> and b <sub>2</sub> fundamental
		1385w		1371w		b <sub>1</sub> fundamental
		1353w		1353w		a <sub>1</sub> fundamental
		1333w		1319w	1319w	540 + 802
1289w						663 x 2
1250w			1250w	1250m	1250m	487 + 808
1213s	1212s	1212s		1202s	1203s	b <sub>1</sub> fundamental
1201w				1194s	1195w	a <sub>1</sub> fundamental
1111vww		1115vww		1111vw	1111vw	487 + 712
						b <sub>1</sub> fundamental

Table 10 (continued)

Saturated solution in				In hexa- chloro- butadiene mull	In Nujol mull	Interpretations
CS <sub>2</sub>	benzene	CH <sub>2</sub> Cl <sub>2</sub>	γ-pico- line			
1093vw		1096w		1094w	1094w	544 x 2
1068s	1067s	1067s		1060s	1061s	b <sub>1</sub> fundamental
1038w		1039w		1038m	1039w	a <sub>1</sub> fundamental
		1026sh				[γ-pic <sub>2</sub> I] <sup>+</sup>
1014s		1019s	1019s	1021s	1022s	a <sub>1</sub> fundamental
969w	970w	973w			975w	b <sub>2</sub> fundamental
					956w	a <sub>1</sub> fundamental
804s	806s	808s			812w	a <sub>1</sub> and b <sub>1</sub> fundamental
793sh						
714m				706m	707m	b <sub>2</sub> fundamental
					663w	b <sub>1</sub> fundamental
535s	537s	540c	540s	544s	540s	a <sub>1</sub> fundamental
485s	485s	486s		487s	487s	b <sub>2</sub> fundamental
	201s		189s		189s	1-Br stretching
			168m			1-Br <sub>2</sub> <sup>-</sup>
	124m		131m		146s	N-I stretching

Table 11

Infrared spectra of the  $\gamma$ -picoline-iodine chloride system in various media

Saturated solution in				In hexa- chloro- butadiene mull	In Nujol mull	Interpretations
CS <sub>2</sub>	C <sub>6</sub> H <sub>6</sub>	CH <sub>2</sub> Cl <sub>2</sub>	$\gamma$ -pico- line			
				3131w		1560 x 2
				3084s		1445 + 1623
3067m				3066m		a <sub>1</sub> and b <sub>1</sub> fundamental
				3045m		a <sub>1</sub> fundamental
3018w				3009m		b <sub>1</sub> fundamental
				2982s		b <sub>1</sub> fundamental
2954s				2960m		b <sub>1</sub> fundamental
				2923w		a <sub>1</sub> fundamental
2855m				2857w		1418 + 1445
1918w		1934w		1937m	1937m	974 x 2
1837vw		1840w		1844w	1841w	808 + 1039
		1764w				711 + 1066
		1667w		1675w	1675w	543 + 1117
		1623s			1623s	) a <sub>1</sub> fundamental )
		1613s			1607m	
		1564w			1560m	b <sub>1</sub> fundamental
		1498w		1497w	1297w	a <sub>1</sub> fundamental
				1445s	1466sh	b <sub>1</sub> and b <sub>2</sub> fundamental
				1418s	1420s	b <sub>1</sub> fundamental
		1383w		1375m		a <sub>1</sub> fundamental
		1355w		1352m		543 + 808
		1333w		1324m	1326m	663 x 2
1250m				1254s	1256s	a <sub>1</sub> fundamental

Table 11 (continued)

Saturated solution in				In hexa- chloro- butadiene mull	In Nujol mull	Interpretations
CS <sub>2</sub>	C <sub>6</sub> H <sub>6</sub>	CH <sub>2</sub> Cl <sub>2</sub>	γ-pico- line			
1212s 1201sh	1213s	1212s		1213m	1213m	a <sub>1</sub> fundamental 487 + 711
		1117vw		1116w	1116w	b <sub>1</sub> fundamental
		1097w		1096w	1096w	543 x 2
1067s	1068s	1066s		1066s	1065s	b <sub>1</sub> fundamental
1039ms		1041w		1038ms	1037ms	a <sub>1</sub> fundamental
1017s		1023s	1022s	1024s	1025s	a <sub>1</sub> fundamental
970m		974w			976m	b <sub>2</sub> fundamental
					960w	a <sub>2</sub> fundamental
804vs	809s	809vs			808vs	a <sub>1</sub> and b <sub>2</sub> fundamental
793w						
714m		711ms		711ms	711ms	b <sub>2</sub> fundamental
535s	540s	543s	543s	547s	549s	a <sub>1</sub> fundamental
485vs	486s	487s		486vs	486vs	b <sub>2</sub> fundamental
	284s		276s		281s	1-Cl stretching
					222s	1 Cl <sub>2</sub> <sup>-</sup>
					167wsh	[γ-pic <sub>2</sub> I] <sup>+</sup> skeletal
	135ms		146ms		166s	N-I stretching

Table 12

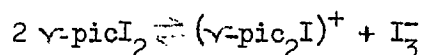
Infrared spectra of the  $\gamma$ -picoline-ICN

Equimolar $\gamma$ -picoline + ICN in			ICN in excess of $\gamma$ -picoline	Interpretation
CS <sub>2</sub>	C <sub>6</sub> H <sub>6</sub>	CH <sub>2</sub> Cl <sub>2</sub>		
3077s				
3059sh				a <sub>1</sub> and b <sub>1</sub> fundamental
3041m				a <sub>1</sub> fundamental
3028m				b <sub>1</sub> fundamental
2995s				1503 x 2
2857w				1420 x 2
			2146w	CN stretching
1931w		1938w		972 x 2
1842w		1845w		802 + 1040
1667m		1667m		526 + 1162
		1639m	1639w	526 + 1111 (?)
		1610s		a <sub>1</sub> fundamental
		1503m		a <sub>1</sub> fundamental
	1420m			b <sub>1</sub> fundamental
1287vw				486 + 802
1239w				526 + 722 b <sub>1</sub> fundamental
1224m	1224m	1228m		a <sub>1</sub> fundamental
1216s	1216s	1216s		a <sub>1</sub> fundamental
1208m	1207w	1200m		486 + 722
1160w		1162s		b <sub>2</sub> fundamental
1070s	1068s	1068s		b <sub>1</sub> fundamental
1040m		1039w		a <sub>1</sub> fundamental
1008s	1009s	1008s	1010s	a <sub>1</sub> fundamental
972w				b <sub>2</sub> fundamental

Table 12 (continued)

Equimolar $\gamma$ -picoline + ICN in			ICN in excess of $\gamma$ -picoline	Interpretation
$\text{CS}_2$	$\text{C}_6\text{H}_6$	$\text{CH}_2\text{Cl}_2$		
806m	806sh			) $a_1$ and $b_2$ fundamental )
800s	802s	803s		
722m				$b_2$ fundamental
526s	528s	529s	530s	$a_1$ fundamental
486s	486s	488s		$b_2$ fundamental
	420s	420s	420s	IC stretching
	336s		338s	ICN bending

The  $I_3^-$  ion observed to be present in excess of  $\gamma$ -picoline or solution of  $\gamma$ -picoline and iodine in nitrobenzene, by comparison with pyridine and iodine, is probably formed by the reaction.



This scheme needs the formation of the ion  $(\gamma\text{-pic}_2\text{I})^+$ . The ion  $(\gamma\text{-pic}_2\text{I})^+$  is found to have only one infra-red band in the low frequency range ( $400\text{--}100\text{cm}^{-1}$ ), the antisymmetric NIN stretching vibration at  $168\text{cm}^{-1}$  (ref.sec.4). Unfortunately this frequency coincides with the I-I stretching vibration of the un-ionised complex and so cannot be separately distinguished. However, supporting evidence is provided by the higher frequency. Here two distinct additional bands can be distinguished in polar solvents such as methylenechloride,  $\gamma$ -picoline etc., one is at  $\sim 545\text{cm}^{-1}$  and the other at  $\sim 1027\text{cm}^{-1}$  and they are found to correspond to the  $\nu_1$  and  $\nu_{6a}$  modes of  $(\gamma\text{-pic}_2\text{I})^+$  ion (ref.sec.4). But these bands are not observed for an equimolar solution of iodine and  $\gamma$ -picoline in benzene. The other higher frequency bands of the  $(\gamma\text{-pic}_2\text{I})^+$  ion lie close to the corresponding bands of  $\gamma\text{-picI}_2$  complex. If it is assumed that the complex is un-ionised in non-polar solvents, and ionised thus

$$\gamma\text{-picI}_2 \rightleftharpoons (\gamma\text{-pic}_2\text{I})^+ + I_3^-$$

in polar solvents, all the bands mentioned in Table 9 are accounted for.

The spectrum obtained from a benzene solution of the solid  $\gamma\text{-picI}_2$  adduct which has been named by Glusker and Miller, (94)

solid II is found to be identical to that of an equilibrium mixture of  $\gamma$ -picoline and iodine in benzene. This agrees with the X-ray data, confirming that this is the solid donor-acceptor complex.

3.2.52.  $\gamma$ -Picoline-iodine bromide: As in iodide the spectra in polar and non-polar solvents differ. Low frequency spectra in benzene solution (Fig. 6a) show two bands (Table 10). By comparison with the PyIBr complex, <sup>(48)</sup> the higher frequency band at  $201\text{cm}^{-1}$  is assigned to the I-Br stretching mode of the complex and the lower frequency band at  $124\text{cm}^{-1}$  assigned to the intermolecular N-I stretching vibration.

In  $\gamma$ -picoline solution, an additional band at  $168\text{cm}^{-1}$  is present. Both the  $\text{IBr}_2^-$  antisymmetric stretching vibration, which appears at  $174\text{cm}^{-1}$  for PyIBr complex in pyridine solution and the NIN antisymmetric stretching vibration of the ion  $(\gamma\text{-pic}_2\text{I})^+$  at  $168\text{cm}^{-1}$ , are possible assignment for this band. The antisymmetric  $\text{IBr}_2^-$  stretch is the more intense band and comparison with the  $\gamma$ -picICl system indicates that it contributes most to the observed absorption. However, a contribution from the antisymmetric  $\gamma$ -pic-I- $\gamma$ -pic stretching vibration cannot be ruled out. In a nujol mull of the solid complex only two bands are observed in the  $100\text{-}400\text{cm}^{-1}$  frequency range; one at  $189\text{cm}^{-1}$  and the other at  $146\text{cm}^{-1}$ , these may be compared with the  $200$  and  $160\text{cm}^{-1}$  bands of pyIBr complex in nujol mull, and indicate that the solid complex is un-ionised.



In the higher frequency region an additional band at  $1026\text{cm}^{-1}$  is observed in methylene-chloride solution which is a polar solvent. This band may be assigned to the  $\nu_1$  mode of the  $(\sqrt{\text{pic}}_2\text{I})^+$  ion (ref.sec.4). Assuming the complex is un-ionised in non-polar media and mulls, and ionised in polar media, all the bands mentioned in Table 10 are accounted for.

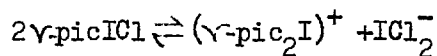
3.2.53.  $\sqrt{\text{Picoline-iodinechloride}}$ : Low frequency spectra of this complex in non-polar solvents such as benzene show only two bands. The higher frequency band at  $284\text{cm}^{-1}$  can be assigned to the I-Cl stretching vibration of the complex, and can be compared with the I-Cl stretching vibration at  $290\text{cm}^{-1}$  for  $\text{pyICl}$  complex in benzene solution. The lower frequency band at  $135\text{cm}^{-1}$  is assigned to the N-I stretching vibration of the un-ionised complex. Furthermore, only two bands are observed in mull in the frequency range  $400-100\text{cm}^{-1}$ ; one at  $281\text{cm}^{-1}$  and the other at  $166\text{cm}^{-1}$ . The  $281\text{cm}^{-1}$  band is assigned to the I-Cl stretching vibration and the  $166\text{cm}^{-1}$  band to the N-I stretching vibration of the complex. All the observed higher frequency bands (Table 11) in benzene solution and in mulls may be assigned to the un-ionised complex.

However, low frequency spectra in  $\sqrt{\text{picoline}}$  solution show two additional bands (Table 11 column 6); one strong band at  $222\text{cm}^{-1}$  and a weak band at  $167\text{cm}^{-1}$ . Spectra in nitrobenzene are similar, although the band at  $167\text{cm}^{-1}$  is somewhat obscured by the strong nitrobenzene

band at  $178\text{cm}^{-1}$ . The weak band at  $167\text{cm}^{-1}$  is also observed in methylenechloride and a solution formed with equal volumes of  $\text{CH}_3\text{CN}$  and benzene. The strong band at  $222\text{cm}^{-1}$  can be assigned to the antisymmetric stretching vibration of the  $\text{ICl}_2^-$  ion. (48,91) The formation of this ion suggests the ionisation

$2\gamma\text{-picICl} \rightleftharpoons (\gamma\text{-pic}_2\text{I})^+ + \text{ICl}_2^-$  is occurring in polar media. The weak band at  $167\text{cm}^{-1}$  may be assigned to the NIN antisymmetric stretching frequency of the ion  $(\gamma\text{-pic}_2\text{I})^+$ . This is confirmed by the presence of a strong infra-red band at  $168\text{cm}^{-1}$  for salts of the ion  $(\gamma\text{-pic}_2\text{I})^+$  (ref.sec.4).

All the higher frequency bands of  $\gamma\text{-picICl}$  in polar solvents lie very close to the corresponding frequencies of the  $(\gamma\text{-pic}_2\text{I})^+$  ion. For example, the  $\nu_1$  and  $\nu_{6a}$  bands of  $\gamma\text{-picICl}$ , appearing at 1023 and  $593\text{cm}^{-1}$  in methylenechloride solution (these two representing the modes of  $\gamma\text{-picoline}$  most sensitive to the nature of complexing at the nitrogen atom) are still too close to the 1025 and  $545\text{cm}^{-1}$  band of  $(\gamma\text{-pic}_2\text{I})^+$  ion (ref.sec.4.) in the same solvent for these latter bands to be distinguished. However, all the observed bands (Table 11) in freshly made up polar solvents are accounted for by the scheme.



3.2.54.  $\gamma$ -Picoline-iodinecyanide: In the present work the frequency range down to  $80\text{cm}^{-1}$  was examined, but no additional low frequency bands were found. The lowest band found at  $\sim 338\text{cm}^{-1}$  can be assigned to I-CN bending. The I-C stretch is observed at  $\sim 420\text{cm}^{-1}$  in benzene, methylenechloride and excess of  $\gamma$ -picoline solutions. As the CN stretching vibration of I-CN appears as a weakband and is expected to be even weaker<sup>(46)</sup> in  $\gamma$ -piclCN complex, there is some doubt regarding the position of this band. However in excess of  $\gamma$ -picoline solution a very weak band at  $2146\text{cm}^{-1}$  is observed and can probably be assigned to the CN stretching mode. The intermolecular N-I stretching mode is expected to be very low, perhaps even below the range of our spectrometer. No evidence of ionisation of the  $\gamma$ -piclC<sub>N</sub> was found in any of the media examined.

3.2.6. Assignments: In the crystalline state the symmetry point group of  $\gamma$ -picI<sub>2</sub> is C<sub>2v</sub><sup>(101)</sup> and it is expected that other  $\gamma$ -picoline-halogen complexes will have the same symmetry point group. It is also expected to retain the same structure in solution. The infra-red data supports the C<sub>2v</sub> symmetry. The presence of a bent N-I-X chain in the complex would reduce the symmetry to C<sub>2</sub>, and allow the vibrations derived from the a<sub>2</sub> class, which is infra-red inactive for C<sub>2v</sub> point group, to become infra-red active. The absence in most of the observed spectra of any bands near to the a<sub>2</sub> class frequencies of  $\gamma$ -picoline ( $937, 866$  and  $384\text{cm}^{-1}$ ) supports a C<sub>2v</sub> structure for the complex.

For  $C_{2v}$  symmetry the vibrations fall into four classes  $a_1, b_1$  (in-plane) and  $a_2, b_2$  (out-of-plane). For  $\gamma$ -picIX ( $X=Cl, Br$  or  $I$ ) the 42 fundamental vibrations fall into the classes  $14a_1+4a_2+14b_1+10b_2$ . Of these vibrations  $12a_1+4a_2+12b_1+8b_2$  will be very similar to vibrations of free  $\gamma$ -picoline. The remaining six vibrations  $2a_1+2b_1+2b_2$  comprise five intermolecular modes and the  $a_1$  IX stretching vibrations, all lying below  $400\text{cm}^{-1}$ . Adopting a  $C_{2v}$  structure the vibrations of  $\gamma$ -picoline-ICN classify as  $15a_1+4a_2+15b_1+11b_2$ , the nine vibrations without being counterparts in free  $\gamma$ -picoline being five intermolecular vibrations ( $a_1+2b_1+2b_2$ ) and four vibrations derived from internal modes of ICN and lying in the classes ( $2a_1+b_1+b_2$ ).

Comparison of the spectra with those of  $\gamma$ -picoline<sup>(88,99)</sup> and  $\gamma$ -picoline metal co-ordinated complexes<sup>(102)</sup> enables one to make an almost complete assignment of the infra-red active fundamentals of the  $\gamma$ -picoline-halogen complexes. Table 13 which shows the assignments for the complexes, also includes those for the  $\gamma$ -picolinium ion given by Spinner<sup>(100)</sup> with some modifications. By comparing with  $\gamma$ -picoline and  $\gamma$ -picoline-halogen complexes, some bands of  $\gamma$ -picolinium ion given by Spinner are reassigned. The  $1259\text{cm}^{-1}$  band of  $\gamma\text{-picH}^+\text{Cl}^-$  was assigned by Spinner to the  $\text{N}^+\text{H}$  in-plane bending, but presence of a band at  $\sim 1250\text{cm}^{-1}$  for all the  $\gamma$ -picoline-halogen complexes suggest it should be assigned to the  $\nu_{9a}$  mode. The frequencies of  $\nu_{12}, \nu_{18a}, \nu_{19a}$  and  $\nu_{19b}$  are also reassigned (Table 13).

Table 13

Assignment of infrared active fundamentals of  $\gamma$ -picoline complexes, and comparison with  $\gamma$ -picoline and  $\gamma$ -picolinium ion ( $\text{cm}^{-1}$ )

Designation [11]	$\gamma$ -Pico- line	$\gamma$ -Pic-I -CN	$\gamma$ -Pic-I <sub>2</sub>	$\gamma$ -Pic-I -Br	$\gamma$ -Pic-I -Cl	( $\gamma$ -PicH) <sup>+</sup>	
$\nu_1$							
$\nu(\text{CH})$	2	3050	3059	3060	3063	3067	-
$\nu(\text{CH})$	20a	3040	3041	3042	3042	3045 <sup>+</sup>	-
$\nu(\text{CC})$	8a	1603	1610 <sup>x</sup>	1616 <sup>x</sup>	1620 <sup>x</sup>	1623 <sup>x</sup>	1633
$\nu(\text{CC}, \text{CC})$	19a	1495	1503 <sup>x</sup>	1499 <sup>x</sup>	1498 <sup>x</sup>	1498 <sup>x</sup>	1504
$\beta(\text{CH})$	9a	1220	1224	1249	1250	1250	1259
$\beta(\text{CH})$	18a	1042	1040	1039	1039	1039	1033
ring	1	994	1008	1012	1014	1017	1007
X-sen.	13	1212	1216	1212	1213	1212	1220
X-sens	12	801	-	-	-	-	-
X-sens	6a	514	526	531	535	535	521
methyl		2924	-	-	-	2923 <sup>+</sup>	-
methyl		1378	-	1382 <sup>6</sup>	1385 <sup>x</sup>	1383 <sup>x</sup>	1377
$\nu(\text{I-X})$	-	-	420 <sup>++</sup>	169 <sup>++</sup>	201 <sup>++</sup>	284 <sup>++</sup>	-
$\nu(\text{N-I})$	-	-	-	-	124 <sup>++</sup>	135 <sup>+</sup>	-
$\nu(\text{C-N})$	-	-	2146	-	-	-	-

Table 13 (continued)

Designation [11]	$\gamma$ -Pico- line	$\gamma$ -Pic-I -CN	$\gamma$ -Pic-I <sub>2</sub>	$\gamma$ -Pic-I -Br	$\gamma$ -Pic-I -Cl	( $\gamma$ -PicH) <sup>+</sup>	
b <sub>1</sub>							
$\nu$ (CH)	20b	3050	3059	3060	3063	3067	-
$\nu$ (CH)	7b	3029	3028	3025	3028	3018	-
$\nu$ (CC)	8b	1561	-	-	1560 <sup>+</sup>	1560 <sup>+</sup>	-
$\nu$ (CC, CN)	19b	1417	-	-	1420 <sup>+</sup>	1420 <sup>+</sup>	-
$\nu$ (CC, CN)	14	1365	-	-	-	1355 <sup>x</sup>	1366
$\beta$ (CH)	3	1283	-	1286	-	-	1311
$\beta$ (CH)	18b	1114	-	-	1115 <sup>x</sup>	1117 <sup>x</sup>	-
$\alpha$ (CCC)	6b	669	-	-	-	-	651
X-sens	15	341	-	-	-	-	351
methyl		2970	-	-	2980	2982 <sup>+</sup>	-
methyl		1449	-	-	1445 <sup>+</sup>	1445 <sup>+</sup>	-
methyl		1068	1070	1067	1068	1067	1069
$\alpha$ (ICN)	-	-	336 <sup>++</sup>	-	-	-	-
b <sub>2</sub>							
$\nu$ (CH)	5	969	972	968	969	970	-
$\nu$ (CH)	10b	799	800	802	804	804	793
$\nu$ (CC)	4	728	722	714	714	714	-
$\nu$ (CC)	11	485	486	485	485	485	477
X-sens	16b	211	-	-	-	-	222
methyl		2960	-	-	-	-	-
methyl		1445	-	-	1445	1445	-
methyl		1148	-	-	-	-	-
$\alpha$ (ICN)	-	-	336 <sup>++</sup>	-	-	-	-

All frequencies refer to CS<sub>2</sub> solution except:

<sup>x</sup> In CH<sub>2</sub>Cl<sub>2</sub>.

<sup>++</sup> In benzene.

<sup>+</sup> In mull.

$\nu$  In CHCl<sub>3</sub>.

### 3.3. Pyridine-bromine and Pyridine bromine chloride complexes.

#### 3.3.1. INTRODUCTION:

The Raman spectra of solutions of bromine and bromine-chloride in various media<sup>(47)</sup> and the infra-red spectra of solutions of bromine in various donors<sup>(43)</sup> have been reported. The infra-red spectra of equimolar pyridine-bromine, and pyridine bromine-chloride solutions in chloroform have been examined over a small frequency range around  $1000\text{cm}^{-1}$  by Zingaro and Witmer<sup>(37)</sup>. The far-infra-red spectra of solutions of pyridine-bromine,  $\nu$ -picoline-bromine and several other similar complexes have been examined by Lake,<sup>(103)</sup> Recently He-Ne Laser Raman spectra of solutions of bromine in various donors have been reported.<sup>(49)</sup> Apart from these few investigations no other infra-red or Raman studies of pyridine- $\text{Br}_2$  and pyridine- $\text{BrCl}$  complexes have been reported. The purpose of the present study is to account for the molecular origins of all the observed bands, to compare the extent of charge-transfer in pyridine-halogen complexes and to examine solvent effects on some sensitive bands.

In this section results are reported for the pyridine-bromine and pyridine-bromine-chloride complexes. The nature of the species present is discussed and the frequencies assigned. Consideration of frequency shift of the pyridine ring vibrations, intensity changes, solvent effect, back charge-transfer, and force constants is deferred until a later section.

3.3.2. EXPERIMENTAL

3.3.21. Purity of Materials: 'Analar' bromine (BDH) was used without further purification. Chlorine gas was dried by bubbling through concentrated sulphuric acid. The purification of other chemicals has already been discussed in section 3.1.21.

3.3.22. Preparation of Complexes:

Pyridine-bromine: This complex has been isolated by Williams.<sup>(84)</sup> To a solution of bromine in carbontetrachloride an equivalent amount of pyridine in the same solvent was added dropwise with constant vigorous shaking. After about 10 minutes the dark red solid was obtained. This was filtered, washed thoroughly with carbontetrachloride and anhydrous ether (sodium dried), and finally dried in a stream of nitrogen. The melting point was found to be  $61^{\circ}\text{C}$  (lit  $62-63^{\circ}\text{C}$ ); calculated from  $\text{pyBr}_2$ , bromine 66.9%; found 66%. This complex was also prepared by mixing the two components in suitable solvents immediately before running the spectrum.

Pyridine-brominechloride: The preparation of this complex has also been described by Williams,<sup>(84)</sup> who obtained a white crystalline solid melting at  $107-8^{\circ}\text{C}$  and stable in dry air, though decomposing on recrystallisation. Chlorine from a cylinder was passed through concentrated sulphuric acid and then into ice-cooled carbontetrachloride until a saturated solution was obtained. A slightly smaller amount of bromine was then added. To the mixture of bromine and chlorine a



solution of pyridine in carbontetrachloride was added slowly with shaking. The white crystalline compound obtained thus was washed with anhydrous ether and dried in a stream of nitrogen, m.pt.  $105^{\circ}$  (lit.  $107-8^{\circ}$ ). An analysis was made for nitrogen and total halogen content.

	N	Br	Cl	Total halogen
{ Calculated (for PyBrCl(%))	7.2	41.1	18.3	59.4
Found	6.82			58.45
Found by Willams		40.8	17.8	58.6

The analysis is in reasonable agreement with Willam's results.

**3.3.3. Spectra:** Solid samples dispersed in mulls were examined using AgCl, KBr and polythene windows. When KBr cell windows were used changes in both colour and spectra were observed within 20 minutes. However, no changes of colour or spectra were observed when AgCl or polythene were used as cell windows. The solutions were prepared as near to the time of measurements as possible, and mixing of the two solutions (e.g. solution of pyridine in benzene) to achieve the desired relative concentrations was done just preceding the measurement. In no case was any change in the spectrum noticed during the first 30 minutes. For studying the infra-red spectra in solutions AgCl cell windows were preferred to KBr windows. This is because changes in both colour and spectra were observed within 15 minutes when KBr cell windows were used. No such changes were observed at least during

the first 30 minutes when AgCl cell windows were used. For the far-infra-red measurements all systems were enclosed in sealed polythene bags, and all spectrum were recorded within 30 minutes of preparation.

No changes in spectra or colour were observed in the first 30 minutes while running the Raman spectra in solutions. However, all the runs used were completed within 15 minutes. Visual examination showed rapid discolouration of the solid pyridine-bromine complex exposed to the laser beam. In addition the band at  $166\text{cm}^{-1}$  which is very strong to begin with disappears completely after 30 minutes exposure. To minimise the decomposition a fresh sample was used for each band in the spectrum thus reducing the time factor to half a minute. Solid pyBrCl gave no evidence of decomposition.

**3.3.4. Results:** The results are presented in Tables 14 - 17.

In all cases only those bands which can be clearly distinguished from the solvent background are reported. The recorded low frequency spectra are shown in Figures 8 and 9 and the higher frequency spectra are shown in Figures 10 and 11.

### **3.3.5. Interpretation of Spectra:**

**3.3.5.1. Pyridine-bromine system:** We will first discuss the low frequency range, as this is the most sensitive to the nature of the species present. Fresh solutions of pyridine and bromine or solution of solid  $\text{PyBr}_2$  in benzene show three infra-red bands in the range  $400-100\text{cm}^{-1}$  (Table 14).

Table 14

Infrared Spectra of the pyridine-bromide complex in different media.

Saturated Solution of PyBr <sub>2</sub> (solid)			Equimolar solution of Py and Br <sub>2</sub>		Bromine in ex- cess of pyridine	Solid PyBr <sub>2</sub> in	
in C <sub>6</sub> H <sub>6</sub>	in CH <sub>2</sub> Cl <sub>2</sub>	in pyri- dine	in C <sub>6</sub> H <sub>6</sub>	in CH <sub>2</sub> Cl <sub>2</sub>		Nujol mull	hexachloro- butadiene mull
cm <sup>-1</sup>	cm <sup>-1</sup>	cm <sup>-1</sup>	cm <sup>-1</sup>	cm <sup>-1</sup>	cm <sup>-1</sup>	cm <sup>-1</sup>	cm <sup>-1</sup>
							3162sh
							3146s
							3142s
							3067s
							3053sh
							2955w
							2931w
							2842w
	1912w			1912w		1912w	
	1841w			1841w		1841w	1845w
	1709m			1711m		1715w	
1599sh	1602sh		1599sh	1602sh			
1591s	1597s		1590s	1597s		1595s	1597s
						1521w	1521m
	1479ms			1480ms			1475s
		1455sh			1455sh		1452s
1447s	1450s	1451s	1447s	1450s	1451s		1402m
1360w			1359w				
1349ms	1349ms		1348ms	1351ms			1351w
		1250ms			1250ms	1254s	1254s
1206s	1206s	1205s	1205s	1208s	1205s	1210m	1210m
						1202s	1202s
1153s	1155s	1154m	1152s	1156s	1154m	1152s	1152s

Table 14 (continued)

Saturated Solution of $\text{PyBr}_2$ (solid)			Equimolar solution of Py and $\text{Br}_2$		Bromine in ex- cess of pyridine	Solid $\text{PyBr}_2$ in	
in $\text{C}_6\text{H}_6$	in $\text{CH}_2\text{Cl}_2$	in pyri- dine	in $\text{C}_6\text{H}_6$	in $\text{CH}_2\text{Cl}_2$		Nujol mull	hexachloro- butadiene mull
							1102w
1062s	1066s		1063s	1067s		1060s	1061s
	1041s			1041s			
	1030s			1030s		1035s	1036s
1009s	1012s	1011s	1009s	1012s	1011s	1007s	1008s
						1004sh	1004sh
941m			941m			984m	
	942m			942m		945m	
784sh			784sh			830w	
						786m	
749s			748s			756s	757s
						749sh	
						699w	
						684s	684s
						673sh	672s
638s	638s	639s	638s	638s	639s	637s	637s
627s	628s	629s	626s	628s	629s		
529vs			529vw			572w	572vw
445m	446ms	446m	445m	446ms	446m	445s	446s
418s	420s	421s	418s	420s	421s		
229s		215s	229s		215s		
187w		185s	187w		185s	180s	
						169sh	
128m		140m	128m		140m		

Table 15

Infrared Spectra of the pyridine-bromine chloride in various media

Saturated solution in			In Nujol mull cm <sup>-1</sup>	In Hexachloro- butadiene mull cm <sup>-1</sup>
C <sub>6</sub> H <sub>6</sub> cm <sup>-1</sup>	CH <sub>2</sub> Cl <sub>2</sub> cm <sup>-1</sup>	pyridine cm <sup>-1</sup>		
				3091s
				3062w
				3059m
				3038m
				3025ms
	1915w		1912w	
	1844w			
1595s	1597s		1595s	1597s
			1570m	
	1517w		1517w	1521w
	1488w			1475w
1449s	1451s	1449s		1449s
				1389s
1348w	1349m		1342s	1342s
				1328m
		1250m	1250s	1251s
1206s	1206s	1205s	1206m	1206m
	1154s		1157m	
			1089w	1089w

Table 15 (continued)

Saturated solution in			In Nujol mull cm <sup>-1</sup>	In Hexachloro- butadiene mull cm <sup>-1</sup>
C <sub>6</sub> H <sub>6</sub> cm <sup>-1</sup>	CH <sub>2</sub> Cl <sub>2</sub> cm <sup>-1</sup>	pyridine cm <sup>-1</sup>		
1065s	1064s		1060s	1060s
	1041ms	1040s		
	1033s		1034ms	1034ms
1011s	1012s	1012s	1015s	1015s
			1006sh	1006sh
	991w			
			972w	
	942w		942ms	
			861w	
			784w	
			769sh	
750s			750s	750s
			700m	700m
			684s	684s
			675sh	677sh
	635sh			
630s	632s	636s	641s	641s
	445ms	446m		
422m	425s	428s	430s	430s
307s		274s	295s	
		226s		
144ms		160ms	196s	
			104ms	
			85w	
			71vw	

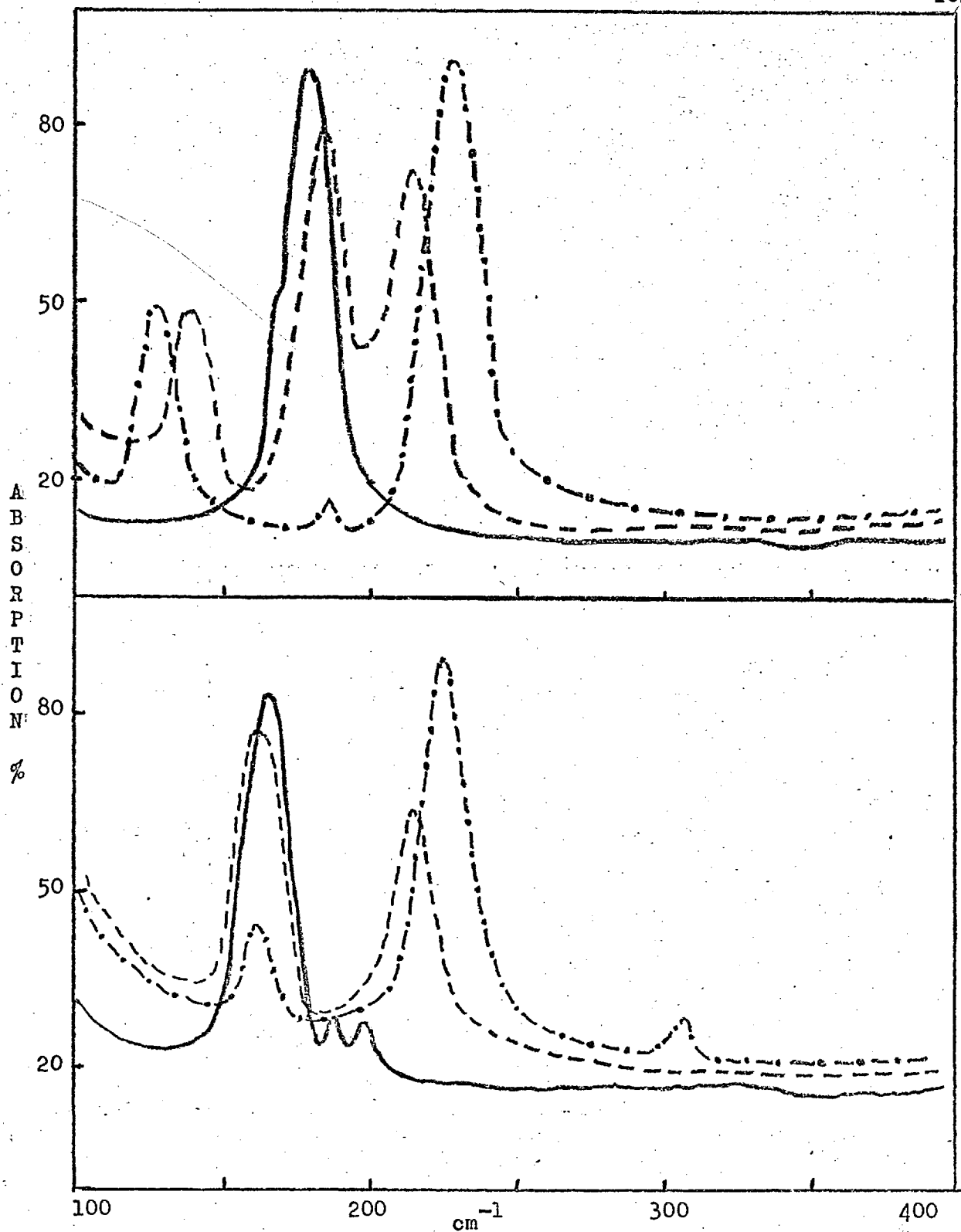


Fig. 8. Top: The infrared spectra of pyridine bromine  
 Bottom: The Raman spectra of pyridine bromine  
 — solid; - - - in pyridine solution; - · - · in  
 benzene solution.

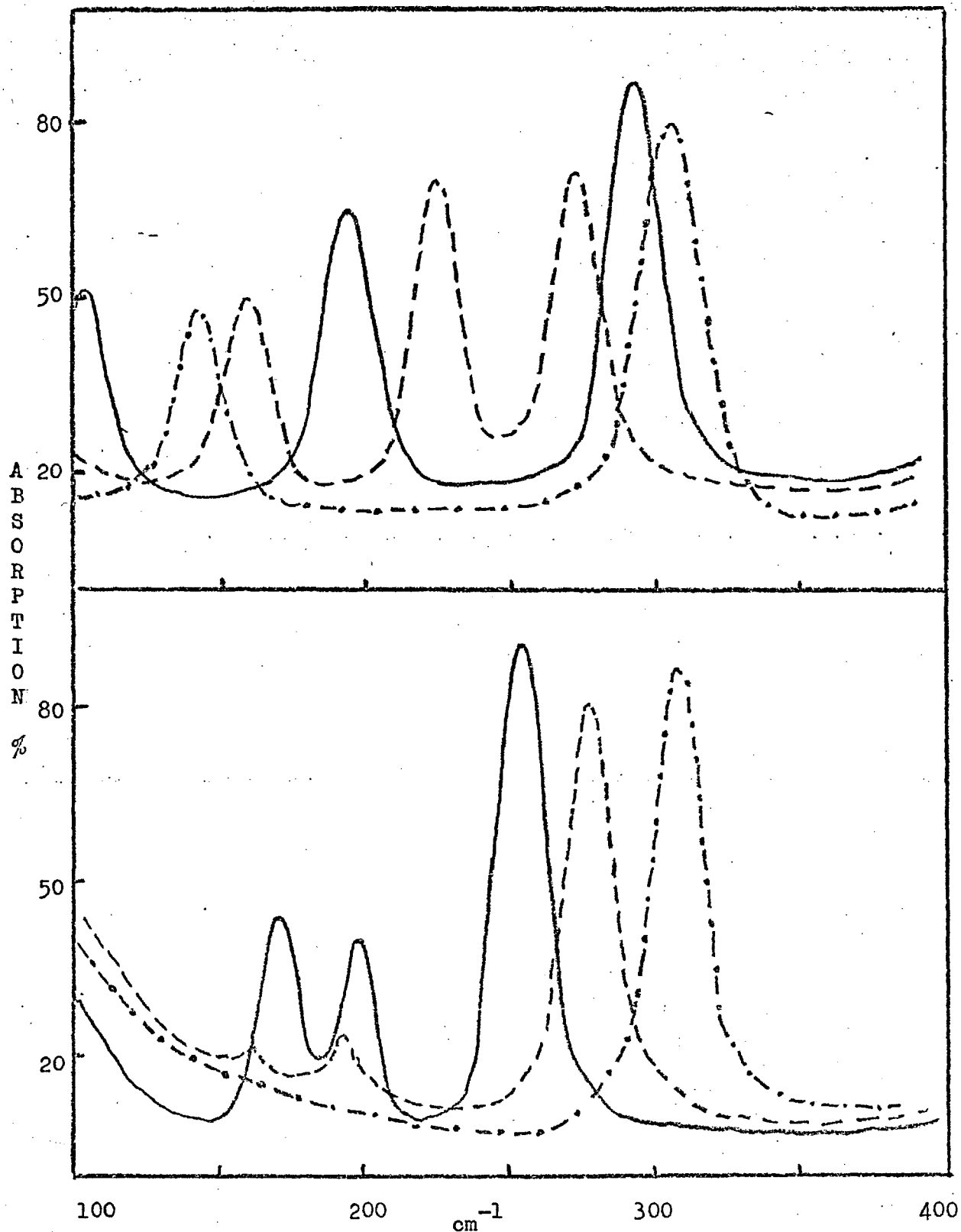


Fig. 9 Top: The infrared spectra of pyridine bromine chloride  
 Bottom: The Raman spectra of pyridine bromine chloride  
 — solid; - - - in pyridine solution; - · - · - in benzene solution.



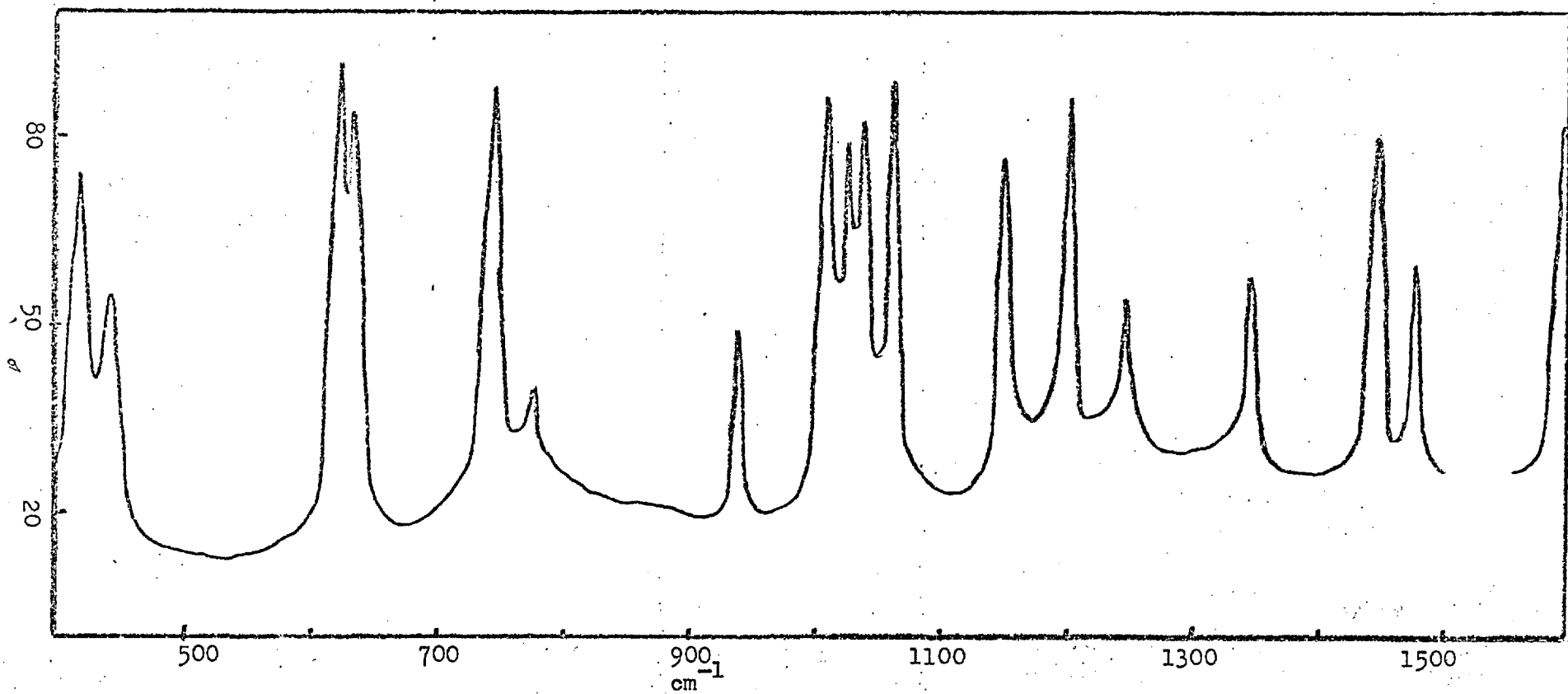


Fig. 10 Composite infrared spectra of  $\text{PyBr}_2$ .

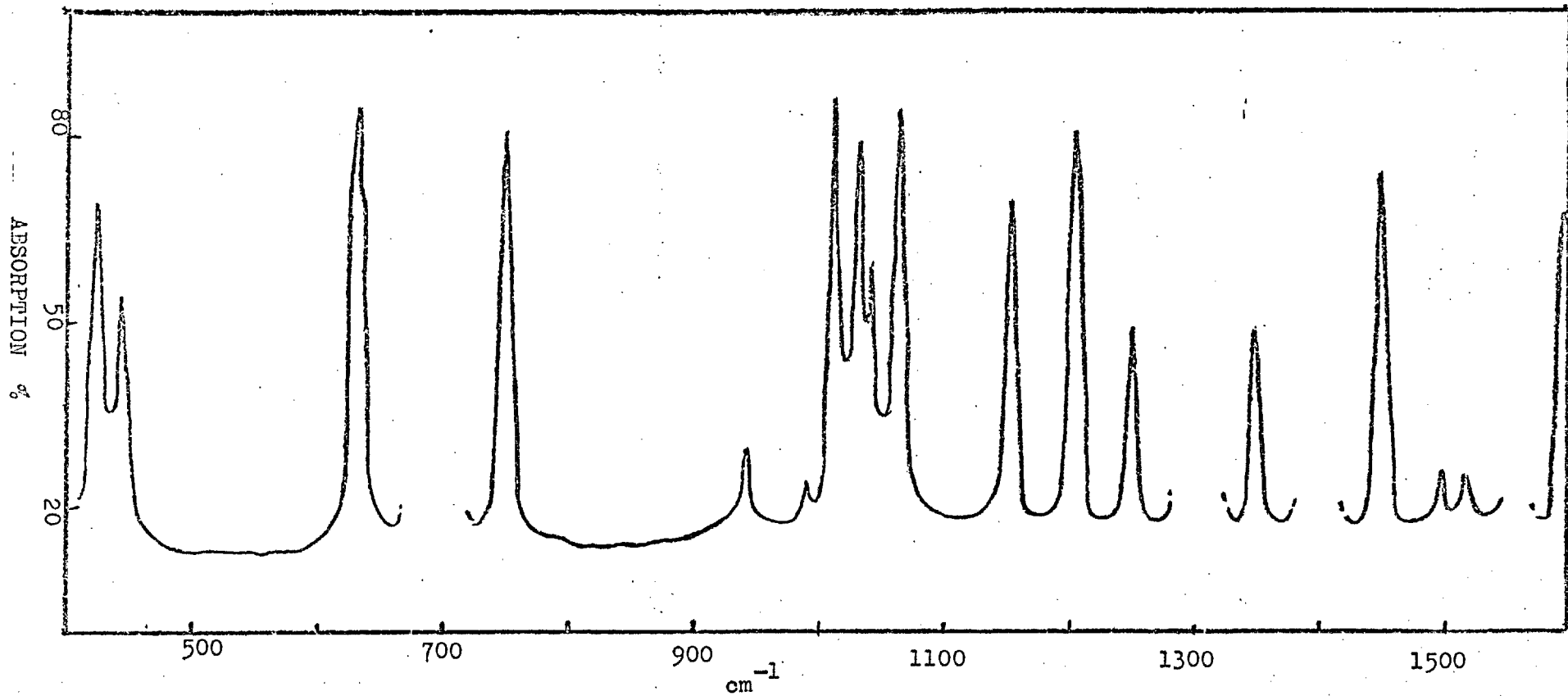
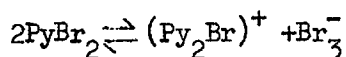


Fig. 11 Composite infrared spectra of PyBrCl.

The weak infra-red band at  $187\text{cm}^{-1}$  can be confidently assigned by comparison with the work of Person et al<sup>(104)</sup> to the antisymmetric vibration of the  $\text{Br}_3^-$  ion. This is further confirmed by examining the spectra of  $\text{Br}_4\text{NBr}_3$  in benzene, which show a single weak band at  $189\text{cm}^{-1}$ . The other two bands, one at  $229\text{cm}^{-1}$  and the other at  $128\text{cm}^{-1}$  can be assigned to Br-Br stretching and N-Br stretching respectively of the un-ionised  $\text{PyBr}_2$  complex.<sup>(103)</sup> The low frequency Raman spectra of  $\text{PyBr}_2$  in benzene show three bands (Table 18). The weak band at  $308\text{cm}^{-1}$  is the Br-Br stretching of the complex benzene- $\text{Br}_2$ .<sup>(47,49)</sup> This is confirmed by the fact that the intensity of this band increases as the concentration of bromine increases, and decreases as the concentration of pyridine increases and finally disappears when excess of pyridine is added. The ~~modified~~ Raman band at  $162\text{cm}^{-1}$  by comparison with the Raman band at  $162\text{cm}^{-1}$  of  $\text{Me}_4\text{N}^+\text{Br}_3^-$  can be assigned to the symmetric  $\text{Br}_3^-$  stretching mode. The strongest Raman polarised band at  $226\text{cm}^{-1}$  can be assigned to the Br-Br stretching vibration of the un-ionised complex  $\text{PyBr}_2$ . The  $\text{Br}_3^-$  ion in solution is possibly formed by the reaction scheme



However, the intensity of Br-Br and N-Br stretching vibration suggest that in benzene solution the predominant species is  $\text{PyBr}_2$ . A salt of the  $(\text{Py}_2\text{Br})^+$  ion has been independently examined (sec.4). This shows that ion  $(\text{Py}_2\text{Br})^+$  has two low frequency stretching vibrations.

Table 16

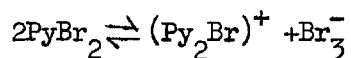
Raman Spectra of the pyridine-bromine complex in various media

Solvent	Observed bands $\text{cm}^{-1}$		
Benzene	162m	226s	308w
Benzene and excess of bromine		235m	308s
* Benzene and excess of pyridine	163s	215s	
1 : 4 Dioxane	162m	221s	300w
Methylene chloride	163m(pol) 218s(p)		
* Pyridine	163s(p) 215s(p)		
Acetone	163m	218s	300w
* Nitrobenzene	164s	214s	
* Acetonitrile	163s	211s	252w
* Nitromethane	165s	210s	258w
Solid $\text{PyBr}_2$	166s	188w	198w

\*  $163 \text{ cm}^{-1}$  band is stronger than  $220 \text{ cm}^{-1}$  band

The antisymmetric stretching vibration of NBrN which is only infra-red active, observed at  $170\text{cm}^{-1}$  and the symmetric stretching mode which is only Raman active, observed at  $195\text{cm}^{-1}$ . Neither of these two bands are observed in a benzene solution of pyridine and bromine or a solution of crystalline  $\text{PyBr}_2$  in benzene.

Most of the higher frequency bands of  $(\text{Py}_2\text{Br})^+$  ion nearly coincide with the bands of  $\text{PyBr}_2$  and are thus of little diagnostic value. However, the ring modes  $\nu_{16b}$  and  $\nu_{6a}$ , which are the two most sensitive to the nature of complexing at the nitrogen atom, are doubled in benzene solution (Table 14 column 1 and 2). For each band, one component, viz, of  $\nu_{6a}$  at  $638$  and of  $\nu_{16b}$  at  $445\text{cm}^{-1}$  closely coincide with the appropriate ring vibrations of  $(\text{Py}_2\text{Br})^+\text{PF}_6^-$ , may be assigned to pyridine ring vibrations of the  $(\text{Py}_2\text{Br})^+$  ion. The other two bands in this region ( $418$  and  $627\text{cm}^{-1}$ ) on comparing with the corresponding bands of  $\text{Py}^+\text{X}$  (ref. sec. 3.1.) complexes can be assigned to the  $\nu_{16b}$  and  $\nu_{6a}$  of the un-ionised  $\text{PyBr}_2$  complex. The band at  $1599\text{cm}^{-1}$  which appears as a shoulder also corresponds to the  $\nu_{8a}$  mode of the  $(\text{Py}_2\text{Br})^+$  ion. All the observed spectra in benzene solution can be accounted for by the scheme



In polar solvents e.g. in excess of pyridine the low frequency infra-red spectra is identical to the spectra in benzene solution. However, in excess of pyridine the intensity of the band assigned to the  $\text{Br}_3^-$  ion increases to a great extent. The Br-Br stretching

vibration drops slightly and the N-Br stretching frequency increases slightly in pyridine solution which is to be expected on passing to more polar solvents. The intensity of Raman active symmetric stretching vibration of the  $\text{Br}_3^-$  ion also increases in excess of pyridine or other polar solvents such as  $\text{CH}_2\text{Cl}_2$ ,  $\text{CH}_3\text{CN}$ , etc.

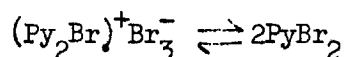
No band at  $308\text{cm}^{-1}$  is observed. However, the low frequency bands of the  $(\text{Py}_2\text{Br})^+$  ion still cannot be distinguished. In the higher frequency region also, apart from an increase in intensity of the bands at  $\sim 445$ ,  $\sim 638$  and  $\sim 1600\text{cm}^{-1}$  no other changes are observed.

In a solution of 0.2M  $\text{Br}_2$  and 1.0M pyridine in benzene, Klaboe<sup>(49)</sup> observed two low frequency Raman bands. The band at  $302\text{cm}^{-1}$  has been ascribed to the Br-Br stretching frequency of benzene- $\text{Br}_2$  complex and the band at  $281\text{cm}^{-1}$  to the Br-Br stretching frequency of  $\text{PyBr}_2$  complex. On repeated examination of the Raman spectra as well as the infra-red spectra we could not observe any bands at  $281\text{cm}^{-1}$  (Table 16).

The vibration spectra of the solid complex show differences from the solution spectra. The most remarkable differences are observed in the low frequency region; below  $400\text{cm}^{-1}$ . Low frequency infra-red spectra of solid pyridine-bromine complex show two bands; a strong and broad band at  $180\text{cm}^{-1}$  and a weaker band at  $169\text{cm}^{-1}$ .

Raman spectra show three bands; one strong band at  $166\text{cm}^{-1}$  and two weaker bands at  $188$  and  $195\text{cm}^{-1}$ . The interesting point is neither of these bands can be assigned to the un-ionised  $\text{PyBr}_2$  complex. The absence of both the Br-Br stretching in the region  $200-230\text{cm}^{-1}$  and the N-Br stretching near  $130\text{cm}^{-1}$ , which are both infra-red and Raman active confirms that the solid is not composed of the un-ionised charge-transfer complex. In fact, all the observed low frequency bands may be accounted for by the  $(\text{Py}_2\text{Br})^+$  and  $\text{Br}_3^-$  ions. The strong infra-red band at  $180\text{cm}^{-1}$  and the Raman band at  $166\text{cm}^{-1}$  can be assigned to antisymmetric and symmetric modes of the ion  $\text{Br}_3^-$ . The infra-red band at  $169\text{cm}^{-1}$  may be assigned either to the symmetric stretching mode of the  $\text{Br}_3^-$  ion which is allowed in the crystalline state or more likely to the antisymmetric stretch of NBrN of the ion  $(\text{Py}_2\text{Br})^+$  (ref.sec.4.). The  $\sim$  Raman band at  $195\text{cm}^{-1}$  may be assigned to the symmetric NBrN stretch of the ion  $(\text{Py}_2\text{Br})^+$ . The weak Raman band at  $188\text{cm}^{-1}$  may be assigned to the antisymmetric  $\text{Br}_3^-$  stretch which is allowed in the crystalline state. Indication that the solid contains the ion  $(\text{py}_2\text{Br})^+$  is supported by the presence of single infra-red bands in the vicinity of  $\nu_{8a}$ ,  $\nu_{6a}$  and  $\nu_{16b}^1$  (Table 14 column 7 and 8) the frequencies of these bands corresponding

with those of the  $(\text{Py}_2\text{Br})^+$  ion (ref. sec.4). From these facts it can be inferred that the solid is entirely composed of  $(\text{Py}_2\text{Br})^+ + \text{Br}_3^-$  ions. In solution the solid gives spectra identical with those obtained directly mixing pyridine and bromine solutions in appropriate solvents (Table 14). This indicates that in solution the ionization is reversible



3.3.52. Pyridine-brominechloride: The low frequency infra-red spectrum of this compound show only two bands in benzene solution. The higher frequency band at  $308\text{cm}^{-1}$  is assigned to the Br-Cl stretching mode of the complex, and can be compared with stretching frequency of BrCl at  $431\text{cm}^{-1}$  in  $\text{CCl}_4$  solution and  $418\text{cm}^{-1}$  in benzene solution. (47) The band at  $144\text{cm}^{-1}$  is assigned to the intermolecular N-Br stretch. (103) Since brominechloride can disproportionate  $2\text{BrCl} \rightleftharpoons \text{Br}_2 + \text{Cl}_2$ , the question arises whether the observed band at  $308\text{cm}^{-1}$  might be due to the benzene- $\text{Br}_2$  complex, which has a band at  $\sim 308\text{cm}^{-1}$ . Since pyridine is a stronger donor than benzene, any bromine would be preferentially complexed with pyridine, giving rise to a Br-Br stretching frequency at  $\sim 220\text{cm}^{-1}$ . The absence of any band near  $\sim 220\text{cm}^{-1}$  show that



disproportion is not taking place. The Raman spectrum in benzene solution (Table 16) below  $400\text{cm}^{-1}$  shows only one strong band at  $308\text{cm}^{-1}$ , which is assigned to the Br-Cl stretching mode of the complex. All the higher frequency bands in benzene solution (Table 15 column 5) can be assigned entirely to a single species, the un-ionised complex.

Low frequency infra-red spectra of PyBrCl in pyridine show three bands (Table 15). Raman spectra also show three bands (Table 17). Comparison with the other pyridine-halogen complexes suggests the ionisation  $2\text{PyBrCl} \rightleftharpoons (\text{Py}_2\text{Br})^+ + \text{BrCl}_2^-$  in polar media. Salts of the ion  $(\text{Py}_2\text{Br})^+$  have two low frequency stretching vibrations; one at  $170\text{cm}^{-1}$  which is observed only in the infra-red and the other at  $195\text{cm}^{-1}$  observed only in the Raman (ref.sec.4.). The ion  $\text{BrCl}_2^-$  has two stretching and one bending vibrations, all lying below  $400\text{cm}^{-1}$ .<sup>(105)</sup> The antisymmetric stretching vibration at  $\sim 220\text{cm}^{-1}$  is only infra-red active, while the symmetric mode at  $\sim 270\text{cm}^{-1}$  is only Raman active and the bending mode at  $\sim 140\text{cm}^{-1}$  is both Raman and infra-red active. All the low frequency vibration bands of PyBrCl in pyridine solution may be assigned assuming the ionisation described above. The  $160\text{cm}^{-1}$  infra-red band and  $162\text{cm}^{-1}$  Raman band may be assigned to the N-Br

Table 17

Raman Spectra of the Pyridine-bromine-chloride in various media

Solvent	Observed bands $\text{cm}^{-1}$			
Benzene				308s
1 : 4 Dioxane			280sh	300s(p)
Methylene chloride		192w	270sh <sup>*</sup>	
Pyridine	162vw	192w	278s(p)	
Acetonitrile		190w	276s	
Solid	102w	171m	198m	255s

\* appears as a shoulder on the  $\nu_4$  band of  $\text{CH}_2\text{Cl}_2$

stretching vibration of the complex. The infra-red band at  $274\text{cm}^{-1}$  can be assigned to the Br-Cl stretching vibration. However, the Raman band at  $278\text{cm}^{-1}$  may be assigned to either the symmetric stretching mode of the  $\text{BrCl}_2^-$  ion or the Br-Cl stretching mode of un-ionised PyBrCl. The fact that this band is also observed as a strong infra-red band, suggests that it should be assigned to the Br-Cl stretch. However, a contribution from the symmetric mode of the  $\text{BrCl}_2^-$  ion cannot be ruled out. In 1:4 dioxane solution the two contributions to the Raman band are more clearly resolved. (Table 17) The sharp infra-red band at  $226\text{cm}^{-1}$  is assigned to the  $\text{BrCl}_2^-$  ion. The weak Raman band at  $192\text{cm}^{-1}$  can be assigned to the symmetric NBrN stretching mode of the ion  $(\text{Py}_2\text{Br})^+$ .

In the higher frequency region the additional band at  $635\text{cm}^{-1}$  which appears as a shoulder in methylene chloride solution can be assigned to  $\nu_{6a}$  mode of the  $(\text{Py}_2\text{Br})^+$  ion. The other higher frequency bands of the PyBrCl in polar solvents nearly coincide with the corresponding vibrations of the  $(\text{Py}_2\text{Br})^+$  ion and so cannot be separately distinguished. Thus it may be concluded that the spectrum in benzene solution is entirely due to the un-ionised PyBrCl complex and the

spectra in polar solvents such as pyridine and methylene chloride are due to  $\text{PyBrCl}$ ,  $(\text{Py}_2\text{Br})^+$  and  $\text{BrCl}_2^-$ .

The vibration spectra of the solid complex, which has been reported by Williams<sup>(84)</sup> to be  $\text{PyBrCl}$ , present several difficulties in interpretation. The solid compound prepared, is identical with William's compound in appearance, melting point and microanalysis of nitrogen and total halogen. The solubility of this compound in organic solvents is similar to the other pyridine-halogen complexes. As the solution spectra of this compound can be easily interpreted, it may be concluded that no substitution reaction has taken place during the preparation. The higher frequency infra-red spectra of the solid complex in mulls is found to be consistent with the un-ionised  $\text{PyBrCl}$  complex, in contrast to the solid pyridine-bromine complex. The single  $\nu_{16b}$  band at  $430\text{cm}^{-1}$  corresponds to the un-ionised  $\text{PyBrCl}$  complex. The  $\nu_{16}$  band for  $(\text{Py}_2\text{Br})^+$  occurs at  $445\text{cm}^{-1}$ , and therefore would have been clearly observed had this ion been present. There is also only one  $\nu_{6a}$  band, the frequency corresponding to the unionised complex. The remaining higher frequency spectrum also corresponds quite closely to that of the unionised complex.

Taken as a whole the spectra give the impression that the solid is entirely in the un-ionised form.

The low frequency infra-red spectra of the solid pyridine-bromine-chloride complex show two strong and four weaker bands (Table 15). The low frequency Raman spectra show three bands (Table 17). None of these low frequency bands can be assigned to  $(\text{Py}_2\text{Br})^+$  and  $\text{BrCl}_2^-$  ions. The absence of the strong infra-red band of  $(\text{Py}_2\text{Br})^+$  near  $170\text{cm}^{-1}$  (see sec.4.) excludes the possibility of presence of the  $(\text{Py}_2\text{Br})^+$  ion in the solid complex. Similarly the absence of the strong infra-red band of  $\text{BrCl}_2^-$  near  $220\text{cm}^{-1}$  and the Raman band near  $276\text{cm}^{-1}$  prove the absence of the  $\text{BrCl}_2^-$  ion in the solid complex. However, the assignment of the low frequency vibration bands entirely to the un-ionised form is not straightforward. The band at  $\sim 196\text{cm}^{-1}$  which appears both in the infra-red and Raman may be assigned to the N-Br stretching frequency of the  $\text{PyBrCl}$  complex, though this appears at  $160\text{cm}^{-1}$  in pyridine solution (Table 15). Such a large frequency shift of the nitrogen-halogen ~~and~~ stretching mode from the solid state to solution spectra is not uncommon. For example, the N-I stretching mode of  $\text{PyICl}$  which appears at  $147\text{cm}^{-1}$  shifts to  $160\text{cm}^{-1}$ (48) in pyridine

solution and finally to  $170\text{cm}^{-1}$ (40) in a mujol mull. The Raman band at  $171\text{cm}^{-1}$  may be due to splitting of the N-Br stretching mode. Splitting of the N-I stretching mode of  $\text{PyI}_3$  in a mull has been observed by Person et al<sup>(50)</sup>. The Raman band at  $102\text{cm}^{-1}$  and the infra-red band at  $104\text{cm}^{-1}$  may be assigned to the N-Br-Cl bending mode. The weak infra-red bands at 85 and  $71\text{cm}^{-1}$  may be assigned to bending, rocking, or crystal lattice vibrations. However, difficulty still arises in assigning the two higher frequency bands. The strong infra-red band at  $295\text{cm}^{-1}$  which might be assigned to the Br-Cl stretching mode is completely absent in the Raman. On the otherhand the strong Raman band at  $255\text{cm}^{-1}$  which could also be assigned to the Br-Cl stretching mode, does not appear in the infra-red. The assignment of both the 295 and  $255\text{cm}^{-1}$  bands to this stretching mode requires strong interaction between the  $\text{PyBrCl}$  units in the crystal, which may not be impossible in such a complex.

The alternative assignment of the low frequency spectra involves the consideration of an asymmetric  $\text{BrCl}_2^-$  ion. Asymmetric polyhalide ions are not frequently observed. However, Tasman and Boswijk<sup>(106)</sup> have found that the  $\text{I}_3^-$  ion in  $\text{CsI}_3$  is asymmetric.

Maki et al<sup>(91)</sup> have also reported asymmetric  $\text{ICl}_2^-$  and  $\text{IBr}_2^-$  ions, where all the three vibrational modes are both infra-red and Raman active. If we consider the  $\text{BrCl}_2^-$  ion in the  $(\text{Py}_2\text{Br})^+\text{BrCl}_2^-$  complex to be asymmetric then all the observed low frequency bands may be assigned. The infra-red band at  $295\text{cm}^{-1}$  and Raman band at  $255\text{cm}^{-1}$  may be assigned to the  $\nu_1$  mode; the band at  $\sim 198\text{cm}^{-1}$  to the  $\nu_3$  mode, and the Raman band at  $171\text{cm}^{-1}$  to the  $\nu_2$  mode of the  $\text{BrCl}_2^-$  ion. However, this assignment requires the  $\nu_1$  infra-red band of  $\text{BrCl}_2^-$  to be separated from the accompanying Raman  $\nu_1$  band by  $40\text{cm}^{-1}$ <sup>(105)</sup>. Assignment of the  $\sim 196\text{cm}^{-1}$  band to the  $\nu_3$  and  $170\text{cm}^{-1}$  Raman band to  $\nu_2$  would also require displacements of some 30 and  $40\text{cm}^{-1}$  respectively from their usual positions. It is also difficult to explain why the  $\nu_2$  band is not observed in the infra-red. Furthermore, the antisymmetric NBrN stretching mode of the  $(\text{Py}_2\text{Br})^+$  ion at  $\sim 170\text{cm}^{-1}$  is not observed in the infra-red spectrum. Finally the rear infra-red spectrum is more difficult to fit to the  $(\text{Py}_2\text{Br})^+$  ion.

The possibility of the formation of  $(\text{Py}_2\text{Cl})^+$  and  $\text{ClBr}_2^-$  ions may be rejected for two main reasons. Firstly the formation of an ion such as  $(\text{Py}_2\text{Cl})^+$  is highly improbable since chlorine as a co-ordination

centre is rare<sup>(108)</sup> and when it occurs it is very unstable; secondly, no bands for the  $\text{ClBr}_2^-$  ion in the vicinity of  $230\text{cm}^{-1}$ <sup>(107)</sup> are observed.

3.3.6. Assignments: As the infra-red spectra of  $\text{PyBrX}$  complexes in solution are comparable to  $\text{PyIX}$  complexes, they may be assumed to have the same symmetry point group, i.e.,  $\text{C}_{2v}$ . The absence in solution infra-red spectra of bands corresponding to the  $a_2$  modes of pyridine also suggests  $\text{C}_{2v}$  symmetry in solution. Comparison with the spectra of pyridine and  $\text{PyIX}$  complexes enables one to make an almost complete assignment of the infra-red active fundamentals of the  $\text{PyBrX}$  complexes. Table 20 shows this assignment.



Table 18

Assignment of infrared active fundamentals of pyridine-bromine and  
pyridine-bromine chloride complexes

Designation		Pyridine-bromine (In $\text{CH}_2\text{Cl}_2$ )	Pyridine-BrCl (In $\text{CH}_2\text{Cl}_2$ )
$a_1$	$\nu(\text{CH})$ 2		
	$\nu(\text{CH})$ 20a		
	$\nu(\text{CC})$ 8a	1597	1597
	$\nu(\text{CC,CN})$ 19a	1480	1488
	$\beta(\text{CH})$ 9a	1206	1206
	$\beta(\text{CH})$ 18a	1067	1067
	Ring 1	1012	1012
	X sens 13		
	X sens 12	1030	1033
	X sens 6a	628	632
	N-Br stretching	128	144
	X-Y stretching	229	307
	$b_1$	$\nu(\text{CH})$ 20b	
$\nu(\text{CH})$ 7b			
$\nu(\text{CC})$ 8b			
$\nu(\text{CC,CN})$ 19b		1450	1451
$\nu(\text{CC,CN})$ 14			
$\beta(\text{CH})$ 3		1206	1206
$\beta(\text{CH})$ 18b			
$\alpha(\text{CCC})$ 6b			
X sens 15		1155	1154
$b_2$	$\nu(\text{CH})$ 5	942	942
	$\nu(\text{CH})$ 10b		
	$\phi(\text{CC})$ 4	748	750
	$\phi(\text{CC})$ 11		
	X sens 16b	420	425

4. The vibration spectra and structure of the bis-pyridine iodine(I); bis-pyridine bromine(I); bis- $\gamma$ -picoline iodine(I) and bis- $\gamma$ -picoline bromine(I) cations.

#### 4.1. INTRODUCTION

Salts containing the ions  $(\text{Py}_2\text{I})^+$  and  $(\text{Py}_2\text{Br})^+$  have long been known. (108,109,110) These ions are in agreement with the requirements of bico-ordination for the  $\text{I}^+$  and  $\text{Br}^+$  species. (111) Ions of this type are generally observed when the anions have slight or no capacity to function as a ligand. Electrolysis of  $(\text{Py}_2\text{I})^+\text{NO}_3^-$  in anhydrous chloroform solution yields iodine at the cathode, while the solution around the anode remains clear. (109) This proves beyond doubt that the iodine is the positive constituent of the salt.

In the compound  $\text{Py}_2\text{I}_7$  obtained by direct interaction of pyridine with iodine, X-ray studies show the presence of an essentially planar cation  $(\text{PyIPy})^+$  along with  $\text{I}_3^-$  and  $\text{I}_2$  molecules. (83) The crystals are monoclinic and of space group  $P2_1/C$  with four molecules of pyridine per unit cell. It has also been shown that, in the crystal, the  $(\text{Py}_2\text{I})^+$  ion has a centrosymmetric structure. Study of infra-red and Raman spectra of the salts of the ion  $(\text{Py}_2\text{I})^+$  in solution may indicate whether the collinearity of the two ligand bands and the co-planarity of the pyridine rings, arise from the internal force field, or from interionic forces dominating the crystal packing.

The infra-red spectra of solid bis-pyridine iodine (I) nitrate and perchlorate have been reported by Zingaro and Tolberg (36) and bis-pyridine bromine (I) nitrate, perchlorate and acetate by Zingaro and Witmer. (37) Their studies were confined to a small frequency range around  $1000\text{cm}^{-1}$ .

The primary object of the present study is to compare the spectra, N-X bond strength and charge distribution of the cations with that of pyridine and  $\gamma$ -picoline charge-transfer complexes. Accordingly several salts of each of the ions  $(\text{Py}_2\text{I})^+$ ,  $(\text{Py}_2\text{Br})^+$ ,  $(\gamma\text{-pic}_2\text{I})^+$  and  $(\gamma\text{-pic}_2\text{Br})^+$  have been prepared and their vibration spectra in the solid state and in solution recorded in the frequency range  $4000\text{--}60\text{cm}^{-1}$ . Many features regarding the structure of these ions have also been explored.

In this section the preparation of the salts is described, and the spectra reported. Possible structures are discussed and frequencies assigned. Consideration of frequency shifts, charge distributions, solvent effects and force constants is deferred until a later section.

#### 4. . . EXPERIMENTAL

4.2.1. Purity of Materials: Sodium-fluoroborate (BDH), ammonium-hexafluorophosphate (Ozark-Mohaning Company) and silvernitrate (BDH) were used without further purification. Purification of other chemicals has already been discussed in sections 3.1.21, 3.2.21 and 3.3.21.

4.2.2. Preparation: Preparation of  $(\text{Py}_2\text{I})^+\text{ClO}_4^-$  has been discussed elsewhere.<sup>(112)</sup> The preparations of  $(\text{Py}_2\text{I})^+\text{PF}_6^-$ ,  $(\text{Py}_2\text{I})^+\text{BF}_4^-$ ,  $(\text{Py}_2\text{Br})^+\text{PF}_6^-$ ,  $(\gamma\text{-pic}_2\text{I})^+\text{BF}_4^-$ ,  $(\gamma\text{-pic}_2\text{I})^+\text{PF}_6^-$  and  $(\gamma\text{-pic}_2\text{Br})^+\text{PF}_6^-$  are all similar and are exemplified below by the preparation of bis-pyridine iodine(I) fluoroborate.

17 grams of silver nitrate was dissolved in 70ml. of water contained in a beaker. 50ml. of pure pyridine was added slowly with stirring, whereupon the solution became warm. Then a solution of 20grms. of sodium fluoroborate in about 100 ml. of water was added to the pyridine/ $\text{AgNO}_3$  solution slowly with stirring. After cooling to about  $0^\circ\text{C}$ , solid crystals were formed at the bottom of the flask and removed by filtration. This product was washed several times with ice-cold water to free it from nitrate, and after drying, it was dissolved in the minimum volume of pyridine-chloroform solution (1:10). This was cooled in an ice bath and to it a saturated solution of iodine in chloroform was added slowly with stirring until the colour turned to a faint purple indicating a slight excess of iodine. The cream coloured precipitate of  $\text{AgI}$  was removed by filtration and washed with two 5 ml. portions of a chloroform-pyridine mixture (20:1), the washings being added to the filtrate. Sodium dried ether was then slowly added with stirring to the filtrate until the precipitation was complete. The white crystalline powder was washed free of iodine with sodium dried ether and air dried. It was further purified by recrystallisation from pure methanol. The white crystalline compound was collected by suction filtration, washed several times with dry ether, dried in a stream of nitrogen and finally dried in vacuo over  $\text{P}_2\text{O}_5$ .

Elemental analyses of the salts are given in Table 19.

TABLE 19

Compound	Iodine %		Bromine %		Nitrogen %		Fluorine %	
	Calc.	Found	Calc.	Found	Calc.	Found	Calc.	Found.
$(\text{Py}_2\text{I})^+\text{ClO}_4^-$	33.03	32.9						
$(\text{Py}_2\text{I})^+\text{BF}_4^-$	34.15	33.9			7.5	7.4		
$(\text{Py}_2\text{I})^+\text{PF}_6^-$	29.5	2.9			6.5	6.3		
$(\text{Py}_2\text{Br})^+\text{PF}_6^-$			20.88	20.4				
$(\gamma\text{-pic}_2)^+\text{BF}_4^-$	31.77	3.2			7.0	7.11	19.0	19.3
$(\gamma\text{-pic}_2\text{I})^+\text{PF}_6^-$	27.7	27.9						
$(\gamma\text{-pic}_2\text{Br})^+\text{PF}_6^-$			19.5	19.0				

4.2.3. Spectra: The solid complexes were examined by dispersing in mujol or hexachlorobutadiene. AgCl, KBr or polythene windows were used. The  $(\text{Py}_2\text{I})^+$ ,  $(\text{Py}_2\text{Br})^+$  and  $(\gamma\text{-pic}_2\text{I})^+$  salts were stable, but  $(\gamma\text{-pic}_2\text{Br})^+\text{PF}_6^-$  became slowly discoloured on standing, with accompanying spectral changes, particularly if KBr windows were employed. For this salt fresh samples were used for the measurement of each band, using AgCl or polythene windows. In methylenechloride and acetonitrile solution all except  $(\gamma\text{-pic}_2\text{Br})^+$  salts were stable for at least two hours. Nevertheless, all solutions were prepared as near to the time of measurement as possible, and a fresh solution was made after every 10 minutes for all salts. The possibility a rapid

decomposition in solution might occur is very real. However, the concentration of decomposition products, if formed, was so small that they were not detectable by infra-red methods. The formation of small amounts of decomposition product may be of much greater importance when methods such as ultraviolet spectroscopy or conductivity are used. To get a reproducible spectrum of  $(\gamma\text{-pic}_2\text{Br})^+\text{PF}_6^-$  in  $\text{CH}_2\text{Cl}_2$  solution, each band was run several times with freshly made up solutions. The  $(\gamma\text{-pic}_2\text{I})^+$  and  $(\gamma\text{-pic}_2\text{Br})^+$  salts in  $\gamma$ -picoline solution were found to be quite unstable; however, by repeatedly renewing the solutions the required spectra were established.

No decomposition of any kind was observed for the salts  $(\text{Py}_2\text{I})^+$ ,  $(\text{Py}_2\text{Br})^+$  and  $(\gamma\text{-pic}_2\text{I})^+$  while running the Raman spectra in solution or in the solid state. However, each observed band was checked by running the spectrum in the region of the band using freshly made up solutions.  $(\gamma\text{-pic}_2\text{I})^+$  salts in  $\gamma$ -picoline were very unstable; however, the band at  $161\text{cm}^{-1}$  was clearly observed in fresh solution, even though it disappears completely after only 10 minutes. Attempts to obtain the Raman spectra of  $(\gamma\text{-pic}_2\text{Br})^+$  salts were unsuccessful, decomposition occurring very rapidly when the sample was exposed to the laser beam.

4.3. Results: The infra-red and Raman data for all the ions investigated are listed in Tables 20-23. The assignments of the Raman and infra-red active fundamentals are shown in Table 24. Figures 12-15 show composite spectra of the cations produced by combining data from the various salts. The spectra in solution and solid are generally similar.

4.4. Discussion: The ion  $(\text{Py}_2\text{I})^+$  in solution may or may not retain its coplanarity depending on whether this feature in the crystal is due to intramolecular ( $\pi$  electron interaction) or inter-ionic forces. In the following section we will consider all the possible structures of this ion and other similar ions  $(\text{Py}_2\text{Br})^+$ ,  $(\nu\text{-pic}_2\text{I})^+$  and  $(\nu\text{-pic}_2\text{Br})^+$ .

If  $\epsilon$  is the angle between the planes of the two pyridine or  $\nu$ -picoline rings (Fig.16), then the free ions may belong to the  $D_{2h}(\epsilon = 0)$ ,  $D_2(\epsilon = 0 < \epsilon < 90^\circ)$  or  $D_{2d}(\epsilon = 90^\circ)$  point groups.  $C_i$  and  $C_{2h}$  are two other possible point groups (Fig.16). One may also imagine a bent N-X-N linkage between the two rings.

First we will deal with the low frequency region of the spectrum as bands of this region are generally easy to assign. Whatever the structure may be, the number of fundamentals which are expected to occur at low frequencies is very small. All the nine skeletal vibrations (Fig.17) which involve the motion of the base rings as a whole are expected to lie below  $400\text{cm}^{-1}$ . In fact,



TABLE 20

I.R. of (Py <sub>2</sub> I)ClO <sub>4</sub> in Nujol mull	(Py <sub>2</sub> I)BF <sub>4</sub>					
	Infra-red					Raman
	In Nujol mull	In hexa- chlorobuta- diene mull	In CH <sub>2</sub> Cl <sub>2</sub> solution	In CH <sub>3</sub> CN solution	Solid	In CH <sub>2</sub> Cl <sub>2</sub> solution
		3159w				
		3109s				
		3102s				
		3079s				
		3049m				
		3035m				
		2950w				
		2922m				
1919w	1926w		1919w			
1843w	1846w	1848w	1846w			
1698w			1699w			
1654w	1652w	1652w	1654w			
1600s	1601s	1602s	1603s	1600s	1606m	1608w
1580w			1575w	1580w	1578m	1578w
			1481w		1485w	1488w
		1455s	1452s		1438w	
1398w	1403w	1400w				
1350m	1355ms	1355m	1354m			

(Py <sub>2</sub> I)PF <sub>6</sub>					Interpretation
Infra-red			Raman		
In Nujol mull	In hexachlorobutadiene mull	In CH <sub>2</sub> Cl <sub>2</sub> solution	Solid	In CH <sub>2</sub> Cl <sub>2</sub> solution	
					(1580 x 2)
					} b <sub>1</sub> fundamental
					a <sub>1</sub> fundamental
					a <sub>1</sub> fundamental
					a <sub>1</sub> &b <sub>1</sub> fundamental
					1354 + 1600
					1355 + 1580
1923w		1919w			760 + 1161
1883w					638 + 1248
1847w	1848w	1845w			638 + 1215
	1700w	1699w			690 + 1010
1651w	1652w	1654w			638 + 1010
1600s	1600s	1602s	1603m	1607w(P?)	a <sub>1</sub> fundamental
1580w		1576w	1576m	1577w(P?)	b <sub>1</sub> fundamental
1506w	1479w	1481w	1486m		a <sub>1</sub> fundamental
	1455s	1452s			b <sub>1</sub> fundamental
1399m	1400m				638 + 760
1355ms	1355ms	1355ms			b <sub>1</sub> fundamental

TABLE 20 (Cont'd)

I.R. of (Py <sub>2</sub> I)ClO <sub>4</sub> in Nujol mull	(Py <sub>2</sub> I)BF <sub>4</sub>					
	Infra-red					Raman
	In Nujol mull	In hexa- chlorobuta- diene mull	In CH <sub>2</sub> Cl <sub>2</sub> solution	In CH <sub>3</sub> CN solution	Solid	In CH <sub>2</sub> Cl <sub>2</sub> solution
1248m	1249m	1250m		1246m		
1205s 1200sh	1207s 1200sh	1209s	1210s	1210s	1216m	1216m
1161ms	1161s		1158s	1156s	1166m	1158m
1055s						
1038ms					1039s	1039s
1010s 1005sh	1009s 1005sh	1010s	1010s 1005sh	1010s	1020s	1021s
	952m		945m		954w	
760s	761s			760s 750sh		
700sh 690s	700sh 690s	691s		707ms 692s		
638s	638s	638s	637s	638s	646s	644s
439s	441ms	441s	437ms	437m	425vw 362vww	422vww
172s	172s		172s *		182s	180s(P) 181 * s

\* In pyridine solution

In these tables, bands due to solvents or the counterion are omitted

(Py <sub>2</sub> I)PF <sub>6</sub>						
Infra-red					Raman	Interpretation
In Nujol mull	In hexa- chlorobuta- diene mull	In CH <sub>2</sub> Cl <sub>2</sub> solution	Solid	In CH <sub>2</sub> Cl <sub>2</sub> solution		
1248m	1247m					b <sub>1</sub> fundamental
1206s 1193sh	1206s	1210s	1216s	1215m(P)		a <sub>1</sub> fundamental 441 + 760
1160m		1158m	1167s	1157s(dp)		b <sub>1</sub> fundamental
1094w	1094w	1090w				b <sub>1</sub> fundamental
1059s	1059s	1062s	1066vw			a <sub>1</sub> fundamental
1040s 1032sh 1010s 1005sh	1038s 1032sh 1009s	1040s 1030w 1009s 1005sh	1036s  1019s	1036s(P)  1019s(P)		} a <sub>1</sub> fundamental } a <sub>1</sub> fundamental
952w		946w	949w			b <sub>2</sub> fundamental
759s			758w			} b <sub>2</sub> fundamental
700sh 690s	701sh 689s					} b <sub>2</sub> fundamental
638s	638s	637s	644s	645s(P)		a <sub>1</sub> fundamental
438s	438s	438s	419w			b <sub>2</sub> fundamental
172s 90w		172s*	181s	181s(P) 182* s		skeletal

TABLE 21

Vibration Spectra of  $(\text{Py}_2\text{Br})\text{PF}_6$ 

in various media

In Nujol Mull	Infra-red		Solid	Raman	Interpretation
	In $\text{CH}_2\text{Cl}_2$ solution	In hexachlorobutadiene mull above $2000\text{cm}^{-1}$		In $\text{CH}_2\text{Cl}_2$ solution	
		3141w			1574 x 2
		3114s			$b_1$ fundamental
		3099sh			
		3073w			$a_1$ fundamental
		3053m			$a_1$ fundamental
		3037			$a_1$ & $b_1$ fundamental
		3015w			1454 + 1584
1929w	1915w				766 + 1160
1845w	1845w				639 + 1213
	<b>1708m</b>				690 + 1021
	1658w				647 + 1011
1600s	1601s		1609m	1608w	$a_1$ fundamental
1574w	1574w		1577m	1584w	$b_1$ fundamental
1538w					(744 x 2)
	1487m		1487m		$a_1$ fundamental
	1454s				$b_1$ fundamental
1408w					(638 + 766)

TABLE 21 (Cont'd)

Vibration Spectra of  $(\text{Py}_2\text{Br})\text{PF}_6$ 

in various media

In Nujol Mull	Infra-red In $\text{CH}_2\text{Cl}_2$ solution	In hexachlorobutadiene mull above $2000\text{cm}^{-1}$	Solid	Raman In $\text{C}_2\text{Cl}_2$ solution	Interpretation
1354m	1351ms				$b_1$ fundamental
1254ms					$b_1$ fundamental
1206s	1205s		1213s	1213s(P)	$a_1$ fundamental
1192sh					
1161m	1158s		1160w		$b_1$ fundamental
1095w	1090w				$b_1$ fundamental
1066s	1062s		1072w		$a_1$ fundamental
1037s 1032sh	1040s 1033sh		1035s	1035s(P)	} $a_1$ fundamental
1011s 1006sh	1011s 1008sh		1021s 1012sh(w)	1022s(P)	
978w					$a_2$ fundamental
953m	945m		952w		$b_2$ fundamental
766s					$b_2$ fundamental
690s 674sh					} $b_2$ fundamental
639s	639s		647s	649s(P)	
452s	450s		635sh(w)		$b_2$ fundamental

TABLE 21 (Cont'd)Vibration Spectra of  $(\text{Py}_2\text{BR})\text{PF}_6$ 

in various media

Infra-red		Raman			Interpretation
In Nujol Mull	In $\text{CH}_2\text{Cl}_2$ solution	In hexachlorobutadiene mull above $2000\text{cm}^{-1}$	Solid	In $\text{CH}_2\text{Cl}_2$ solution	
170s	170s*		189s	193s(P)	skeletal
			168w		
			138w		

\* In pyridine solution

TABLE 22

( $\nu$ -Pic <sub>2</sub> I)BF <sub>4</sub>				
Infra-red			Raman	
In Nujol mull	In CH <sub>2</sub> Cl <sub>2</sub> solution	In CH <sub>3</sub> CN solution	Solid	In CH <sub>2</sub> Cl <sub>2</sub> solution

1938w	1941w	1945w		
1848w	1838w	1838w		
1689w				
1623s	1620s	1618s	1620ms	1621m(P)
1613s	1613s	1610s		
1560w	1557w	1560w		
1504w	1499m	1506m	1506m	1506w
	1383m		1387s	1385ms(P)
	1366w			
1333w	1333w	1333w		
1284m				



$(\nu - \text{Pic}_2\text{I})\text{PF}_6$ 

Infra-red		Raman			
In Nujol mull	In hexa- chlorobuta- diene mull	In $\text{CH}_2\text{Cl}_2$ solution	Solid	In $\text{CH}_2\text{Cl}_2$ solution	Interpretation
	3133w				1560 x 2'
	1307m				1610 + 1502
	3067m				$a_1$ & $b_1$ fundamental
	3053m				$a_1$ fundamental
	3021w				$b_1$ fundamental
	2992w				1502 + 1506
	2924w				$a_1$ fundamental
1944w	1941w	1930w			712 + 1228
1848w	1848w	1835w 1767w			810 + 1028 813 + 1952
1680w	1680w				712 + 958
1618s 1610s	1621s 1610s	1618s 1610s	1620m	1622w	) $a_1$ fundamental & ) 810 + 813
1557w		1560m			$b_1$ fundamental
1502m	1502w	1499m	1506m	1501w	$a_1$ fundamental
	1447s				$b_1$ & $b_2$ fundamental
	1439s				$b_1$ fundamental
	1387m	1383m	1387ms	1383ms	$a_1$ fundamental
		1366w			662 + 712
1333w	1333w	1331w	1338w		660 + 662

TABLE 22 (Cont'd)

$(\gamma\text{-Pic}_2\text{I})\text{BF}_4$				
Infra-red			Raman	
In Nujol mull	In $\text{CH}_2\text{Cl}_2$ solution	In $\text{CH}_3\text{CN}$ solution	Solid	In $\text{CH}_2\text{Cl}_2$ solution
1254m		1253m		
1231w	1225w	1225w	1233s	1227s(P)
1211s	1212s	1211s	1216s	1215s(P)
1125w				
1096w				
1067s	1068s			
1037m	1036m			
1022s	1025s	1025s	1027s	1031s(P)
		983vw	990vw	
			970vw	
873w		871w		
820s	813s	814s	813s	813s(P)
813s				
713m		712m	714vw	
666w				
660w		662w	663s	663s(dp)
545s	545s	546s	553s	554s(P)
490s	490s	494s	484m	
164s	168s*		164s	162s(P)
80m				161s*

\* In  $\gamma$ -picoline solution

( $\gamma$ -Pic <sub>2</sub> I)PF <sub>6</sub>					
Infra-red			Raman		
In Nujol mull	In hexa- chlorobuta- diene mull	In CH <sub>2</sub> Cl <sub>2</sub> solution	Solid	In CH <sub>2</sub> Cl <sub>2</sub> solution	Interpretation
1297vw	1297vw				491 + 808
1258m	1255m				b <sub>1</sub> fundamental
1228w	1228w	1226w	1228s	1226s	a <sub>1</sub> fundamental
1209s	1209s	1207s	1215s	1211s	a <sub>1</sub> fundamental
1121w	1121w	1120w			b <sub>1</sub> fundamental
1098vw	1098vw	1096w			549 + 551
1063s	1063s	1061s	1072m	1069w	b <sub>1</sub> fundamental
1043w	1042w	1038w			a <sub>1</sub> fundamental
1024s	1025s	1024s	1028s	1028s	a <sub>1</sub> fundamental
			988vw		494 + 484
975w		975w	968vw		b <sub>2</sub> fundamental
952w					a <sub>2</sub> fundamental
810s	808s	810s	813s	813s	} a <sub>1</sub> &b <sub>2</sub> fundamental
712m	711m				b <sub>2</sub> fundamental
666w					} b <sub>1</sub> fundamental
660w			662s	662s	
545s	545s	549s	551s	553s	a <sub>1</sub> fundamental
491s	491s	491s	485w	487w	b <sub>2</sub> fundamental
			162s	160s	skeletal

TABLE 23Infra-red Spectra of ( $\nu$ -Pic<sub>2</sub>Br)PF<sub>6</sub>

in various media

In Nujol Mull	In hexachloro- butadiene mull	In CH <sub>2</sub> Cl <sub>2</sub> solution	Interpretation
	3130w		5 x 1562
	3105m		(1502 + 1610)
	3077ms		a <sub>1</sub> & b <sub>1</sub> fundamental
	3058ms		a <sub>1</sub> fundamental
	3023m		b <sub>1</sub> fundamental
	2990w		(2 x 1502)
	2923w		a <sub>1</sub> fundamental
1943w	1943w	1932w	(712 + 1222)
1848w	1848w	1838w	(810 + 1026)
	1680w		(810 + 873)
		1644m	(666 + 975)
1621s	1621s	1623s	} a <sub>1</sub> fundamental and (810 x 2)
1608s	1610s	1613s	
1562w		1568w	b <sub>1</sub> fundamental
1496w	1502m	1509m	a <sub>1</sub> fundamental
	1450s		b <sub>1</sub> & b <sub>2</sub> fundamental
	1435s		b <sub>1</sub> fundamental
	1387ms	1385m	a <sub>1</sub> fundamental
		1366w	b <sub>1</sub> fundamental

TABLE 23 (Cont'd)

Infra-red Spectra of ( $\gamma$ -Pic<sub>2</sub>Br)PF<sub>6</sub>

in various media

In Nujol Mull	In hexachloro- butadiene mull	In CH <sub>2</sub> Cl <sub>2</sub> solution	Interpretation
1332w	1332w	1328w	(666 x 2)
1259m	1260m		(543 + 712)
1223w	1223w		a <sub>1</sub> fundamental
1205s	1205s	1206s	a <sub>1</sub> fundamental
1120w	1120w	1121w	b <sub>1</sub> fundamental
1099vw	1100vw	1098w	(2 x 543)
1062s	1062s	1063s	b <sub>1</sub> fundamental
1041sh	1045sh	1040sh	a <sub>1</sub> fundamental
1025s	1024s	1026s	a <sub>1</sub> fundamental
975m		976m	b <sub>2</sub> fundamental
954w		941w	a <sub>2</sub> fundamental
810s	808s	811s	a <sub>1</sub> & b <sub>2</sub> fundamental
711ms	712ms		b <sub>2</sub> fundamental
666w			) b <sub>1</sub> fundamental
660w			
536s	538s	543s	a <sub>1</sub> fundamental
493s	495s	494s 486s	) b <sub>2</sub> fundamental
170s		170s*	skeletal

\* In  $\gamma$ -picoline solution

TABLE 24

Assignment of vibrational frequencies related to  
internal vibrations of the base groups:

Designation (8)	$(\text{Py}_2\text{I})^+$				$(\text{Py}_2\text{Br})^+$				
	I.R. in Soln.	Raman in Soln.	I.R. in mull	Raman Solid	I.R. in Soln.	Raman in Soln.	I.R. in mull	Raman solid	
$a_1 \nu(\text{CH})$ 2			3079				3073		
$\nu(\text{CH})$ 20a			3049				3053		
$\nu(\text{CC})$ 8a	1602	1607	1600	1603	1601	1608	1600	1609	
$\nu(\text{CC.CN})$ 19a	1481	1488	1479	1486	1487			1487	
$\beta(\text{CH})$ 9a	1210	1216	1207	1216	1205	1213	1206	1213	
$\beta(\text{CH})$ 18a	1062		1059	1066	1062		1066	1072	
Ring 1	{1009 1005	1019	1010 1005	1019	1011 1008	1022	1011 1006	1021	
X-sens 13			3035				3037		
X-sens 12	1040 1030	1036	1040 1032	1036	1040 1033	1035	1037 1032	1035	
X-sens 6a	637	644	638	645	639	649	639	647	
$b_1 \nu(\text{CH})$ 20b			3109 3102				3114		
$\nu(\text{CH})$ 7b			3035				3037		
$\nu(\text{CC})$ 8b	1576	1577	1580	1576	1574	1584	1574	1577	
$\nu(\text{CC.CN})$ 19b	1452		1455	1438	1454				
$\beta(\text{CC.CN})$ 14	1355		1355		1351		1354		
$\beta(\text{CH})$ 3	1246		1248				1254		

TABLE 24 (Cont'd)

Assignment of vibrational frequencies related to internal vibrations of the base groups.

Designation (8)	(Py <sub>2</sub> I) <sup>+</sup>				(Py <sub>2</sub> Br) <sup>+</sup>			
	I.R. in Soln.	Raman in Soln.	I.R. in Mull	Raman Solid in	I.R. in Soln.	Raman in mull	I.R. in mull	Raman Solid
α(CCC) 6b								
X-sens 15	1158	1157	1160	1167	1158		1161	1160
a <sub>2</sub> ν(CH) 17a							978	
ν(CH) 10a								
ν(CC) 16a				362				
b <sub>2</sub> ν(CH) 5	945		952		945		953	952
ν(CH) 10b								
ν(CC) 4	760		761	758			766	
ν(CC) 11	692 707							
X-sens 16b	438	422	438	425	450		452	

TABLE 24 (Continued)

Designation (8) (9)	$(\gamma\text{-Pic}_2\text{I})^+$			$(\gamma\text{-Pic}_2\text{Br})^+$ ( $\text{PF}_6^-$ )		
	I.R. in soln. ( $\text{CH}_2\text{Cl}_2$ or $\text{CH}_3\text{CN}$ )	Raman in soln. ( $\text{CH}_2\text{Cl}_2$ )	I.R. of mull	Raman solid	I.R. in $\text{CH}_2\text{Cl}_2$ soln.	I.R. in mull
$a_1 \nu(\text{OH})$ 2			3067			3077
$\nu(\text{OH})$ 20a			3053			3058
$\nu(\text{CO})$ 8a	1618 1610	1622	1618 1610	1620	1623 1613	1621 1610
$\nu(\text{CO.CN})$ 19a	1499	1501	1502	1506	1509	1502
$\nu(\text{CH})$ 9a	1226	1226	1228	1228		1223
$\nu(\text{CH})$ 18a	1038		1043		1040	1045
Ring	1	1024	1028	1024	1028	1026
X-sens	13	1207	1211	1209	1215	1206
X-sens	12	814	813	{ 820 813	813	811
X-sens	6a	545	554	545	553	543
Methyl	$M_1$		2924			2923
Methyl	$M_2$	1383	1383	1387	1387	1385
$b_1 \nu(\text{CH})$ 20b			3053			3058
$\nu(\text{CH})$ 7b			3021			3023
$\nu(\text{CC})$ 8b	1560		1557		1568	1562
$\nu(\text{CC.CN})$ 19b			1439			1435
$\nu(\text{CC.CN})$ 14	1366				1366	



TABLE 24 (Cont'd)

		$(\gamma\text{-Pic}_2\text{I})^+$			$(\gamma\text{-Pic}_2\text{Br})^+ (\text{PF}_6^-)$		
Designation (8) (9)	I.R. in soln. ( $\text{CH}_2\text{Cl}_2$ or $\text{CH}_3\text{CN}$ )	Raman in soln. ( $\text{CH}_2\text{Cl}_2$ )	I.R. of mull	Raman solid	I.R. in $\text{CH}_2\text{Cl}_2$ solution	I.R. in mull	
(CH) 3			2197				
(CH) 18b	1121		1121		1120	1120	
(CCC) 6b	662	663	666 660	663		{ 666 660	
X-sens 15							
Methyl $M_2(b_1)$			2992?			2990	
Methyl $M_4(b_1)$			1447			1450	
Methyl $M_6(b_1)$	1061	1069	1063	1072	1063	1062	
$a_2$ (CH) 17a			952		941	954	
(CH) 10a	871		873				
(CC) 16a							
$b_2$ (CH) 5	975		975	970	976	975	
(CH) 10b	813		{ 820 813		811	810	
(CC) 4	712		713	714		711	
(CC) 11	491	487	490	485	494	495	
X-sens 16b							
Methyl $M_2(b_2)$			2992?			2990	
Methyl $M_4(b_2)$			1447			1450	
Methyl $M_6(b_2)$							

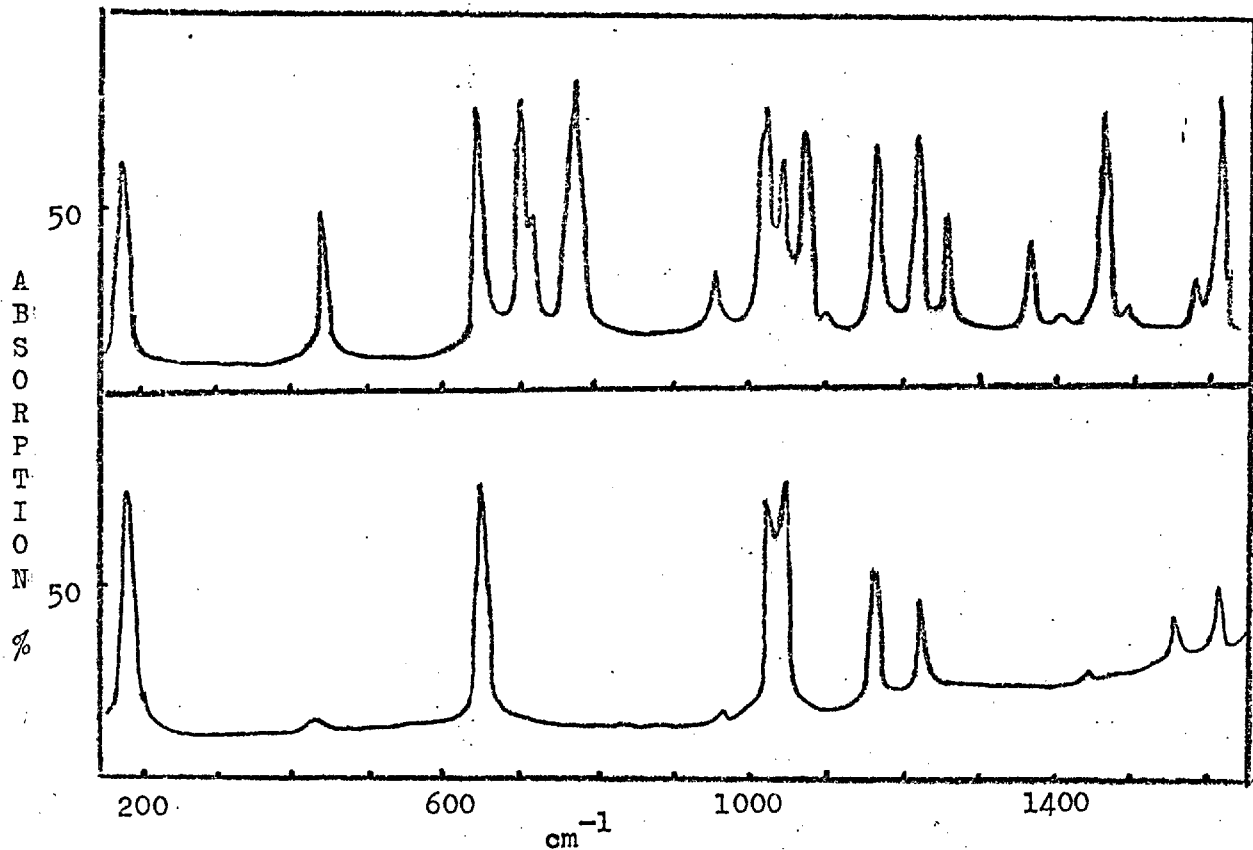


Fig. 12 . Top: Infrared spectrum of the  $(\text{Py}_2\text{I})^+$  cation. Above  $400\text{ cm}^{-1}$  in  $\text{CH}_2\text{Cl}_2$ , below  $400\text{ cm}^{-1}$  in pyridine solution.

Bottom: Raman spectrum in  $\text{CH}_2\text{Cl}_2$  solution.

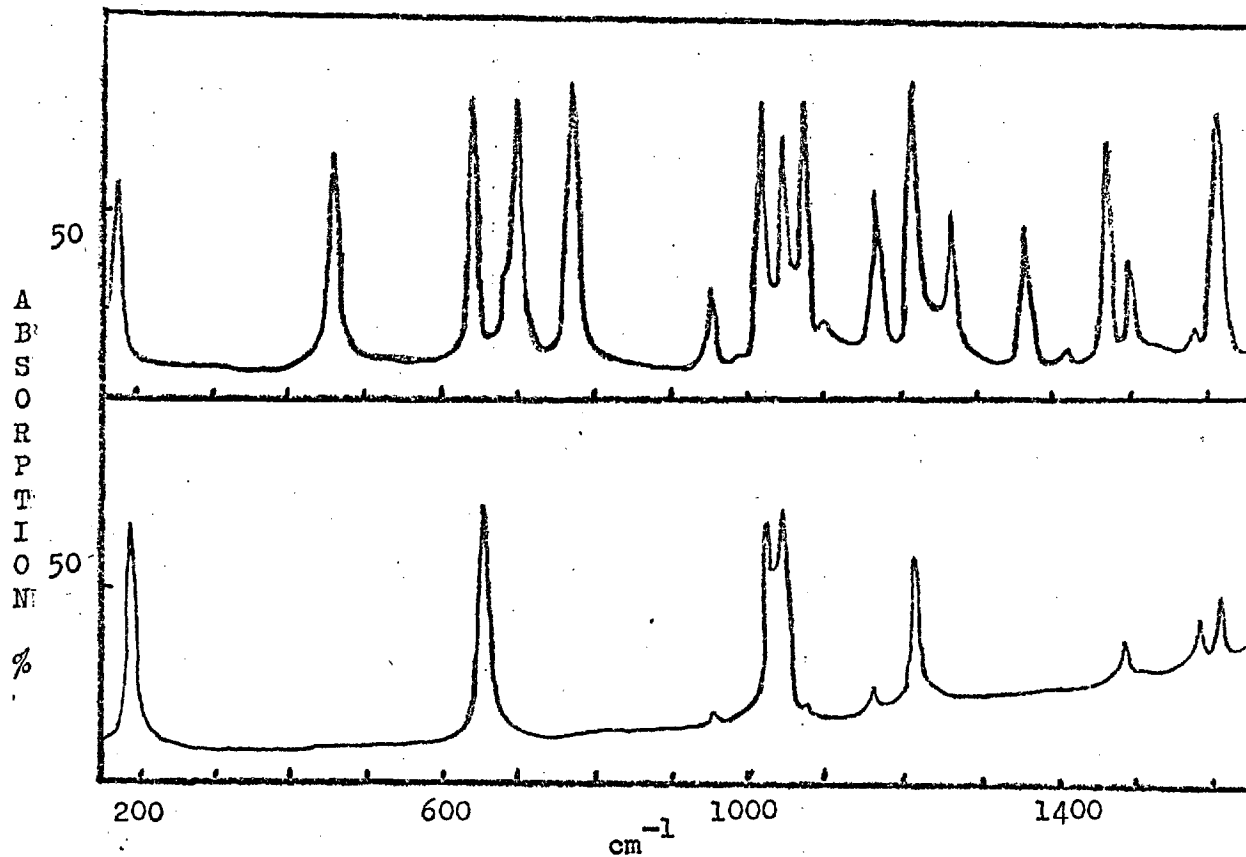


Fig. 13 . Top: Infrared spectrum of the  $(\text{Py}_2\text{Br})^+$  cation. Above  $400 \text{ cm}^{-1}$  in  $\text{CH}_2\text{Cl}_2$ , below  $400 \text{ cm}^{-1}$  in pyridine solution.

Bottom: Raman spectrum in  $\text{CH}_2\text{Cl}_2$  solution.

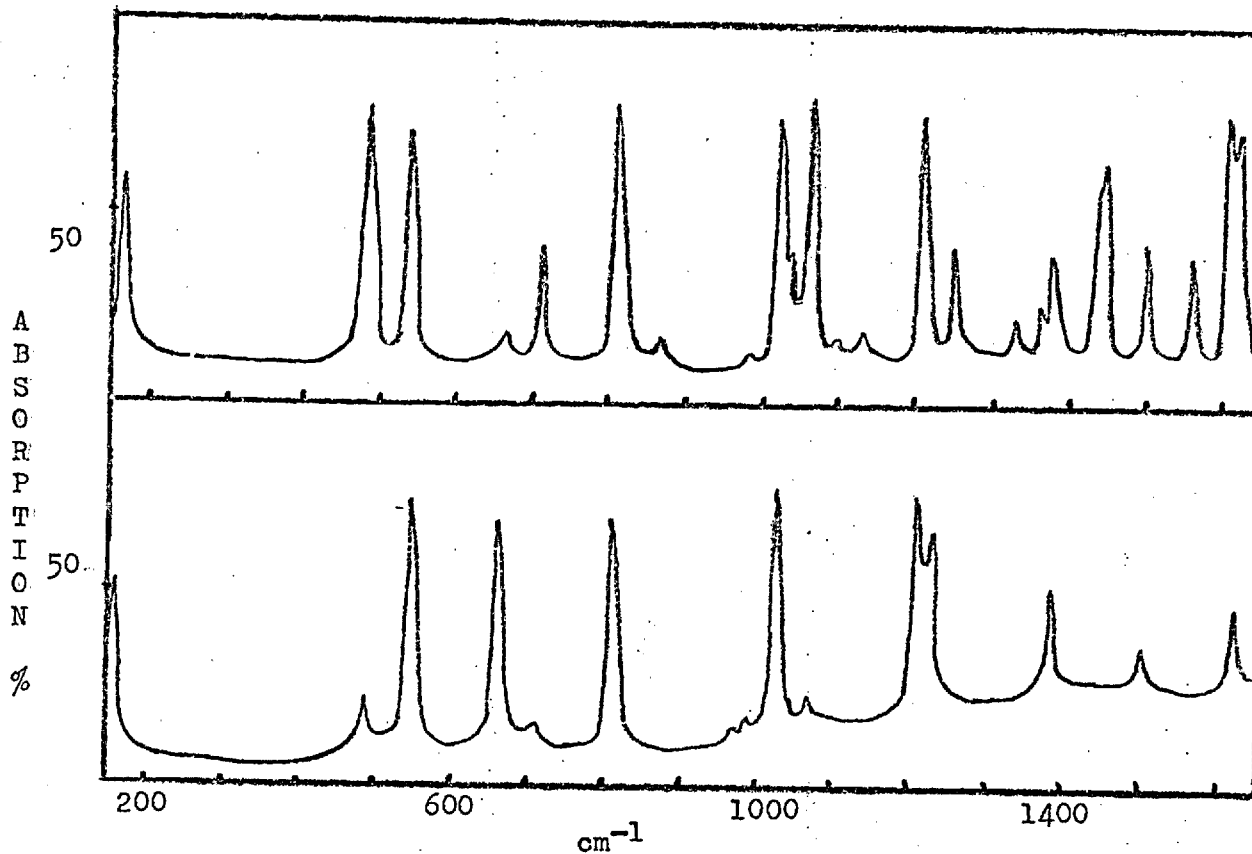


Fig. 14. Top: Infrared spectrum of the  $(\gamma\text{-Pic}_2\text{I})^+$  cation. Above  $400\text{ cm}^{-1}$  in  $\text{CH}_2\text{Cl}_2$ , below  $400\text{ cm}^{-1}$  in  $\gamma$ -picoline solution.

Bottom: Raman spectrum in  $\text{CH}_2\text{Cl}_2$  solution.

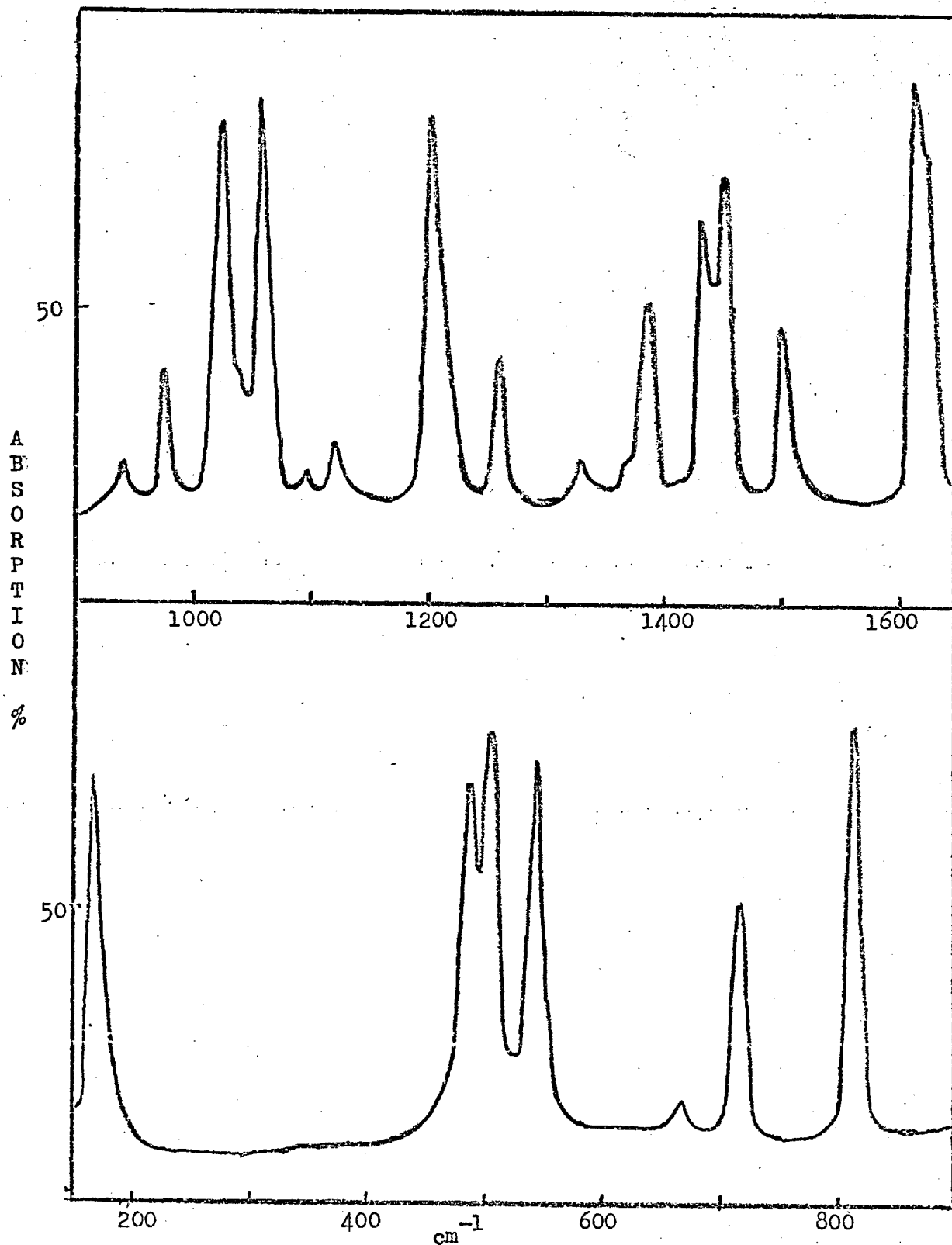


Fig. 15 Infrared spectrum of the  $(\gamma\text{-Pic}_2\text{Br})^+$  cation. Above 400  $\text{cm}^{-1}$  in  $\text{CH}_2\text{Cl}_2$ , below 400  $\text{cm}^{-1}$  in  $\gamma$ -picoline solution.

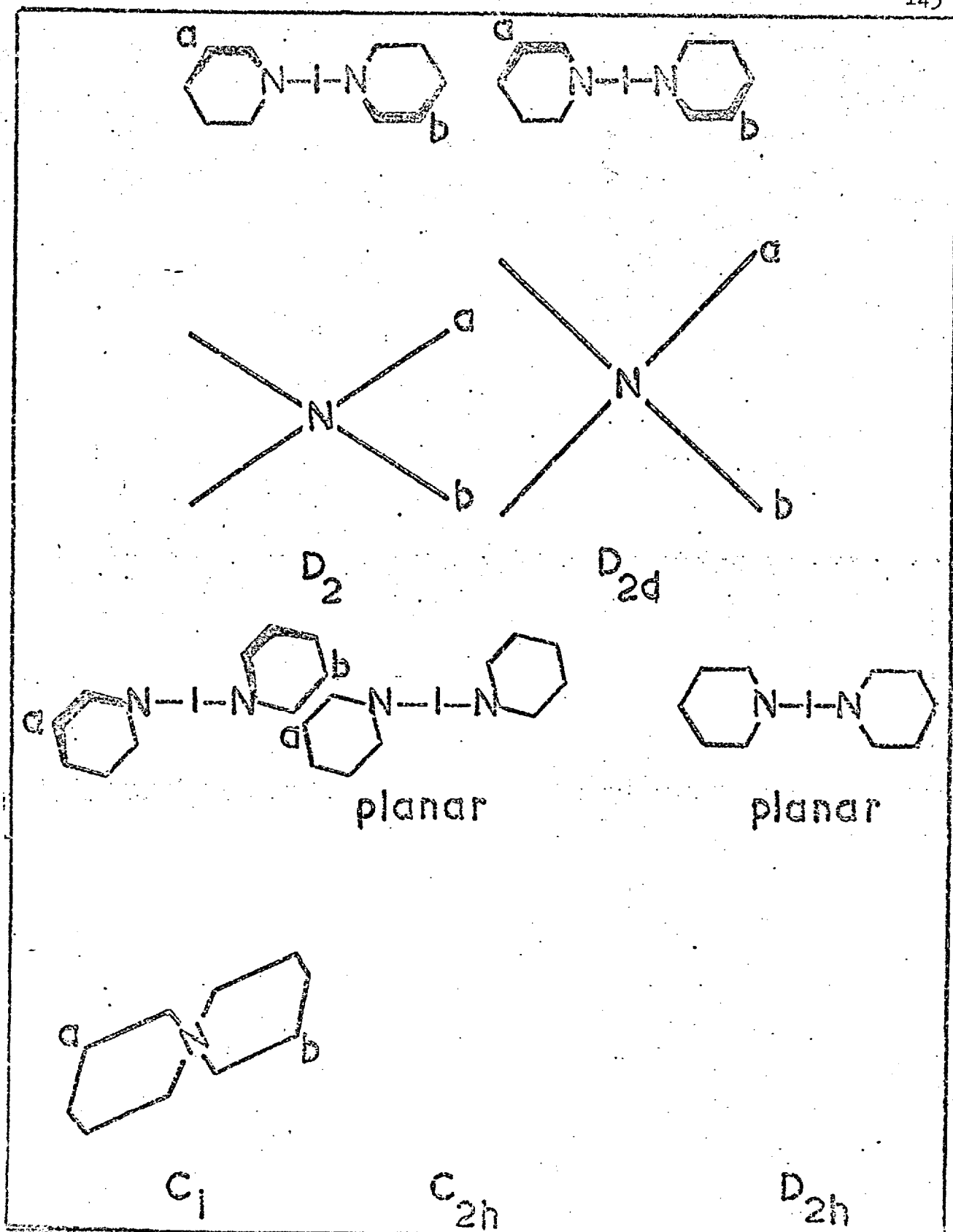


Fig. 16 Some possible rigid structures of the  $(Py_2I)^+$  cation, incorporating a linear N-I-N group.

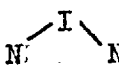
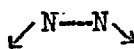
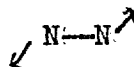
1. N—I—N    antisymmetric stretch
2.    "        symmetric stretch
3.     in-plane bend.
4.    "        out-of-plane bend
5.     in-plane
6.    "        out-of-plane
7.     in-plane
8.    "        out-of-plane
9. Torsion

Fig. 17    Modes involving the N-I-N atoms.

in the frequency range, only two strong bands are observed for each of the ions in solution as well as in the solid state. One of these is observed in the Raman but completely disappears in the infra-red. The other is infra-red active but is not seen in the Raman. For example, for the ion  $(\text{Py}_2\text{I})^+$  (Table 20), the Raman spectra show a strong polarised band at  $181\text{cm}^{-1}$  and infra-red spectra a strong band at  $172\text{cm}^{-1}$ . Neither of these bands is present in pure pyridine nor in the anions  $(\text{BF}_4^-, \text{PF}_6^- \text{ or } \text{ClO}_4^-)$ . The most likely assignments of these two bands are to the N-I-N stretching vibrations which are likely to be very intense. The position of these vibrations for the ion  $(\text{Py}_2\text{I})^+$ , may be crudely estimated from the relations,

$$\lambda_1 = (K + K_{12}) \mu_y$$

$$\lambda_3 = (K - K_{12}) \left( \mu_y + 2\mu_n \right)$$

where  $\mu_y$  and  $\mu_n$  are the reduced masses of pyridine and iodine respectively, and  $K$  and  $K_{12}$  are the stretching and interaction force constants respectively. We may assume the value of  $K$  to be approximately equal to the N-I force constant of  $\text{PyICl}$ , which is the strongest among the pyridine halogen charge-transfer complexes. This value has been calculated by Person et al to be  $1.02\text{mdyn}^{(50)}/\text{\AA}^0$ . A value of  $0.4\text{ mdyn}/\text{\AA}^0$  for  $K_{12}$  is not unreasonable.<sup>(50)</sup> Putting these values in the above equations one calculates the symmetric and antisymmetric stretching frequencies to be at  $174$  and  $172\text{cm}^{-1}$  respectively. By comparing with these values, the band at  $181\text{cm}^{-1}$ ,



which is observed only in Raman spectra may be assigned to the NIN symmetric stretching vibration and the band at  $172\text{cm}^{-1}$ , which is observed only in infra-red, to the antisymmetric stretching vibration of the ion  $(\text{Py}_2\text{I})^+$ . The mutual exclusion of these two bands between the infra-red and Raman spectra clearly demonstrates the colinearity of the N-I-N bonds. This immediately eliminates the bent N-I-N bond since in this case one would expect both the stretching vibrations to be Raman as well as infra-red active. By comparing with the  $(\text{py}_2\text{I})^+$  ion, the Raman bands of  $(\text{Py}_2\text{Br})^+$  at 193 and  $(\gamma\text{-pic}_2\text{I})^+$  at  $169\text{cm}^{-1}$  may be assigned to the NBrN and NIN symmetric stretching vibrations respectively, and the infra-red bands of  $(\text{Py}_2\text{Br})^+$  at 170,  $(\gamma\text{-pic}_2\text{I})^+$  at 164 and  $(\gamma\text{-pic}_2\text{Br})^+$  at  $170\text{cm}^{-1}$  to the NBrN, NIN and NBrN antisymmetric stretching vibrations. It may be concluded that all the ions possess a linear NXN bond.

The higher frequency vibrations may be considered to be counterparts of modes in the corresponding free base. To a quite good approximation, linear combination of the fundamentals of the free bases, give rise to pairs of bands in the cation spectrum, each pair split by interaction via the halogen atom. These  $2 \times 27$  vibrations (bis-pyridine ion) or  $2 \times 36$  vibrations (bis- $\gamma$ -picoline ions) may therefore be classified under the point group  $C_{2v}$  (symmetry of free bases). All the observed bands may be assigned by comparison with pyridine and pyridine-halogen complexes, and  $\gamma$ -picoline and  $\gamma$ -picoline-halogen complexes. In the following section we will

discuss the assignments of  $(\text{Py}_2\text{Br})^+$  and  $(\nu\text{-pic}_2\text{Br})^+$  are identical with their iodine counterparts. The following considerations refer to both solution and solid spectra.

$a_1$ -type vibrations:

$(\text{Py}_2\text{I})^+$  ion.

On the basis of intensity and polarisation data the Raman bands 1215, 1036, 1019 and  $645\text{cm}^{-1}$  are unequivocally correlated to the  $\nu_{8a}$ ,  $\nu_{9a}$ ,  $\nu_{12}$ ,  $\nu_1$  and  $\nu_{6a}$  modes of pyridine respectively. Similarly the strong infra-red bands at 1602, 1210, 1040, 1009 and  $638\text{cm}^{-1}$  may be correlated to the  $\nu_{8a}$ ,  $\nu_{9a}$ ,  $\nu_{12}$ ,  $\nu_1$  and  $\nu_{6a}$  modes of pyridine respectively. The most remarkable feature of these observations is the non co-incidence of Raman and infra-red frequencies deriving from the same mode of pyridine. The weak Raman bands at 1488 and  $1066\text{cm}^{-1}$ , and also infra-red bands at 1488 and  $1066\text{cm}^{-1}$ , and also infra-red bands at 1481 and  $1066\text{cm}^{-1}$  may be correlated to  $\nu_{19a}$  and  $\nu_{18a}$  modes of pyridine respectively.

$(\nu\text{-pic}_2\text{I})^+$  ion.

Similar correlations may also be made for this ion. Strong and polarised Raman bands at 1622, 1385, 1227, 1215, 1032, 818 and  $554\text{cm}^{-1}$ , and also the corresponding infra-red bands at 1618, 1383, 1226, 1207, 1024, 814 and  $545\text{cm}^{-1}$  may confidently be correlated to the  $\nu_{8a}$ ,  $\nu_{12}$ ,  $\nu_{9a}$ ,  $\nu_{13}$ ,  $\nu_1$ ,  $\nu_{12}$  and  $\nu_{6a}$  modes of  $\nu$ -picoline respectively.

The weak Raman band at  $1506\text{cm}^{-1}$  and infra-red band at  $1499\text{cm}^{-1}$  may both be related to the  $\nu_{19a}$  mode.

$b_1$ -type vibrations:

$(\text{Py}_2\text{I})^+$  ions.

Only a very few Raman bands may be assigned to this class. Generally bands of this class are weak in Raman spectra. However, at  $1157\text{cm}^{-1}$  the only depolarised band is observed, and this without doubt derives from the  $\nu_{15}$  mode of pyridine. Two other Raman bands at  $1576$  and  $1438\text{cm}^{-1}$  may be correlated to  $\nu_{18b}$  and  $\nu_{16b}$  modes respectively. The infra-red bands at  $1576$ ,  $1452$ ,  $1355$ ,  $1246$ ,  $1158$  and  $1090\text{cm}^{-1}$  may be related to the  $\nu_{8b}$ ,  $\nu_{19b}$ ,  $\nu_{14}$ ,  $\nu_3$ ,  $\nu_{15b}$  and  $\nu_{18b}$  respectively.

$(\gamma\text{-pic}_2\text{I})^+$  ion.

The very weak infra-red band at  $662\text{cm}^{-1}$  and the very strong depolarised Raman band at  $663\text{cm}^{-1}$  may be correlated to the  $\nu_{6b}$  mode of  $\gamma$ -picoline. For all 4-substituted pyridines this planar ring deformation ( $\nu_{6b}$ ) always appears especially intense in the Raman spectrum whilst, in the infra-red it is weak.<sup>(88)</sup> Strong infra-red bands in the spectra at  $1439$  and  $1447\text{cm}^{-1}$  may readily be assigned to  $\nu_{16b}$  and  $M_4$  modes of  $\gamma$ -picoline. The infra-red band at  $1283\text{cm}^{-1}$  of  $\gamma$ -picoline which has been assigned to  $\nu_3$ <sup>(88)</sup> modes requires some comments. In both the cations and the  $\gamma$ -picoline-halogen charge-transfer complexes two bands are observed in this region; one at

1260cm<sup>-1</sup> and the other at 1297cm<sup>-1</sup>. The former is the stronger, and would therefore seem more likely to be the fundamental derived from  $\nu_3$ . As the vibrations of this class are not sensitive to complexing; it seems that the assignment<sup>(88)</sup> of a band at 1283cm<sup>-1</sup> in  $\nu$ -picoline to the  $\nu_3$  fundamental may need revision. Other vibrations which may very easily be related to the corresponding  $\nu$ -picoline modes needs no comment (Table 24).

### a<sub>2</sub>-type vibrations:

(Py<sub>2</sub>I)<sup>+</sup> ion:

The frequencies of these modes are expected to be very close to those of the corresponding pyridine modes. Only one band, the Raman band at 362cm<sup>-1</sup> may be assigned to this class and may be related to  $\nu_{16a}$  mode of pyridine.

( $\nu$ -pic<sub>2</sub>I)<sup>+</sup> ion:

The Raman bands at 952 and 873 may be related to  $\nu_{17a}$  and  $\nu_{10a}$  modes of  $\nu$ -picoline. The infra-red band at 871cm<sup>-1</sup> may also be related to  $\nu_{10a}$ .

### b<sub>2</sub>-type vibrations:

(Py<sub>2</sub>I)<sup>+</sup> ion:

The two ring deformations ( $\nu_4$  and  $\nu_{11}$ ) are identified with the strong infra-red bands at 760 and 690cm<sup>-1</sup>. The latter appears also in the Raman spectrum as a weak band. The X-sensitive ( $\nu_{16b}$ ) band

is identified with a strong infra-red band at  $438\text{cm}^{-1}$ , and a weak Raman band at  $422\text{cm}^{-1}$ . The infra-red bands at  $945$  and  $813\text{cm}^{-1}$  may be assigned to  $\nu_5$  and  $\nu_{10b}$  modes of pyridine respectively.

( $\gamma$ -pic<sub>2</sub>I)<sup>+</sup> ion:

The infra-red band at  $712\text{cm}^{-1}$  and the Raman band at  $714\text{cm}^{-1}$  may be assigned to the  $\nu_4$  ring deformation of  $\gamma$ -picoline. The other ring deformation,  $\nu_{11}$ , appears at  $491\text{cm}^{-1}$  in the infra-red and  $485\text{cm}^{-1}$  in the Raman. The infra-red bands at  $2992$  and  $1447\text{cm}^{-1}$  may be related to the  $M_2$  and  $M_6$  modes respectively.

Now we are in a position to discuss the possible rigid structures which incorporate a linear N-I-N linkage. The correlation of fundamentals of  $D_2$ ,  $D_{2d}$ ,  $C_i$ ,  $C_{2h}$  and  $D_{2h}$  with  $C_{2v}$  are shown in Table 25, together with their infra-red and Raman activity. (113)

The  $D_2$  and  $D_{2d}$  structures do not have a centre of symmetry, while the  $C_i$ ,  $C_{2h}$  and  $D_{2h}$  do. It is clear from the correlation table that the cation modes derived from the  $b_1$  and  $b_2$  classes of the  $C_{2v}$  point group should be active in both the infra-red and Raman spectra in  $D_2$  and  $D_{2d}$  symmetry; while the pair of cation vibrations derived from the  $a_1$  mode should both be Raman active. These requirements are not observed. For example, of the pair of bands  $1009$  and  $1019\text{cm}^{-1}$  (Table 20) in the ( $\text{py}_2\text{I}$ )<sup>+</sup> ion derived from  $992\text{cm}^{-1}$  ( $a_1$  class) of pure pyridine, only the  $1019\text{cm}^{-1}$  band which is observed in infra-red completely disappears in the Raman. This fact eliminates the  $D_2$  and  $D_{2d}$  structures.

Table 25

Correlation between the symmetry classes; and selection rules.

$D_2$	$D_{2d}$	$C_{2v}$	$C_i$	$C_{2h}$	$D_{2h}$
$a$ (R)	$a_1$ (R)	$a_1$	$a_g$ (R)	$a_g$ (R)	$a_g$ (R)
$b_1$ (IR+R)	$b_2$ (IR+R)	$(R+IR)$	$a_u$ (IR)	$b_u$ (IR)	$b_{1u}$ (IR)
$b_1$ (IR+R)	$a_2$ (inactive)	$a_2$	$a_g$ (R)	$b_g$ (R)	$b_{1g}$ (R)
$a$ (R)	$b_1$ (R)	$(R)$	$a_u$ (IR)	$a_u$ (IR)	$a_u$ (inactive)
$b_2$ (IR+R)	$e$ (IR+R)	$b_1$	$a_g$ (R)	$a_g$ (R)	$b_{2g}$ (R)
$b_3$ (IR+R)		$(R+IR)$	$a_u$ (IR)	$b_u$ (IR)	$b_{3u}$ (IR)
$b_2$ (IR+R)	$e$ (IR+R)	$b_2$	$a_g$ (R)	$b_g$ (R)	$b_{3g}$ (R)
$b_3$ (IR+R)		$(R+IR)$	$a_u$ (IR)	$a_u$ (IR)	$b_{2u}$ (IR)

The mutual exclusion of Raman and infra-red bands indicates that the cation structure must have a centre of symmetry.  $C_1$  and  $C_{2h}$  structures demand that the modes derived from the  $a_2$  class should be infra-red active. The absence in most of the observed infra-red spectra, of any bands near to the  $a_2$  class frequencies of pyridine (986, 891 and  $375\text{cm}^{-1}$ ) for the  $(\text{py}_2\text{X})^+$  ions, and of  $\nu$ -picoline (937, 872 and  $384\text{cm}^{-1}$ ) for the  $(\nu\text{-pic}_2\text{X})^+$  ions, supports a  $D_{2h}$  structure for the cations. The difference between the infra-red and Raman frequencies of the most prominent fundamentals  $\nu_{8a}, \nu_{9a}, \nu_1, \nu_{6a}$  and  $\nu_{16b}$  remains the same, within experimental error both in solution and in the solid state (Table 24). This indicates a similar interaction between the rings in the two states and provides further evidence that the  $D_{2h}$  structure of the solid is preserved in solution. Retention of the planar structure in solution needs a strong  $\pi$  electron interaction extended over both the rings. This means that back-donation from the halogen atom to the ring may be an important factor in the bonding (ref. sec.5). In an LCAO-SCF treatment, Singh<sup>(114)</sup> has calculated the stabilisation energy due to  $\pi$  electron overlap and has shown that the increased stabilisation energy for the configuration at  $\Theta = 0(D_{2h})$  over that  $\Theta = 90^\circ(D_{2d})$  is 2.6 KCal/mole. All these considerations favour a  $D_{2h}$  structure of the cations.

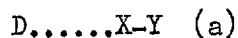
The possibility of free rotation about the N-X-N axes and torsion has been fully discussed in the paper No.5. attached at the back of the thesis.

4.5. Classification of Modes: The  $C_{2v}$  fundamental modes of the  $C_5H_5N$  or  $4-CH_3C_5H_4N$  molecules give rise in  $(Py_2X)^+$  or  $(\nu-pic_2X)^+(D_{2h})$  to two modes; a 'g' and a 'u' mode. Since all 'g' modes are infra-red inactive and all 'u' modes are Raman inactive no confusion is likely to arise in referring to the vibrations in terms of the  $C_{2v}$  classes from which they are derived. This is shown in Table 7. However, we may classify the vibrations in the various  $D_{2h}$  symmetry classes. For  $D_{2h}$  symmetry the vibrations fall into eight classes. Taking into account the skeletal vibrations, the  $D_{2h}$  fundamentals for  $(py_2X)^+$  ion separate as  $11A_g(R-P)+10B_{2g}(R-dp)+6B_{3g}(R-dp)+3B_{1g}(R-dp)+4A_u(\text{inactive})+7B_{eu}(IR)+11B_{3u}(IR)+11B_{1u}(IR)$ . Out of these 63 fundamentals 2 x 27 vibrations will be similar to those in pyridine. Going from 2 pyridine to  $(py_2X)^+$  results in the appearance of nine new modes. These nine vibrations  $1A_g+2B_{1u}+B_{2u}+1B_{2g}+2B_{3u}+1A_u+1B_{3g}$  arise from motion of the base rings as a whole, and would expect to be below  $300cm^{-1}$ . Similarly the 91 vibrations of  $(\nu-pic_2X)^+$  may be distributed among the classes,  $13A_g+13B_{2g}+9B_{3g}+4B_{1g}+5A_u+10B_{2u}+14B_{3u}+13B_{1u}$ .



## 5. GENERAL DISCUSSIONS

5.1. Force Constants: The structure of charge-transfer complexes between 'n' donors and halogen acceptors has been described (46) in terms of two resonance structures,



This model predicts that the X-Y (halogen-halogen) force constant will decrease, and the D-X (donor-halogen) force constant increase, as the contribution of the structure (b) increases. This study has provided information on force constants in a series of related charge-transfer complexes. Accordingly the force constants of the D-X and X-Y bonds of pyridine-halogen and picoline-halogen charge-transfer complexes, and also the N-X-N bonds of the  $(Py_2X)^+$  and  $(\gamma-pic_2I)^+$  ions have been estimated. To calculate these stretching force constants a linear simplified triatomic model and a simple valency force field are assumed (nomenclature given in Figure 18). This assumption

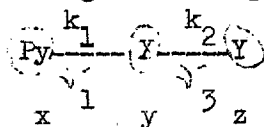


Figure 18

has some justification, since in these cases other molecular vibrations are well separated from the stretching modes under consideration, and so interaction with them should be relatively small. Justification for taking the whole mass of the pyridine or picoline molecule as a point mass in the model, is provided by comparison with

hydrogen-bonding studies<sup>(115)</sup> where, for a series of phenols and pyridines, a linear relationship between the stretching frequencies and reduced mass has been demonstrated, i.e.

$$\Delta \nu \propto \mu \nu_0^2$$

where  $\nu$  is the change in O-H stretching frequency on complex formation,  $\nu_0$  is the hydrogen bond stretching frequency and  $\mu$  is the reduced mass of the complex given by

$$\mu = \frac{1}{M_1} + \frac{1}{M_2}$$

where  $M_1$  and  $M_2$  are the total masses of phenol and pyridine.

The stretching force constants for the cations and charge-transfer complexes are given in Tables 26 and 27. The vibrational frequencies used to calculate the force constants are also included. These constants were calculated using the equations for a linear x y z type molecule;

$$\lambda_1 + \lambda_2 = \frac{K_1}{\mu_x} + \frac{K_2}{\mu_z} + (K_1 + K_2 - 2K_{12}) \mu_y \text{-----(1)}$$

$$\lambda_1 \lambda_3 = \frac{(K_1 K_2 - K_{12}^2)}{\mu_x \mu_y + \mu_y \mu_z + \mu_x \mu_z} \text{-----(2)}$$

where  $\mu_i$  are the reciprocal masses and  $K_1$  and  $K_2$  are force constants of the x-y and y-z bonds respectively;  $K_{12}$  is the interaction constant. For a symmetrical linear molecule of the type yxy equations(1)and (2) may be simplified thus:

$$\lambda_1 = (K + K_{12}) \mu_y \text{-----(3)}$$

$$\lambda_3 = (K - K_{12}) \left( \frac{\mu_y}{\mu_x} + 2 \mu_x \right) \text{-----(4)}$$

Equations (3) and (4) were used to calculate the stretching force constants of the cations  $(\text{Py}_2\text{I})^+$ ,  $(\text{Py}_2\text{Br})^+$  and  $(\gamma\text{-pic}_2\text{I})^+$ .

In using equations (1) and (2) there are three unknown for constants  $K_1, K_2$  and  $K_{12}$  and only two frequencies (D-X and X-Y stretching). Lake and Thompson<sup>(52)</sup> in calculating the force constants  $K_{\text{I-I}}$  and  $K_{\text{N-I}}$  for pyridine iodine and related complexes assumed that the  $K_{12}=0$ . However, certain considerations make this assumption seem rather unjustified. For instance when the D-X bond stretches, the complex may be considered to be of the 'no bond' structure (a) and the X-Y molecule as a free halogen. Conversely when the D-X bond contracts the dative bond structure (b) with a weak interhalogen bond will predominate. Thus we might expect the interaction constant between the D-X and X-Y bonds to be larger than for a normal co-valent molecule. Person and Coworkers<sup>(50)</sup> have evaluated force constants for  $\text{PyI}^+\text{Br}^-$  and  $\text{PyI}^+\text{Cl}^-$  complexes assuming  $K_{12}=0.40 \text{ mdyn/\AA}^2$ . By comparison with the interaction constant of the trihalide ions,<sup>(91,104)</sup> their assumed value seems to be quite reasonable. On the other hand, Watri<sup>(40)</sup> finds this constant, for the  $\text{PyI}^+\text{Cl}^-$  complex, to be  $K_{12}=0.22 \text{ mdyn/\AA}^2$ . He estimated this value from the known I-Cl stretching force constant calculated by Badger's rule.<sup>(116)</sup> In view of these differences, perhaps the best value for the interaction constant may be obtained from the N-X-N bonds of the cations and trihalide ions. For example,  $K_{12}$  for the  $\text{PyI}^+\text{Cl}^-$  molecule may be assumed to be the average of the NIN interaction

TABLE 26

Stretching and interaction force constants for cations  
and related molecules

Compound	$\nu_{1-1}$ cm <sup>-1</sup>	$\nu_{3-1}$ cm <sup>-1</sup>	K (mdyn/A°)	K <sub>12</sub> (mdyn/A°)	K <sub>12</sub> /K	K+K <sub>12</sub> (mdyn/A°)	K-K <sub>12</sub> (mdyn/A°)
(Py <sub>2</sub> I) <sup>+</sup>	182	172	1.08	0.46	0.42	1.54	0.62
(Py <sub>2</sub> Br) <sup>+</sup>	193	170	1.09	0.64	0.59	1.73	0.45
(ν-pic <sub>2</sub> I) <sup>+</sup>	163	161	1.02	0.40	0.40	1.42	0.62
Br <sub>3</sub> <sup>-(c)</sup>	162	193	0.91	0.32	0.35	1.23	0.59
ICl <sub>2</sub> <sup>-(b)</sup>	254	226	1.02	0.33	0.33	1.35	0.69
lBr <sub>2</sub> <sup>-(b)</sup>	160	171	0.91	0.30	0.33	1.21	0.61
HF <sub>2</sub> <sup>-(b)</sup>	600	1425	2.31	1.72	0.74	4.03	0.59
CO <sub>2</sub> <sup>(a)</sup>	1337	667	15.50	1.30	0.08	16.80	14.2
CS <sub>2</sub> <sup>(a)</sup>	657	397	7.50	0.60	0.08	8.10	6.90

(a) See Ref. (118) P.173 and 187

(b) See Ref. (104)

(c) See Ref. (91)

TABLE 27

Stretching force constants for charge-transfer  
complexes and free halogens.

Compound	$\nu_1$ cm <sup>-1</sup>	$\nu_2$ cm <sup>-1</sup>	$K_1$ (mdyn/Å <sup>2</sup> )	$K_2$ (mdyn/Å <sup>2</sup> )	$K_{12}$ (mdyn/Å <sup>2</sup> )	$\frac{1}{2}(K_1+K_2)-K_{12}$ (mdyn/Å <sup>2</sup> )
PyI <sub>2</sub> <sup>(c)</sup>	100	171	0.36	1.28	0.29	0.53
PyIBr <sup>(d)</sup>	134	204	0.63	1.38	0.38	0.63
PyICl <sup>(d)</sup>	147	290	0.73	1.48	0.39	0.71
γ-picI <sub>2</sub> <sup>(a)</sup>	88	181	0.32	1.40	0.26	0.60
γ-picIBr	124	201	0.638	1.30	0.35	0.62
γ-picICl	135	284	0.68	1.42	0.36	0.63
PyBr <sub>2</sub>	128	229	0.61	1.49	0.48	0.57
PyBrCl	144	307	0.69	1.58	0.55	0.58
I <sub>2</sub> <sup>(b)</sup>		207		1.60		
IBr <sup>(b)</sup>		261		1.97		
ICl <sup>(b)</sup>		375		2.30		
Br <sub>2</sub> <sup>(b)</sup>		312		2.29		
BrCl <sup>(b)</sup>		431		2.69		

(a) Frequencies from Ref. (52)

(b) Frequencies from Ref. (47)

(c) Frequencies from Ref. (103)

(d) Frequencies from Ref. (48)

constants for the  $(\text{Py}_2\text{I})^+$  and  $\text{ICl}_2^-$  ions. This assumption is justified by the fact that the bonding and charge on the central atom of a trihalide ion, and the charge on the nitrogen atoms of a cation are comparable with that found in charge-transfer complexes.<sup>(48)</sup> We believe that this is the most reliable method for deriving values of  $K_{12}$ , which does not involve an explicit normal co-ordinate treatment. Some support of the value of  $K_{12}$  calculated by a method is given by the fact that relation  $\frac{1}{2}(K_1+K_2)-K_{12} \approx 0.6$  is found for all the complexes studied (Table 27 column 7). This relation was proposed by Maki and Forneris<sup>(104)</sup> from the force constants of trihalide ions. Column 6 of Table 27 shows the values of  $K_{12}$  which were used in calculating the stretching force constants.

$K_1$  and  $K_2$  reported in Table 27 are in disagreement with previously reported values.<sup>(40,50)</sup> This is for two reasons, (i) different choice of interaction constants and (ii) most of the previously reported stretching force constants were calculated using frequencies in the solid state. The skeletal vibration frequencies of charge-transfer complexes in the solid state are generally higher than those found in solution. It seems that the force constants of this type of complex have little meaning without mentioning the solvent used in the measurement of the spectrum from which they were calculated.

The relative change in X-Y force constant  $(K_0 - K_2/K_0)$  has been used to estimate the weight of the dative state,  $(51)_{b^2+abS}$ , in the

structure of the complex. These two are related by the equation

$$(K_0 - K_{12})/K_0 = (1 - \frac{K_1}{K_2})(b^2 + abS) \text{-----} (5)$$

where  $K_0$  and  $K_1$  are the X-Y stretching force constants in the free X-Y and  $(X-Y)^-$  molecules, respectively; 'a' and 'b' are the co-efficients of no-bond and dative bond structures respectively; and S is the overlap integral. Frequencies for some  $(X-Y)^-$  ions have been shown to be about one-half the frequencies for the free molecules. Thus one can derive the ratio  $K_1/K_0 \cong 0.25$ . Equation (5) may be approximated thus: <sup>(117)</sup>

$$(K_0 - K_2)/K_0 = \Delta K/K \cong b^2 + abS \text{-----} (6)$$

Table 28 shows the estimates of the weight of the dative structure obtained from the equations (5) and (6) for the charge-transfer complexes. In Table 27, the frequencies of the halogens in carbontetrachloride solution are chosen as reference frequencies from which to derive  $K_0$ , the force constant of the free halogen. The weight of the dative structure for the  $PyI_2$  complex (calculated by using equation (6)) has been reported by Yarwood and Person <sup>(117)</sup> to be in the range 0.13-0.29, depending mainly on  $K_{12}$ . In fact we calculated a value of 0.20 for this complex. Again this value has little meaning without mentioning the solvent used. To get internally comparable values within a series of complexes one must take frequencies measured in the same solvent. All our results refer to benzene solution, except  $\nu\text{-picI}_2$  which was studied in cyclohexane. It is quite clear from Table 28 that the weight of

TABLE 28

Estimates for the weight of the dative structure

$$(b^2 + abS)$$

Complex	from equation (6)		from equation (5)	
		%		%
PyI <sub>2</sub>	20.00		26.6	
PyIBr	29.9		39.8	
PyICl	35.58		47.4	
γ-picI <sub>2</sub>	12.5		16.66	
γ-picIBr	33.72		45.00	
γ-picICl	38.08		51.00	
PyBr <sub>2</sub>	35.02		46.69	
PyBrCl	41.26		55.01	



the dative structure increases on going from iodine to ICl complexes. Moreover, the weights for  $\gamma$ -picoline-halogen complexes are larger than those for the pyridine-halogen complexes. This is to be expected, considering the order of the acid strength of the halogens which follows the series  $\text{ICl} > \text{IBr} > \text{I}_2$ , and from the fact that the ionization potential of  $\gamma$ -picoline is smaller than pyridine. The values for bromine complexes are also found to be greater than those for iodine complexes. This indicates a greater charge-transfer from the pyridine ring.

Now returning to the force constants of cations given in Table 26, a value for the interaction constant which approaches 50% of the stretching constant is indeed unusual. High interaction constants are also observed in trihalides and in the  $\text{HF}_2^-$  ion (given at the bottom of the Table 26). For a normal co-valent molecule e.g.  $\text{CO}_2, \text{CS}_2$  etc. the order of magnitude of the interaction constant is approximately 10%<sup>(118)</sup> of the stretching constant.

The effect of high interaction constant may be understood from the following consideration. The potential energy of a linear symmetric triatomic molecule may be written as (neglecting cubic and higher order terms).

$$2V = K_A \nu_1^2 + K_A \nu_2^2 + K_{12} \Delta \nu_1 \nu_2 \text{-----} (7)$$

Where  $\nu_1$  and  $\nu_2$  are the distances from the central to the end atoms. The N-X-N antisymmetric vibration for the cations may be regarded as

involving only motion of the central halogen atom between the two end atoms i.e. the N-N distance remains fixed during this vibration. In this case  $\Delta v_1 = -\Delta v_2$  and the equation (7) reduces to

$$2V = (2K - K_{12}) \Delta v_1^2 \text{-----} (8)$$

From this it is clear that the higher the value of the interaction constant the lower is the **energy** required to execute the antisymmetric mode. In other words the central halogen atom is very loosely bound at the equilibrium position.

Table 29 gives the bending force constants. These were calculated using the equation for a linear xyz type molecule

$$4\pi^2 c^2 \nu_2^2 = \frac{1}{b_1^2 b_2^2} \left[ \frac{b_1^2}{M_z} + \frac{b_2^2}{M_x} + \frac{(b_1 + b_2)^2}{M_y} \right] K \sigma$$

Where  $\nu_2$  is the bending frequency and  $b_1$  and  $b_2$  are the distances of x and z respectively from y. Since the bond distance of the  $(\text{pic}_2\text{I})^+$  ion is not known, it was assumed to be same as the  $(\text{Py}_2\text{I})^+$  ion. For comparison purposes, the bending force constants of several other molecules are also included in the Table.

TABLE 29

Bending force constants

Compound	$\nu_2$ ( $\text{cm}^{-1}$ )	$K_S/1_1 1_2$ ( $\text{mdyn}/\text{A}^0$ )
PyICl	92	0.07
PyIBr	94	0.09
(Py <sub>2</sub> I) <sup>+</sup>	90	0.09
( $\nu$ -pic <sub>2</sub> I) <sup>+</sup>	80	0.087
I <sub>3</sub> <sup>-</sup> (a)	69	0.06
IBr <sub>2</sub> <sup>-</sup> (a)	98	0.10
ICl <sub>2</sub> <sup>-</sup> (a)	138	0.13

(a) See Ref. (104)

5.2. Effect of Environment: A polar solvent is expected to favour the charge separated, dative-bond structure of the charge-transfer complex, giving rise to a large contribution of this structure in the ground state. In other words, as the polarity of the environment increases, the transfer of charge from the donor to the acceptor should increase resulting in shifts of the vibration frequencies of pyridine and  $\gamma$ -picoline ring modes to higher values. In addition, the X-Y stretching frequency should drop and the D-X frequency rise. Furthermore, greater environmental effects are likely to be observed in stronger complexes. Studies of these effects are now reported.

The solvents used in this study are not sufficiently strong donors to displace the pyridine or  $\gamma$ -picoline from the complex. Considering first the donor frequencies; it is observed that the vibrations which are sensitive to the degree of electron transfer move in the same direction through a series of environments of increasing polarity as they do in a series of complexes where the acceptor strength increases. This is shown in Table 30, for  $\nu_1$  and  $\nu_{6a}$  modes (these two being the most sensitive to complexation). The precise position of both these modes seems to be dependent upon the nature of the environment. Thus, the frequency shifts of the  $\nu_1$  and  $\nu_{6a}$  vibrations are dependent upon a common factor, and should therefore be directly related to each other. Figure 19 shows plots of  $\Delta\nu_1$  against  $\Delta\nu_{6a}$  for the complexes  $\gamma$ -picI<sub>2</sub>Br and  $\gamma$ -picI<sub>2</sub>Cl in a variety of environments. These two complexes are



TABLE 30 (Cont'd)

Complex	Solvent					
	CS <sub>2</sub>	C <sub>6</sub> H <sub>6</sub>	CH <sub>2</sub> Cl <sub>2</sub>	Py	γ-pic	Mull
γ-picICl	( $\lambda$ )	1017	1023		1022	1024
	( $\lambda$ ) <sub>6a</sub>	535	540		543	549
(γ-pic <sub>2</sub> I) <sup>+</sup>	( $\lambda$ )		1025			1025
	( $\lambda$ ) <sub>6a</sub>		545			545

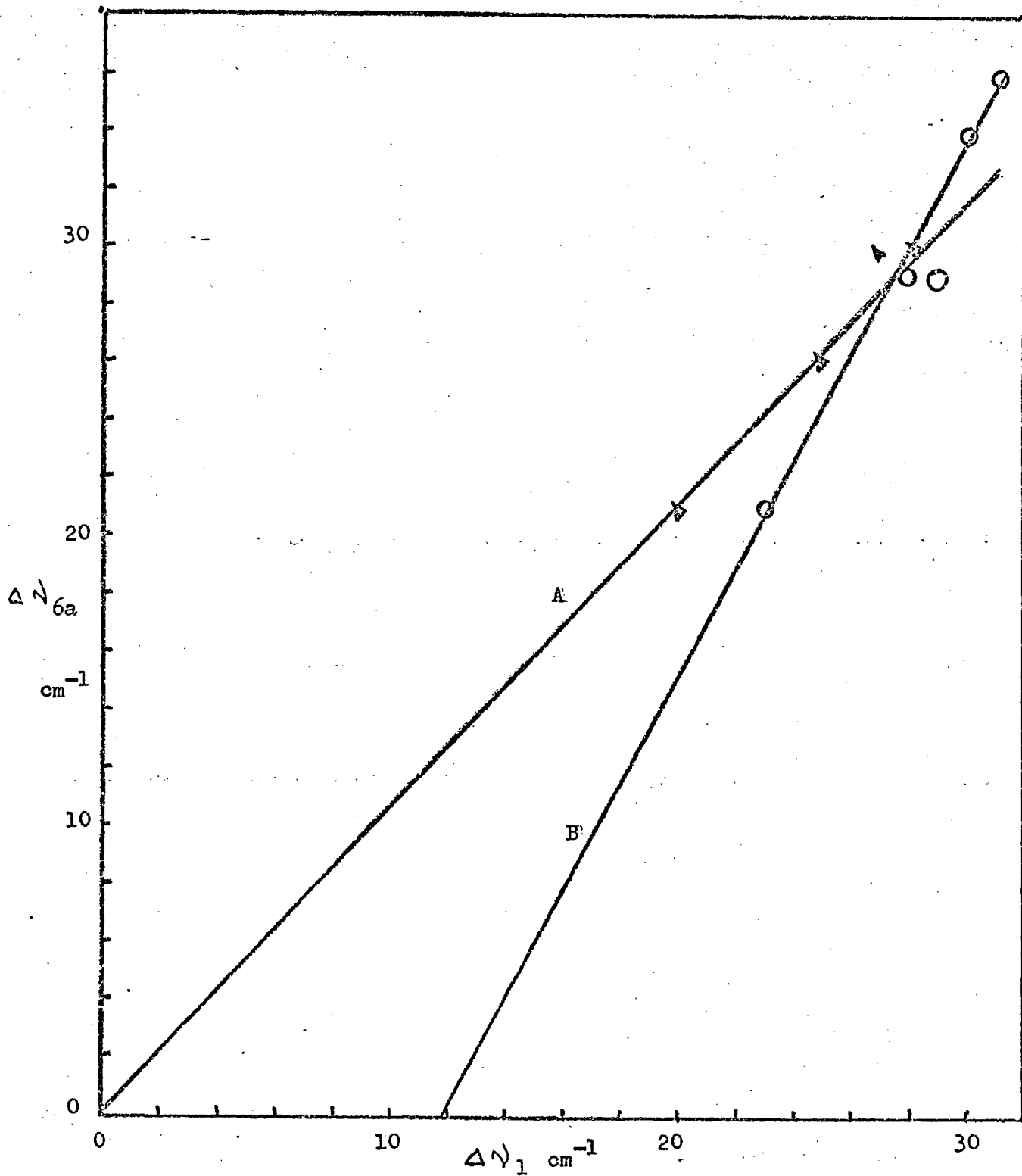


Fig. 19. Plots of  $\Delta\nu_1$  against  $\Delta\nu_{6a}$  in a variety of solvents

(A)  $\gamma$ -PicIBr; (B)  $\gamma$ -PicICl.

chosen because a large amount of data is available on them. Evidence for similar effects in different complexes is given by the fact that, when the shifts in a sensitive vibration of a complex, for example,  $\Delta \nu_1$ , are plotted against  $\Delta \nu_1$  for another complex (same donor) in a variety of common solvents, then a series of points is obtained corresponding to the different solvent used, which all fall on a straight line. This is shown in Figure 20, for  $\nu_1$  and  $\nu_{6a}$  of the complexes  $\gamma$ -picI<sub>2</sub>Br and  $\gamma$ -picI<sub>2</sub>Cl.

The X-Y and D-X stretching vibrations are found to be the most sensitive to solvent changes (Table 31 and 32). The former frequency falls and the latter rises as the polarity of the environment increases. This rise in the D-X stretching frequency is just the reverse of what is generally observed for a simple stretching vibration. Generally in solution the band peak of all stretching vibrations are displaced to lower frequencies as the polarity of the solvent is increased.<sup>(119)</sup> However, in a few exceptional cases, for example the N=O stretch of nitrosyl chloride, the stretching frequency increases as the polarity of the environment increases.<sup>(120)</sup> This is because more polar solvents bring about an increase in the proportion of the ionic canonical form  $(O \equiv N)^+ - Cl^-$ , thereby increasing the N=O frequency towards that of the  $(N \equiv O)^+$  radical. A similar explanation may be given for the D-X stretching frequency. With the increase in polarity of the environment the contribution of the structure  $(D-X)^+ - Y^-$  increases.



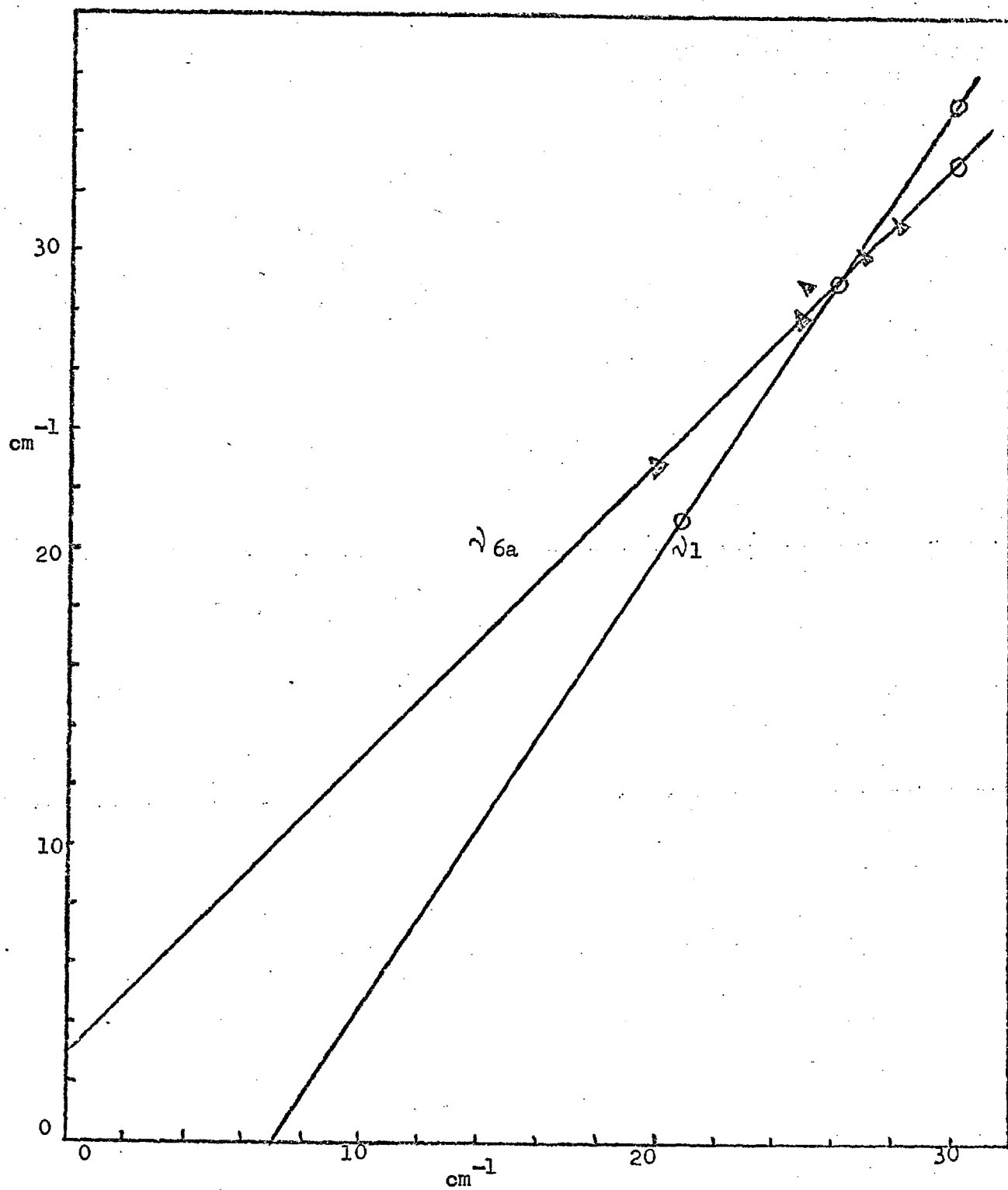


Fig. 20 Plots of  $\Delta\nu_1$  and  $\Delta\nu_{6a}$  for  $\gamma$ -PicICl against the corresponding modes for  $\gamma$ -PicIBr in a variety of solvents.

TABLE 31

Effect of solvent on X-Y stretching  
vibration (Raman).

Solvent	PyIBr		PyICl		PyBr <sub>2</sub>		PyBrCl	
	$\frac{\text{I-Br}}{\text{cm}^{-1}}$	$\Delta$ %	$\frac{\text{I-Cl}}{\text{cm}^{-1}}$	$\Delta$ %	$\frac{\text{Br-Br}}{\text{cm}^{-1}}$	$\Delta$ %	$\frac{\text{Br-Cl}}{\text{cm}^{-1}}$	$\Delta$ %
Benzene	204	21.8	292	22.1	226	27.6	308	28.5
1:4 Dioxane	203	22.2	290	22.9	221	29.2	300	30.3
Acetone	197	24.5	280	25.3	218	30.1		
Methylenechloride	199	23.7			218	30.1		
Pyridine	196	24.9	275	26.6	215	31.1	278	35.4
Nitrobenzene	195	25.3	276	26.4	214	31.4		
Acetonitrile	194	25.7	274	26.9	211	32.4	276	36.0
Nitromethane	193	26.0	272	27.4	210	32.7		

TABLE 32

Solvent effect on X-Y and D-X stretching frequency  
(Infra-red)

Complex	Solvent			
	$C_6H_6$	Pyridine	$\gamma$ -picoline	Mull
	$cm^{-1}$	$cm^{-1}$	$cm^{-1}$	$cm^{-1}$
$PyI_2$ (a) $\left\{ \begin{array}{l} \Delta (I-I) \\ \Delta (N-I) \end{array} \right\}$	171(17.4)	167(19.3)		
$PyIBr$ (a) $\left\{ \begin{array}{l} \Delta (I-Br) \\ \Delta (N-I) \end{array} \right\}$	204(21.8) 134	195(25.3) 144		200(23.4) 160
$PyICl$ (a) $\left\{ \begin{array}{l} \Delta (I-Cl) \\ \Delta (N-I) \end{array} \right\}$	290(22.7) 147	277(26.1) 160		265(29.3) 170
$PyBr_2$ $\left\{ \begin{array}{l} \Delta (Br-Br) \\ \Delta (N-Br) \end{array} \right\}$	229(26.6) 128	215(31.1) 140		
$PyBrCl$ 1 $\left\{ \begin{array}{l} \Delta (Br-Cl) \\ \Delta (N-Br) \end{array} \right\}$	307(28.8) 144	274(36.4) 160		
$\gamma$ -pic $I_2$ $\left\{ \begin{array}{l} \Delta (I-I) \\ \Delta (N-I) \end{array} \right\}$	169(18.3)		162(21.7)	
$\gamma$ -pic $IBr$ $\left\{ \begin{array}{l} \Delta (I-Br) \\ \Delta (N-I) \end{array} \right\}$	201(23.0) 124		189(27.6) 131	189(27.6) 146
$\gamma$ -pic $ICl$ $\left\{ \begin{array}{l} \Delta (I-Cl) \\ \Delta (N-I) \end{array} \right\}$	135		276(26.4) 146	281(25.1) 166

(a) Frequencies from Ref. (48)

Values of  $\Delta$  are given in brackets.

As a result the D-X bond becomes stronger and hence the stretching frequency rises. On the other hand, the X-Y bond becomes weaker resulting in a decrease in frequency.

The relative frequency shifts,  $\Delta = (\nu_{\text{free}} - \nu_{\text{complex}} / \nu_{\text{free}})$ , for the X-Y stretching vibration is shown in Tables 31 and 32. This follows the order  $\text{ICl} > \text{IBr} > \text{I}_2$  and also  $\text{BrCl} > \text{Br}_2$ . It definitely indicates that L<sub>r</sub> complexes are more polar than I<sub>2</sub> complexes, but less polar than those of ICl. It also shows that BrCl complexes are more polar than Br<sub>2</sub>. The relative frequency shifts are greater in BrX complexes than in IX, suggesting greater electron transfer in the former series.

The ring frequencies as well as the skeletal vibrations of the cation are found to be insensitive to the change of environment. This is to be expected considering the fact that these cations have no dipole moment.

As the most extensive data we have is on the X-Y stretching frequency for the complexes PyIBr, PyICl and PyBr<sub>2</sub>, we used this information to examine the validity of some of the relations between the frequency shift and solvent character reported in the literature.

Ballamy and workers<sup>(121)</sup> found that when the X-H (X=halogen or oxygen) stretching vibration of a number of compounds was examined in a large number of solvents, the frequency shift observed

could be correlated with the corresponding shifts of  $\nu(N-H)$  of another compound in the same solvent. For example, if  $\Delta \nu/\nu$  of phenol in a given solvent was plotted against  $\Delta \nu/\nu$  of pyrrole in the same solvent, then a series of points was obtained, corresponding to the different solvents, which all fall on a straight line. Similar linear relations are found for the PyIBr, PyICl and PyBr<sub>2</sub> complexes. Figure 21, illustrates the results of plotting (i)  $\Delta \nu/\nu$  of IBr against ICl and (ii)  $\Delta \nu/\nu$  of IBr against Br<sub>2</sub>. It is seen that a fairly good linear relationship exists, indicating that common factors are involved in changing the frequencies.

The best quantitative relation between the frequency shift and the nature of the solvent so far reported seems to be David-Hallan's<sup>(122)</sup> equation:-

$$\Delta \nu = C_1 + C_2(n^2 - 1)/(n^2 + 2) + C_3(e - 1)/(e + 2)$$

Where  $n$  is the solvent refractive-index,  $e$  is the dielectric constant and  $C_1, C_2$  and  $C_3$  are constants. Our data in Table 32, is fitted to this relation by the least square method; the values of the least square constants are given in Table 33. Table 34 shows that the observed and calculated shifts are in close agreement.

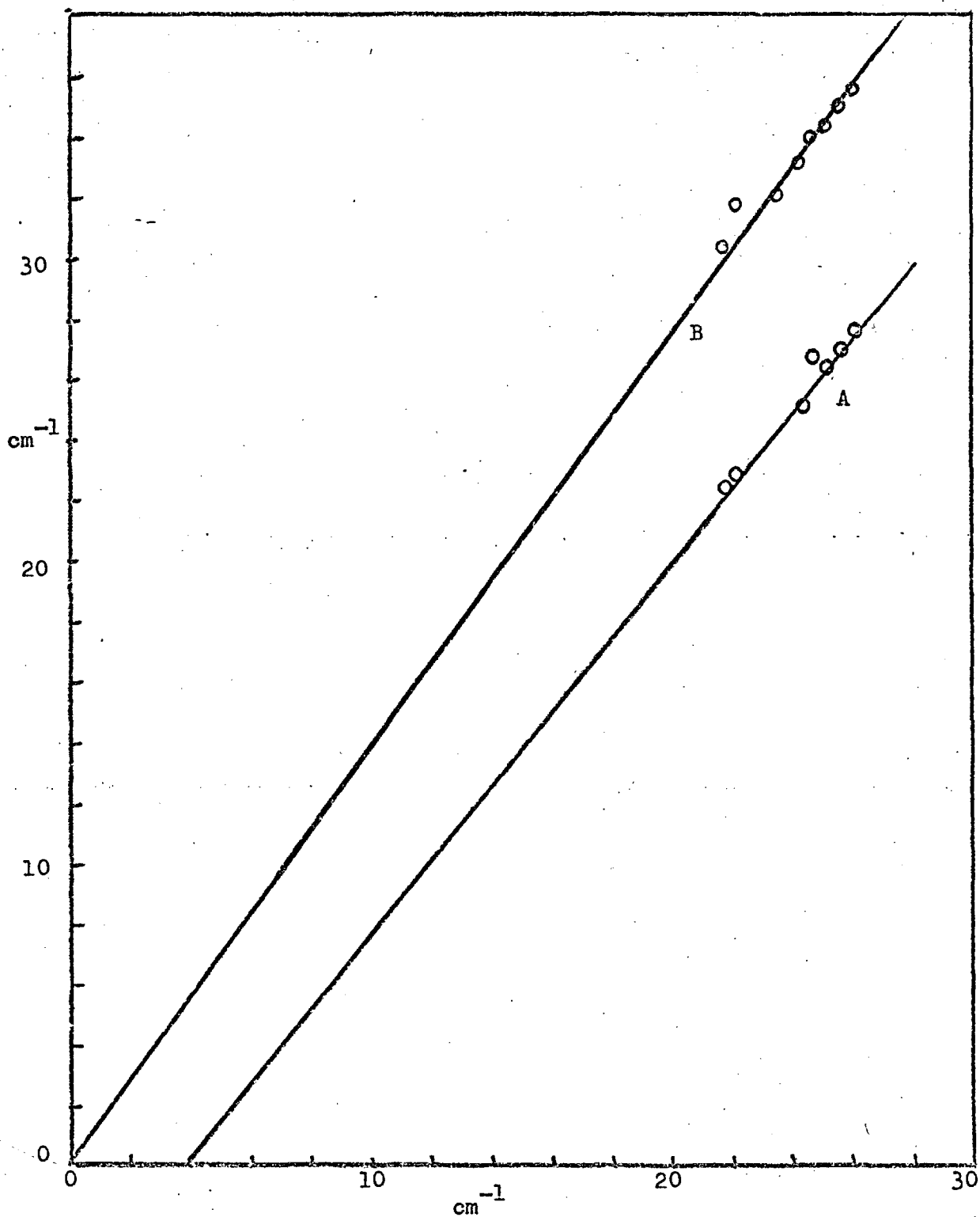


Fig. 21 . Plots of  $\Delta\tilde{\nu}/\tilde{\nu}$  for the I-Br stretch of PyIBr against (A)  $\Delta\tilde{\nu}/\tilde{\nu}$  for the I-Cl stretch of PyICl; (B)  $\Delta\tilde{\nu}/\tilde{\nu}$  for the Br-Br stretch of PyBr<sub>2</sub>.

TABLE 33

Least square constants of the David-Hallam equation.

Complex	$C_1$	$C_2$	$C_3$
PyI <sub>2</sub> Br	49.65	9.90	15.46
PyIOl	71.06	15.54	27.66
PyBr <sub>2</sub>	86.29	4.85	22.20

TABLE 34Difference between calculated and observed frequency shift (in  $\text{cm}^{-1}$ )

Solvent	PyI <sub>2</sub> Br	PyIOl	PyBr <sub>2</sub>
Benzene	+0.2	+0.9	-0.6
1:4 Dioxane	-0.6	-0.7	-4.7
Acetone	+1.2	+3.4	+3.6
Methylenechloride	+1.0		
Pyridine	-0.2	-2.4	-0.7
Nitrobenzene	+1.0	+1.4	+1.2
Acetonitrile	-1.0	-1.1	-1.8
Nitromethane	-1.7	-2.6	-3.0

5.3. Frequency Shift: In the spectra of complexes of pyridine or  $\gamma$ -picoline it is observed that certain ring vibrations of the pyridine or  $\gamma$ -picoline shift to higher frequencies. However, the shifts are generally less than 10%. There seems to be no correlation between the extent of frequency shift and the mass of the adjacent co-ordination atom. Perhaps the best explanation may be given in terms of charge-transfer from the ring to the acceptor.

In pyridine or  $\gamma$ -picoline halogen charge-transfer complexes electron transfer is likely to take place from the nitrogen  $2SP^2$  lone pair orbital to the vacant  $\sigma^* p_z$  ( $n=4$  for  $Br_2$  and 5 for  $I_2$ ) antibonding orbital of halogen. (1) The amount of charge-transfer should increase with the increase in acid strength of the halogen. The acid strength in order of increasing strength (71) are  $Cl_2 \ll Br_2 \ll I_2 \ll IBr \ll BrCl \ll ICl$  and also  $ICN \ll I_2$ . The changes in the  $\sigma$  bonding frame work will indirectly modify the  $\pi$  orbitals of the rings. The effect of changes in bonding may be correlated with the pyridinium or  $\gamma$ -picolinium ion, for these represent extreme cases of electron removal. Assuming that the coupling with the X-Y vibration is small, the vibration frequency of the nucleus may be expected to lie between those of free pyridine or  $\gamma$ -picoline, and the corresponding frequencies of the pyridinium or  $\gamma$ -picolinium ions. Table 35, which tabulates the frequencies of the most sensitive modes before and after complexation, shows that this is



TABLE 35

Compound	$\nu_1 \text{ cm}^{-1}$	$\nu_{6a} \text{ cm}^{-1}$
Pyridine	992	605
PyICN	1003	617
PyI <sub>2</sub>	1005	620
PyIBr	1009	625
PyICl	1009	627
PyBr <sub>2</sub>	1009	626
PyBrCl	1011	630
PyH <sup>+</sup>	1010	633
(Py <sub>2</sub> I) <sup>+</sup>	1009	637
$\gamma$ -picoline	994	514
$\gamma$ -picICN	1008	526
$\gamma$ -picI <sub>2</sub>	1012	631
$\gamma$ -picIBr	1014	535
$\gamma$ -picICl	1017	535
$\gamma$ -picH <sup>+</sup>	1007	521
( $\gamma$ -pic <sub>2</sub> I) <sup>+</sup>	1024	545

nearly always observed. It is also observed that charge-transfer has proceeded even further in the cations ( $[\text{Py}_2\text{I}]^+$  etc) than in those complexes (with ICl) which involve the greatest extent of charge-transfer. For example, the  $605\text{cm}^{-1}$  band of pyridine which is shifted by  $12\text{cm}^{-1}$  to  $617\text{cm}^{-1}$  for the  $\text{PyICN}$  is shifted further to  $620, 625, 627$  and  $637\text{cm}^{-1}$  for the  $\text{PyI}_2$ ,  $\text{PyIBr}$ ,  $\text{PyICl}$  and  $[\text{Py}_2\text{I}]^+$  respectively. The change of frequency  $\Delta\nu$ , for one of the sensitive modes is found to be proportional to the  $\Delta\nu$  for another sensitive mode of the same complex. For example, if  $\Delta\nu_1$  of  $\gamma$ -picoline for a given complex is plotted against  $\Delta\nu_{6a}$  of the same complex, then a series of points are obtained, as different charge-transfer complexes of  $\gamma$ -picoline are used, all of which fall on a straight line (Fig.22). It is to be noted that the points for  $[\text{Py}_2\text{I}]^+$  or  $[\gamma\text{-pic}_2\text{I}]^+$  ion do not fall on the straight line plots for their corresponding charge-transfer complexes.

The study of pyridine and  $\gamma$ -picoline metal co-ordinated<sup>(90,102)</sup> and hydrogen-bonded<sup>(125)</sup> complexes have shown changes in a number of sensitive ring frequencies. The frequencies affected, and the magnitude and direction of the frequency shifts are almost the same as those in the present halogen series. However, no relation between  $\Delta\nu_1$  and  $\Delta\nu_{6a}$  is observed for these complexes. Perhaps this indicates that a fundamentally different type of bonding is present in charge-transfer complexes from that in hydrogen-bonded or metal co-ordinated complexes.

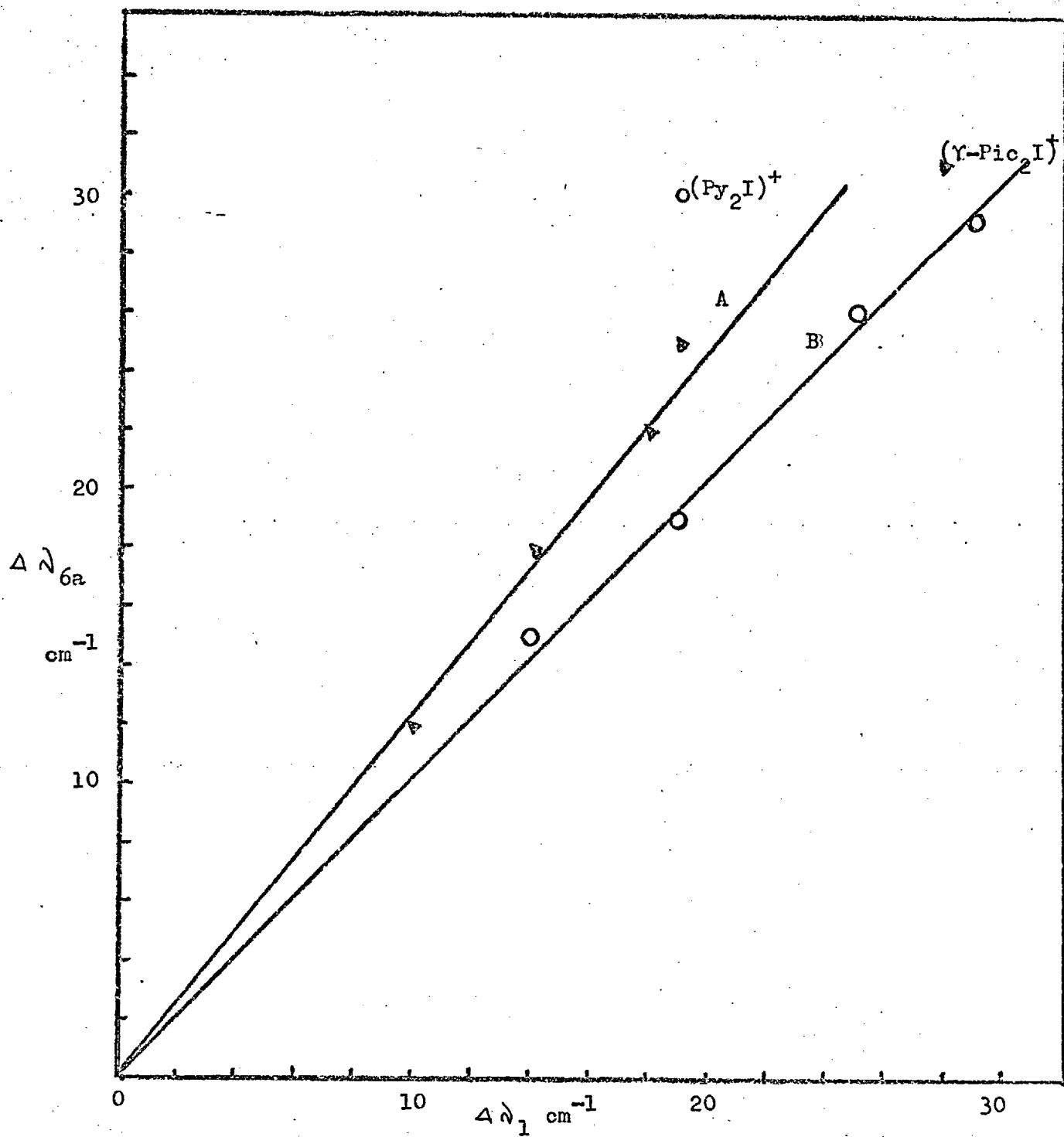


Fig. 22 Plots of  $\Delta \nu_1$  against  $\Delta \nu_{6a}$  in a given solvent

A. for PyIX complexes; B. for  $\gamma$ -PicIX complexes.

An increase in electron transfer should result in a weakening of the interhalogen bond. This is reflected in a decrease in the halogen-halogen stretching frequency. Table 36 shows the proportional decrease of this frequency. It is clear from the table that the relative change in frequency ( $\nu_{\text{free}} - \nu_{\text{complex}} / \nu_{\text{free}}$ ),  $\Delta$ , is greater for ICl complexes than for IBr, which is again greater than  $I_2$  complexes. In the bromine series of complexes also,  $\Delta$ , is found to be greater for the BrCl than for the  $Br_2$  complex. This supports the behaviour of the sensitive donor modes.

Comparison of Pyridine-halogen and picoline-halogen complexes:

From Table 35 and 36 it is quite clear that the magnitude of the frequency shifts are greater in  $\nu$ -picoline complexes than those of the corresponding pyridine ones. This is what is expected considering the fact that  $\nu$ -picoline because of its lower ionization potential is a stronger donor than pyridine. However, the N-I stretching frequency of  $\nu$ -picoline complexes are lower than the corresponding pyridine complexes, whereas the greater stability of the  $\nu$ -picoline complexes would lead to the expectation of higher frequency. This anomaly may be accounted for in terms of a change of mass. For example, substituting the values of the force constants of PyIBr (Table 27) in Equations(1) and (2) of section 5.1. the N-I stretching frequency of  $\nu$ -picIBr is calculated to be  $126\text{cm}^{-1}$ , compared with  $134\text{cm}^{-1}$  for the PyIBr. Thus, by changing the mass from 79a.m.u.(pyridine) to 93a.m.u.( $\nu$ -picoline) the N-I stretching frequency drops by  $8\text{cm}^{-1}$ .

TABLE 36

Complex	$\frac{D-X}{\text{cm}^{-1}}$	$\frac{X-Y}{\text{cm}^{-1}}$ (b)	$\frac{\nu \text{ free} - \nu \text{ complex}}{\text{free}} \%$ (a)
PyICN (b)		423	13.0
PyI <sub>2</sub> (c)	100	171	17.4
PyIBr (d)	134	204	21.8
PyICl (d)	147	290	22.7
PyBr <sub>2</sub>	128	226	27.6
PyBrCl	144	307	28.7
$\nu$ -picICN (b)		420	13.6
$\nu$ -picI <sub>2</sub>		169	18.4
$\nu$ -picIBr	124	201	23.0
$\nu$ -picICl	135	284	24.3

All frequencies refer to benzene solution.

(a)  $\nu$  free from Table 27

(b)  $\nu$  free for ICN from Ref. (46)

(c) Frequencies from Ref. (103)

(d) Frequencies from Ref. (48)

Comparison of PyIX and PyBrX complexes

Since  $I_2$  has a greater acid strength than  $Br_2$ , one would expect a greater charge-transfer from the pyridine ring accompanied by a larger shift in the ring frequency when complexing with the former. Surprisingly, the observed extent of the frequency shifts in the present bromine complexes are found to be as great as in the corresponding iodine ones (Table 35). The relative change of halogen-halogen stretching frequency,  $\Delta$ , is also found to be greater for bromine complexes (Table 36). This and the study of force constants and solvent effects suggest that the net electron transfer from pyridine ring to the halogen is greater for the  $Br_2$  and  $BrCl$  complexes than for the  $I_2$  and  $ICl$  complexes respectively.

A possible explanation for this anomaly may be given in terms of a back transfer mechanism.<sup>(124)</sup> Pyridine may act both as a 'n' donor and  $\pi$  acceptor, the donor action being centred at the nitrogen atom and the acceptor action spread over the entire ring.<sup>(10)</sup> Halogen may donate electrons from the  $\pi_g$  antibonding orbital to the lowest unoccupied  $e_{2u}$   $\pi$  orbital of pyridine. The drift of halogen electrons into pyridine orbitals will tend to make the latter as a whole more negative and hence to increase its basicity; at the same time the drift of electrons to the halogen in the  $\sigma$  bond tends to make the pyridine positive, thus enhancing the acceptor strength of the  $\pi$  orbitals. As the ionization potential of iodine is lower than that of bromine, the electron transfer will

take place more efficiently in the former than in the latter.

The effect would be to increase the stability of the iodine series, reduce the net charge-transfer, and increase the strength of the IX bond compared to the BrX bond.

5.4. Change in Intensity: Besides the frequency shifts the most remarkable change in the spectra of pyridine or  $\gamma$ -picoline on complex formation, is the change in intensity of some vibrations. Although no quantitative measurements were made, large intensity change of a few vibrations may be qualitatively discussed.

When pyridine forms a complex with iodine, the  $1030\text{cm}^{-1}(\nu_{12})$  band of pure pyridine largely diminishes in intensity. It is interesting to note that the decrease in intensity of this band seems to be directly related to the acid strength of the halogen. With the increase in strength of the complex this band gradually becomes weaker and for the cations it appears as a weak band. The  $\nu_{18a}$  mode of  $\gamma$ -picoline behaves similarly. The intensity change of pyridine-halogen complexes has been discussed elsewhere. (46,51)

This is due to the change in electronic charge on pyridine or  $\gamma$ -picoline from the free molecule to the complex.



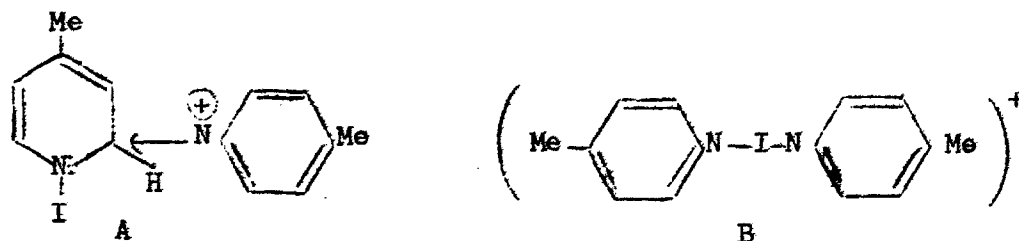
### 5.5. Conclusions

The contribution of the dative bond structure to the ground state of the charge-transfer complex is qualitatively indicated by the study of force constants, solvent effects and frequency shifts. Evidence is also found for greater charge transfer in the case of bromine complexes than that of iodine. Further information on these points could be observed from a dipole-moment study of these complexes in different solvents. Extension of this work to other complexes of this type e.g. aliphatic amine-halogen complexes, is clearly desirable.

6. The Reaction Products of  $\gamma$ -picoline and iodine

## 6.1. INTRODUCTION

In the course of their study of the spectra of  $I_2$  in  $\gamma$ -picoline, Glusker and Thompson<sup>(35)</sup> observed that a rapid reaction soon set in, resulting in the eventual solidification of the whole mixture. However, they were unable to identify the product. Glusker and Miller<sup>(94)</sup> isolated two distinct solid compounds from solutions of iodine in  $\gamma$ -picoline. Their compound(II) which is a charge-transfer complex has already been discussed in section 3.2. The other compound(I) is insoluble in many organic solvents but soluble in water. The authors draw the conclusion from radial distribution analysis that this compound had no I-I distance shorter than  $3\text{\AA}$ , and suggested the structure A. By comparison with the reaction product of pyridine and iodine, Hassel and coworkers<sup>(95)</sup> have argued that structure B was more probable. However, the infrared spectra

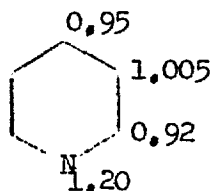


of compound(I) is found to be completely different from the bis- $\gamma$ -picoline iodine(I) cation and so the Hassel's structure is invalidated.

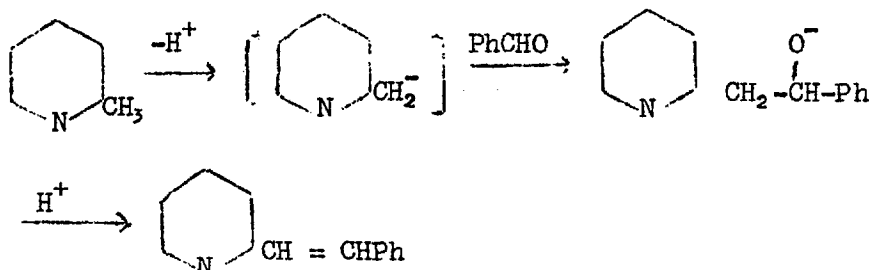
We also found Glusker and Miller's arguments regarding the structure of compound(I), somewhat inconclusive. We have therefore sought to determine the structure of this product by spectroscopic means.

Experimental details, results and structures have been discussed in the paper No.6 attached at the end of the thesis. In this section only the possible reaction mechanism is discussed.

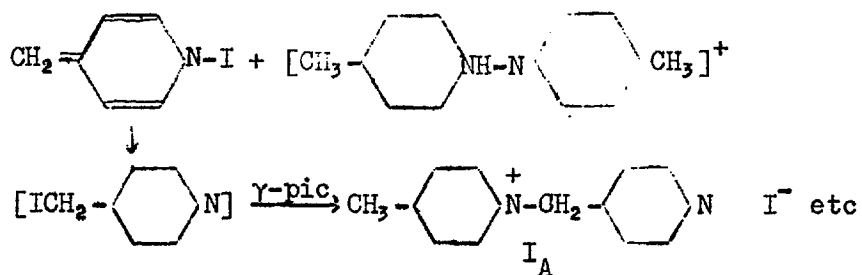
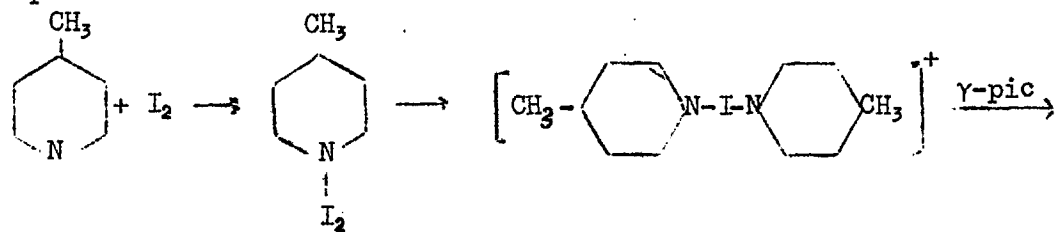
6.2. Discussion: The  $\pi$  electron density at the various positions of the pyridine ring have been calculated by molecular orbital methods and show that there is a considerable drift of electrons from the ring towards the nitrogen atom<sup>(125)</sup>; Further, the  $\alpha$  and  $\gamma$  carbon atoms are found to have partial positive charges. As a result protons from methyl substituent groups at the  $\alpha$  and  $\gamma$  positions



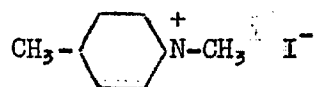
of the pyridine ring are easily lost under suitable conditions<sup>(126,127)</sup>. In consequence, for instance, condensation takes place between  $\alpha$ -picoline and benzaldehyde in the presence of acetic anhydride or zinc chloride:-



In a similar way the formation of solid  $I_A$ ,  $I_B$  and  $I_C$  may be explained



These compounds may be compared with the N-methyl- $\gamma$ -picolinium iodide for example



REFERENCES

- 1a G. Briegleb, 'Electronen Donator-Acceptor Komplex', Springer-verlag  
Berlin 1961.
- 1b L.J. Andrews and R.M. Keefer, 'Molecular Complexes in Organic  
Chemistry', Holden-Day, San Francisco, London,  
Amsterdam, 1964.
- 1c J. Rose, 'Molecular Complexes', Pergamon Press, London, 1967.
2. L.J. Andrews, Chem. Rev., 54, 713, (1954).
3. L.E. Orgel, Quart. Rev., 8, 432, (1954).
4. A.N. Terenin, Uspekhi Khim., 24, 121, (1955).
5. S.P. McGlinn, Chem. Rev., 58, 1113, (1958).
6. J.N. Murrell, Quart. Rev., 15, 191, (1961).
7. S.F. Mason, Quart. Rev., 15, 287, (1961).
8. L.J. Andrews and R.M. Keefer, Adv. Inorg. Chem. Radiochem., 3,  
91, (1961).
9. R.S. Mulliken and W.B. Person, Ann. Rev. Phys. Chem. 13, 107, (1962).
10. R.S. Mulliken, J. chim. phy., 61, 20, (1964).
11. R.L. Scott, J. Amer. Chem. Soc., 75, 1550, (1953).
12. P. Pfeiffer, 'Organische Molekulverbindungen', 2nd ed. Germany (1927).
13. G.M. Bennett and G.H. Wills, J. Chem. Soc., 256, (1929).
14. J.S. Anderson, Nature, 140, 583, (1937).
15. G. Briegleb, Z. physik. chem., B16, 249 (1932).
16. R.E. Gibson and O.H. Loeffler, J. Amer. Chem. Soc., 62, 1234, (1940).
17. D. LL. Hammick and R.M.B. Yule, J. Chem. Soc., 1439, (1940).

18. J. Weiss, J. Chem. Soc., 245, (1942).
19. R.B. Woodward, J. Amer. Chem. Soc., 64, 3058, (1942).
20. W. Brackman, Rec. Trav. Chim., 68, 147, (1949).
21. R.S. Mulliken, J. Amer. Chem. Soc., 74, 811, (1952).
22. R.S. Mulliken, J. Amer. Chem. Soc., 72, 600, 4493 (1950)  
id., J. Chem. Phys., 19, 514, (1951);  
id., J. chim. phys., 51, 341, (1954);  
id., J. Chem. Phys., 23, 397, (1955);  
id., Rec. Trav. Chim., 75, 845, (1956);  
id., J. Phys. Chem. 56, 801, (1952).
23. H. McConnel, J.S. Ham and J.R. Platt, J. Chem. Phys., 21, 66, (1953).
24. E.M. Voigt and C. Reid, J. Amer. Chem. Soc., 86, 3930, (1964).
25. K. Nakamoto, J. Amer. Chem. Soc., 74, 1739, (1952).
26. E.E. Ferguson, J. Chem. Phys., 25, 577, (1956).
27. E.E. Ferguson, J. Chem. Phys., 26, 1357, (1957).
28. E.E. Ferguson and F.A. Matsen, J. Chem. Phys., 29, 105, (1958).
29. E.E. Ferguson and F.A. Matsen, J. Amer. Chem. Soc., 82, 3268 (1960).
30. W.B. Person, C.F. Cook and H.B. Friedrich, J. Chem. Phys., 46,  
2521, (1967).
31. E.E. Ferguson, J. chim. phys., 61, 257, (1964).
32. E.E. Ferguson and I.Y. Chang, J. Chem. Phys., 34, 628, (1961).
33. H. Yada, J. Tanaka and S. Nagakura, J. Mol. Spec., 9, 461, (1962).
34. N.S. Ham, A.L.G. Ren and A. Walsh, Nature, 169, 110, (1952).
35. D.L. Glusker and H.W. Thompson, J. Chem. Soc., 471, (1955).
36. R.A. Zingaro and W.E. Tolberg, J. Amer. Chem. Soc., 81, 1353, (1959).

37. R.A. Zingaro and W.B. Witmer, J. Phys.Chem., 64, 1705, (1960).
38. A.I. Popov, J.C. Marshall, F.B. Stute and W.B. Person,  
J. Amer. Chem. Soc., 83, 3586, (1961).
39. F. Watari and S. Kimumaki, Sci. Rep. Res. Inst. Tokaku Univ.  
Ser. A14, 64, (1962).
40. F. Watari, Spec. Acta, 23A, 1917, (1967).
41. J. Collin and L. D'Or, J. Chem. Phys., 23, 397, (1955).
42. L. D'Or, R. Alewaters and J. Collin, Rec. Trav. Chim., 75, 862,  
(1956).
43. W.B. Person, R.E. Erickson and R.F. Buckles, J. Amer. Chem. Soc.,  
82, 29, (1960).
44. E.K. Plyler and R.S. Mulliken, J. Amer. Chem. Soc., 81, 823, (1959).
45. W.B. Person, R.E. Humphrey, W.A. Deskin and A.I. Popov,  
J. Amer. Chem. Soc., 80, 2049, (1958).
46. W.B. Person, R.E. Humphrey and A.I. Popov, J. Amer. Chem. Soc.,  
81, 27, (1959).
47. H. Strammreich, R. Forneris and Y. Tavares, Spec. Acta, 17,  
1173, (1961).
48. S.G.W. Ginn and J.L. Wood, Trans. Faraday Soc., 62, 777, (1966).
49. P. Klaboe, J. Amer. Chem. Soc., 89, 3667, (1967).
50. Y. Yagi, A.I. Popov and W.B. Person, J. Phys. Chem., 71, 2439,  
(1967).
51. H.W. Friedrich and W.B. Person, J. Chem. Phys., 44, 2161, (1966).
52. R.F. Lake and H.W. Thompson, Proc. Roy. Soc., A297, 440, (1967).
53. R.S. Mulliken, J. chim. phys., 51, 341, (1954).

54. C. Reid and R.S. Mulliken, *J. Amer. Chem. Soc.*, 76, 3869, (1954).
55. G. Kortum and H.Z. Walz, *Z. Electrochem.*, 57, 73, (1953).
56. H. Tasubomura and S. Nagakura, *J. Chem. Phys.*, 27, 819, (1957).
57. K. Toyoda and W.B. Person, *J. Amer. Chem. Soc.*, 88, 1629, (1966).
58. S. Nagakura, *J. Amer. Chem. Soc.*, 80, 520, (1958).
59. O. Hassel and C.H.R. Romming, *Quart. Rev.*, 16, 1, (1962).
60. T. Dahl, O. Hassel and K. Sky, *Act. chem. Scand.*, 21, 592, (1967).
61. O. Hassel and Hvosef, *Act. chem. Scand.*, 8, 873, (1954).
62. O. Hassel and Stromme, *Act. chem. Scand.*, 13, 275, (1959).
63. O. Hassel and Stromme, *Act. chem. Scand.*, 12, 1146, (1958).
64. H.A. Benesi and J.H. Hildebrand, *J. Amer. Chem. Soc.*, 71, 2703, (1949).
65. J.A.A. Ketelaar, C. van de Stolpe, A. Goudsmit and W. Dzeubar,  
*Rec. Trav. chim.*, 71, 1104, (1952).
66. L.E. Orgel and R.S. Mulliken, *J. Amer. Chem. Soc.*, 79, 4939, (1957).
67. S. Carter, J.N. Murrell and E.J. Rosch, *J. Chem. Soc.*, 2048, (1965).
68. M.J.S. Dewar and C.C. Thompson Jr., *Tetrahedron, Suppl. No.7*,  
97, (1966).
69. A.G. Maki and E.K. Plyler, *J. Phys. Chem.*, 66, 766, (1962).
70. A.V. Chekunev and P.A. Bazhulin, *Teor. i Ehzperim. Kim. Akad.*  
*Nauk. USSR*, 1, 536, (1965).
71. H.D. Bist and W.B. Person, *J. Phys. Chem.*, 71, 2750, (1967).
72. R.M. Keefer and L.J. Andrews, *J. Amer. Chem. Soc.*, 77, 2164, (1955).
73. H. Yada, J. Tanaka and S. Nagakura, *Bull. Chem. Soc. Japan*, 33,  
1660, (1960).



74. S.F. Mason, *Quart. Rev.*, 15, 287, (1961).
75. K.M.C. Davis and M.C.R. Symons, *J. Chem. Soc.*, 7079, (1965).
76. K.M.C. Davis, *J. Chem. Soc. (B)*, 1167, (1967).
77. H.M. Rosenberg, E. Eimutis and D. Half, *Can. J. Chem.*, 44, 2405, (1966).
78. S. Kobinta and S. Nagakura, *J. Amer. Chem. Soc.*, 88, 3905, (1966).
79. H.G. Silver, Ph.D. Thesis, London (1963).
80. P. Taimsalu, Ph.D. Thesis, London (1963).
81. S.G.W. Ginn, Ph.D. Thesis, London (1966).
82. R.A. Oetjen et al., *J. Opt. Soc. Am.*, 42, 559, (1952).
83. O. Hassel and H. Hope, *Acta Chem. Scand.*, 15, 407, (1961).
- 84.a D.M. Williams, *J. Chem. Soc.*, 2783, (1931).
- b D.M. Williams, *Inorg. Syn.*, 7, 176, (1961).
85. D.M. Williams, *Org. Syn.* 32, 29, (1951).
- 86.a Corrsin, Fax and Lord, *J. Chem. Phys.*, 21, 1170, (1953).
- b Wilmshurst and Bernstein, *Can. J. Chem.*, 35, 1183, (1957):
87. D.A. Long, F.S. Murfin and E.L. Thomas, *Trans. Faraday Soc.*, 59, 12, (1963).
88. J.H.S. Green, W. Kynaston and H.M. Paisely, *Spec. Acta*, 19 549, (1963).
89. D. Cook, *Can. J. Chem.*, 39, 2009, (1961).
90. N.S. Gill, R.H. Nuttal, D.E. Scaife and D.W.A. Sharp, *J. Inorg. and Nucl. Chem.*, 18, 79, (1961).
91. A.G. Maki and R. Forneris, *Spectrochim. Acta*, 23Am 867, (1967).

92. V.G. Krishna and Benoy B. Bhowmik, *J. Amer. Chem. Soc.*, 90, 1700, (1968).
93. V. Lorenzelli, *Compt. Rend.* 258, 5386, (1964).  
*ibid. Grazz. chim. Ital.*, 95, 218, (1965).
94. D.L. Glusker and A. Miller, *J. Chem. Phys.*, 26, 331, (1957).
95. O. Hassel, C. Rønning and T. Tufte, *Acta Chem. Scand.*, 15, 967, (1961).
96. R.D. Whittaker, J.R. Ambrose and C.W. Hickam, *J. Inorg. Nucl. Chem.* 17, 254, (1961).
97. Hari D. Bist and W.B. Person, *J. Phys. Chem.*, 71, 3288, (1967).
98. W.B. Person, R.E. Humphrey and A.I. Popov, *J. Amer. Chem. Soc.*, 81, 273, (1959).
99. D.A. Lang and W.O. George, *Spectrochim. Acta*, 19, 1777, (1963).
100. E. Spinner, *J. Chem. Soc.*, 3960, (1963).
101. O. Hassel, C.H.R. Rønning and T. Tufte, *Acta Chem. Scand.*, 15, 967, (1961).
102. M. Goodgame and P.J. Hayward, *J. Chem. Soc.(A)*, 632, (1966).
103. R.F. Lake, Contribution to "Symposium on the physical chemistry of weak complexes", Chemical Society Anniversary Meeting, 1967.
104. W.B. Person, G.R. Anderson, J.N. Fordemwalt, H. Stammreich and R. Forneris, *J. Chem. Phys.*, 35, 308, (1961).
105. J.C. Evans and G. Y-S. Lo, *J. Chem. Phys.*, 44, 4356, (1966).
106. H.A. Tasman and K.H. Bosneijk, *Acta Cryst.*, 8, 59 (1955);  
8, 857, (1955).
107. J.C. Evans and G. Y-S. Lo, *J. Chem. Phys.*, 45, 1069, (1966).

108. H. Carlsohn, Habilitation Thesis "Über eine neue Klasse von Verbindungen des Positive Einwertigen Jods", Verlag S. Hinzl, Leipzig, 1932.
109. J. Kleinberg, J. Chem. Ed., 23, 559, (1946).
110. R.A. Zingaro, C.A. van der Werf and J. Kleinberg, J. Amer. Chem. Soc., 71, 575, (1949).
111. F.A. Cotton and G. Wilkinson, "Advanced Inorganic Chemistry", 2nd Ed. Interscience, 1966.
112. Inorganic Synthesis, 7, 169, (1963).
113. Wilson, Decious and Cross, "Molecular Vibrations", McGraw-Hill, 1955.
114. T.R. Singh, private communication.
115. A. Hall and J.L. Wood, unpublished results.
116. G.M. Badger, J. Chem. Phys., 3, 710, (1935).
117. J. Yarwood and W.B. Person, J. Amer. Chem. Soc., 90, 594, (1968).
118. G. Herzberg, "Infrared and Raman Spectra of Polyatomic Molecules", D. van Nostrand Company, 1945.
119. H.E. Hallam, "Infrared Spectroscopy and Molecular Structure" Ed. by M. Davis, Elsevier Publishing Company, 1963, p.420.
120. L.J. Bellamy, "The infrared spectra of complex molecules", Methuen, 2nd Ed. 1956, p.382.
121. L.J. Bellamy, H.E. Hallam and R.L. Williams, Trans. Faraday Soc., 54, 1120, (1958).
122. J.G. David and H.E. Hallam, Spectrochim. Acta, 23A, 593, (1967).

123. H. Takahashi, K. Mamola, and E.K. Plyler, *J. Mol. Spec.*, 21,  
217 (1966).
124. I. Hillier, private communication.
125. J.N. Murrell, S.F.A. Kettle and J.M. Tedder, "Valency Theory",  
John Wiley, 1965, p.280.
126. R.M. Acheson, "The Chemistry of Heterocyclic Compounds",  
Interscience, 1960, p.174.
127. J. Packer and J. Vaughan, "A Modern Approach to Organic Chemistry",  
Oxford Press, 1958, p.911.

## The Iododipyridinium Ion

By J. A. CREIGHTON

(Chemical Standards Division, National Physical Laboratory, Teddington, Middlesex)

and INAMUL HAQUE and J. L. WOOD

(Chemistry Department, Imperial College of Science and Technology, Imperial Institute Road, London, S.W.7)

IN the course of examining the far-infrared spectra of charge-transfer complexes formed by pyridine with iodine, iodine bromide, and iodine chloride in solution in nitromethane or an excess of pyridine, hean ions  $I_3^-$ ,  $IBr_2^-$  and  $ICl_2^-$  in addition to the dissociated complexes were identified.<sup>1</sup> A possible cationic species in these solutions is the iododipyridinium ion



which a molecular-orbital calculation suggests might possess a linear N-I-N skeleton.

To identify the bands due to this cation, the infrared spectra of iododipyridinium tetrafluoroborate and perchlorate\* in solution in pyridine, and the Raman spectrum of the tetrafluoroborate in pyridine solution, have now been examined. Comparison of the infrared bands above 300  $cm^{-1}$

with those of the solutions of iodine and iodine halides previously studied,<sup>1</sup> confirms the presence of the iododipyridinium ion in the latter solutions. Above 300  $cm^{-1}$  the frequencies are close to those of free pyridine and arise from the internal vibrations of co-ordinated pyridine. Between 300 and 100  $cm^{-1}$  the only bands are 172 (infrared) and 181  $cm^{-1}$  (Raman, polarized), which are assigned to asymmetric and symmetric N-I-N skeletal stretching respectively. The absence of coincident skeletal stretching frequencies in the infrared and Raman is consistent with a linear N-I-N skeleton as suggested by the molecular-orbital calculation. Analysis of the spectra above 300  $cm^{-1}$  is now being undertaken to investigate the coplanarity of the pyridine rings.

(Received, March 23rd, 1966; Com. 184.)

\* Explosive.

<sup>1</sup>S. G. W. Ginn and J. L. Wood, *Trans. Faraday Soc.*, to be published.

## The infra-red spectra of pyridine-halogen complexes

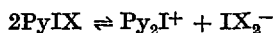
I. HAQUE and J. L. WOOD

Chemistry Department, Imperial College, London S.W.7

(Received 15 June 1966)

**Abstract**—The infra-red spectra of the complexes  $\text{PyI}_2$ ,  $\text{PyIBr}$ ,  $\text{PyICl}$  and  $\text{PyICN}$  have been examined in a range of environments.

In polar solvents the ionization



takes place. The vibrations of the complexes are assigned, and discussed on the basis of a molecular orbital treatment.

### INTRODUCTION

PYRIDINE forms relatively stable complexes with iodine, iodine bromide, iodine chloride, and iodine cyanide immediately on mixing [1]. The initial small electrical conductivity of pyridine-iodine solutions rises rapidly on standing, and the anion formed is identified by both u.v. [2] and far infra-red spectroscopy [3] as the tri-iodide ion. This dissociation is found in other polar solvents, and a corresponding process takes place with the interhalogen complexes giving the  $\text{IX}_2^-$  anion [4]. It has been suggested by POPOV and PFLAUM [4] that the corresponding cation formed is the iodo-dipyridinium ion  $(\text{Py}_2\text{I})^+$ , the net process being represented by



Centrosymmetric  $(\text{Py}_2\text{I})^+$  cations have been identified in the crystalline material which deposits from alcoholic pyridine-iodine solutions, by X-ray examination [5].

Numerous investigations have been made of particular aspects of the infra-red spectra of these complexes [6], but there has been no comprehensive discussion of the entire spectra. It is the purpose of the present paper to account for the molecular origin of all the observed bands, and to provide a nearly complete assignment of the vibrational fundamentals.

- 
- [1] G. BRIEGLER, *Elektronen Donator Acceptor Komplexe*, Springer, Berlin (1961). R. S. MULLIKEN and W. B. PERSON, *Ann. Rev. Phys. Chem.* **107** (1962). L. J. ANDREWS and R. M. KEEFER, *Molecular Complexes in Organic Chemistry*, Holden-Day, San Francisco (1964).
- [2] J. KLEINBERG *et al.*, *J. Am. Chem. Soc.* **75**, 442, 1953.
- [3] S. G. W. GINN and J. L. WOOD, *Trans. Faraday Soc.* **62**, 777 (1966).
- [4] A. I. POPOV and R. T. PFLAUM, *J. Am. Chem. Soc.* **79**, 570 (1957).
- [5] O. HASSEL and H. HOPE, *Acta Chem. Scand.* **15**, 407 (1961). O. HASSEL and C. RØMMING, *Quart. Rev. Chem. Soc.* **16**, 1 (1962).
- [6] E. K. PLYLER and R. S. MULLIKEN, *J. Am. Chem. Soc.* **81**, 823 (1959). R. A. ZINGARO and W. E. TOLBERG, *J. Am. Chem. Soc.* **81**, 1353 (1959). W. B. PERSON *et al.*, *J. Am. Chem. Soc.* **82**, 29 (1960). R. A. ZINGARO and W. B. WITMER, *J. Phys. Chem.* **64**, 1705 (1960). A. I. POPOV *et al.*, *J. Am. Chem. Soc.* **83**, 3586 (1961). F. WATARI and S. KINMUMAKI, *Sci. Rep. Res. Inst. Tohoku Univ.* **A14**, 64 (1962).

Table 1. Infra-red spectra of pyridine-iodine system

Iodine in excess of pyridine	Equimolar pyridine and iodine in CS <sub>2</sub>	Equimolar pyridine and iodine in benzene	Equimolar pyridine and iodine in <i>n</i> -heptane	Equimolar pyridine and iodine in cyclohexane
	3149 w			
	3085 m			
	3065 s			
	3042 w			
	3032 w			
	2999 s			
	2952 w			
	2910 s			
	1990 w			
	1911 m			
	1888 w			
		1594 s		
		1445 m		
1445 s		1351 w		
	1351 w			
	1295 vw			
1240 w	1236 m			
1209 s	1209 s	1209 s		1212 w
	1151 s			
	1067 s	1067 s		1067 w
1038 vw	1039 vw			
	1030 m			
1007 s	1005 vs	1006 s	1003 w	
	939 w	944 w		
	746 vs	748 s		746 s
	694 vs			
	677 w			
	653 w			
636 m*	639 vw*			
625 s	620 vs	623 s‡	617 s‡	617 s‡
436 w*				
421 sh	420 vw			420 s
167 s		171 s	180 s	
137†				

\* Py<sub>2</sub>I<sup>+</sup>† IX<sub>2</sub><sup>-</sup>‡ as these solvents are clear below about 650 cm<sup>-1</sup> longer path length was used (1 mm).

Only bands clearly distinguishable from the background are included in these tables.

the bands of pyridine overlie those of the complexes, so in this solvent only bands that can be clearly distinguished from the solvent background are noted in the tables.

### DISCUSSION

If the pyridine IX complexes in solution have the expected linear  $C_{2v}$  structure the 33 fundamental vibrations fall into the classes  $12a_1 + 3a_2 + 11b_1 + 7b_2$ .\* Only the  $a_2$  modes are inactive in the infra-red. Of these vibrations  $10a_1 + 3a_2 + 9b_1 + 5b_2$  are closely related to vibrations of free pyridine, and, since the interaction between pyridine and the halogen is relatively weak, these vibrations will have frequencies close to their counterparts in pyridine. The remaining six vibrations  $2a_1 + 2b_1 + 2b_2$  comprise five intermolecular modes and the  $a_1$  IX stretching vibrations, all lying below 400 cm<sup>-1</sup>. Consequently above 400 cm<sup>-1</sup> the spectra of the complexes will closely resemble that of the pyridine parent. Adopting a  $C_{2v}$  structure the vibrations of pyridine ICN classify as  $13a_1 + 3a_2 + 12b_1 + 8b_2$ , the nine vibrations without

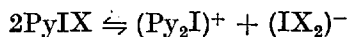
\* The axes are chosen as in Ref. [13].

Table 3. Infra-red spectra of the pyridine iodine chloride system in various media

Saturated solution of PyICl in pyridine	Saturated solution of PyICl in carbon disulphide (4000-400 cm <sup>-1</sup> )	Saturated solution of PyICl in benzene (2000-400 cm <sup>-1</sup> )	PyICl in Nujol Mull (2000-400 cm <sup>-1</sup> )	PyICl in Hexachlorobutadiene Mull (Only from 2000 cm <sup>-1</sup> )	Saturated solution of PyICl in CH <sub>3</sub> CN
	3149 w				
	3085 w			3099 m	
	3068 m			3089 m	
				3065 m	
	3039 w			3053 s	
	2999 w			3039 w	
				2999 w	
	2925 s			2952 w	
				2928 m	
	1910 w		1980 vw		
			1915 w		
			1838 vw		
			1647 w		
		1597 s	1597 s		
			1569 m		
1449 s		1449 s	1449 s		
			1390 w		
	1347 m	1350 w	1344 s		
1244 w	1239 m		1247 s		
1209 sh	1209 s	1209 s	1209 s		
			1197 s		
	1150 s		1154 w		
			1087 w		
	1067 s	1064 s	1056 vs		
	1030 ms		1035 m		
1011 s	1009 s	1011 s	1013 s		
	941 vw		948 w		
			869 vw		
			851 vw		
	748 s	749 s	752 vs		
	702 w		704 w		
	692 s		689 vs		
	676 w				
	655 w		649 w		
632 s	627 s	630 s	636 vs		633 vs
					603 w
434*					436 sh*
424 s	421 sh	421 s	426 s		423 m
					406 w
277 s		290 s			
223 w†					
160 m		147 m			

\* Py<sub>2</sub>I<sup>+</sup>† ICl<sub>2</sub><sup>-</sup>

entirely accounted for by the equilibria



the possibility that species such as (PyI)<sup>+</sup> are present in small amounts cannot be eliminated, for the vibration frequencies of such a species would lie very close to the bands of the species known to be present.

The presence of a band at 636 cm<sup>-1</sup> in a freshly made solution of ICN in pyridine indicates the presence of Py<sub>2</sub>I<sup>+</sup>, but no bands which could be attributed to anions were observed. The PyICN spectra also showed the most noticeable changes with



Table 5. Assignment of infra-red active fundamentals of pyridine complexes, and comparison with pyridine and pyridinium ion

Designation [12]	Pyridine	Pyridine ICN	Pyridine I <sub>2</sub>	Pyridine IBr	Pyridine ICl	Pyridinium <sup>+</sup> (I <sup>-</sup> )
<i>a</i> <sub>1</sub>						
ν <sub>1</sub>	992	1003	1005	1009	1009	1010
ν <sub>2</sub>	3054	3065	3065	3067	3068	
ν <sub>3</sub>	605	617	620	625	627	633†
ν <sub>4</sub>	1583	1597	1594	1597	1597	1638
ν <sub>5</sub>	1218	1213	1209	1210	1209	1194
ν <sub>6</sub>	1030	1032	1030	1031	1030	
ν <sub>7</sub>	3054	3065	3065	3067	3068	3060
ν <sub>8</sub>	1068	1068	1067	1067	1067	1030
ν <sub>9</sub>	1482					1484
ν <sub>10</sub>	3036	3048	3042	3034	3039	
N—I stretching			120(?)	134	147	
I—X stretching		423	171	204	290	
C—N stretching		2155				
<i>b</i> <sub>1</sub>						
ν <sub>11</sub>	1218	1213	1209	1210	1209	1326
ν <sub>12</sub>	652	656	653	655	649	
ν <sub>13</sub>	3036	3048	3042			3045
ν <sub>14</sub>	1572					1608
ν <sub>15</sub>	1375					
ν <sub>16</sub>	1148	1149	1151	1152	1150	1161
ν <sub>17</sub>	1085					1050
ν <sub>18</sub>	1439	1445	1445	1449	1449	1535
ν <sub>19</sub>	3083	3085	3085	3089	3085	
ICN bending		336*				
<i>b</i> <sub>2</sub>						
ν <sub>23</sub>	749	748	746	749	748	738
ν <sub>24</sub>	981					980
ν <sub>25</sub>	886					855
ν <sub>26</sub>	700	698	694	693	692	671
ν <sub>27</sub>	405	413	420	420	421	
ICN bending		336*				

\* Ref [9]

† Present work

The low frequency intermolecular bending modes, which have not yet been observed, are omitted.

the complexes, also includes that for the pyridinium ion, given by COOK [13]. All frequencies in this table refer to solution in carbon disulphide, except where bands are obscured, when data from other solvents is utilized. All the complexes have a strong band between 2910 and 2930 cm<sup>-1</sup>, which has no counterpart in either pyridine or the pyridinium ion. It seems unlikely that a CH stretching frequency in the complexes should lie so far outside the range found in these compounds, and a combination mode origin for this band is preferred.

### DISCUSSION

The formation, stability and electronic spectra of the complexes can be accounted for by a simple 3-centre molecular orbital treatment, which combines the 2*sp*<sup>2</sup> orbital of pyridine with appropriate *p<sub>z</sub>* orbitals of the halogens [3]. Figure 2 shows the resulting charge on the nitrogen, iodine, and X atoms when the valence parameters lie in their most probable ranges. This positive charge acquired by the nitrogen atom on formation of a complex corresponds to their charge-transfer nature. These effects are in the σ-bonding framework; the resulting increase in the electronegativity of the nitrogen atom will modify the π-orbitals of the pyridine ring.

[13] D. COOK, *Can. J. Chem.* **39**, 2009 (1961).

that vibrations of the pyridine nucleus will move in the pyridinium<sup>+</sup> ion direction. This effect is generally observable (Tables 1-4), and is particularly clearly shown by the sensitive vibration  $\nu_3$  (Table 6), change of solvent being equivalent to changing the X atom electronegativity. The data also show that charge-transfer proceeds furthest in the crystal. The stability of the complexes is increased by greater charge transfer [3].

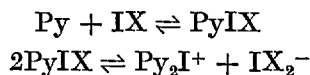
Table 6. Effect of medium in increasing polarity

Medium	PyICN	PyI <sub>2</sub>	PyIBr	PyICl
<i>n</i> -hexane		617	*	*
Cyclohexane		617	*	*
Carbon disulphide	617	620	625	627
Benzene	617	623	627	630
Pyridine	623	625	629	632
Acetonitrile				633
Mull			632	636

\* Increasing polarity reduces the solubility in non-polarizing solvents.

#### CONCLUSION

The presence of the iodo-dipyridinium ion in polar solutions of the complex, suggested by the molecular orbital calculations [3] is confirmed. In freshly made up solutions the species involved in the equilibria



can account for all the bands in the vibrational spectra. Slight ionization occurs in CS<sub>2</sub>, but there is no evidence for ionization in other non-polar media. On standing for some days, irreversible decomposition occurs, probably due to substitution in the ring. The changes in the force constants of the pyridine nucleus are predicted with a simple molecular orbital treatment of the complexes. The agreement in addition indicates that dynamical coupling of the pyridine nucleus and the halogen moiety is relatively small, as would be anticipated from the relative weakness of the intermolecular forces.

*Acknowledgement*—We wish to thank the Education Department, Government of Assam, for a grant to one of us (I. H.).

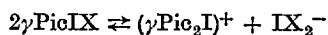
## The infra-red spectra of $\gamma$ -picoline-halogen complexes

I. HAQUE and J. L. WOOD

Department of Chemistry, Imperial College, Imperial Institute Road, London S.W.7

(Received 6 January 1967)

**Abstract**—The infra-red spectra of the complexes  $\gamma$ PicI<sub>2</sub>,  $\gamma$ PicIBr,  $\gamma$ PicICl and  $\gamma$ PicICN have been recorded from 80–3500 cm<sup>-1</sup> in a range of environments. In polar solvents the first three complexes ionise



further reaction occurring on standing. There is no evidence for the ionisation of the  $\gamma$ PicICN complex.

The vibrations of the complexes are assigned on the basis of  $C_{2v}$  symmetry, and compared with those of the pyridine analogues.

### INTRODUCTION

WE have recently examined the infra-red spectra of the complexes PyI<sub>2</sub>, PyIBr, PyICl and PyICN [1] and found that in freshly prepared solutions in non-polar solvents the pyridine complexes are not ionised, while in polar solvents ionisation of the first three complexes according to the scheme  $2\text{PyIX} \rightleftharpoons (\text{Py}_2\text{I})^+ + \text{IX}_2^-$  takes place. The introduction of a *p*-Me group increases the basicity of the electron donor, with a consequent rise in the stability of the complex [2]. We have now examined the infra-red spectra of the  $\gamma$ -picoline complexes in various environments over a frequency range extending to 80 cm<sup>-1</sup>. It has been possible to determine the origin of almost all the observed bands, and to account for the effects of the change in the basicity of the donor, and of variation in the solvent, or the acceptor, in terms of increasing charge transfer.

The  $\gamma$ -picoline complexes have not been as extensively examined as the corresponding pyridine series. Glusker and Thompson observed changes in the frequencies of a number of  $\gamma$ -picoline bands on addition of iodine [3] providing evidence of complex formation in this solution, and recently Lorenzelli has observed the I—I stretching vibration of the  $\gamma$ -picoline-iodine complex in *cyclohexane* solution [4].

Two distinct solids have been reported to be obtained from solutions of iodine in  $\gamma$ -picoline. These solids have been designated compound I and compound II by GLUSKER and MILLER [5], who concluded from an X-ray examination that compound I, which is water soluble, contained no pairs of directly bonded atoms. In contrast compound II, which is soluble in organic solvents, was found to contain a pair of

- [1] S. G. W. GINN and J. L. WOOD, *Trans. Faraday Soc.* **62**, 777 (1966); I. HAQUE and J. L. WOOD, *Spectrochim. Acta* **23A**, 959 (1967).  
 [2] G. BRIEGLEB, *Elektronen Donator Acceptor Komplexe* **23A**, 959 (1967). Springer (1961).  
 [3] D. L. GLUSKER and H. W. THOMPSON, *J. Chem. Soc.* 471 (1955).  
 [4] V. LORENZELLI, *Gazz Chim. Ital.* **95**, 218 (1965).  
 [5] D. L. GLUSKER and A. MILLER, *J. Chem. Phys.* **26**, 331 (1957).

## NATURE OF THE SPECIES PRESENT

 $\gamma$  picoline-iodine

Only a single strong band is present in the 100–200  $\text{cm}^{-1}$  range in freshly made-up solutions in non-polar solvents, and this can be confidently ascribed to the I—I stretching of the un-ionised complex. (c.f. Ref [4]). In fresh solutions in excess  $\gamma$ -picoline, a further band at 137  $\text{cm}^{-1}$  is present, which is the asymmetric stretching

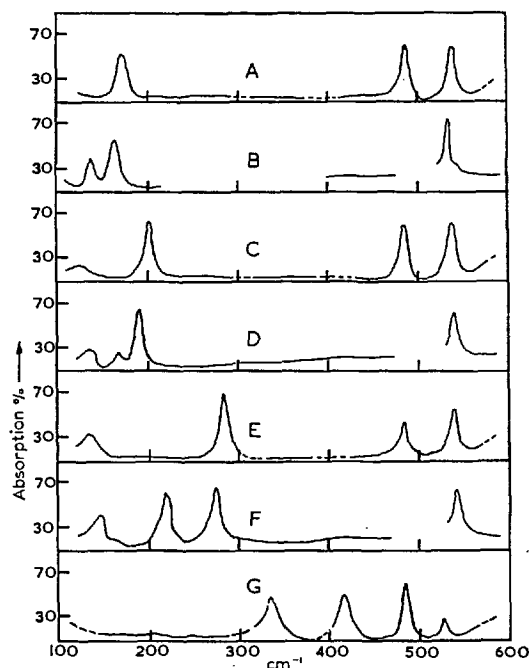


Fig. 1. A. Equimolar  $\gamma$ -picoline and  $\text{I}_2$  in benzene. B.  $\text{I}_2$  in excess  $\gamma$ -picoline. C.  $\gamma$ -picoline IBr in benzene. D. IBr in excess  $\gamma$ -picoline. E.  $\gamma$ -picoline ICl in benzene. F. ICl in excess  $\gamma$ -picoline. G.  $\gamma$ -picoline ICN in benzene.

frequency of the  $\text{I}_3^-$  ion [1]. Low frequency spectra of  $\gamma$ -picoline +  $\text{I}_2$  in nitrobenzene—previously found to be a good ionising solvent—also show the 137  $\text{cm}^{-1}$  band. Comparison with pyridine complexes suggests that the counter-ion is  $(\gamma\text{Pic}_2\text{I})^+$ . This ion has only one strong infra-red band in the low frequency range, the asymmetric NIN stretching at 168  $\text{cm}^{-1}$  [9], but this frequency coincides with the I—I stretch of the un-ionised complex and so cannot be separately distinguished. Most of the higher frequency bands of the  $(\gamma\text{Pic}_2\text{I})^+$  ion lie close to corresponding bands of complexed  $\gamma\text{Pic}$ , and are thus of little diagnostic value. However the additional bands at  $\sim 545 \text{ cm}^{-1}$  and  $\sim 1027 \text{ cm}^{-1}$ , observed in polar solvents only, both correspond with  $(\gamma\text{Pic}_2\text{I})^+$  frequencies. If it is assumed that the complex is un-ionised in benzene, chloroform, and cyclohexane, slightly ionised as  $(\gamma\text{Pic}_2\text{I})^+ + \text{I}_3^-$

[9] I. HAQUE and J. L. WOOD, To be published.

*$\gamma$ -Picoline iodine-bromide*

In non-polar solvents a single species, the un-ionised complex  $\gamma\text{Pic}-\text{I}-\text{Br}$  can account for all the bands observed (Table 2). In freshly prepared solutions of most of the polar solvents, no additional bands are found, and it appears that the ionisation  $2\gamma\text{PicI} \rightleftharpoons (\gamma\text{Pic}_2\text{I})^+ + \text{IBr}_2^-$  does not occur as extensively as in the iodine

Table 2. Infra-red spectra of the  $\gamma$ -picoline-iodine bromide system in various media

Saturated solution of $\gamma\text{-Pi-I-Br}$ in $\text{CS}_2$	Saturated solution of $\gamma\text{-Pi-I-Br}$ in $\text{C}_6\text{H}_6$	Saturated solution of $\gamma\text{-Pi-I-Br}$ in $\text{CH}_2\text{Cl}_2$	$\gamma\text{-Pi-I-Br}$ hexachloro-butadiene mull	$\gamma\text{-Pi-I-Br}$ in Nujol mull	Saturated solution of $\gamma\text{-Pi-I-Br}$ in $\gamma$ -picoline
3150 w					
3080 w			3082 m		
3063 s			3057 m		
3042 vvw					
3028 vvw					
2980 w (broad)					
1930 w		1937 w	1923 w	1927 w	
1838 w		1845 w			
1667 w		1667 w	1674 w	1673 w	
		1620 s		1613 s	
				1602 sh	
				1560 w	
		1498 vw			
	1429 w		1445 sh		
			1418 s	1420 s	
		1385 w	1371 w		
		1353 w	1353 w		
		1333 w	1319 w	1319 w	
1289 w					
1250 w			1250 m	1250 m	1250 w
1213 s	1212 s	1212 s	1202 s	1203 s	
1201 w			1194 s	1194 s	
1111 vvw		1115 vvw	1111 vw	1111 vw	
1093 vw		1096 w	1094 w	1094 w	
1068 s	1067 s	1067 s	1060 s	1061 s	
1039 w		1039 w	1038 m	1039 w	
		1026 sh			
1014 s		1019 s	1021 s	1022 s	1019 s
969 w	970 w	973 w		975 w	
				956 w†	
804 s	806 s	808 s		812 s	
793 sh					
714 m			706 m	707 m	
				663 w	
535 s	537 s	540 s	544 s	544 s	540 s
485 s	485 s	486 s	487 s	487 s	
	201 s			189 s	189 s
					168 m
	124 m(?)			146 s	131 m

complex. Only in fresh solutions in excess  $\gamma$ -picoline is an additional low frequency band observed at  $168\text{ cm}^{-1}$ . Both the  $\text{IBr}_2^-$  antisymmetric stretching vibration ( $174\text{ cm}^{-1}$  in pyridine [1]) and the  $(\gamma\text{Pic}_2\text{I})^+$  antisymmetric NIN stretching vibration ( $168\text{ cm}^{-1}$ ) are possible origins. The former is the stronger band, and comparison with the  $\gamma\text{PicICl}$  system (q.v.) indicates that it gives the main contribution to the observed absorption. The characteristic bands of the  $(\gamma\text{Pic}_2^+\text{I})$  ion at  $\sim 545\text{ cm}^{-1}$

to the  $\text{ICl}_2^-$  ion (antisymmetric stretch =  $223\text{ cm}^{-1}$  in pyridine solution [1]). A band is also present at this frequency in nitrobenzene solution. The solution in excess  $\gamma$ -picoline also shows a shoulder at  $167\text{ cm}^{-1}$ , a  $(\gamma\text{Pic}_2\text{I})^+$  ion frequency. Nitrobenzene is not clear in this region, but a weak shoulder is also found at  $\sim 167\text{ cm}^{-1}$  in both the ionising solvent  $\text{CH}_2\text{Cl}_2$ , and in an equal volume mixture of MeCN and benzene. The higher frequency  $(\gamma\text{Pic}_2\text{I})^+$  bands at  $545\text{ cm}^{-1}$  and  $1025\text{ cm}^{-1}$  are unfortunately again obscured by bands of the un-ionised complex. One thus finds that all the bands observable in freshly prepared solutions, and in mulls, are accountable by the scheme



and the evidence for the ionic species is better supported than in the case of the iodine bromide complex.

#### *$\gamma$ -Picoline iodine cyanide*

The infra-red spectra of a number of ICN complexes have been reported by PERSON *et al.* [10]. The three ICN vibrations, modified by complexing, were observed in the frequency ranges  $310\text{--}340\text{ cm}^{-1}$  (bending)  $390\text{--}490\text{ cm}^{-1}$  (I—C stretching) and  $2150\text{--}2170\text{ cm}^{-1}$  (CN stretching). In the present work the frequency range down to  $80\text{ cm}^{-1}$  was examined, but no additional low frequency absorption bands were found. The lowest frequency band observed (Table 4) which occurs in benzene, nitrobenzene and in excess  $\gamma$ -picoline, at  $\sim 338\text{ cm}^{-1}$ , can be assigned to ICN bending. The IC stretching is observed at  $\sim 420\text{ cm}^{-1}$  in benzene,  $\text{CH}_2\text{Cl}_2$ , and in excess  $\gamma$ -picoline solutions. Iodine cyanide is the weakest acceptor in the series, and it is to be expected that the NI stretching band is too low in frequency to be within the range covered. A band at  $2146\text{ cm}^{-1}$  in excess  $\gamma$ -picoline is probably the CN stretching lowered from its value in free ICN. The absence of a higher "intermolecular" vibration frequency, and the close similarity between the vibrations of the ICN complex and the other members of the series clearly indicate that donation is to the I, not the N atom of ICN.

In none of the media examined was any evidence for ionisation of the  $\gamma\text{PicICN}$  complex found.

#### ASSIGNMENT

The normal vibrations of free  $\gamma$ -picoline have been assigned by GREEN *et al.* [11] and by LONG and GEORGE [12]. There is a large measure of agreement in these assignments; where they differ, we have followed Long and George, since this assignment has the benefit of a force constant calculation. The notation of Green *et al.* however is used, since this is more suited to comparison with related systems.

Inter-comparison of the spectra, and comparison with  $\gamma$ -picoline readily permits the assignment of all the bands ascribed to the unionised complexes (apart from a few weak ones). The infra-red inactive bands of  $\gamma$ -picoline ( $a_2$  class,  $C_{2v}$  point

[10] W. B. PERSON, R. E. HUMPHREY and A. I. POPOV, *J. Am. Chem. Soc.* **81**, 273 (1959).

[11] J. H. S. GREEN, W. KNYASTON and H. M. PAISLEY, *Spectrochim. Acta* **19**, 549 (1963).

[12] D. A. LONG and W. O. GEORGE, *Spectrochim. Acta* **19**, 1777 (1963).

Table 5. Assignment of infra-red active fundamentals of  $\gamma$ -picoline complexes, and comparison with  $\gamma$ -picoline and  $\gamma$ -picolinium ion ( $\text{cm}^{-1}$ )

Designation [11]	$\gamma$ -Picoline	$\gamma$ -Pic-I-CN	$\gamma$ -Pic-I <sub>2</sub>	$\gamma$ -Pic-I-Br	$\gamma$ -Pic-I-Cl	( $\gamma$ -PicH) <sup>†</sup>
<i>a</i> <sub>1</sub>						
$\nu$ (CH) 2	3050	3059	3060	3063	3067	—
$\nu$ (CH) 20a	3040	3041	3042	3042	3045†	—
$\nu$ (CC) 8a	1603	1610*	1616*	1620*	1623*	1633
$\nu$ (CC, CN) 19a	1495	1503*	1499*	1498*	1498*	1504
$\beta$ (CH) 9a	1220	1224	1249	1250	1250	1259
$\beta$ (CH) 18a	1042	1040	1039	1039	1039	1033
ring 1	994	1008	1012	1014	1017	1007
X-sens 13	1212	1216	1212	1213	1212	1220
X-sens 12	801	—	—	—	—	—
X-sens 6a	514	526	531	535	535	521
methyl	2924	—	—	—	2923†	—
methyl	1378	—	1382§	1385*	1383*	1377
$\nu$ (I—X)	—	420†	169†	201†	284†	—
$\nu$ (N—I)	—	—	—	124‡	135†	—
$\nu$ (C—N)	—	2146	—	—	—	—
<i>b</i> <sub>1</sub>						
$\nu$ (CH) 20b	3050	3059	3060	3063	3067	—
$\nu$ (CH) 7b	3029	3028	3025	3028	3018	—
$\nu$ (CC) 8b	1561	—	—	1560†	1560†	—
$\nu$ (CC, CN) 19b	1417	—	—	1420†	1420†	—
$\nu$ (CC, CN) 14	1365	—	—	—	1355*	1366
$\beta$ (CH) 3	1283	—	1286	—	—	1311
$\beta$ (CH) 18b	1114	—	—	1115*	1117*	—
$\alpha$ (CCC) 6b	669	—	—	—	—	651
X-sens 15	341	—	—	—	—	351
methyl	2970	—	—	2980	2982†	—
methyl	1449	—	—	1445†	1445†	—
methyl	1068	1070	1067	1068	1067	1069
$\alpha$ (ICN)	—	336†	—	—	—	—
<i>b</i> <sub>2</sub>						
$\nu$ (CH) 5	969	972	968	969	970	—
$\nu$ (CH) 10b	799	800	802	804	804	793
$\phi$ (CC) 4	728	722	714	714	714	—
$\phi$ (CC) 11	485	486	485	485	485	477
X-sens 16b	211	—	—	—	—	222
methyl	2960	—	—	—	—	—
methyl	1445	—	—	1445	1445	—
methyl	1148	—	—	—	—	—
$\alpha$ (ICN)	—	336†	—	—	—	—

All frequencies refer to CS<sub>2</sub> solution except:\* In CH<sub>2</sub>Cl<sub>2</sub>.

† In mull.

‡ In benzene.

§ In CHCl<sub>3</sub>.

demonstrated for  $\nu_1$ ,  $\nu_{6a}$ , and  $\nu_{10b}$  in Table 6 and reference can be made to Tables 1-4 for further examples. At the same time, the expected rise in the N—I stretching frequency, and corresponding fall in the IX stretching frequency is also observed (Table 6.)

#### COMPARISON WITH PYRIDINE COMPLEXES

Since the ionisation potential of  $\gamma$ -picoline (9.6 eV) is lower than that of pyridine (9.8 eV) [15] stronger complexes should result. Some evidence of this appears in the "sensitive" ring vibrations, which show greater frequency changes on complexing in the  $\gamma$ -picoline series, than do their counterparts in the pyridine series. The IX vibrations are also indicative of greater charge transfer in the  $\gamma$ -picoline series, being at lower frequency than in the corresponding pyridine complexes, thus:

Solvent: benzene	I <sub>2</sub>	IBr	ICl
$\gamma$ -picoline	169	201	284
Pyridine	171	204	290

The effect however, is quite small, less than that produced by change of solvent. The NI vibration frequencies of the  $\gamma$ -picoline complexes, however, are *lower* than those of the corresponding pyridine ones, whereas the greater stability of the  $\gamma$ -picoline complexes would lead to the expectation of a higher frequency. Although some part of the frequency decrease may be due to changes in the G matrix resulting from the increased mass, it is necessary to regard the entire donor molecule as a point mass to account for the observed decrease in frequency. This is certainly unrealistic, and a more detailed examination of the intermolecular force field is called for.

*Acknowledgement*—We wish to thank the Education Department, Government of Assam, for a grant to one of us (I. H.)

[15] See Ref. [2], p. 156.



## ERRATA

I. HAQUE and J. L. WOOD, The infra-red spectra of  $\gamma$ -picolene-halogen complexes. *Spectrochimica Acta* **23A**, 2523 (1967).

Owing to a printing error subsequent to the galley proofs, the notation and key to Table 6 of this paper was omitted.

The Table should read:

Table 6. Effect of environment of some vibration frequencies

		$\gamma$ -PicICN	$\gamma$ -PicI <sub>2</sub>	$\gamma$ -PicIBr	$\gamma$ -PicICI
$\nu_{6a}$	1	526	531	535	535
	2	528	532	537	540
	3	529	533	540	543
	4	530	536	540	543
	5			544	549
$\nu_{10b}$	1	800	802	804	804
	2	802	802	806	809
	3	803	805	808	809
	5			812	808
$\nu_1$	1	1008	1012	1014	1017
	2	1009	1010		
	3	1008	1013	1019	1023
	4	1010	1012	1019	1022
	5			1022	1024
IX stretching	2		169	201	284
	6			189*	284
	4		162	189	276
	5			189	281
NI stretching	2			124	135
	6			127	138
	7				143
	4			131	146
	5			146	166(?)

1, carbon disulphide solution; 2, benzene solution; 3, methylene chloride solution; 4,  $\gamma$ -picoline solution; 5, nujol mull; 6, chlorobenzene solution; 7, benzene + acetonitrile solution.

\* This band merges with the solvent band at 195 cm<sup>-1</sup>.

J. E. CHAMBERLAIN, A. E. COSTLEY and H. A. GEBBIE, Sub-millimetre dispersion of liquid tetrabromoethane. *Spectrochimica Acta* **23A**, 2255 (1967).

The conversion factor given in Table 1 should read  $W/(10^3 \rho)$ . To correct for this error the values published (as darks) in the last column of Table 1 should be multiplied by  $1.36 \times 10^{-2}$  to give the correct values in darks.

THE VIBRATION SPECTRA OF THE COMPLEXES PYRIDINE-BROMINE,  
AND PYRIDINE-BROMINE CHLORIDE

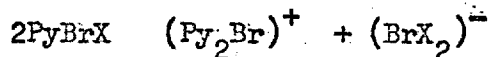
by

S.G.W. GINN, INAMUL HAQ<sup>u</sup> and J.L. WOOD

Chemistry Department, Imperial College  
of Science and Technology,  
Imperial Institute Road, London S.W.7.

ABSTRACT

The vibrational spectra extending to  $80 \text{ cm}^{-1}$  of the complexes formed by pyridine with bromine, and with bromine chloride have been examined by infrared grating spectrometers and a He/Ne laser Raman spectrometer. In non-polar solvents complexes are predominantly un-ionised. The spectra of the complexes are consistent with  $C_{2v}$  symmetry, the halogens atoms lying on the  $C_2$  axis. Electron transfer appears to be as great as in the corresponding iodine complexes. Additional bands, prominent in polar media, are identified as due to the cation  $(\text{Py}_2\text{Br})^+$ , and the anions  $\text{Br}_3^-$  or  $\text{BrCl}_2^-$  in the bromine and bromine chloride complexes respectively,



## INTRODUCTION

The rôle of both bromine and bromine chloride to accept electrons and form charge-transfer complexes is well established<sup>(1)</sup>. The complexes with pyridine are sufficiently stable to be isolated<sup>(2)</sup> as crystalline solids. The infrared spectra of the equimolar pyridine-bromine, and pyridine bromine chloride solutions in chloroform have been examined over a small frequency range around  $1000\text{ cm}^{-1}$  by Zingaro and Witmer<sup>(3)</sup>, but no extensive study of the vibrational spectra of these complexes appears to have been made. Recently features of the low frequency infrared spectrum of the pyridine bromine complex have been described<sup>(4)</sup>, and these agree substantially with the present results. We understand an account of this parallel investigation will shortly be published<sup>(5)</sup>. The He/Ne laser Raman spectra of solutions of bromine in various donors have been recently reported<sup>(6)</sup>, but a more extensive examination of the Raman spectra of the pyridine-bromine complex in various solvents fails to support these results.

## EXPERIMENTAL

### Materials

All reagents and solvents were 'AnalaR' grade except nitromethane, acetonitrile, and methylene chloride,

which were 'Reagent Grade'. All were purified and dried by standard methods. Pyridine bromine and pyridine bromine chloride were prepared as described by Williams<sup>(2)</sup>  $\text{PyBr}_2$  m.p.  $61^\circ$  (lit.  $62-3^\circ$ ) Br 66% calc. 66.9%;  $\text{PyBrCl}$  m.p.  $105^\circ$  (lit.  $107-8^\circ$ ) N 6.8% calc. 7.2% total halogen 58.5% calc. 59.4% . \*

### Spectroscopy

Above  $400\text{ cm}^{-1}$  infrared spectra were recorded with a Grubb-Parsons 'Spectromaster'. There were no differences between the spectra of fresh solutions using KBr, AgCl or polythene windows, but more rapid decomposition ensues in cells with KBr windows. Spectra below  $400\text{ cm}^{-1}$  were obtained using a single beam vacuum grating spectrometer constructed in the Department. For these spectra all samples were enclosed in sealed polythene bags, and examination completed within 30 minutes of preparation.

Raman spectra were recorded with a Cary 81 spectrometer equipped with a 'Spectra-Physics' model 125 He-Ne laser, giving  $6328\text{ \AA}$  radiation. Solutions were

---

\* The poor total halogen analysis probably results from the difficulty of recrystallising the solid, due to decomposition cf. ref. 2.

irradiated along the axis of a conventional 'Hilger' Raman sample tube, shortened to 12 cm. Glycerol was employed between the end optical flat of the sample tube and the condensing lens to reduce reflection losses. Tests showed that liquid phase Raman spectra were stable for at least 30 minutes, but all runs were completed within 15 minutes. Visual examination showed rapid discolouration of solid  $\text{PyBr}_2$  samples placed in the laser beam. To minimise the effects of decomposition a fresh sample was used for each band in the spectrum. In addition, the wavelength shift was fixed on the strong  $166 \text{ cm}^{-1}$  band, which was recorded without wavelength drive, from the onset of irradiation. This showed that the band (assigned to  $\text{Br}_2^-$ ) appears to be present ab initio, and disappears after  $\sim 30$  minutes exposure. Solid  $\text{PyBrCl}$  gave no evidence of decomposition under Raman examination.

### Results

The complexes were examined over the frequency range  $50 - 2000 \text{ cm}^{-1}$  in various solvents, and as mulls in the range  $50 - 3500 \text{ cm}^{-1}$ . Although some bands are obscured in each solvent, by intercomparison, the entire complex spectrum can be built up, and certain bands can be followed through a range of environments. All the

bands shown in Tables 1 and 2 have thus been clearly distinguished from solvent bands, though many may nearly coincide with these in a particular solvent such as pyridine. The appearance of the low frequency spectra are shown in Fig.1 and 2.

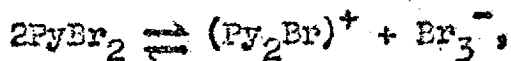
### DISCUSSION

#### IDENTIFICATION OF SPECIES PRESENT

##### The Pyridine-Bromine System

The low frequency range is the most useful for identifying the species present. In benzene solution, the weak infrared band at  $187\text{ cm}^{-1}$  and the medium Raman band at  $162\text{ cm}^{-1}$  indicate the presence of a small amount of  $\text{Br}_3^-$  ion (7). The weak Raman band at  $308\text{ cm}^{-1}$  is due to bromine solvated by benzene, as shown by the intensity change of this band when the pyridine/bromine ratio is changed (Table 3). The remaining bands below  $400\text{ cm}^{-1}$ , viz.  $229\text{ cm}^{-1}$  (infrared)  $226\text{ cm}^{-1}$  (Raman) and  $128\text{ cm}^{-1}$  are ascribed to the un-ionised  $\text{PyBr}_2$  complex, which is the predominant species present. The anticipated counter ion to the tribromide is the bis-pyridine bromine I cation  $(\text{Py}_2\text{Br})^+$ . Salts of this cation have been examined (8) and show that two bands occur in the present frequency range,  $170\text{ cm}^{-1}$  (infrared) and  $195\text{ cm}^{-1}$  (Raman)

Both bands are rather weak compared to  $\text{Br}_3^-$  bands, and neither is observed in benzene solutions of the complex. In the higher frequency range most of the  $(\text{Py}_2\text{Br})^+$  bands nearly coincide with corresponding  $\text{PyBr}_2$  bands arising from the same pyridine ring mode. The ring modes  $\nu_{16b}$  and  $\nu_{6a}$  giving rise to strong infrared bands around  $430 \text{ cm}^{-1}$  and  $630 \text{ cm}^{-1}$  are, however, sensitive to the nature of complexing at the nitrogen atom<sup>(9,13)</sup>. These bands are doubled in benzene solution. In each case the weaker component closely coincides with the appropriate ring vibration of the  $(\text{Py}_2\text{Br})^+$  ion, to which it is ascribed. All the remaining observations on benzene solution are consistent with the presence of the equilibrium



the un-ionised complex being favoured. Examination of  $\text{Me}_4\text{NBr}_3$  solutions show that the  $\text{Br}_3^-$  ion is not insoluble in benzene.

On passing to more polar solvents, e.g.  $\text{CH}_2\text{Cl}_2$  or excess pyridine the  $163 \text{ cm}^{-1}$  Raman band and the  $185 \text{ cm}^{-1}$  infrared band of the  $\text{Br}_3^-$  ion increase in intensity, as expected, as do the two higher frequency bands  $\nu_{6a}$ ,  $\nu_{16b}$  of the  $\text{Py}_2\text{Br}^+$  ion. However the low frequency bands of this ion still cannot be distinguished. The

bands due to the un-ionised complex show small and progressive solvent shifts as the polarity of the solvent increases, in the same direction as in the iodine complexes<sup>(9)</sup>. In a solution of 0.2 M Br<sub>2</sub> and 1.0 M pyridine in benzene, Klaboe<sup>(6)</sup> observed two low frequency bands in the Raman spectra, a weak band at 302 cm<sup>-1</sup> ascribed to the benzene Br<sub>2</sub> complex, and a stronger band at 281 cm<sup>-1</sup> ascribed to the pyridine Br<sub>2</sub> complex. In repeated examination of the Raman spectra of this solution we find two strong bands, at 163 cm<sup>-1</sup> (assigned to Br<sub>3</sub><sup>-</sup>) and 215 cm<sup>-1</sup> (assigned to Br-Br stretch of complex). In an attempt to resolve the disagreement with Klaboe's result, we have examined the Raman spectra of the pyridine complex in various solvents. The observed bands, shown in Table 3, can be satisfactorily accounted for in a manner consistent with the other observations reported in this paper, but we are unable to offer an explanation of Klaboe's observations.

The low frequency spectra of the solid "complex" show some notable differences from the solution spectra. Most remarkable is the absence in both the infrared and Raman spectra of any band near the frequency of the Br-Br stretching of the un-ionised complex. Even



after making allowance for the change of environment, this band would still be expected in the range  $200-220 \text{ cm}^{-1}$ , strong in both the infrared and Raman. The indication that the solid is not composed of the un-ionised charge transfer complex is supported by the presence of only single infrared bands in the  $\nu_{6a}$  and  $\nu_{16b}$  vicinity, the frequencies of these bands corresponding with those of the  $(\text{Py}_2\text{Br})^+$  ion. All the low frequency bands can be accounted for by the  $(\text{Py}_2\text{Br})^+$  and  $\text{Br}_3^-$  ions. Thus the strong infrared band at  $180 \text{ cm}^{-1}$  and the strong Raman band at  $166 \text{ cm}^{-1}$  can be confidently assigned to  $\nu_3$  and  $\nu_1$  of the  $\text{Br}_3^-$  ion respectively. The weak Raman band at  $188 \text{ cm}^{-1}$  and the shoulder on the infrared band at  $169 \text{ cm}^{-1}$  may also be assigned to these vibrations, weakly allowed by relaxation of the symmetry in the lattice. An infrared band of the  $(\text{Py}_2\text{Br})^+$  ion also lies at  $170 \text{ cm}^{-1}$ , and may contribute to the observed shoulder. The only Raman band of the  $(\text{Py}_2\text{Br})^+$  ion in this range is a fairly weak one at  $\sim 195 \text{ cm}^{-1}$ , and satisfactorily accounts for the observed band at this frequency. In other  $\text{Py}_2\text{Br}^+$  salts this Raman band is not split<sup>(8)</sup>, so the assignment of  $188 \text{ cm}^{-1}$  to the  $\text{Br}_3^-$  ion is more probable than that  $188 \text{ cm}^{-1}$  and  $198 \text{ cm}^{-1}$  form a doublet arising from the  $\text{Py}_2\text{Br}^+$  ion. As the appearance, and position,

of all the higher frequency bands of the solid also closely correspond to those of  $(\text{Py}_2\text{Br})^+$  salts (again frequencies vary slightly with the anion) we infer that the solid 'complex' is entirely in the form of  $(\text{Py}_2\text{Br})^+$  +  $\text{Br}_3^-$  ions. The ionisation is reversible. On solution the solid gives spectra identical with those obtained by directly mixing pyridine and bromine solutions in the appropriate solvent (Table 1).

#### Pyridine Bromine-Chloride

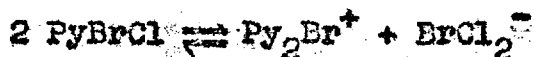
In benzene solution the low frequency range contains only two infrared bands. The higher frequency band at  $\sim 308 \text{ cm}^{-1}$ , which is strong in both the infrared and Raman spectrum is assigned to the BrCl stretching of the un-ionised charge transfer complex. Since bromine chloride can disproportionate  $2\text{BrCl} \rightleftharpoons \text{Br}_2 + \text{Cl}_2$ , the question arises whether the observed band might be due to the benzene- $\text{Br}_2$  complex, which has a band at  $\sim 308 \text{ cm}^{-1}$ . Any  $\text{Br}_2$  however would preferentially complex with the pyridine present, - that the latter is associated is clearly shown by the higher frequency spectrum. The distinction from the low frequency spectrum of the  $\text{PyBr}_2$  complex in benzene shows that disproportionation has not occurred. Further evidence is the fact that no  $\text{Cl}_2$  is evolved.  $\text{Cl}_2$  does not form

a stable pyridine complex under these conditions. The lower frequency band is assigned to the N--Br stretching of the complex. The remaining high frequency spectrum can be assigned entirely to a single species, the un-ionised complex. This is supported by the presence of only single  $\nu_{6a}$  and  $\nu_{16b}$  bands.

In excess pyridine solution the low frequency infrared range contains an additional strong band at  $\sim 226 \text{ cm}^{-1}$ . Although the asymmetric stretching frequency of the  $\text{BrCl}_2^-$  was originally reported at  $305 \text{ cm}^{-1}$  (7), this is high in comparison with other trihalide ions (11), and recently Evans and Lo (10) have determined the frequency of this mode at  $227 \text{ cm}^{-1}$  in the spectra of tetraalkylammonium<sup>+</sup>  $\text{BrCl}_2^-$  salts in a benzene/acetonitrile mixture as solvent. We therefore ascribe the  $226 \text{ cm}^{-1}$  band to the  $\text{BrCl}_2^-$  ion. The strong polarised Raman band at  $275 \text{ cm}^{-1}$  agrees with the reported  $\nu_1$  frequency of the ion (10). A strong band is also present in the infrared spectrum at this frequency, and cannot be due to  $\nu_1$  of  $\text{BrCl}_2^-$ . Comparison with the spectrum in benzene solution suggests its ascription to the Br-Cl stretching of the un-ionised complex. If so, there should also be a contribution from this mode to the Raman band.

The latter is appreciably asymmetric (polarisation is found not to change the asymmetry), and in 1:4 dioxane solution the two contributions to the Raman band are more clearly resolved. The fairly strong band in the infrared at  $160\text{ cm}^{-1}$  is very weak in the Raman. Although this suggests its assignment to the bending vibration of the  $\text{BrCl}_2^-$  ion, which in crystalline salts is found near  $140\text{ cm}^{-1}$  (10), there are two reasons for preferring its assignment to the N-Br stretching of the un-ionised complex. The first is that the  $\text{BrCl}_2^-$  bending frequency would be expected to be lower in solution than in the solid rather than higher, secondly, a similar infrared band is observed at  $144\text{ cm}^{-1}$  in a benzene solution of the complex, which contains no  $\text{BrCl}_2^-$  ions. This band is unobservable in the Raman spectrum. Further support for the occurrence of dissociation  $2\text{PyBrCl} \rightleftharpoons (\text{Py}_2\text{Br})^+ + (\text{BrCl}_2)^-$  is provided by the  $(\text{Py}_2\text{Br})^+$  bands. The Raman band at  $\sim 192\text{ cm}^{-1}$  (this is the  $\nu_1$  type vibration) is observable, and in the higher frequency range the presence of an additional band in polar solvents at  $\sim 445\text{ cm}^{-1}$  corresponds to the  $\nu_{16b}$  band of  $\text{Py}_2\text{Br}^+$ . The  $\nu_{6a}$  band of this ion is at  $639\text{ cm}^{-1}$ , and although a strong infrared band is present at this frequency in pyridine solutions,

the  $\nu_{6a}$  band of the un-ionised complex is also expected near this frequency. No indication of a doublet structure is observed in pyridine solution, but in  $\text{CH}_2\text{Cl}_2$  a second contribution becomes apparent. Thus all the features of the solution spectra are consistent with the equilibrium



no detectable dissociation occurring in benzene, but appreciable ionisation taking place in polar solvents.

The interpretation of the vibrational spectra of the solid complex presents several difficulties. From the appearance and m.p. the solid appears to be identical with the material reported by Williams<sup>(2)</sup>. The solubility is similar to that of the other solid complexes examined, and after solution the spectra (see above) are readily interpreted. It can be concluded that no chemical reaction such as substitution in the pyridine ring has taken place during preparation. In the frequency range of the ring vibrations, only single  $\nu_{16b}$  and  $\nu_{6a}$  occur in the infrared, the frequency corresponding to the un-ionised complex. Comparison with, e.g. the bromine complex, suggests that a 'solvent' shift is unlikely to be sufficiently large to permit an alternative interpretation as  $(\text{Py}_2\text{Br})^+ + (\text{BrCl}_2)^-$ .

The remaining higher frequency spectrum also corresponds quite closely to that of the un-ionised complex, except for some notable intensity changes, as in the 1206 and 1250  $\text{cm}^{-1}$  bands,--but taken as a whole gives the general impression that the solid is entirely in the un-ionised form - in contrast to the  $\text{PyBr}_2$  complex. In the low frequency range the absence of the strong infrared band of  $\text{BrCl}_2^-$  near 220  $\text{cm}^{-1}$  and the Raman band near 276  $\text{cm}^{-1}$  at first sight also supports this view. However the assignment of the observed bands entirely to the un-ionised form is not straightforward, firstly because four, instead of two bands, occur in the 160 - 300  $\text{cm}^{-1}$  range, secondly, because the 255  $\text{cm}^{-1}$  band is entirely absent in the infrared, while the 295  $\text{cm}^{-1}$  band is entirely absent in the Raman. The near mutual exclusion of the infrared and Raman spectra indicates the presence of centrosymmetric units. Formally this means a centrosymmetric unit cell. Such a model, with each cell containing 2n un-ionised  $\text{PyBrCl}$  units has the merit of being in accordance with the higher frequency spectra. The low frequency spectra can be accounted for if there is strong interaction between the  $\text{PyBrCl}$  units, the 295 and 255  $\text{cm}^{-1}$  bands both deriving from the  $\text{BrCl}$  stretching mode, and the

196 and 171  $\text{cm}^{-1}$  bands from the NBr stretching mode. The band at 104  $\text{cm}^{-1}$  and lower bands are then assigned to bending or rocking modes. If the intermolecular interaction is sufficiently great to produce splittings of this magnitude, the distinction between internal vibrations and lattice modes dissolves, as does the concept of molecular units. This assignment however still conflicts with the depolarisation of the 255  $\text{cm}^{-1}$  band.

It is also possible to assign the low frequency spectra to  $(\text{Py}_2\text{Br})^+$  and  $\text{BrCl}_2^-$  units, not necessarily situated in a centrosymmetric unit cell. <sup>However</sup> The assignment requires the  $\nu_1$  band of  $\text{BrCl}_2^-$  to be activated in the infrared (cf ref.10) and to be separated from the accompanying Raman  $\nu_2$  band by 40  $\text{cm}^{-1}$ . Assignment of the 196  $\text{cm}^{-1}$  band to  $\nu_3$  would also require a displacement of some 30  $\text{cm}^{-1}$  from the usual position. A further difficulty is that no band is found near the expected  $\text{BrCl}_2^-$  bending frequency  $\sim 140 \text{ cm}^{-1}$ . Thus much larger than usual displacements of the  $\text{BrCl}_2^-$  band positions are implied. As, further, the  $(\text{Py}_2\text{Br})^+$  infrared band at  $\sim 170 \text{ cm}^{-1}$  is not observed, and the higher frequency bands are more difficult to fit to the  $(\text{Py}_2\text{Br})^+$  ion, the preferred interpretation is on the basis of un-ionised

PyBrCl units. This contrasts with solid PyBr<sub>2</sub>, but in a crystal where the strong intermolecular or inter-ionic forces are comparable to the weak charge-transfer type intramolecular or intraionic forces, the ionic or un-ionised models represent only limiting structures, the spectra showing that neither exactly represents the solid PyBrCl complex.

#### Assignment

The bands ascribable to the un-ionised complexes<sup>a</sup> may readily be assigned by comparison with the spectra of pyridine and its iodo-complexes, and is shown in Table 4. The absence in the solution infrared spectra of bands corresponding to the a<sub>2</sub> modes of pyridine suggest that C<sub>2v</sub> symmetry is retained in the complexes, i.e. that the halogen atoms lie on the C<sub>2</sub> axis of pyridine. As usual, inferences from the absence of vibrational bands do not exclude the possibility of a small amount of asymmetry.

#### Comparison with iodo complexes

On forming complexes, certain pyridine or  $\gamma$ -picoline vibrations show appreciable frequency shifts. The modes involved and the direction of the shifts are the same in series of hydrogen bonded<sup>(12)</sup> charge-transfer<sup>(9,13)</sup> or metal-co-ordination<sup>(14,15)</sup> complexes. There is no



correlation of the frequency shifts with the mass of the adjacent co-ordinated atom, which can vary from H to I, and so mechanical coupling does not appear to be the cause. The shifts, however, fit in well with the expected extent of electron transfer out of the pyridine or  $\gamma$ -picoline rings. In Table 5 the frequencies of some of the most sensitive vibrations ( $\nu_1$ ,  $\nu_{6a}$ ,  $\nu_{19b}$  and  $\nu_{16b}$ ) are shown for the bromo and iodo complexes. The frequency shifts indicate greater charge transfer in the bromine chloride than in the bromine complex. This parallels the increasing electron transfer in the passing through the  $I_2 - IBr - ICl$  series. Less expected is the observation that the shifts in the bromine complexes are as great as in the corresponding iodine ones, suggesting a comparable amount of charge transfer.

In the iodine and iodine halide complexes, increasing electron transfer is accompanied by a progressive weakening of the interhalogen bond, as manifested in the decrease of the halogen stretching frequency<sup>(16)</sup>. Table 6 shows the proportional decrease  $\Delta$  of this frequency in the present series, and, for comparison, that in the corresponding iodine and iodine halide complexes. The order supports the observations in

the sensitive donor modes thus  $\Delta$  is greater for the  $\text{BrCl}$  than for the  $\text{Br}_2$  complex. It is also greater for the bromide complexes than for the corresponding iodine ones, suggesting greater electron transfer in the bromine series. Despite this, the bromine and bromine chloride complexes give the impression of being less stable than the iodine complexes. Continuing the series through, attempts to prepare a  $\text{PyCl}_2$  complex have failed, supporting the order of stability  $\text{PyI}_2 > \text{PyBr}_2 > \text{PyCl}_2$ .

#### Extent of Electron Transfer

It has been seen above that the vibrational spectra indicate that the extent of charge transfer in the bromine series of complexes is as great, or greater than in the corresponding iodine series, despite the greater stability of the latter. A possible explanation in terms of 'back-transfer' - the contribution of a valence bond structure  $\text{Py}^{\ominus} \dots (\text{XY})^{\oplus}$  has been suggested by Dr. I. Hillier<sup>(20)</sup>. Such an electron transfer, involving donation from the antibonding  $\bar{\text{a}}_g$  orbital of the halogen to the lowest unoccupied  $\pi$  orbital of the pyridine would occur more readily in the iodine than in the bromine series. The effect would be to increase the stability of the iodine series, reduce the net

charge transfer in these complexes, and to increase the strength of the IX bond compared to the BrX bond. An attempt is now being made to explore the implications of this suggestion quantitatively.

#### Effect of Environment

We are examining here, as before<sup>(9,13)</sup> the effect of change of solvent or phase on a given complex. This is in distinction to most previous work, in which a given acceptor has been examined in various solvents, which act both as donor and as solvent. The pyridine-iodine halide and  $\gamma$ -picoline iodine halide complexes the effect of the environment was clearly established, - increasing polarity facilitates charge transfer, with the result that the 'sensitive' vibrations of the donor moiety move in the same direction in environments of increasing polarity as they do with a series of increasingly electron attracting acceptors. Exactly similar behaviour is exhibited by the present complexes (see Table 7). The skeletal vibrations are particularly sensitive to solvent changes and also follow the previously established pattern: as the polarity of the environment increases, the NBr stretching frequency rises, and the BrX stretching frequency falls. Both these changes are in the same direction as those

produced by increasing electron transfer. The frequency shifts are noticeably greater in the more polar  $\text{ErCl}$  complex. It is also apparent that the magnitude of the frequency shifts produced by changes of environment are comparable with those produced by a change of acceptor - thus it is as important to pay regard to the solvent in measuring or considering the properties of a charge transfer complex, as to consider the chemical nature of the donor and acceptor. This seems to have been rather overlooked in some earlier work.

#### ACKNOWLEDGEMENTS

We thank the S.R.C. for a postdoctoral Fellowship, and the Government of Assam for a maintenance grant.

REFERENCES

1. G. Briegleb, Elektronen-Donator Acceptor Komplexe  
Springer, Berlin 1961, Andrews and Keefer.
2. D.M. Williams, J. Chem. Soc. 2781, 1931.
3. W.B. Person, R.E. Erickson and R.E. Buckles,  
J.A.C.S., 82, 29, 1960.  
R.A. Zingaro and W.B. Wittmer, J. Phys. Chem. 64  
1705, 1960.
4. R.F. Lake, contribution to "Symposium on the Physical  
Chemistry of Weak Complexes", Chemical Society  
Anniversary Meeting 1967.
5. W.H. Thompson, private communication.
6. P. Kláboe, J.A.C.S., 89, 3667, 1967.
7. W.B. Person, G.R. Anderson, J.N. Fondenwalt,  
H. Stammerich and R. Formeris, J. Chem. Phys.  
35, 908, 1961.
8. I. Haque and J.L. Wood, to be published.
9. I. Haque and J.L. Wood, Sp. Acta 23A 959, 1967.
10. J.C. Evans and G. Y-S Lo, J. Chem. Phys. 44, 4356, 1966.
11. A.G. Maki and R. Formeris, Sp. Acta, 23A, 867, 1967.
12. H. Takahashi, K. Mamola and E.K. Plyler, J. Mol. Spect.  
21, 217, 1966.
13. I. Haque and J.L. Wood, Sp. Acta, 23A, 2523, 1967.
14. M. Goodgame and P.J. Hayward, J.C.S. (A) 632, 1966.
15. N.S. Gill and H.F. Kington, Aust. J. Chem. 19, 2197, 1966.

16. E.K. Plyler and R.S. Mulliken, J. Am. Chem. Soc. 81,  
823 (1959).
17. H. Stammerich, R. Fornieris and Y. Tavares, Sp. Acta,  
17, 1173, 1961.
18. S.G.W. Ginn and J.L. Wood, Trans. Faraday Soc. 62,  
777, 1966.
19. J.H.S. Green, W. Kynaston and H.M. Paisley, Sp. Acta,  
19, 549, 1963.
20. I. Hillier, private communication.

Table 1

## Infrared Spectra of the Pyridine-Bromide Complex in different media

Saturated Equimolar soln of $\text{PyBr}_2$ (solid) in $\text{C}_6\text{H}_6$	Saturated Equimolar soln of $\text{PyBr}_2$ (solid) in $\text{CH}_2\text{Cl}_2$	Equimolar soln of Py and $\text{Br}_2$ in $\text{CH}_2\text{Cl}_2$	Saturated soln of $\text{PyBr}_2$ (solid) in pyridine	Bromine in excess of pyridine	Solid $\text{PyBr}_2$ in Nujol	Solid $\text{PyBr}_2$ in hexachlorobutadiene
$\text{cm}^{-1}$	$\text{cm}^{-1}$	$\text{cm}^{-1}$	$\text{cm}^{-1}$	$\text{cm}^{-1}$	$\text{cm}^{-1}$	$\text{cm}^{-1}$
1599 sh 1591 s	1912 w 1841 w 1709 m 1602 sh 1597 s	1912 w 1841 w 1711 m 1602 sh 1597 s	1455 sh 1451 s	1455 sh 1451 s	1912 w 1841 w 1715 w	1597 s 1521 m 1475 s 1402 m 1351 w
1447 s 1360 w 1349 ms	1479 ms 1450 s 1349 ms	1480 ms 1450 s 1351 ms	1250 ms 1205 s	1250 ms 1205 s	1595 s 1521 w	1254 s 1210 m 1202 s 1152 s 1102 w 1061 s
1206 s 1153 s 1062 s	1206 s 1155 s 1066 s 1041 s	1208 s 1156 s 1067 s 1041 s	1154 m	1154 m	1060 s	

Table I - continued

1009 s	1009 s	1030 s 1012 s	1030 s 1012 s	1011 s	1011 s	1035 s 1007 s 1004 sh 984 m 945 m 830 w 786 m 756 s 749 sh 699 w 684 s 672 sh 637 s	1036 s 1008 s 1004 sh      757 s  684 s 672 s 637 s  572 vw 446 s
941 m	941 m	942 m	942 m				
784 sh	784 sh						
749 s	748 s						
638 s	638 s	638 s	638 s	639 s	639 s		
627 s	626 s	628 s	628 s	629 s	629 s		
529 vw	529 vw					572 w	572 vw
445 m	445 m	446 ms	446 ms	446 m	446 m	445 s	446 s
418 s	418 s	420 s	420 s	421 s	421 s		
229 s	229 s			215 s	215 s		
187 w	187 w			185 s	185 s	180 s	
128 m	128 m			140 m	140 m	169 sh	

NS



Table 2

Infrared Spectra of the Pyridine-Bromine chloride in various media

Saturated solution in $C_6H_6$ $cm^{-1}$	Saturated solution in $CH_2Cl_2$ $cm^{-1}$	Saturated solution in Pyridine $cm^{-1}$	In Nujol Mull $cm^{-1}$	In hexachlorobutadiene Mull $cm^{-1}$
				3091 s
				3068 w
				3059 m
				3038 m
				3025 ms
	1915 w		1912 w	
1595 s	1844 w		1595 s	1597 s
	1597 s		1570 m	
	1517 w		1517 w	1521 w
1449 s	1488 w	1449 s		1475 w
	1451 s			1449 s
1348 w	1349 m		1342 s	1389 m
		1250 m	1250 s	1342 s
1206 s	1206 s	1205 s	1206 m	1251 s
	1154 s		1157 m	1206 m
1065 s	1064 s		1089 w	1089 w
	1041 ms	1040 s	1060 s	1060 s
1011 s	1033 s		1034 ms	1034 ms
	1012 s	1012 s	1015 s	1015 s
			1006 sh	1006 sh
	991 w		972 w	
	942 w		942 ms	
			861 w	
			784 w	
750 s			769 sh	
			750 s	750 s
			700 m	700 m
			684 s	684 s
			675 sh	677 sh
630 s	635 sh			
	632 s	636 s	641 s	641 s
	445 ms	446 m		

Table 2 - continued

---

422 m	425 s	428 s	430 s	430 s
307 s		274 s	295 s	
		226 s		
144 ms		160 ms	196 s	
			104 ms	
			85 w	
			71 vw	

---

Table 3Raman Spectra of the Pyridine-Bromine Complex  
in various media

Solvent		Observed bands cm <sup>-1</sup>	
Benzene	162 m	226 s	308 w
Benzene and excess of Br <sub>2</sub>		235 m	308 s
*Benzene and excess of Pyridine	163 s	215 s	
1:4 Dioxane	162 m	221 s	300 w
Methylene chloride	163 m (Pol)	218 s (Pol)	
*Pyridine	163 s (Pol)	215 s (Pol)	
Acetone	163 m	218 s	300 w
*Nitrobenzene	164 s	214 s	
*Acetonitrile	163 s	211 s	252 w
*Nitromethane	165 s	210 s	258 w
Solid PyBr <sub>2</sub>	166 s	188 w	198 w

\* ~163 cm<sup>-1</sup> band is stronger than ~220 cm<sup>-1</sup> band

Table 3 continued

## Raman Spectra of the PyBrCl Complex in various media

Solvent	Observed bands cm <sup>-1</sup>		
Benzene			308 s
1:4 Dioxane			280 sh 300 s(Pol)
Methylene chloride	192 w	~270 sh*	
Pyridine	162 vw	192 w	278 s(Pol)
Acetonitrile		190 w	276 s
Solid	102 w	171 m(dp <sub>ol</sub> )	255 s(dp <sub>ol</sub> ) 198 m (dp <sub>ol</sub> )

\* appears as a shoulder on the  $\nu_4$  band of  $\text{CH}_2\text{Cl}_2$

Table 4

Assignment of Infrared active fundamentals of Pyridine-bromine and pyridine-bromine chloride complexes, and comparison with pyridine and pyridine-iodine chloride

Designation (19)	Pyridine (liquid)	Pyridine Iodine chloride (In $CS_2$ )	Pyridine- $Br_2$ (In $CH_2Cl_2$ )	Pyridine- $BrCl$ (In $CH_2Cl_2$ )
$a_1$ $\nu_{NH}$ (CH) 2	3054	3058	-	-
$\nu$ (CH) 20a	3054	3068	-	-
$\nu$ (CO) 8a	1583	1597*	1597	1597
$\nu$ (CO, CH) 19a	1432	-	1430	1488
$\beta$ (CH) 9a	1218	1209	1206	1206
$\beta$ (CH) 18a	1068	1067	1067	1064
Ring 1	992	1009	1012	1012
X sens 13	3036	3039	-	-
X sens 12	1030	1030	1030	1033
X sens 6a	605	627	628	632
NI or NBr stretching	-	147*	128*	144*
X-Y stretch- ing	-	290*	229*	307*
$b_1$ $\nu$ (CH) 20b	3080	3085	-	-
$\nu$ (CH) 7b	3036	-	-	-
$\nu$ (CO) 8b	1572	-	-	-
$\nu$ (CO, CH) 19b	1439	1449*	1450	1451
$\nu$ (CO, CH) 14	1375	-	-	-
$\beta$ (CH) 3	1218	1209	1206	1206
$\beta$ (CH) 18b	1065	-	-	-
$\alpha$ (COO) 7b	652	655	-	-
X sens 15	1148	1150	1155	1154
$b_2$ $\gamma$ (CH) 5	942	-	942	942
$\gamma$ (CH) 10b	886	-	-	-

Table 4 - continued

Designation	Pyridine	Pyridine Iodine chloride	Pyridine-Br <sub>2</sub>	Pyridine- BrCl
φ (CC) 4	749	748	748*	750*
φ (CC) 11	700	692	-	-
X sens. 16b	405	421	420	425

\* In benzene solution

Table 5

Sensitive vibrations compared with those of Iodine  
1 Br- and 1 Cl complexes

(All frequencies refer to benzene solution)

	Py I <sub>2</sub> cm <sup>-1</sup>	Py 1 Br cm <sup>-1</sup>	Py 1 Cl cm <sup>-1</sup>	PyBr <sub>2</sub> cm <sup>-1</sup>	PyBrCl cm <sup>-1</sup>
v <sub>1</sub>	1006	1010	1011	1009	1011
v <sub>9</sub> <sup>A</sup>	623	627	630	627	630
v <sub>19</sub> <sup>A</sup>	1445	1449	1449	1447	1449
v <sub>16</sub> <sup>A</sup>		420	421	418	422

Table 6

Complex	$\nu$ complex in Benzene soln. $\text{cm}^{-1}$	$\nu$ free (17) (halogen- halogen) $\text{cm}^{-1}$	$\frac{\nu \text{ free} - \nu \text{ complex}}{\nu \text{ free}}$	%
PyI <sub>2</sub>	171 (ref.18)	213	20	
Py 1 Br <sub>2</sub>	204 (ref.18)	266	23.3	
Py 1 Cl	290 (ref.18)	381	24	
Py Br <sub>2</sub>	226	316	28.5	
Py Br Cl	307	439.5	30	



Table 7

Effect of medium on 'sensitive' vibrations

Mode of vibration	Solvent	PyBr <sub>2</sub> cm <sup>-1</sup>	PyBrCl cm <sup>-1</sup>
v <sub>1</sub>	Benzene	1009	1011
	Methylene chloride	1012	1012
	Pyridine	1011	1012
v <sub>6a</sub>	Benzene	627	630
	Methylene chloride	628	632
	Pyridine	629	635
v <sub>16b</sub>	Benzene	418	422
	Methylene chloride	420	425
	Pyridine	421	428
v(Br-X)*	Benzene	226	308
	1:4 Dioxane	221	300
	Acetone	218	
	Methylene chloride	218	
	Pyridine	215	278
	Nitrobenzene	214	
	Acetonitrile	211	276
	Nitromethane	210	
v(N-Br)	Benzene	128	144
	Pyridine	140	160

\* Raman data

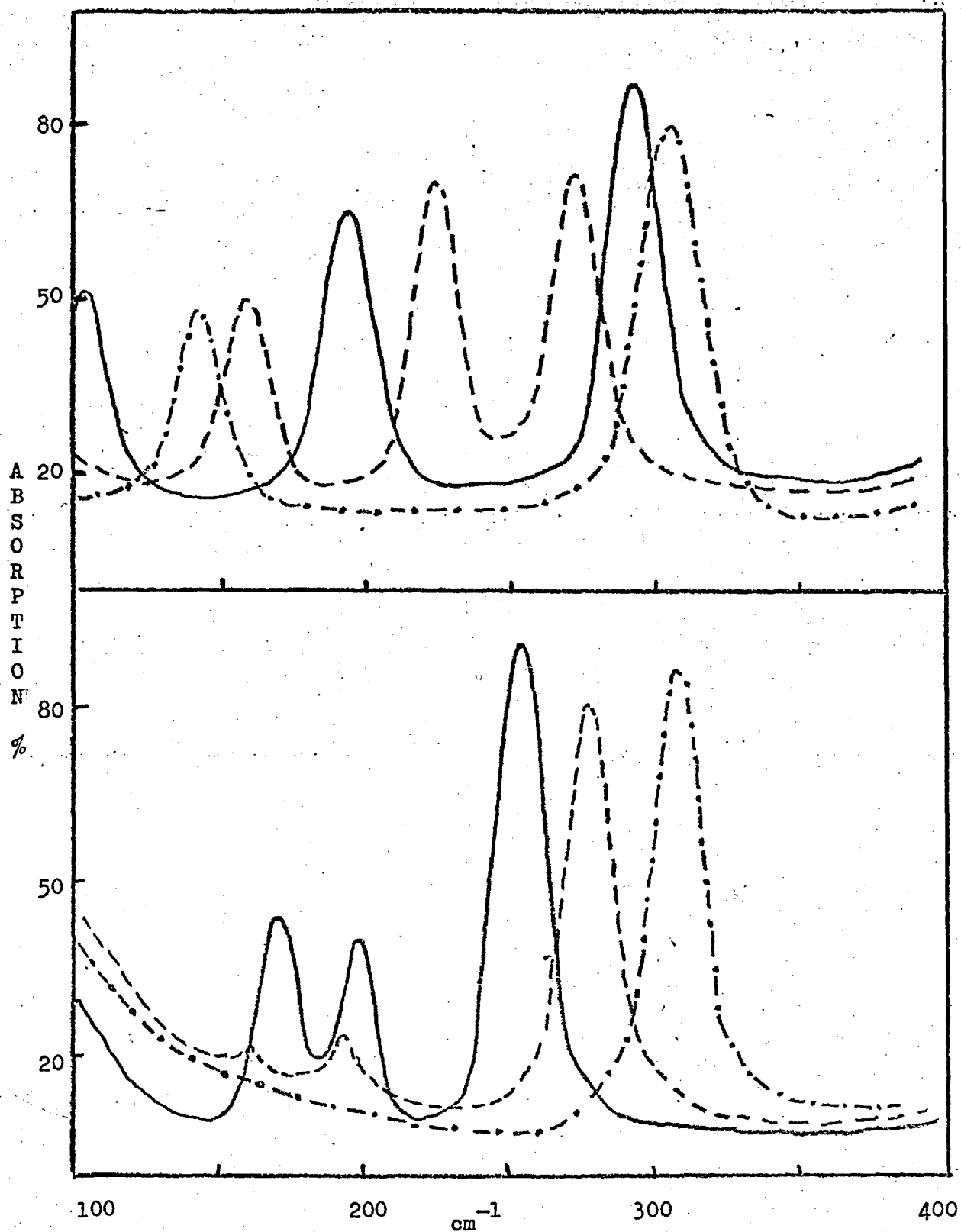


Fig. 2 Top: The infrared spectra of pyridine bromine chloride  
 Bottom: The Raman spectra of pyridine bromine chloride  
 — solid; - - - in pyridine solution; - . - . in benzene solution.

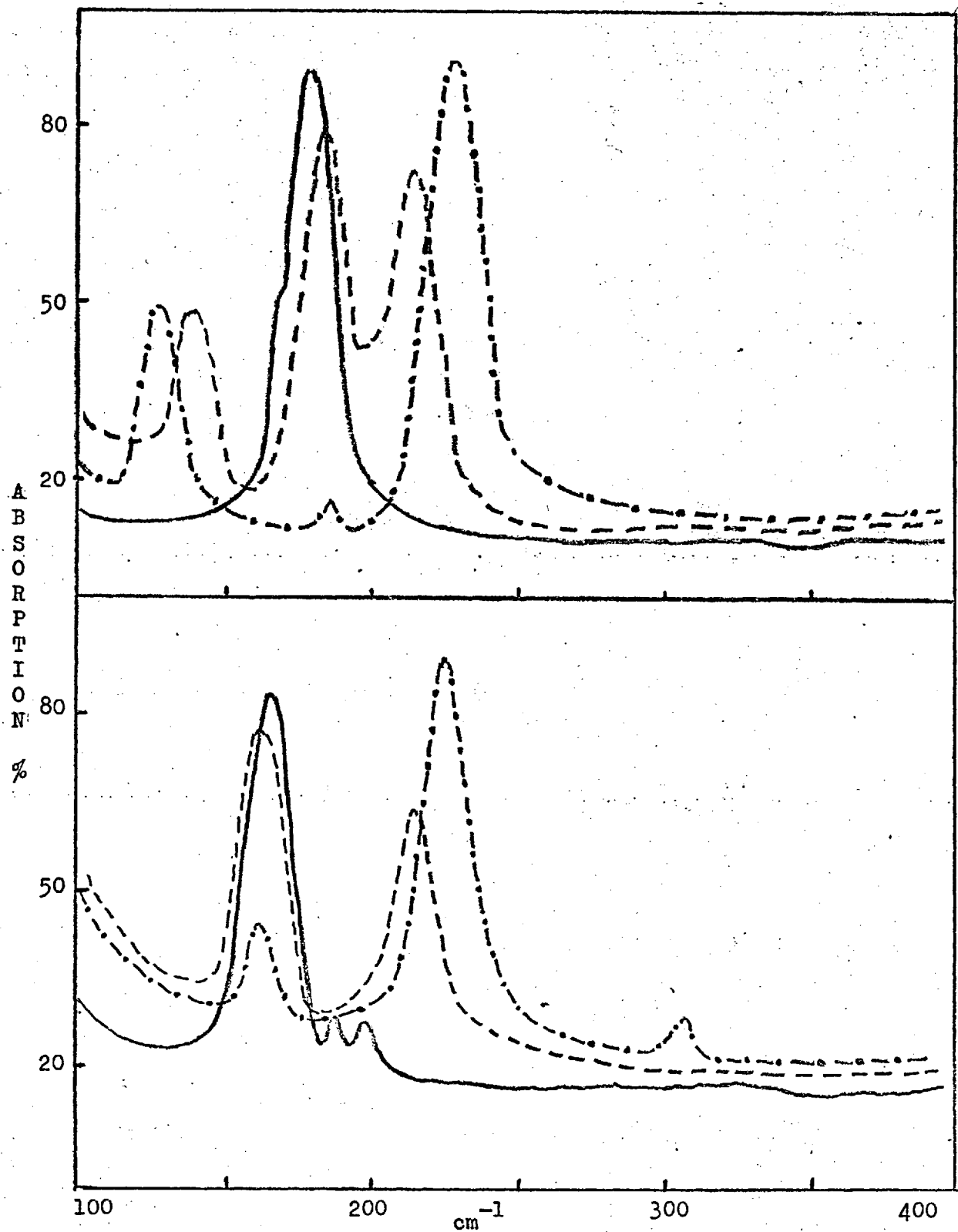


Fig. 1. Top: The infrared spectra of pyridine bromine  
 Bottom: The Raman spectra of pyridine bromine  
 ——— solid; - - - - in pyridine solution; - · - · in  
 benzene solution.

17-5-1968

Slips 1—22

1st proof

NO. 5

*Journal of Molecular Structure*

Elsevier Publishing Company, Amsterdam. Printed in the Netherlands

AUTHOR

THE VIBRATIONAL SPECTRA AND STRUCTURE OF THE BIS(PYRIDINE)IODINE(I), BIS(PYRIDINE)BROMINE(I), BIS( $\gamma$ -PICOLINE)IODINE (I) AND BIS( $\gamma$ -PICOLINE)BROMINE(I) CATIONS

I. HAQUE AND J. L. WOOD

*Chemistry Department, Imperial College of Science and Technology, London, S.W. 7.*

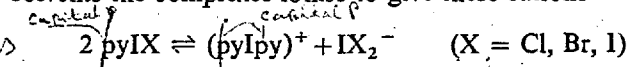
(Received March 27th, 1968)

## SUMMARY

IR (80–4000  $\text{cm}^{-1}$ ) and Raman spectra of various perchlorate, tetrafluoroborate, and hexafluorophosphate salts of bis(pyridine)iodine (I), bis(pyridine)bromine (I), bis( $\gamma$ -picoline)iodine (I) and bis( $\gamma$ -picoline)bromine (I) have been examined in various media. For the first three cations, the spectra are sufficient to establish the linearity of the N–I–N and N–Br–N atoms, and the presence of a centre of symmetry, in both mull and solution. In the iodine cations the mull spectra indicate coplanarity of the two ligand rings, and there is slight evidence that this persists in solution. Shifts of sensitive ring modes indicate the charge distribution, which is compared with the corresponding charge-transfer complexes. In contrast to the charge-transfer complexes, solvent effects are slight.

## INTRODUCTION

Salts of the bis(pyridine)iodine (I),  $(\text{pyIpy})^+$ , and bis(pyridine)bromine (I),  $(\text{pyBrpy})^+$  cations have been known for a considerable time<sup>1–3</sup>. Some bands in the 700  $\text{cm}^{-1}$  and 1000  $\text{cm}^{-1}$  region of the IR spectra of solid bis(pyridine)iodine nitrate and perchlorate were observed by Zingaro and Tolberg<sup>4a</sup>, and of solid bis(pyridine)bromine nitrate and acetate by Zingaro and Witmer<sup>4b</sup>, but no full account of the spectra were given. The bis(pyridine)iodine (I) cation has also been shown by X-ray diffraction to be present in the pyridine–iodine adduct<sup>5</sup>. Our interest in these cations derived from an examination of the IR spectra of pyridine and  $\gamma$ -picoline–halogen and interhalogen charge-transfer complexes<sup>6–8</sup>. In polar solvents the complexes ionise to give these cations



which were identified by comparison of the spectra of the solutions with those

now reported. In addition to their occurrence in these solutions the cations have a number of intrinsic features of interest. In the crystal, X-ray data show that the  $(pyIpy)^+$  ion has a centrosymmetric structure, with the two py rings nearly coplanar<sup>5</sup> (point group  $D_{2h}$ ). Determination of the structure in solution will indicate whether the two salient structural features above, viz. the collinearity of two ligands bonds, and the coplanarity of the pyridine rings, arise from the internal force field, or result from interionic forces dominating the crystal packing. Preservation of the N-I-N collinearity in solution would emphasise the similarity with the  $pyIX$  charge-transfer complexes, and with the  $IX_2^-$  ions, which may be regarded as isoelectronic in that two 3-centre  $\sigma$ -type M.O.'s involving four electrons (each halogen providing none, and each nitrogen two) can be formed throughout<sup>6</sup>.

The question of the possible retention of the coplanarity of the pyridine (or  $\gamma$ -picoline) rings in solution is particularly interesting. As far as the authors are aware, in all instances of restricted rotation so far established, the tops involved are directly united by a single bond\*. If (as will be seen) the cations are linear, restricted relative rotation of the pyridine or  $\gamma$ -picoline rings would imply a torsional interaction extending over two collinear single bonds. The similarity of the present cations with the corresponding charge-transfer complexes also suggests an intercomparison of the N-I bond strengths, and of the charge distribution. A measure of the latter is provided by the shift of the frequency of a number of characteristic "sensitive" vibrations which are largely localised in the pyridine or  $\gamma$ -picoline rings<sup>7</sup>. The effect of the environment on the vibration frequencies, which appears to be closely related to the charge distribution in the C.T. complexes<sup>6, 7b</sup> has also been examined in the cations.

## EXPERIMENTAL

### Materials

"Analar" pyridine was dried over KOH and BaO for several days and distilled from fresh BaO. The IR spectrum of purified pyridine did not show any bands of picolines, which are the most likely contaminants.  $\gamma$ -picoline was dried over KOH and BaO and distilled under reduced pressure. The purity of  $\gamma$ -picoline, checked by v.p.c., was found to be 98.8%. "Reagent-grade" methylene chloride and acetonitrile were dried and purified by standard methods. "Analar" bromine (BDH), "Analar" iodine (BDH), sodium fluoroborate (BDH), ammonium hexafluorophosphate (Orzak) Mohaning Company) and silver nitrate (BDH) were used without further purification. Nujol (liquid paraffin) and hexachlorobutadiene were kept over molecular sieves "type 4A" for several days, prior to use.

\* In, for instance, dimethyl ether, torsion is about a C-O bond, which unites a Me group and an -OMe group. There are two torsions in all in dimethyl ether, and two torsional azimuthal angles are involved. In collinear  $(pyIpy)^+$  only a single torsion is possible.

### Preparations

<sup>Bis</sup> Dipyridine silver (I) fluoroborate and <sup>bis</sup> dipyridine silver (I) hexafluorophosphate were prepared by the same method as <sup>bis</sup> dipyridine silver (I) perchlorate<sup>3</sup>; NaBF<sub>4</sub> and NH<sub>4</sub>PF<sub>6</sub> respectively being used in place of NaClO<sub>4</sub>. From these salts [py<sub>2</sub>I]BF<sub>4</sub>, [py<sub>2</sub>I]PF<sub>6</sub> and [py<sub>2</sub>Br]PF<sub>6</sub> were prepared in the same way as [py<sub>2</sub>Br]ClO<sub>4</sub> and [py<sub>2</sub>I]ClO<sub>4</sub> were prepared<sup>2,3</sup> from [py<sub>2</sub>Ag]ClO<sub>4</sub>. The corresponding  $\gamma$ -picoline salts were similarly prepared. All the salts were purified by recrystallisation from methanol.

### Analysis:

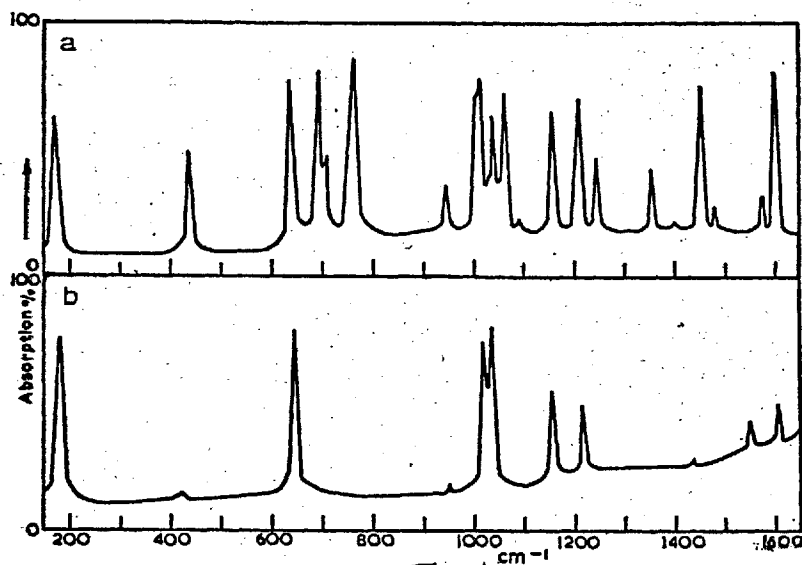
<sup>Cap P</sup> [py<sub>2</sub>I]BF<sub>4</sub>: I 33.9 %, calc. 34.15 %; N 7.4 %, calc. 7.5 %.  
<sup>Cap P</sup> [py<sub>2</sub>I]PF<sub>6</sub>: I 29 %, calc. 29.5 %; N 6.3 %, calc. 6.5 %.  
[py<sub>2</sub>Br]PF<sub>6</sub>: Br 20.4 %, calc. 20.88 %.  
[ $\gamma$ -pic<sub>2</sub>I]BF<sub>4</sub>: I 32 %, calc. 31.75 %; N 7.11 %, calc. 7 % F 19.3 %, calc. 19 %.  
[ $\gamma$ -pic<sub>2</sub>I]PF<sub>6</sub>: I 27.9 %, calc. 27.7 %.  
[ $\gamma$ -pic<sub>2</sub>Br]PF<sub>6</sub>: Br 19 %, calc. 19.5 %.

### Spectroscopy

Two instruments were used to obtain IR spectra. A single-beam vacuum grating spectrometer constructed in the department was used for measurements from 400 to 70 cm<sup>-1</sup>. On carefully drying the cell compartment with P<sub>2</sub>O<sub>5</sub> and by passing dry nitrogen gas, no background absorption due to water vapour was observed. In this frequency range all the samples were examined in polythene bags.

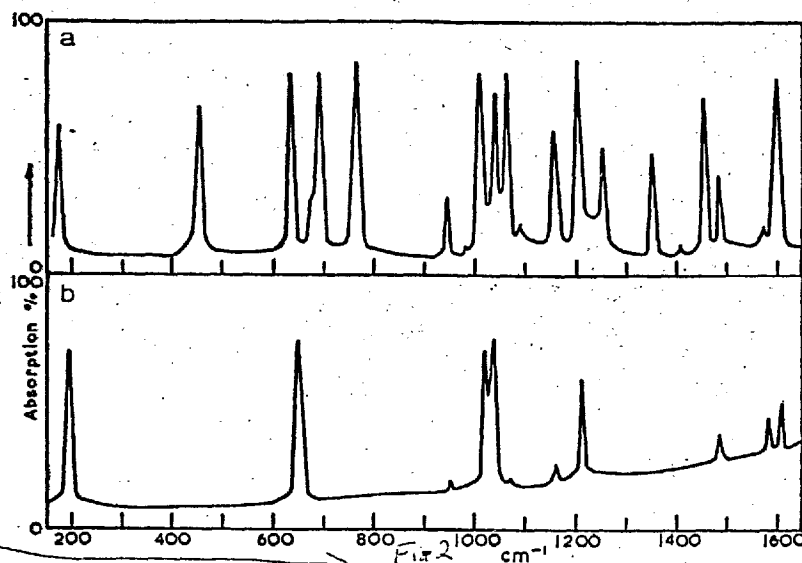
A Grubb-Parsons' spectrometer was used for measurements from 4000 to 400 cm<sup>-1</sup>. In this range, samples were usually examined in cells with KBr or AgCl windows.

<sup>Cap P</sup> Solid samples were examined by dispersing in nujol or in hexachlorobutadiene. AgCl, KBr and polythene windows were used. The (py<sub>2</sub>I)<sup>+</sup>, (py<sub>2</sub>Br)<sup>+</sup> and ( $\gamma$ -pic<sub>2</sub>I)<sup>+</sup> salts were stable, but ( $\gamma$ -pic<sub>2</sub>Br)<sup>+</sup>(PF<sub>6</sub>)<sup>-</sup> slowly discoloured, with accompanying spectral changes, particularly if KBr windows were employed. For this salt, fresh samples were used for the measurement of each band, using AgCl or polythene windows. In methylene chloride solutions, all except ( $\gamma$ -pic<sub>2</sub>Br)<sup>+</sup> salts were stable for at least two hours. Nevertheless, the precaution of using a fresh solution after every 10 minutes was made for all salts. AgCl or polythene windows were preferred. For comparison with charge-transfer complexes, some bands of ( $\gamma$ -pic<sub>2</sub>I)<sup>+</sup> and ( $\gamma$ -pic<sub>2</sub>Br)<sup>+</sup> salts in  $\gamma$ -picoline solution were required. These solutions are not stable; however by repeatedly renewing the solutions ~~are the solutions~~ the required spectra were established. Measurements on the ( $\gamma$ -pic<sub>2</sub>Br)<sup>+</sup> salts were particularly difficult, as these react more rapidly than ( $\gamma$ -pic<sub>2</sub>I)<sup>+</sup> salts, but by distinguishing between bands increasing and decreasing



N.B.

Fig 1



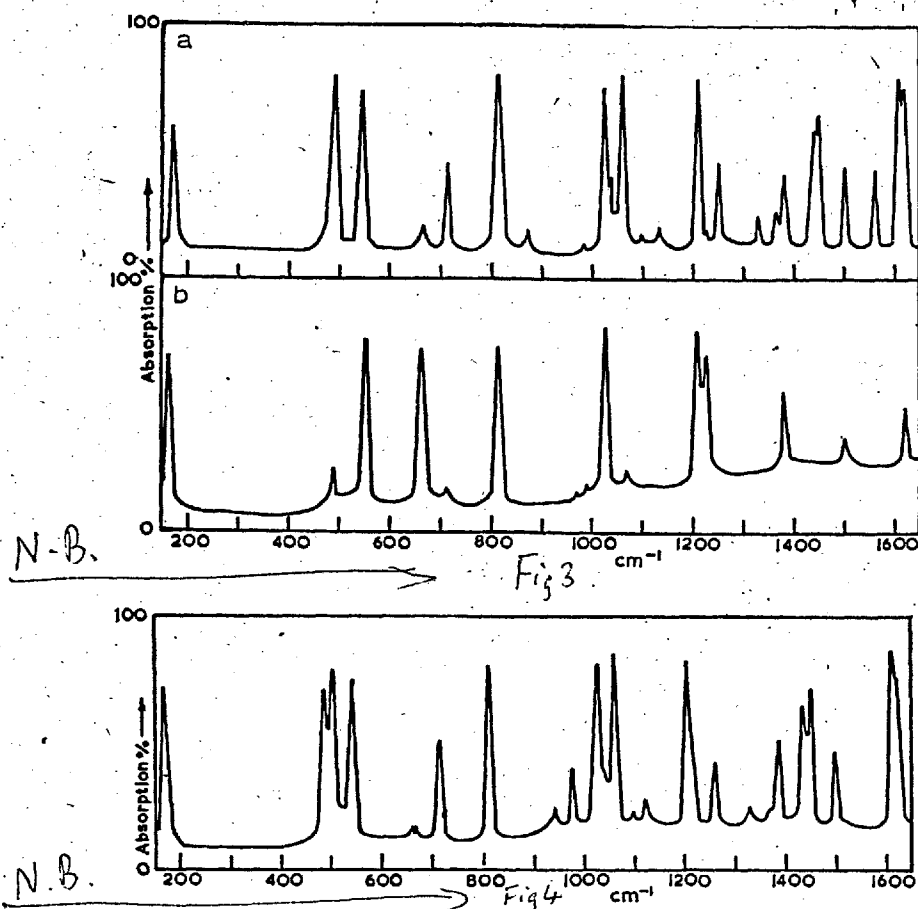
N.B.

Fig 2

O.K. → Figs. 1-2: (a) IR spectra, 400-1650  $\text{cm}^{-1}$  in  $\text{CH}_2\text{Cl}_2$ , 150-400  $\text{cm}^{-1}$  in pyridine soln.; (b) Raman spectra in  $\text{CH}_2\text{Cl}_2$  soln. Fig. 1, the  $(\text{py}_2\text{I})^+$  cation; fig. 2, the  $(\text{pyBr}_2)^+$  cation.

in intensity, the spectrum ascribable to the  $(\gamma\text{-pic}_2\text{Br})^+$  ion was determined.

Raman spectra were recorded with a Cary 81 spectrometer equipped with a "spectra physics" model 125 He/Ne laser, giving 6328Å radiation. The solutions were contained in a 10 cm long glass capillary tube of approximately 1 mm internal



Figs. 3-4. (3a) and (4), IR spectra, 400-1650  $\text{cm}^{-1}$  in  $\text{CH}_2\text{Cl}_2$ , 150-400  $\text{cm}^{-1}$  in  $\gamma$ -picoline soln.; (3b) Raman spectrum in  $\text{CH}_2\text{Cl}_2$  soln. Fig. 3, the  $(\gamma\text{-pic}_2\text{I})^+$  cation; fig. 4, the  $(\gamma\text{-pic}_2\text{Br})^+$  cation.

capillary  
Caps

diameter sealed at one end. The sealed end of the capillary was flattened with a fine file. After filling the tube with solution it was "sealed" with plasticine, leaving a small gap of about 2 mm between the solution and plasticine. Glycerol was employed between the flat end of the capillary cell and the spectrometer lens to ensure good contact and thereby reduce reflection losses. The pyridine salts were quite stable, as was the  $(\gamma\text{-pic}_2\text{I})^+$  in  $\text{CH}_2\text{Cl}_2$  solution. As a precaution, however, all observed bands were checked individually with freshly prepared samples. For comparison with the IR, the frequency of the skeletal stretching band of  $(\gamma\text{-pic}_2\text{I})^+$  was required in the same medium, viz.  $\gamma$ -picoline. In this solvent decomposition is rapid, however the band at  $161\text{ cm}^{-1}$  is strong in fresh solutions, but disappears completely after 10 minutes. All attempts to obtain the Raman spectra of  $(\gamma\text{-pic}_2\text{Br})^+$  salt solutions were unsuccessful, decomposition occurring very rapidly on laser illumination.



TABLE I

ASSIGNMENT OF VIBRATIONAL FREQUENCIES RELATED TO INTERNAL VIBRATIONS OF THE BASE GROUPS

Designation <sup>a, b</sup>	$[py_3I]^+$ <i>capital P</i>				$[py_3Br]^+$				$[\gamma-pic_3I]^+$ <i>capital P</i>				$[\gamma-pic_3Br]^+(PF_6)^-$	
	IR in soln.	Raman in soln.	IR in mull	Raman solid	IR in soln.	Raman in soln.	IR in mull	Raman solid	IR in soln. (CH <sub>2</sub> Cl <sub>2</sub> , CH <sub>3</sub> CN)	Raman in soln. (CH <sub>2</sub> Cl <sub>2</sub> )	IR in mull	Raman solid	IR in CH <sub>2</sub> Cl <sub>2</sub> soln.	IR in mull
<i>a</i> <sub>1</sub>														
$\nu$ (CH) 2			3079				3073				3067		3077	
$\nu$ (CH) 20a			3049				3053				3053		3058	
$\nu$ (CC) 8a	1602	1607	1600	1603	1601	1608	1600	1609	1618, 1610	1622	1618, 1610	1620	1623, 1613	1621, 1610
$\nu$ (CC,CN)19a	1481	1488	1479	1486	1487		1487	1499	1499	1501	1502	1506	1509	1502
$\beta$ (CH) 9a	1210	1216	1207	1216	1205	1213	1206	1213	1226	1226	1228	1228		1223
$\beta$ (CH) 18a	1062		1059	1066	1062		1066	1072	1038		1043		1040	1045
Ring 1	1009, 1005	1019	1010, 1005	1019	1011, 1008	1022	1011, 1006	1021	1024	1028	1024	1028	1026	1024
X-sens 13			3035				3037		1207	1211	1209	1215	1206	1205
X-sens 12	1040, 1030	1036	1040, 1032	1036	1040, 1033	1035	1037, 1032	1035	814	813	820, 813	813	811	808
X-sens 6a	637	644	638	645	639	649	639	647	545	554	545	553	543	538
Methyl M <sub>1</sub>											2924			2923
Methyl M <sub>2</sub>									1383	1383	1387	1387	1385	1387
<i>b</i> <sub>1</sub>														
$\nu$ (CH) 20b			3109, 3102				3114				3053			3058
$\nu$ (CH) 7b			3053				3037				3021			3023

116 — MOLESTRUC — 1st proof

$\nu(\text{CC})$	8b	1576	1577	1580	1576	1574	1584	1574	1577	1560		1557		1568	1562
$\nu(\text{CC,CN})$	19b	1452		1455	1438	1454						1439			1435
$\nu(\text{CC,CN})$	14	1355		1355		1351		1354		1366				1366	
$\beta(\text{CH})$	3	1246		1248				1254				1297			
$\beta(\text{CH})$	18b	1090		1094		1090		1095		1121		1121		1120	1120
$\alpha(\text{CCC})$	6b									662	663	666, 660	663		666, 660
X-sens	15	1158	1157	1160	1167	1158		1161	1160						
Methyl $M_2$												2992?			2990
Methyl $M_4$												1447			1450
Methyl $M_6$										1061	1069	1063	1072	1063	1062
$a_2$															
$\gamma(\text{CH})$	17a							978				952		941	954
$\gamma(\text{CH})$	10a									871		873			
$\varphi(\text{CC})$	16a				362										
$b_2$															
$\gamma(\text{CH})$	5	945		952		945		953	952	975		975	970	976	975
$\gamma(\text{CH})$	10b									813		820, 813		811	810
$\varphi(\text{CC})$	4	760		761	758			766		712		713	714		711
$\varphi(\text{CC})$	11	692, 707								491	487	490	485	494	495
X-sens	16b	438	422	438	425	450		452							
Methyl $M_2$												2992?			2990
Methyl $M_4$												1447			1450
Methyl $M_6$															

Conductivity studies indicate that in concentrated electrolyte solutions, particularly in solvents of low dielectric constant, the major part of the ions present are associated as pairs, triplets or higher clusters. In order to ensure that the observed spectra did not reflect the influence of the counter ion the hexafluorophosphate, the tetraphenylborate, and occasionally the perchlorate salts were compared. No effects due to the counter ion were observed. Variation of the counter ion also permitted the entire range of the cation spectra to be built up.

fluoro  
fluoro

## RESULTS

Figures 1-4 show composite spectra of the cations, produced by combining data from the various salts. The spectra shown refer to  $\text{CH}_2\text{Cl}_2$  solution, supplemented, where solvent bands obscure the spectrum by data from other media. In other solvents, or in the crystal, the spectra are generally similar and tables detailing the observations are given in the Appendix.

## DISCUSSION

### 1. Vibrational Assignment

It is apparent that the higher-frequency vibrations are the counterparts of modes in the corresponding free base. To a quite good approximation two normal modes of the ion are formed by linear combination from each base mode, each pair of cation modes being split by interaction via the halogen atom. These  $2 \times 27$  vibrations (bis(pyridine)ions) or  $2 \times 36$  vibrations (bis( $\gamma$ -picoline)ions) may therefore be classified according to their parentage in the isolated base (Table 1). Assignments to the corresponding parent mode are made by comparison with the spectra of pyridine<sup>8</sup>,  $\gamma$ -picoline<sup>9</sup> and their halogen charge-transfer complexes<sup>7b</sup>, which are of very similar appearance. The only problem in relating the cation bands to those of the free bases arises with the  $b_1$  mode  $\nu_3$  of ( $\gamma$ -pic<sub>2</sub>X)<sup>+</sup> salts. In both cations and the  $\gamma$ -picoline C.T. complexes a band at  $\sim 1260 \text{ cm}^{-1}$  is much stronger than that at  $\sim 1297 \text{ cm}^{-1}$ , suggesting that the former is the fundamental derived from  $\nu_3$ . As the frequency is not sensitive to complexing, this suggests that the assignment of a band at  $\sim 1297 \text{ cm}^{-1}$  in  $\gamma$ -picoline to the  $\nu_3$  fundamental may need revision. Fortunately the question is not essential to any of the arguments employed here. Most of the weak bands can be plausibly explained as overtones or combinations. As the ions have a centre of symmetry, the  $g \dots u$  rule requires IR-active combinations to be formed from one IR-active and one Raman-active component. This has been followed where possible. In addition to modes derived from ring vibrations the ions have 9 skeletal vibrations which involve the motion

Comp. R

of the base rings as a whole, and which have no counterpart in the isolated base. The only modes of this type which can be identified in the observed spectra are the symmetric and antisymmetric "N-I-N stretching" modes. The mutual exclusion of these between the IR and Raman spectrum particularly clearly demonstrates the collinearity of the N-I-N bonds.

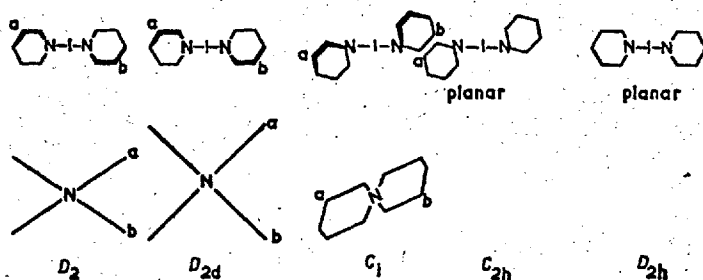


Fig. 5. Some possible rigid structures of the  $(\text{py}_2\text{I})^+$  cation, incorporating a linear N-I-N group.

*Some*  
 The possible rigid structures which incorporate a linear N-I-N grouping are shown in Fig. 5, and Table 2 gives the correlations between the internal vibrations of a single ring, and the in-phase and out-of-phase binary combinations which represent the corresponding normal modes in the cation, together with the IR and Raman activity. The  $D_2$  and  $D_{2d}$  structures do not contain a centre of symmetry, and consequently cation modes derived from the  $b_1$  and  $b_2$  ring vibrations should be active in both the IR and Raman spectra, while the pair of cation vibrations derived from each  $a_1$  ring mode should both be Raman active. The fact that these requirements are not observed eliminates these structures, and only those incorporating a centre of symmetry remain. The  $D_{2h}$  structure is distinguished from the  $C_{2h}$  and  $C_1$  structures by the inactivity in the IR of either of the cation modes derived from a particular  $a_2$  ring mode. *Only a very few, weak* No IR bands corresponding to these ring modes are observed, so that of the rigid structures,  $D_{2h}$  is preferred.

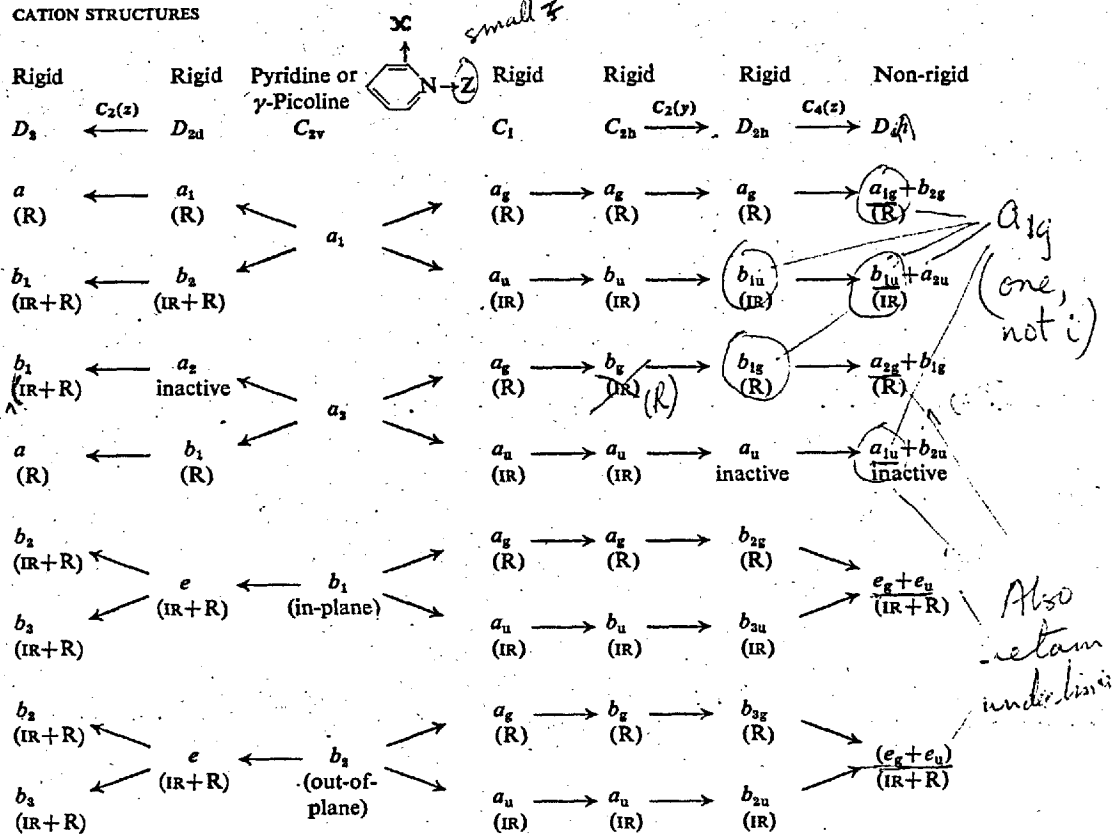
#### The torsional barrier

One of the most interesting features of the cation structure is the question of hindered rotation of the pyridine or  $\gamma$ -picoline rings about the N-I bonds. As far as we are aware all established cases of restricted rotation relate to the torsional orientation of tops containing off-axis atoms directly attached by a single bond. This includes cases such as dimethyl ether, where the non-linearity of the C-O-C bonds means that a single C-O bond, directly links two tops (Me and OMe) containing off-axis atoms. Where more than a single bond separates tops containing off-axis atoms, e.g. in dimethylacetylene, there is no barrier to internal rotation. In the present cations it is possible to conceive of a  $\pi$ -orbital extending over both rings and the halogen atom, stabilising the planar configuration. Such a coplanar

structure is observed in the crystal<sup>5</sup>, where it may be the result of packing factors. It is therefore particularly interesting to examine the evidence relating to the structure in solution, where the internal force field can be expected to play a more decisive part in determining the structure.

TABLE 2

CORRELATION BETWEEN THE SYMMETRY CLASSES, AND SELECTION RULES, FOR VARIOUS POSSIBLE CATION STRUCTURES



To explore the spectroscopic consequences of internal rotation it is necessary to employ the group theory of non-rigid systems, which has been developed by Longuet-Higgins<sup>10</sup>, Bunker<sup>11</sup> and Hougen<sup>12</sup> in particular. We have examined in some detail the effect of adding the torsional operation (the rotation of a pyridine or  $\gamma$ -picoline ring by  $\pi$ -radians about the N-I-N axis) to the rigid  $D_{2h}$  configuration. Although the effects of adding the torsional operation to the other possible rigid configurations have not been examined in any detail, we expect them to be closely similar to those for  $D_{2h}$ . The consequences relating to the interpretation of the vibrational spectra will be given here, and the detailed group theoretical discussion reserved for separate treatment.

analogous

If torsional rotation is a permitted symmetry operation, a group isomorphic with  $D_{4h}$  must be employed to classify the vibrational levels, the operations being the analogue of those found by Finch et al.<sup>13</sup> for the similar diboron tetrafluoride molecule. It should of course be appreciated that the non-rigid group is always the appropriate basis for the symmetry classification; when the torsional barrier is high the rigid model serves as a satisfactory approximation.

Big

Table 2 shows the relationship between the modes ( $q_i$ ) of the rigid  $D_{2h}$  model, and the corresponding ones of the labile  $D_{4h}$  model, established by use of the correlation rule of Watson<sup>14</sup>. Each of the vibrations derived from the  $A_g, B_{1g}, B_{2g}$  or  $A_u$  modes of the  $D_{2h}$  model gives a pair of non-degenerate vibrations under the  $D_{4h}$  group. The reason why each mode under  $D_{2h}$  correlates with two modes under  $D_{4h}$  is as follows. With a twofold torsional symmetry axis, as here, the torsional ground state  $\tau = 0$  is comprised of two sublevels, the lower of species  $A_{1g}$ , the upper  $B_{1g}$  under  $D_{4h}$ . With a high barrier, these sublevels coincide; with a low barrier they are still only separated by an energy comparable with that of free rotation about the N-I-N ( $z$ )<sup>15</sup> axis. The entries shown in column seven of Table 2 represent the symmetry of the wave functions which can be approximately described as the product of the first excited state of the  $q_i$  mode with the torsional levels  $A_{1g}$  and  $B_{1g}$  respectively. These wave functions can be symbolised as  $|1,0\rangle_+$  or  $|1,0\rangle_-$ , the first index referring to  $q_i$ , the second to  $\tau$ , and the parity to the torsional sublevel. Since the ground-state torsional sublevels have the same parity with respect to inversion, application of the selection rules to the individual transitions from the  $|0,0\rangle_{\pm}$  levels to the various  $|1,0\rangle_{\pm}$  levels shows no change in the mutual exclusion rule based on consideration of the symmetry of  $q_i$  alone. This means that the non-coincidence of the IR and Raman cation modes derived from the  $a_1$  and  $a_2$  modes of the constituent bases provides no information about the torsional barrier. The fact that these modes do not coincide, and follow the mutual exclusion rule simply shows that there is a large vibrational interaction between the rings, and that the ions have a centre of symmetry.

B<sub>1u</sub>

✓  
O.K.

The situation however is different with the cation modes derived from the  $b_1$  and  $b_2$  modes of the bases. Here for each ring mode, the correlation rule gives a fourfold representation  $E_g + E_u$  under  $D_{4h}$ . If  $q_1$  represents the normal coordinate of say, a  $b_{2g}$  mode under  $D_{2h}$ , and  $q_2$  that of the corresponding  $b_{3u}$  mode derived from the same ring vibration,  $q_j$ , then the four wave functions  $|1,0,0\rangle_+, |1,0,0\rangle_-, |0,1,0\rangle_+, |0,1,0\rangle_-$ ,  $|| \rangle = |q_1 q_2 \tau \rangle$  form the basis of a fourfold representation of  $D_{4h}$ , reducible to  $E_g + E_u$ . Descriptively we may say that  $E_g + E_u$  represents the symmetry of the first excited levels of  $q_1$  or  $q_2$  combined with the torsional ground state. When the torsional barrier is zero (free internal rotation), or if there is no vibrational interaction between the two parent  $q_j$  vibrations, one in each of the two rings, the  $E_g$  and  $E_u$  levels coincide\*. Thus although formally the mutual ex-

\* Not taking account of energy differences of the order of the overall rotational energy about the z-axis.

clusion selection rule is preserved under  $D_{4h}$ , the IR and Raman vibrations derived from a particular ring mode  $q_j$  will occur at the same frequency. If a twofold torsional barrier is present, and at the same time, there is a torsionally dependent vibrational interaction between the  $q_1$  and  $q_2$  modes, i.e. of the form  $k_1 q_1 q_2 \cos \theta$ , then the coincidence of the modes under  $D_{4h}$  derived from e.g. the  $B_{2g}$  and  $B_{3u}(D_{2h})$  vibrations is removed. For a given interaction parameter  $k$  the splitting increases with the torsional barrier. The appearance of the spectrum then goes over to that derived on the basis of the rigid  $D_{2h}$  model, one of the transitions derived from  $q_j$  lying in the IR, the other in the Raman spectrum. It should be noted that the introduction of the interaction term does not formally decrease the symmetry from  $D_{4h}$ , simply that with a high barrier the  $D_{2h}$  rules suffice, and when vibrational interaction is also present, the IR and Raman lines do not coincide.

In examining the spectra to determine whether the vibrations derived from the  $b_1$  or  $b_2$  ring modes show any evidence for restricted rotation, it is important to bear in mind that the assignment must be reliable, and that the frequency calibration of the IR and Raman spectra should be better than the difference in the observed frequencies. This requires a difference of  $> 2\text{cm}^{-1}$  in the band frequencies. The pairs of cation vibrations derived from  $a_1$  ring modes show splittings of up to  $10\text{cm}^{-1}$ , so vibrational interaction between the rings appears to be quite substantial, and may hopefully be sufficient to produce appreciable effects in the modes derived from the  $b_1$  and  $b_2$  vibrations.

Examination of Table I shows that few of the vibrations derived from the  $b_1$  and  $b_2$  ring modes are observable in the Raman spectrum. This is true even for the solid, which provides better spectra than the solutions with He/Ne laser excitation. In the solid  $(\text{py}_2\text{I})^+$  the best evidence appears to be the non-coincidence of the pairs of modes derived from  $\nu_4$  and  $\nu_{16b}$  of pyridine, since the possibility of alternative assignments of ring modes in the low-frequency range is least. The coplanarity of the pyridine rings in the solid salts thus indicated harmonises with the X-ray data. The only slight evidence for solutions relates to the  $\nu_{16b}$  mode, to which a weak Raman line at  $422\text{cm}^{-1}$  is assigned, also supporting a coplanar structure. It should perhaps be added that the coincidences of the IR and Raman modes derived from  $\nu_{8b}$  or  $\nu_{15}$  does not provide counter-evidence. With free rotation, all the IR and Raman modes derived from  $b_1$  and  $b_2$  parents will coincide; with a rigid structure, some may, and some may not, coincide, depending on the magnitude of the interaction constant,  $k_j$ .

In solid  $(\gamma\text{-pic}_2\text{I})^+$  salts, coplanarity of the  $\gamma$ -picoline rings is also indicated by the non-coincidence of the IR and Raman lines derived from the  $b_2$  parent modes  $\nu_3$  and  $\nu_{11}$ . The Raman lines, particularly  $\nu_{11}$  are stronger than in  $(\text{py}_2\text{I})^+$ , and the occurrence, frequency and assignment of the lines are well established. Less weight can be given to higher frequency lines. e.g.  $M_6$ , where more possibilities of alternative assignments arise. In solution, both the IR and Raman lines derived from  $\nu_{11}$  are quite reliable, providing some evidence that coplanarity is preserved

MR

in solution. It would be desirable to examine whether the presence of a torsional interaction in solution, if it can be more definitely established, is independent of the solvent. The present measurements refer to  $\text{CH}_2\text{Cl}_2$ , which seems unlikely to provide a solvent interaction resulting in the coplanarity of the rings. The data for the  $(\text{py}_2\text{Br})^+$  and  $(\gamma\text{-pic}_2\text{Br})^+$  salts is insufficient to throw any light on the relative orientation of the rings.

Capital P

### Charge distribution

Certain pyridine and  $\gamma$ -picoline ring-vibration frequencies. e.g.  $\nu_1$ ,  $\nu_{6a}$ ,  $\nu_{8a}$ , and  $\nu_{16b}$  are sensitive to the electron affinity of the acceptor<sup>7</sup>. Thus these frequencies show increasing shifts through the series of acceptors ICN,  $\text{I}_2$ , IBr and ICl. Table 3 compares the frequencies of some of these sensitive modes in the free bases, in the iodine chloride complexes, and in the present cations. The shifts indicate that charge transfer has proceeded even further in the ions than in those complexes (with iodine chloride) which involve the greatest extent of charge transfer. Direct comparison of the ICl etc. complexes with the  $(\text{py}_2\text{Br})^+$  and  $(\gamma\text{-pic}_2\text{Br})^+$  ions may be affected by the change in the inertial coupling consequent on the change in mass of the central atom. This does not generally appear to be very important, and the closeness of the corresponding bromine and iodine cation frequencies also suggests that the mass change has only a minor effect. Thus it appears that similar charges are borne by the rings in the two pairs of ions.

Capital P

Capital P

TABLE 3

THE FREQUENCIES OF SOME RING MODES WHICH ARE SENSITIVE TO THE CHARGE BORNE BY THE BASE GROUPS

Capital P

Capital P throughout

Mode	py	pyICl <sup>a</sup>	$(\text{py}_2^+\text{Br})^b$	$(\text{py}_2^+\text{I})^b$	$\gamma\text{-pic}$	$\gamma\text{-picICl}^c$	$(\gamma\text{-pic}_2\text{Br})^{+c}$	$(\gamma\text{-pic}_2\text{I})^{+b}$
$\nu_{8a}$	1583	1597	1605	1605	1603	1623	1618	1619
$\nu_1$	992	1009	1016	1013	994	1023	1026	1026
$\nu_{6a}$	605	627	644	640	514	543	543	550
$\nu_{16b}$	405	421	450	438	—	—	—	—
$\nu_4$	749	748	766	760	728	711	(712) <sub>null</sub>	(712) <sub>null</sub>

<sup>a</sup> IR frequencies in  $\text{CS}_2$  soln.

<sup>b</sup> mean of IR and Raman frequencies in  $\text{CH}_2\text{Cl}_2$  soln., where available.

<sup>c</sup> IR only.

<sup>d</sup> IR frequencies in  $\text{CH}_2\text{Cl}_2$  soln.

### Influence of environment

In the C.T. complexes, solution in polar solvents was observed to facilitate electron transfer, as evidenced by the shifts in the sensitive frequencies<sup>7</sup>. This may be regarded as due to the stabilisation by the solvent of the resulting more-polar



form. This effect may not be expected to be so pronounced in the cations, which have no dipole moment, the quadrupole being the first term which can be influenced by solvation. Reference to the tables in the Appendix does indeed show that the sensitive frequencies do not change with the environment. The mull spectra refer to the crystalline salts. Experience with the C.T. complexes shows that these can be regarded as equivalent to a very polar medium, and even here only small frequency shifts are observed.

*The NX stretching and interaction force constants*

Without undertaking a complete normal-coordinate analysis, only limited inferences can be made regarding the strength and interaction in the N-X bonds. The absence of other normal-vibration frequencies in the neighbourhood permits the assignment of the symmetric and antisymmetric NX stretching modes to be

TABLE 4

THE SKELETAL VIBRATION FREQUENCIES OF THE CATIONS COMPARED WITH THE N-X (HALOGEN) STRETCHING FREQUENCIES OF XCl CHARGE-TRANSFER COMPLEXES

<i>py</i> Cl	<i>(py<sub>3</sub>I)</i> <sup>+</sup>	<i>pyBr</i> Cl	<i>(py<sub>3</sub>Br)</i> <sup>+</sup>	<i>γ-pic</i> Cl	<i>(γ-pic<sub>2</sub>I)</i> <sup>+</sup>	<i>(γ-pic<sub>2</sub>Br)</i> <sup>+</sup>
147 <sup>b</sup> IR	180 <sup>a</sup> Raman 181 <sup>c</sup> 172 <sup>c</sup> IR	144 <sup>b</sup> IR	193 <sup>a</sup> Raman 170 <sup>c</sup> IR	135 <sup>b</sup> IR	160 <sup>a</sup> Raman 161 <sup>d</sup> 168 <sup>d</sup> IR	170 <sup>c</sup> IR

<sup>a</sup> in CH<sub>2</sub>Cl<sub>2</sub> soln. <sup>b</sup> in C<sub>6</sub>H<sub>6</sub> soln. <sup>c</sup> in pyridine soln. <sup>d</sup> in *γ*-picoline soln.

made with confidence. Table 4 compares these frequencies with those in the corresponding XCl charge-transfer complexes. The increase in frequency in the cations is much larger than could arise\* from the change in the effective mass, and is a clear indication of a greater N-X bond order in the ions than in the strongest complex. This increase in the NX force constant may reflect additional  $\pi$ -bonding in the cations, compared to the neutral complexes. Individual values for the N-X stretching and interaction force constants properly require the internal flexibility of the pyridine or *γ*-picoline units to be accounted. A rather crude approximation, depending on the separation of the low skeletal frequencies from the higher base unit modes is to replace these by rigid units of 79 and 93 a.m.u. respectively. Some justification for utilising the entire mass of the pyridine or *γ*-picoline units is provided by comparison with hydrogen-bonding studies<sup>16</sup>. The resulting stretching and interaction force constants are given in Table 5, and compared with those for

\* Indeed this would probably lead to lower frequencies in the cations.

TABLE 5

STRETCHING AND INTERACTION FORCE CONSTANTS

	$k$ ( $\text{mdyn } \text{Å}^{-1}$ )	$k'$ ( $\text{mdyn } \text{Å}^{-1}$ )	$k/k'$	$k+k'$ ( $\text{mdyn } \text{Å}^{-1}$ )	$k-k'$ ( $\text{mdyn } \text{Å}^{-1}$ )
<i>capital P</i> (py <sub>2</sub> I) <sup>+</sup>	1.08	0.46	0.42 <sub>s</sub>	1.54	0.62
(py <sub>2</sub> Br) <sup>+</sup>	1.09	0.64	0.59	1.73	0.45
( $\gamma$ -pic <sub>2</sub> I) <sup>+</sup>	1.02	0.40	0.40	1.42	0.62
Br <sub>3</sub> <sup>-17</sup>	0.91	0.32	0.35	1.23	0.59
ICl <sub>3</sub> <sup>-17</sup>	1.02	0.33	0.33	1.35	0.69
(Br <sub>2</sub> ) <sup>-17</sup>	0.91	0.30	0.33	1.21	0.61

the XY<sub>2</sub> trihalide ions<sup>16</sup> – which involve no approximation. The interaction force constant is exceptionally large for the trihalide ions<sup>17</sup>. Table 5 shows that those for the cations are even larger. As Maki and Forneris<sup>17</sup> have pointed out for linear YXY molecules, the equations relating the frequencies to the force constants;

$$4\pi^2 \nu_s^2 = \lambda_s = (k+k')\mu_y$$

$$4\pi^2 \nu_A^2 = \lambda_A = (k-k')(\mu_x + 2\mu_y)$$

may be interpreted as involving a composite force constant ( $k+k'$ ) for the N...N stretching vibration, and ( $k-k'$ ) for the antisymmetric vibration, in which the N-N distance remains constant, while the halogen atom oscillates in a one-dimensional potential well bounded by the fixed N atoms. The values of ( $k-k'$ ) for the cations with a central iodine atom are very similar to those found for the trihalide ions. These are very low, i.e. indicative of a tendency to a flat potential well. ( $k-k'$ ) for the (py<sub>2</sub>Br)<sup>+</sup> cation is still lower. Ultimately this tendency would result in a double minimum potential for the central atom, emphasising the similarity between the present "charge-transfer" cations, and the corresponding H-bonded complex ions (pyHpy)<sup>+</sup> and ( $\gamma$ -picHy-pic)<sup>+</sup>.<sup>18</sup>

The possibility that the halogen atom is asymmetrically situated between the N...N atoms, i.e. in a high-barrier double-minimum potential can be rejected since it would imply the activity of the  $\nu_s$  skeletal mode in the IR, and of  $\nu_A$  in the Raman. No indication of either band is observed.

## ACKNOWLEDGEMENTS

We thank the Education Department, Government of Assam, for a maintenance grant, and Dr. T. A. Creighton, National Physical Laboratory and Dr. R. E. Hester, York University, for early attempts to obtain the laser Raman Spectra, which was superseded with the availability of the Cary 81 spectrometer.

1963

REFERENCES

- 1 H. CARLSOHN, *Habilitation Thesis: Über eine neue Klasse von Verbindungen des positiv Einwertigen Jods*, Verlag S. Hinzel, Leipzig, 1932.
- 2 R. A. ZINGARO, C. A. VAN DER WERF AND J. KLEINBERG, *J. Am. Chem. Soc.*, 71 (1949) 575.
- 3 *Inorg. Synt.* 7 (1961) 169.
- 4a R. A. ZINGARO AND W. E. TOLBERG, *J. Am. Chem. Soc.*, 81 (1959) 1353.
- 4b R. A. ZINGARO AND W. B. WITMER, *J. Phys. Chem.*, 64 (1960) 1705.
- 5 O. HASSEL AND H. HOPE, *Acta Chem. Scand.*, 15 (1961) 407.
- 6 S. G. W. GINN AND J. L. WOOD, *Trans. Faraday Soc.*, 62 (1966) 777.
- 7a M. GOODGAME AND P. J. HAYWARD, *J. Chem. Soc. A*, (1966) 632.
- 7b I. HAQUE AND J. L. WOOD, *Spectrochim. Acta*, 23A (1967) 959, 2523.
- 8 J. H. S. GREEN, W. KYNASTON AND H. M. PAISLEY, *Spectrochim. Acta*, 19 (1963) 549.
- 9 D. A. LONG AND W. O. GEORGE, *Spectrochim. Acta*, 19 (1963) 1777.
- 10 H. C. LONGUET-HIGGINS, *Mol. Physics*, 5 (1963) 445.
- 11 P. R. BUNKER, *Mol. Physics*, 8 (1964) 81; *J. Chem. Phys.*, 42 (1965) 2991; P. R. BUNKER AND H. C. LONGUET-HIGGINS, *Proc. Roy. Soc. (London)*, A280 (1964) 340.
- 12 J. T. HOUGEN, *Can. J. Phys.*, 42 (1964) 1920.
- 13 A. FINCH, I. HYAMS AND D. STEELE, *Spectrochim. Acta*, 21 (1965) 1423.
- 14 J. K. G. WATSON, *Can. J. Phys.*, 43 (1965) 1996.
- 15 J. S. KOEHLER AND D. M. DENNISON, *Phys. Rev.*, 57 (1940) 1006.
- 16 C. PERCHARD, A. M. BELLOCQ AND A. NOVAK, *J. Chim. Phys.*, 62 (1965) 1344.
- 17 A. G. MAKI AND R. FORNERIS, *Spectrochim. Acta*, 23A (1967) 867.
- 18 R. CLEMENTS, T. R. SINGH AND J. L. WOOD, to be published.

APPENDIX. TABLE 1

(In these tables, bands due to solvents or the counterion are omitted)

[py <sub>2</sub> I]BF <sub>4</sub>					[py <sub>2</sub> I]PF <sub>6</sub>					Interpretation		
IR of [py <sub>2</sub> I]ClO <sub>4</sub> in nujol mull					Raman	IR			Raman			
In nujol mull	In hexachlorobutadiene mull	In CH <sub>2</sub> Cl <sub>2</sub> soln.	In CH <sub>2</sub> CN soln.	In CH <sub>2</sub> Cl <sub>2</sub> soln.	Solid	In CH <sub>2</sub> Cl <sub>2</sub> soln.	In nujol mull	In hexachlorobutadiene mull	In CH <sub>2</sub> Cl <sub>2</sub> soln.	Solid	In CH <sub>2</sub> Cl <sub>2</sub> soln.	
	3159w										(1580 × 2)	
	3109s,										b <sub>1</sub> fundamental	
	3102s											
	3079s										a <sub>1</sub> fundamental	
	3049m										a <sub>1</sub> fundamental	
	3035m										a <sub>1</sub> & b <sub>1</sub> fundamental	
	2950w										1354 + 1600	
	2922m										1355 + 1580	
1919w	1926w		1919w				1923w		1919w		760 + 1161	
							1883w				638 + 1248	
1843w	1846w	1848w	1846w				1847w	1848w	1845w		638 + 1215	
1698w			1699w					1700w	1699w		690 + 1010	
1654w	1652w	1652w	1654w				1651w	1652w	1654w		638 + 1010	
1600s	1601s	1602s	1603s	1600s	1606m	1608w	1600s	1600s	1602s	1603m	1607w(P?)	a <sub>1</sub> fundamental
1580w			1575w	1580w	1578m	1578w	1580w		1576w	1576m	1577w(P?)	b <sub>1</sub> fundamental
			1481w		1485w	1488w	1506w	1479w	1481w	1486m		a <sub>1</sub> fundamental

		1455s	1452s		1438w			1455s	1452s				$b_1$ fundamental
1398w	1403w	1400w						1399m	1400m				638+760
1350m	1355ms	1355m	1354m					1355ms	1355ms	1355ms			$b_1$ fundamental
1248m	1249m	1250m		1246m				1248m	1247m				$b_1$ fundamental
1205s	1207s	1209s	1210s	1210s	1216m	1216m		1206s	1206s	1210s	1216s	1215m(P)	$a_1$ fundamental
1200sh	1200sh							1193sh					441+760
1161ms	1161s		1158s	1156s	1166m	1158m		1160m		1158m	1167s	1157s(dp)	$b_1$ fundamental
								1094w	1094w	1090w			$b_1$ fundamental
1055s								1059s	1059s	1062s	1066vw		$a_1$ fundamental
1038ms					1039s	1039s		1040s, 1032sh	1038s, 1032sh	1040s, 1030w	1036s	1036s (P)	$a_1$ fundamental
1010s, 1005sh	1009s, 1005sh	1010s	1010s, 1005sh	1010s	1020s	1021s		1010s, 1005sh	1009s	1009s, 1005sh	1019s	1019s (P)	$a_1$ fundamental
	952m		945m		954w			952w		946w	949w		$b_2$ fundamental
760s	761s			760s, 750sh				759s			758w		$b_2$ fundamental
700sh, 690s	700sh, 690s	691s		707ms, 692s				700sh, 690s	701sh, 689s				$b_2$ fundamental
638s	638s	638s	637s	638s	646s	644s		638s	638s	637s	644s	645s (P)	$a_1$ fundamental
439s	441ms	441s	437ms	437m	424vw, 362vw	422vw		438s	438s	438s	419w		$b_2$ fundamental
172s	172s		172s <sup>a</sup>		182s	180s(P)	172s			172s <sup>a</sup>	181s	181s (P)	skeletal
						181s <sup>a</sup>						182s <sup>a</sup>	

<sup>a</sup> In pyridine soln.

replace by 'a'

172s<sup>a</sup>

APPENDIX. TABLE 2 <sup>capital P!</sup> <sup>1005</sup>  
 VIBRATION SPECTRA OF  $[\text{py}_2\text{Br}]\text{PF}_6$  IN VARIOUS MEDIA

IR			Raman		Interpretation
In nujol mull	In $\text{CH}_2\text{Cl}_2$ soln.	In hexachlorobutadiene mull above 2000 $\text{cm}^{-1}$	Solid	In $\text{CH}_2\text{Cl}_2$ soln.	
		3141w			1574 × 2
		3114s			$b_1$ fundamental
		3099sh			
		3073w			$a_1$ fundamental
		3053m			$a_1$ fundamental
		3037			$a_1$ & $b_1$ fundamental
		3015w			1454 + 1584
1929w	1915w				766 + 1160
1845w	1845w				639 + 1213
	1708m				690 + 1021
	1658w				647 + 1011
1600s	1601s		1609m	1608w	$a_1$ fundamental
1574w	1574w		1577m	1584w	$b_1$ fundamental
1538w					(744 × 2)
	1487m		1487m		$a_1$ fundamental
	1454s				$b_1$ fundamental
1408w					(638 + 766)
1354m	1351ms				$b_1$ fundamental
1254ms					$b_1$ fundamental
1206s	1205s		1213s	1213s(P)	$a_1$ fundamental
1192sh					
1161m	1158s		1160w		$b_1$ fundamental
1095w	1090w				$b_1$ fundamental
1066s	1062s		1072w		$a_1$ fundamental
1037s	1040s		1035s	1035s(P)	} $a_1$ fundamental
1032sh	1033sh				
1011s	1011s		1021s	1022s(P)	} $a_1$ fundamental
1006sh	1008sh		1012sh(w)		
978w					$a_2$ fundamental
953m	945m		952w		$b_2$ fundamental
766s					$b_2$ fundamental
690s					} $b_2$ fundamental
674sh					
639s	639s		647s	649s(P)	$a_1$ fundamental
452s	450s		635sh(w)		$b_2$ fundamental
170s	170s <sup>a</sup>		189s	139s(P)	skeletal
			168w		
			138w		

<sup>a</sup> In pyridine soln.

193

APPENDIX. TABLE 3

*supradial p.*

$[\gamma\text{-pic}_2\text{I}]\text{BF}_4$					$[\gamma\text{-pic}_2\text{I}]\text{PF}_6$					Interpretation
IR			← Raman		IR			← Raman		
In nujol mull	In $\text{CH}_2\text{Cl}_2$ soln.	In $\text{CH}_3\text{CN}$ soln.	Solid	In $\text{CH}_2\text{Cl}_2$ soln.	In nujol mull	In hexachlorobutadiene mull	In $\text{CH}_2\text{Cl}_2$ soln.	Solid	In $\text{CH}_2\text{Cl}_2$ soln.	
						3133w 3107(1307m)				1560
						3067m				1560x2
						3053m				1610+1502
						3021w				$a_1$ & $b_1$ fundamental
						2992w				$a_1$ fundamental
						2924w				$b_1$ fundamental
1938w	1941w	1945w			1944w	1941w	1930w			1502+1506
1848w	1838w	1838w			1848w	1848w	1835w			$a_1$ fundamental
							1767w			810+1028
1689w					1680w	1680w				813+1952 <i>delete 1</i>
1623s,	1620s,	1618s,	1620ms	1621m (P)	1618s,	1621s,	1618s,	1620m	1622w	712+1228
1613s	1613s	1610s			1610s	1610s	1610s			810+1028
1560w	1557w	1560w			1557w		1560m			812+952
1504w	1499m	1506m	1506m	1506w	1502m	1502w	1499m	1506m	1501w	712+958
						1447s				$a_1$ fundamental and
						1439s				810+813
						1387m	1383m	1387ms	1383ms	$b_1$ fundamental
			1387s	1385ms (P)						$a_1$ fundamental

	1366w									1366w		662+712
1333w	1333w	1333w			1333w	1333w	1331w	1338w				660+662
1248m					1297vw	1297vw						491+808
1254m		1253m			1258m	1255m						$b_1$ fundamental
1231w	1225w	1225w	1233s	1227s (P)	<sup>1209</sup> 1228w	<sup>1209</sup> 1228w	1226w	1228s	1226s			$a_1$ fundamental
1211s	1212s	1211s	1216s	1215s (P)	1290s	1290s	1207s	1215s	1211s			$a_1$ fundamental
1125w					1121w	1121w	1120w					$b_1$ fundamental
1096w					1098vw	1098vw	1096w					549+551
1067s	1068s				1063s	1063s	1061s	1072m	1069w			$b_1$ fundamental
1037m	1036m				1043w	1042w	1038w					$a_1$ fundamental
1022s	1025s	1025s	1027s	1031s (P)	1024s	1025s	1024s	1028s	1028s			$a_1$ fundamental
		983vw	990vw	990vw	975w		975w	968vw	988			$b_2$ fundamental
		970vw						988vw	968			494+484
873w		871w			952w							$a_2$ fundamental
820s,	813s	814s	813s	813s (P)	810s	808s	810s	813s	813s			$a_2$ fundamental
813s												$a_1$ & $b_2$ fundamental
713m		712m	714vw		712m	711m						$b_2$ fundamental
666w,		662w	663s	663s(dp)	666w,			662s	662s			$b_1$ fundamental
660w					660w							
545s	545s	546s	553s	554s (P)	545s	545s	549s	551s	553s			$a_1$ fundamental
490s	490s	494s	484m		491s	491s	491s	485w	487w			$b_2$ fundamental
164s	168s*		164s	162s (P)				162s	160s			skeletal
				161s*								

\* In  $\gamma$ -picoline soln.



APPENDIX. TABLE 4.

 IR SPECTRA OF  $[\gamma\text{-pic}_2\text{Br}]PF_6$  IN VARIOUS MEDIA

<i>In nujol mull</i>	<i>In hexachloro- butadiene mull</i>	<i>In CH<sub>2</sub>Cl<sub>2</sub> soln.</i>	<i>Interpretation</i>
	3130w		5 × 1562
	3105m		(1502 + 1610)
	3077ms		<i>a</i> <sub>1</sub> & <i>b</i> <sub>1</sub> fundamental
	3058ms		<i>a</i> <sub>1</sub> fundamental
	3023m		<i>b</i> <sub>1</sub> fundamental
	2990w		(2 × 1502)
	2923w		<i>a</i> <sub>1</sub> fundamental
1943w	1943w	1932w	(712 + 1222)
1848w	1848w	1838w	(810 + 1026)
	1680w		(810 + 873)
		1644m	(666 + 975)
1621s, 1608s	1621s, 1610s	1623s, 1613s	<i>a</i> <sub>1</sub> fundamental and (810 × 2)
1562w		1568w	<i>b</i> <sub>1</sub> fundamental
1496w	1502m	1509m	<i>a</i> <sub>1</sub> fundamental
	1450s		<i>b</i> <sub>1</sub> & <i>b</i> <sub>2</sub> fundamental
	1435s		<i>b</i> <sub>1</sub> fundamental
	1387ms	1385m	<i>a</i> <sub>1</sub> fundamental
		1366w	<i>b</i> <sub>1</sub> fundamental
1332w	1332w	1328w	(666 × 2)
1259m	1260m		(543 + 712)
1223w	1223w		<i>a</i> <sub>1</sub> fundamental
1205s	1205s	1206s	<i>a</i> <sub>1</sub> fundamental
1120w	1120w	1121w	<i>b</i> <sub>1</sub> fundamental
1099vw	1100vw	1098w	(2 × 543)
1062s	1062s	1063s	<i>b</i> <sub>1</sub> fundamental
1041sh	1045sh	1040sh	<i>a</i> <sub>1</sub> fundamental
1025s	1024s	1026s	<i>a</i> <sub>1</sub> fundamental
975m		976m	<i>b</i> <sub>2</sub> fundamental
954w		941w	<i>a</i> <sub>2</sub> fundamental
810s	808s	811s	<i>a</i> <sub>1</sub> & <i>b</i> <sub>2</sub> fundamental
711ms	712ms		<i>b</i> <sub>2</sub> fundamental
666w, 660w			<i>b</i> <sub>1</sub> fundamental
536s	538s	543s	<i>a</i> <sub>1</sub> fundamental
493s	495s	494s, 486s	<i>b</i> <sub>2</sub> fundamental
170s		170s <sup>a</sup>	skeletal

<sup>a</sup> in  $\gamma$ -picoline sol.

The Reaction Products of  $\gamma$ -Picoline and Iodineby I. Hague and J.L. WoodImperial College of Science and Technology,  
Imperial Institute Road, London, S.W.7.Summary

Solutions of iodine in  $\gamma$ -picoline contain the  $(\gamma\text{-Pic I } \gamma\text{-Pic})^+$  ion. In the presence of free  $\gamma$ -picoline this reacts to give solid  $1_a$ , with structure  $\text{Me}-\text{C}_5\text{H}_4\overset{+}{\text{N}}-\text{CH}_2-\text{C}_5\text{H}_4\text{N}$ ,  $1^-$ , established by infrared and N.M.R. spectra. Further reaction produces solid  $1_b$ ,  $\text{Me}-\text{C}_5\text{H}_4\overset{+}{\text{N}}-\text{CH}_2-\text{C}_5\text{H}_4\overset{+}{\text{N}}-\text{CH}_2-\text{C}_5\text{H}_4\text{N}$ ,  $21^-$ , and also solid  $1_c$ ,  $\text{Me}-(\text{C}_5\text{H}_4\overset{+}{\text{N}}-\text{CH}_2)_3-\text{C}_5\text{H}_4\text{N}$ ,  $31^-$ . The protons eliminated in these reactions are incorporated in the  $(\gamma\text{-PicHY-}\gamma\text{-Pic})^+$  ion.

## Introduction

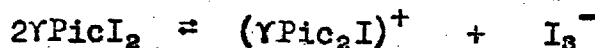
Two distinct solid compounds can be isolated from solutions of iodine in  $\gamma$ -picoline.<sup>(1)</sup> The first, which is rapidly formed on mixing, is soluble in  $\gamma$ -picoline and other organic solvents, but insoluble in water. Both crystal structure studies<sup>(2)</sup> and the infrared spectrum show this to be the charge-transfer complex  $\gamma$ -PicI<sub>2</sub>. The second compound is formed more slowly, and eventually precipitates from the  $\gamma$ -picoline solution. It is insoluble in many organic solvents, but soluble in water. This compound ("compound 1" of Glusker and Miller) was shown by these authors to contain no I-I distance shorter than 3.0Å, and suggested the structure A. Hassel et al<sup>(2)</sup> however, proposed that B was more probable, by analogy with the corresponding pyridine salt.

We have recently determined the infrared and Raman spectra of various iododi $\gamma$ -picolinium salts<sup>(3)</sup>. Comparison with the infrared spectrum of the water-soluble compound show decisively that Hassel's conjecture is untenable. (see fig. 1).

We have therefore sought to determine the structure of this product, and the nature of the process by which "compound 1" is formed, largely using spectroscopic means. The situation turns out to be appreciably more complicated than initially envisaged—nevertheless, many features have been elucidated.

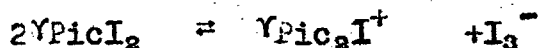
### The Reaction Process

If equimolar proportions of  $\gamma$ -picoline and iodine are mixed in an inert solvent, e.g. n-hexane, or benzene, the molecular charge-transfer complex  $\gamma$ -picoline  $I_2$  is formed, the equilibrium strongly favouring the complex. (4) At room temperature these solutions show no spectroscopic changes, either in daylight or the dark, at least over a period of  $\approx 12$  hours, provided no excess  $\gamma$ -picoline is present. The presence of excess, and consequently free,  $I_2$  also does not lead to reaction in inert solvents. In polar solvents, and also in  $CS_2$  to a lesser extent, partial ionisation takes place. (5)



the cation being the iododi $\gamma$ picolinium ion. When  $I_2$  is added to excess  $\gamma$ -picoline in an inert solvent, or when  $\gamma$ -picoline is itself the solvent - in both cases necessarily implying the possibility of ionisation, spectroscopic changes are immediately apparent, culminating in the precipitation of the water-soluble solid. Owing to the opacity of the solution it is not possible to fix a time at which precipitation commences, but it is apparent within 30 minutes. The spectroscopic changes are most clearly shown in the  $500-700\text{cm}^{-1}$  region, which in the freshly made up solution contains only bands at  $515\text{cm}^{-1}$  ( $\nu_{82}$  (6) of free  $\gamma$ -picoline),  $536\text{cm}^{-1}$  is the corresponding band of  $\gamma\text{Pic}I_2$ , and  $546\text{cm}^{-1}$  that of  $(\gamma\text{Pic}_2I)^+$ .

The changes in this frequency range are shown in fig. 2, and display the rise in a strong band at  $\sim 605\text{cm}^{-1}$ , one of the most characteristic features in the spectrum of the product. The band at  $546\text{cm}^{-1}$  due to  $(\gamma\text{Pic}_2\text{I})^+$  rapidly disappears, and eventually the band at  $515\text{cm}^{-1}$  also decreases in intensity, a consequence of the utilisation of  $\gamma$ -picoline in forming the product. The retention of the  $535\text{cm}^{-1}$  band arising from the  $\gamma$ -picoline  $\text{I}_2$  complex is apparently irreconcilable with the disappearance of  $\gamma\text{Pic}_2\text{I}^+$ , since the equilibrium

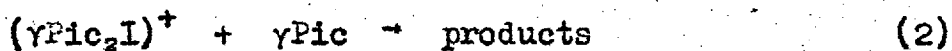


is found to be rapidly set up, i.e. within the time that the first observations can be made, so that the concentrations of  $\gamma\text{PicI}_2$  and  $\gamma\text{Pic}_2\text{I}^+$  should keep proportionate. The difficulty is resolved by examination of the spectral range around  $1000\text{cm}^{-1}$ . The charge transfer complex  $\gamma\text{PicI}_2$  has a single sharp band at  $1011\text{cm}^{-1}$  in  $\gamma$ -picoline solution (this is  $\nu_1^{(6)}$  of the complex). The corresponding band of  $(\gamma\text{Pic}_2\text{I})^+$  is at  $1025\text{cm}^{-1}$ . As reaction proceeds, both the  $1011$  and  $1025\text{cm}^{-1}$  bands disappear, and are replaced by a sharp band of the product at  $1018\text{cm}^{-1}$  (fig. 3). This shows that as reaction proceeds, the  $535\text{cm}^{-1}$  band is no longer due to  $\gamma\text{PicI}_2$ , and therefore arises from a product. Further, it is apparent that the bands at  $1011$  and  $1025\text{cm}^{-1}$

disappear, and  $1018\text{cm}^{-1}$  appears before the appearance of  $605\text{cm}^{-1}$ . It will be seen later that  $605\text{cm}^{-1}$  and  $1018\text{cm}^{-1}$  arise from different products. The  $1018\text{cm}^{-1}$  band is still present in old solutions which also show the  $605\text{cm}^{-1}$  band, and is consequently not due to a forerunner of the " $605\text{cm}^{-1}$ " product. The changes of the spectrum in other frequency ranges are generally complex, but it is significant that in the low frequency range the strong band initially present at  $137\text{cm}^{-1}$ , due to the  $\text{I}_3^-$  ion<sup>(5)</sup> and the band at  $\sim 162\text{cm}^{-1}$  which comprises both the I-I stretching of the un-ionised complex ( $162\text{cm}^{-1}$ ) and the antisymmetric (N-I-N) stretching of  $(\text{YPic}_2)^+$  at ( $168\text{cm}^{-1}$ ) both disappear, and the lower frequency range ( $100-300\text{cm}^{-1}$ ) becomes devoid of all bands except a weak band at  $\sim 210\text{cm}^{-1}$ . The rate of reaction, as shown by the intensity of the  $606\text{cm}^{-1}$  band, is the same in the dark and in daylight. These observations do not permit us to distinguish whether it is the ion,  $(\text{YPic}_2\text{I})^+$ , or the complex  $\text{YPicI}_2$ , which reacts with  $\gamma$ -picoline. It is easy to demonstrate that at least the  $(\text{YPic}_2\text{I})^+$  cation reacts with  $\gamma$ -picoline to give a product containing the bands at  $535\text{cm}^{-1}$ ,  $606\text{cm}^{-1}$  and  $1018\text{cm}^{-1}$  (fig. 4). The characteristic  $(\text{YPic}_2\text{I})^+$  bands at  $545\text{cm}^{-1}$  and  $168\text{cm}^{-1}$  (not shown) rapidly disappear. The accompanying anion ( $\text{BF}_4^-$  or  $\text{PF}_6^-$ ) remains unchanged. The reaction of  $(\text{YPic}_2\text{I})^+$  salts with  $\gamma$ -picoline can also be demonstrated in  $\text{CH}_2\text{Cl}_2$  solution, forming the same product. Examination of the electronic spectrum shows

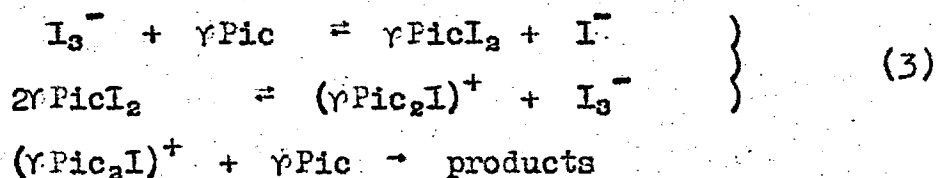
that no free  $I_2$  is formed. Further the  $(\gamma\text{Pic}_2\text{I})^+$  cation (in the form of the fluoroborate salt) is stable in a polar solvent (nitrobenzene) for at least 24 h., and there is also no reaction when free  $I_2$  is added to  $(\gamma\text{Pic}_2\text{I}^+ \text{BF}_4^-)$  in  $\text{CH}_2\text{Cl}_2$ , for at least 6 h. The fact that  $(\gamma\text{Pic}_2\text{I})^+$  reacts with  $\gamma$ -picoline does not exclude the possibility that in solutions  $\gamma\text{PicI}_2$  also reacts directly with  $\gamma$ -picoline. As it is not possible to have  $\gamma\text{PicI}_2$  alone present in  $\gamma$ -picoline solutions, since equilibrium<sup>(I)</sup> always provides

$(\gamma\text{Pic}_2\text{I})^+$ , a detailed kinetic investigation is required to decide whether  $\gamma\text{PicI}_2$  is also reacting directly with  $\gamma$ -picoline. We shall adopt, simply to economise on hypotheses, that the reaction is due to the ~~reaction of~~ the  $(\gamma\text{Pic}_2\text{I})^+$  ion



Although for simplicity we have referred so far to "the product" this turns out to comprise several chemical species, and the proportions can vary with the reaction conditions.

The observation that the  $\text{I}_3^-$  counterion disappears in the original process could be easily accounted for, using equilibria which are known to occur in  $\gamma$ -picoline solution

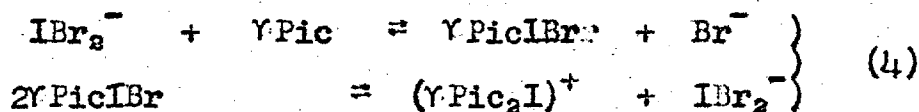


This possibility can be tested directly by dissolving  $(\text{NAlk}_4)^+ \text{I}_3^-$  in  $\gamma$ -picoline. After one day the characteristic product bands at  $535\text{cm}^{-1}$  and  $1018\text{cm}^{-1}$  are clearly present (fig. 5), while the  $137\text{cm}^{-1}$  band disappears. Neither the  $1011\text{cm}^{-1}$   $\gamma\text{PicI}_2$  nor the  $1025\text{cm}^{-1}$   $(\gamma\text{Pic}_2\text{I})^+$  bands can be picked up in rapid scans of this frequency range (fig. 5),



but the speed with which these bands disappear from  $\gamma$ Picoline +  $I_2$  solutions (fig. 3) shows that their absence is not inconsistent with the reaction scheme 3.

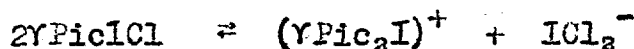
The reaction of  $I_3^-$  with  $\gamma$ Picoline suggests that  $IBr_2^-$  should also react to give the same product, since the corresponding equilibria



would produce the  $(\gamma Pic_2I)^+$ . This expectation is borne out, as the spectrum of a solution  $(NAlk_4)^+ IBr_2^-$  in  $\gamma$ -picoline after 1 day (fig. 6) shows. The  $IBr_2^-$  band at  $174cm^{-1}$  (not shown) correspondingly disappears.

In this case scans of the  $1000cm^{-1}$  region of freshly prepared solutions show evidence of the transient presence of  $\gamma PicIBr$ , which has a sharp band at  $1019cm^{-1}$ (5). This band rapidly decreases at first (fig. 6), the weaker permanent residuum being ascribed to  $1018cm^{-1}$  of the product.

We have also examined the reaction of  $\gamma PicICl$  with  $\gamma$ -picoline. Since  $(\gamma Pic_2I)^+$  is formed in this solvent(5),



the same product can be expected. Fig. 7 shows that both  $\gamma PicICl$  and  $(\gamma Pic_2I)^+$  disappear from a solution in

$\gamma$ -picoline, as evidenced by the disappearance of the  $545\text{cm}^{-1}$  band (The frequency corresponding to  $\nu_{\text{C}_2}$  is almost the same in the two compounds a reflection of the similarity of the electron transfer from the  $\gamma$ -picoline ring). The characteristic product band at  $606\text{cm}^{-1}$  arises, but is now accompanied by other bands at  $570$  and  $630\text{cm}^{-1}$ , indicating the production of further species.

Taken together, these observations show that  $\gamma\text{Pic}_3\text{I}^+$  reacts with  $\gamma$ -picoline to form a product or products which are comprised in "compound 1". The possibility of other reactions, e.g. directly between  $\gamma\text{PicI}_2$  or  $\gamma\text{PicICl}$  and  $\gamma$ -picoline, cannot be excluded.

#### The nature of the reaction product

The only previous examination of the reaction product is by Glusker and Miller,<sup>(1)</sup> and we quote their description - "a saturated solution of resublimed iodine in pure  $\gamma$  picoline was prepared under anhydrous conditions. It set to a solid mass after approximately two hours. The mixture was partially soluble in ethyl alcohol. The insoluble residue, (I), which proved to be water-soluble, and insoluble in the common organic solvents, was washed with ether and recrystallized from water-alcohol mixtures as a light brown microcrystalline solid. Its melting point

is 223-4°C with decomposition, and its density approximately 1.9 g/cm.<sup>3</sup>. Chemical analysis and equivalent weight determined from the freezing point depression of water solutions were consistent with an ionic formula  $C_{12}H_{14}N_2I^+I^-$ . A precipitate of silver iodide is formed immediately upon the addition of acidified silver nitrate solution to an aqueous solution of (I)".

Extraction of the  $I_2$ /Ypicoline reaction product with ethanol gave a solution from which addition of ether precipitated a cream coloured solid (Ia), m.p. 175° very soluble in water, which gives an analysis (Table I) corresponding more nearly to 2YPic:I, in contrast to Glusker and Miller's result. The infrared spectrum of this substance, shown in fig. 8 contains the characteristic 606  $cm^{-1}$  band, but not bands near 535 or 570-580  $cm^{-1}$ . The product of the reaction of  $(YPic_2I)^+ PF_6^-$  with Y-picoline, when worked up in the same way, gives an identical infrared spectrum (fig. 8) if allowance is made for the presence of  $(PF_6)^-$  bands. Both observations suggest that Ia is the salt  $(2YPic)^+, X^-$ . The analysis of the product from the second reaction bears this out (Table I), showing that  $PF_6^-$  has partially replaced  $I^-$ . This hypothesis was supported by dissolving the  $I_a$  iodide in water, and adding aqueous

$\text{AgNO}_3$  solution, which gave an immediate ppt of  $\text{AgI}$ . On extraction, a non-crystalline residue was obtained, which contained no iodine. The presence of nitrate bands is clearly shown in the infrared spectrum. The remaining bands, although bearing a general similarity to those of solid  $\text{I}_2$ , show shifts of up to  $10\text{cm}^{-1}$ . We take this to indicate that the  $\text{I}_2$  infrared spectrum does not depend on the presence of iodine, and that the nitrate salt is rather unstable, as indicated by its slow brownish discolouration.

To determine the nature of the cation more precisely, the N.M.R. spectrum of the  $\text{I}_2$  iodide was examined (fig. 9). Decoupling experiments show the doublets d and b were coupled, likewise the doublets e and c, each individual doublet representing two protons, relative to  $\text{Me} = 3$  protons. This indicates the structure  $\text{I}_2$  as shown, the d b pair of doublets being assigned to the ring bearing the formal charge. The structure is consistent with the analytical results.- The absence of an  $\text{NH}^+$  stretching vibration in the infrared, and the overall cation:anion ratio shows the cation is the free base and bears only a single unit charge. Although we have not attempted a complete vibrational assignment of the infrared spectrum, (see Appendix) comparison with closely related compounds<sup>(5,6,7)</sup> shows that it is consistent with structure  $\text{I}_2$ , in particular the  $605\text{cm}^{-1}$  band is identified as a  $\text{CH}_2$  deformation mode.

The mass spectrum (see Appendix) generally supports the structure shown, the peaks assigned to  $\text{CH}_2\text{C}_6\text{H}_{11}\text{N}$  at  $m/e = 92$  and  $\text{MeC}_6\text{H}_{11}\text{N}$  at  $m/e = 93$  being particularly prominent. The peaks at  $m/e = 184$  and  $185$  suggest the presence of  $\text{CH}_2\text{C}_6\text{H}_{11}\text{N}-\text{CH}_2\text{C}_6\text{H}_{11}\text{N}$  and  $\text{MeC}_6\text{H}_{11}\text{N}-\text{CH}_2\text{C}_6\text{H}_{11}\text{N}$ . In view of the pronounced thermal instability of  $\text{I}_a$  (see the following section) the agreement with the proposed structure appears reasonable.

In earlier work on the product, we followed Glusker and Miller's procedure, and recrystallised from ethanol-water mixtures. The light brown product (m.p. decomp  $218^\circ$ ) gave an infrared spectrum having strong, sharp bands at  $\approx 580\text{cm}^{-1}$  and  $\approx 606\text{cm}^{-1}$ . The variation in the relative intensities of these two bands indicated that a mixture was present. Repeated recrystallisation to constant infrared spectrum gave a product  $\text{I}_b$  containing sharp bands at  $580$  and  $608\text{cm}^{-1}$  of nearly equal intensity. (fig.10). Despite the close coincidence of many bands in the spectrum with bands of  $\text{I}_a$ , there are many distinct lines in the  $\text{I}_b$  infrared spectrum that have no counterparts in  $\text{I}_a$  (see Appendix table) and vice versa. Consequently, if  $\text{I}_a$  and  $\text{I}_b$  are single species (which we believe because of the constancy of their infrared and N.M.R. spectra) they must be distinct.

The N.M.R. spectrum of  $I_b$  is shown in fig. 9. The lines b, c, d, e and g found in  $I_a$  are still present, with the same intensity relative to Me, the same coupling, and almost the same position. There are in addition a further pair of 2 proton doublets a d, and a 2 proton resonance at f. As with the infrared spectra one is concerned whether the sample could be a mixture of  $I_a$  and a b proton species 'X' giving the new lines. In samples recrystallised to constant infrared spectrum the intensity ratio of the common and new lines would represent equimolar proportions of  $I_a$  and X - this is unlikely to arise fortuitously in a mixture.

Decisive proof that  $I_b$  is not a mixture of  $I_a$  and X is provided by the N.M.R. of a nearly equimolar mixture of  $I_a$  and  $I_b$  (fig. 9). If  $I_b$  already contained  $I_a$ , line g would be simply enhanced. In fact, two lines are seen, hence  $I_b$  contains no  $I_a$ , and is a distinct species. The N.M.R. spectrum is readily assigned to the structure  $I_b$  shown.

Structures involving substitution in the rings would involve a single proton resonance, which is not observed.

Further, the spectrum of  $I_b$  indicates that still only a single methyl group is present, so that an alternative such as  $I_b'$  can be eliminated. If structure  $I_b$  is adopted, the similarities in the N.M.R. spectrum to that of  $I_a$  are readily explicable, as are also the positions and coupling of the new lines. The composition  $I_b$  is also supported by the analysis (Table I). Further, the similarities in the infrared spectra

of  $I_a$  and  $I_b$  are now simply explained. The band at  $608\text{cm}^{-1}$  (the slight change in frequency is apparent on detailed examination) can be assigned to the end  $\text{CH}_2$  group, while  $580\text{cm}^{-1}$ , of almost equal intensity can be ascribed to the new  $\text{CH}_2$  group. The  $580\text{cm}^{-1}$  line is often much weaker than the line near  $605\text{cm}^{-1}$  in the infrared spectra of the initial reaction products, and it appears that  $I_b$  has largely been produced as a result of the heating involved in the recrystallisation. The mass spectrum (see Appendix) resembles that of  $I_a$ , and while supporting the close relationship of  $I_a$  and  $I_b$ , appears to be indecisive in confirming the detailed proposal for  $I_b$ . The larger proportion of iodine in this compound is apparent. // In some earlier samples we noticed that the band near  $580\text{cm}^{-1}$  was more intense than that  $\approx 606\text{cm}^{-1}$ . This could not result from a mixture of  $I_a$  and  $I_b$ . Recrystallisation from methanol also resulted in a solid  $I_c$  (m.p. (decomp)  $227^\circ$ ) with the  $580\text{cm}^{-1}$  band stronger than the  $605\text{cm}^{-1}$  in the infrared spectrum shown in fig.10. The N.M.R. spectrum is shown in fig. 9. It corresponds closely to that of  $I_b$ , with the addition of a yet further pair of two proton doublets at the a d position, and also a further two proton resonance at f'. Assignment to the 'tetramer' structure  $I_c$  is suggested by comparison with  $I_b$ . The absence of further lines at g, together with the nearly integral

intensity ratios shows  $I_c$  does not contain  $I_b$  or  $I_a$ . The elemental analysis (Table I) however, is not very satisfactory, and indicates that  $I_c$  has not been cleanly isolated. The frequency and relative intensity of the  $CH_2$  modes in the infrared spectrum further support this structure; there are now two chain  $CH_2$  groups, contributing to the  $580\text{cm}^{-1}$  band, for one end  $CH_2$  group.

The proposed structures for  $I_a$ ,  $I_b$  and  $I_c$  also explain the surprising absence of any marked absorption bands in the low frequency range, the sole weak band at  $210\text{cm}^{-1}$  is due to the end Me group<sup>(5)</sup>.

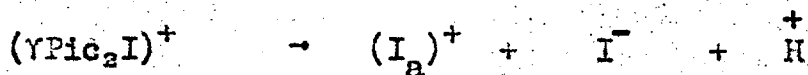
It is notable that more prolonged refluxing was entailed in the recrystallisation from methanol, further supporting the view that polymerisation proceeds in the recrystallisation process.

As the chain length of the polycation increases, the empirical formula approaches  $(C_6H_7NI)_n$ , if the counterion is entirely iodide. This is the composition observed by Glusker and Miller suggesting that the substance isolated by them was the polymer. The cryoscopic depression observed by these authors also agrees with this interpretation as do the remainder of their observations. (see quotation). In the species we have examined, the



presence of the Me group and the general features of the N.M.R. spectra show there is no appreciable ring closure to give polymers such as shown. This, however, cannot be excluded as the substance reported by Glusker and Miller.

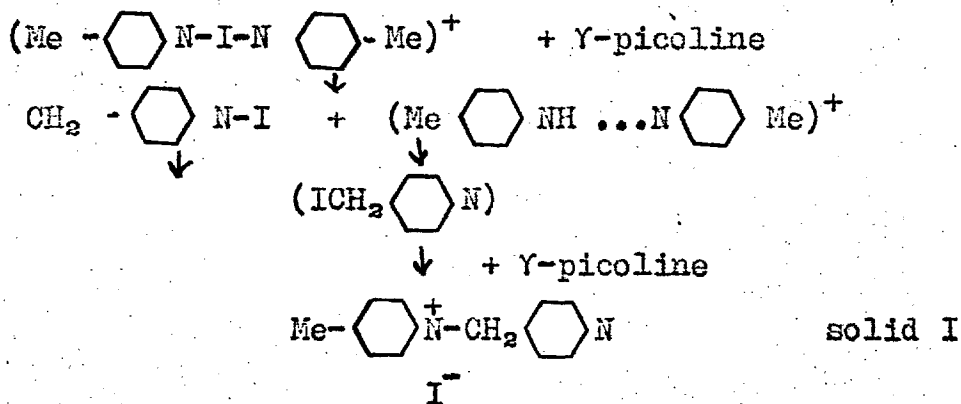
Finally, we return to the nature of the reaction product which gives rise to the bands at  $536\text{cm}^{-1}$  and  $1018\text{cm}^{-1}$ , present in aged solutions of  $I_2$  in  $\gamma$ -picoline (product II)). These bands are absent in solids  $I_a$ ,  $I_b$  and  $I_c$ , and presumably have been eliminated in the washing involved in working-up these solids. Direct spectroscopic examination of a  $\text{CH}_2\text{Cl}_2$  wash of the reaction product confirms the presence of both the  $536\text{cm}^{-1}$  and  $1018\text{cm}^{-1}$  bands. Owing to the presence in the solution spectrum of bands due to unreacted  $\gamma$ -picoline, and some dissolved solid  $I_2$ , only a few further characteristic bands of product II can be identified. These are at  $478\text{cm}^{-1}$ , and a broad band centred about  $2720\text{cm}^{-1}$ , with a smaller shoulder near  $3376\text{cm}^{-1}$ . These bands strongly suggest that II is a H-bonded  $\gamma$ -picoline species; we have therefore examined the infrared spectrum of  $\gamma$ -picoline hydrogen iodide dissolved in an equimolar mixture of  $\text{CH}_2\text{Cl}_2$  and  $\gamma$ -picoline. The frequency, intensity, and contours of all the four identifiable bands of compound II are reproduced, showing this to be a solution of  $\gamma\text{PicHI}$ , and accounting for the proton eliminated in the reaction.



Comparison of the spectra with those of pyridinium salts in solutions containing pyridine (8) indicates that the H-bonded species II is  $(\gamma\text{PicH}\gamma\text{Pic})^+$ ,  $\text{I}^-$  rather than  $(\gamma\text{PicH})^+$ ,  $\text{I}^-$ .

### Conclusion

No attempt has been made to formulate a detailed course, or to quantitatively examine the kinetics of the reactions. The absence of a direct reaction between  $\text{I}_2$  (in excess) and  $\gamma$ -picoline, the absence of reaction in non-polarising, <sup>solvents</sup> and the lack of any notable distinction between the rates in daylight and the dark suggest that a heterolytic, rather than a homolytic process is involved. Electron transfer from the  $\gamma$ -picoline ring increases in the series  $(\gamma\text{Pic}_2\text{I})^+ > \gamma\text{PicI}_2 > \gamma$ -picoline, (3,5) and the following reaction scheme involving the removal of a proton from the  $(\gamma\text{Pic}_2\text{I})^+$  ion by the free  $\gamma$ -picoline base present may be tentatively proposed<sup>(10)</sup>



etc.

Establishment of the detailed mechanism of the reaction process requires extensive investigation beyond the objectives of the present examination, which has been to explain the main temporal changes in the spectra of solutions of iodine in  $\gamma$ -picoline, and the nature of the products formed.

#### Acknowledgements

It is a pleasure to thank Mr. P.N. Jenkins and Drs. L. Pratt, J.K. Sutherland and D.W. Turner for practical help with and advice on N.M.R. spectroscopy, and Dr. E.S. Waight for help with the mass spectroscopy. We are also indebted to Dr. J.H. Ridd for suggesting a mechanism for the reaction.

## Experimental

### Materials:

B.D.H.  $\gamma$ -picoline was first dried over Sodium Sulphate (anhydrous) and then over barium oxide and fractionated. The purity of  $\gamma$ -picoline thus obtained and examined by V.P.C., was found to be 99%. A.R. Iodine was used without further purifications.

### Reaction:

A saturated solution of Iodine in  $\gamma$ -picoline was prepared and kept for 24 hours, when it had become a solid mass. This was washed several times with ethanol and finally with sodium-dried-ether and dried. Column-chromatography of this solid showed the presence of three components.

### Product Isolation

#### Solid Ia

A saturated solution of Iodine in  $\gamma$ -picoline was kept for about 3 hours. 2 volumes of ethanol were added, the solid remaining removed by filtration, and again washed with ethanol. On adding ether to the combined filtrates a precipitate was obtained, separated, washed, dried and recrystallised from ethanol. The solid was then dissolved in hot ethanol and cooled in ice-salt freezing mixture, the light microcrystalline substance obtained was separated by filtration. To the filtrate.

dried ether was added until precipitation was complete.

Solid Ib.

A saturated solution of Iodine in  $\gamma$ -picoline was prepared and kept for 24 hours, becoming a solid mass. This was ground, washed with alcohol several times, finally washed with dried ether, and dried. It was then dissolved in a mixture of water and alcohol (1:100) boiled for one minute, then filtered. The filtrate was cooled in dry ice for two hours - a microcrystalline light brown solid was precipitated, filtered, washed, dried, and again crystallised.

m.p. (decomposes) 218

Solid Ic.

A saturated solution of Iodine in  $\gamma$ -picoline was kept for about six hours. The solid thus obtained was filtered, washed several times with ethanol and then ether. The dried substance was mixed with Analar methanol and boiled for one minute, when most of the solid dissolved. The filtrate was then cooled in solid carbondioxide for 2 hours. The resulting precipitate filtered, washed with ethanol, then ether, and dried by passing dry nitrogen. It was again recrystallised from methanol washed and dried.

m.p. (decomposes) 227°

### Infrared Spectroscopy

Above  $400\text{cm}^{-1}$  infrared spectra were recorded using a Grubb-Parsons 'Spectromaster'; below  $400\text{cm}^{-1}$  a vacuum grating spectrometer constructed in the Department was used. In general KBr windows were used in the high frequency region and polythene in the lower range. No differences were found between the spectra of samples kept in the cell, and samples stored in flasks. Kinetic runs (Fig. 2) showed similar development using KBr, AgCl or polythene windows.

### Mass-spectroscopy

Mass spectra were obtained with an A.E.I. MS.9 spectrometer, with direct insertion, at  $T = 200^\circ\text{C}$ ,  $p = 5 \times 10^{-7}$  torr: Electron impact source, 75 e.v.,  $18\mu\text{A}$ .

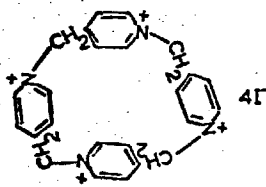
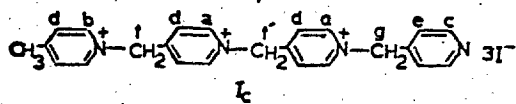
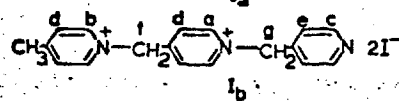
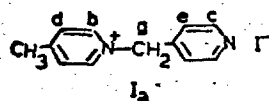
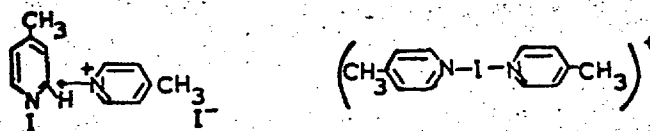
The main peaks above  $m/e = 37$  are tabulated in the Appendix.

### N.M.R. Spectroscopy.

Most of the N.M.R. Spectra were recorded using a Marian HA.100 N.M.R. Spectrometer. Solutions in both D.M.S.O. (D.M.S.O. used as lock signal) and in  $\text{D}_2\text{O}$  (T.M.S. used as external lock signal) were examined.

References

- (1) D.L. Glusker and A. Miller, *J.Chem.Phys.*, 26, 331, (1957).
- (2) O. Hassel, C. Romming and T. Tufte, *Acta Chem Scand*, 15, 967, (1961).
- (3) I. Haque and J.L. Wood, In preparation.
- (4) R.F. Lake and H.W. Thompson, *Proc.Roy.Soc.*, 297A, 440, (1967).
- (5) I. Haque and J.L. Wood, *Spectrochim. Acta* (In press).
- (6) J.H.S. Green et al. *Spectrochim Acta*, 19, 549, (1963).
- (7) E. Spinner, *J.Chem.Soc.*, 3860 (1963).
- (8) T.R. Singh and J.L. Wood. (To be published).
- (9) J.E. Collin and R. Cahay, *Bull Acad Royale Belg., Classe des Sciences*, 52, 606, (1966).
- (10) J.H. Ridd, Private Communication.



Possible reaction products of γ-picoline and iodine.



Captions

- (1) Upper. Infrared spectrum of reaction product of  $I_2$  with  $\gamma$ -picoline. Washed with ethanol to remove excess  $\gamma$ -picoline, but not otherwise treated (Nujol mull). Lower. Composite infrared spectrum of  $(\gamma\text{Pic}_2\text{I})^+$  ion, from data using the  $\text{BF}_4^-$  and  $\text{PF}_6^-$  salts (Nujol + HCBD mulls).
- (2) Scans of the  $500\text{-}650\text{cm}^{-1}$  range of a nearly saturated solution of  $I_2$  in  $\gamma$ -picoline at successive periods after preparation. The cell containing the solution remained in the beam for the first five scans. The final scan refers to a sample kept throughout in a closed flask until examined. A - 5 mins., B - 25 mins, C - 40 mins, D - 65 mins, E - 2 hrs., F - 24 hrs. after mixing.
- (3) Scans of the  $1000\text{-}1050\text{ cm}^{-1}$  range of a nearly saturated solution of  $I_2$  in  $\gamma$ -picoline at successive periods after preparation. The cell containing the sample remained in the beam throughout. A - 5 mins., B - 15 mins., C - 2 hrs., D - 24 hrs.
- (4) The reaction of  $(\gamma\text{Pic}_2\text{I})^+$  with  $\gamma\text{Pic}$ . Both the  $\text{BF}_4^-$  and  $\text{PF}_6^-$  salts were examined. Anion bands are omitted. A - 5 mins., B - 20 mins., C - 40 mins., D - 5 hrs.
- (5)  $\text{NBu}_4^+ \text{I}_3^-$  in  $\gamma$ -picoline after 1 day in vitro.
- (6)  $\text{Me}_4^+ \text{IBr}_2^-$  in  $\gamma$ -picoline A - 5 mins. Note the bands at  $540$  and  $1019\text{ cm}^{-1}$ , characteristic of  $\gamma\text{PicIBr}$ . B - after

one day in vitro. Note the bands of the reaction product at 536, 606 and  $1018\text{cm}^{-1}$ . The band at  $558\text{cm}^{-1}$  has not been accounted for.

(7)  $\gamma$ -PicICl in  $\gamma$ -picoline A - 5 mins., B - 25 mins., C - 45 mins., D - 2 hrs. The bands at  $545\text{cm}^{-1}$  ( $\gamma\text{Pic}_2\text{I}^+$ , and  $\gamma\text{PicICl}$ )  $1022$   $\gamma\text{PicICl}$  and  $1025$  ( $\gamma\text{Pic}_2\text{I}^+$ ) disappear and product bands at 536, 570, 608 and  $1018\text{cm}^{-1}$  arise.

(8) A. Product  $\text{I}_a$ . As in C, but after metathesis of anion with  $\text{NO}_3^-$ .  $\alpha$  indicates  $\text{NO}_3^-$  bands.

B. Product  $\text{I}_a$  obtained by reaction of  $(\gamma\text{Pic}_2\text{I})^+\text{PF}_6^-$  with  $\gamma$ -picoline.  $\alpha$  indicates  $\text{PF}_6^-$  bands.

C. Product  $\text{I}_a$  obtained by reaction of  $\text{I}_a$  with  $\gamma$ -picoline.

(9) Top left N.M.R. Spectrum of  $\text{I}_a$ . Intensities relative to Me = 5 protons indicated.

Top right N.M.R. spectrum of  $\text{I}_b$ .

Bottom left N.M.R. spectrum of a mixture of  $\text{I}_a$  and  $\text{I}_b$ .

Bottom right N.M.R. spectrum of  $\text{I}_c$ .

(10) A. Infrared spectrum of  $\text{I}_c$  (null).

B. " " "  $\text{I}_b$  (null).

Null bands omitted.

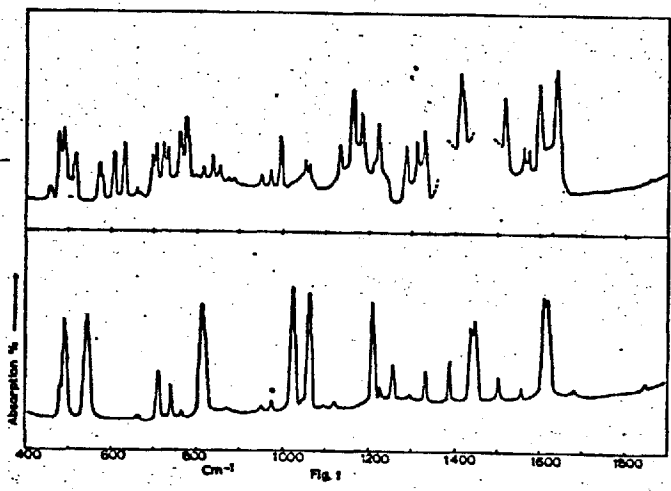


Fig. 1

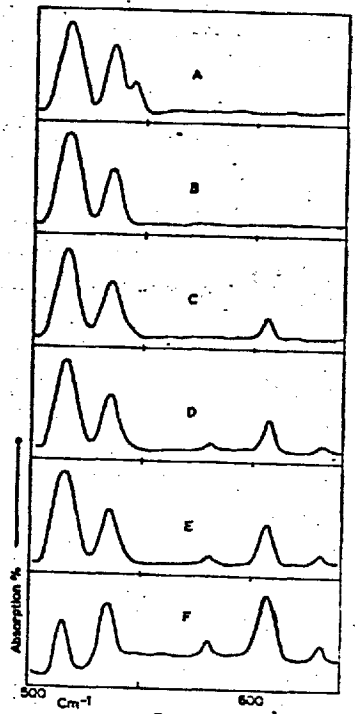


Fig 2

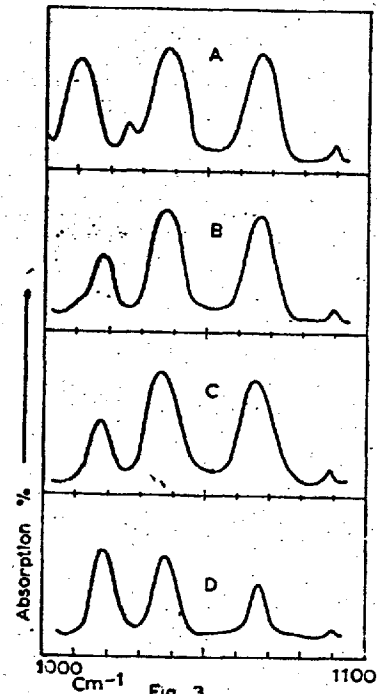
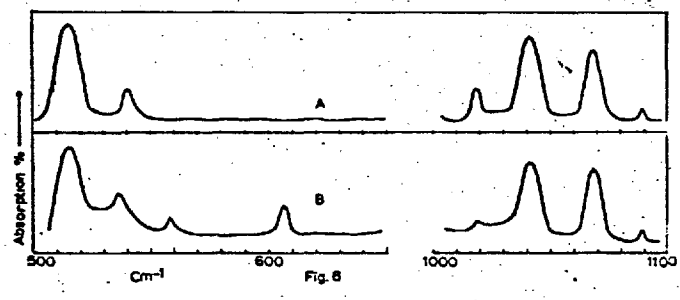
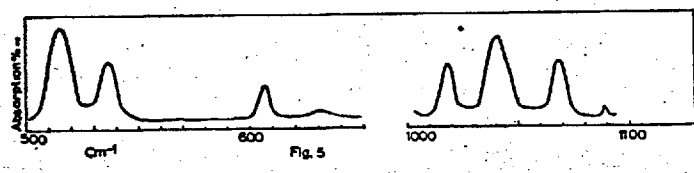
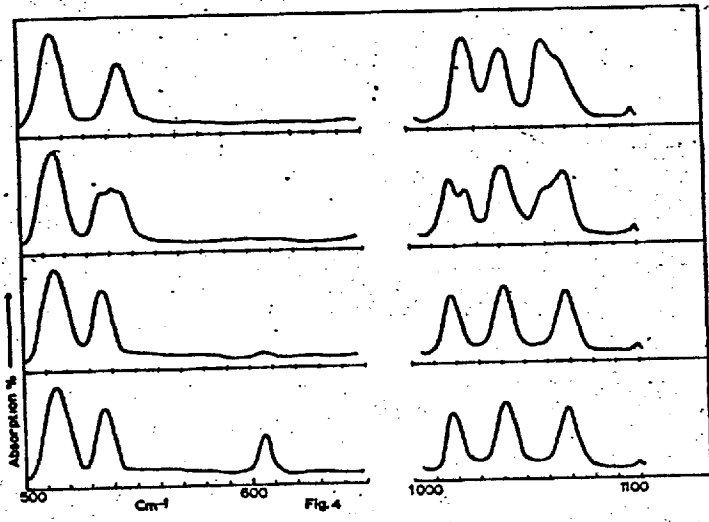
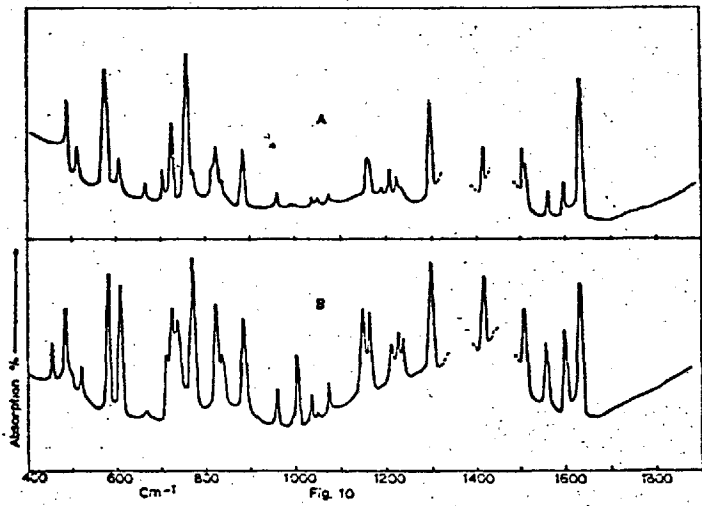
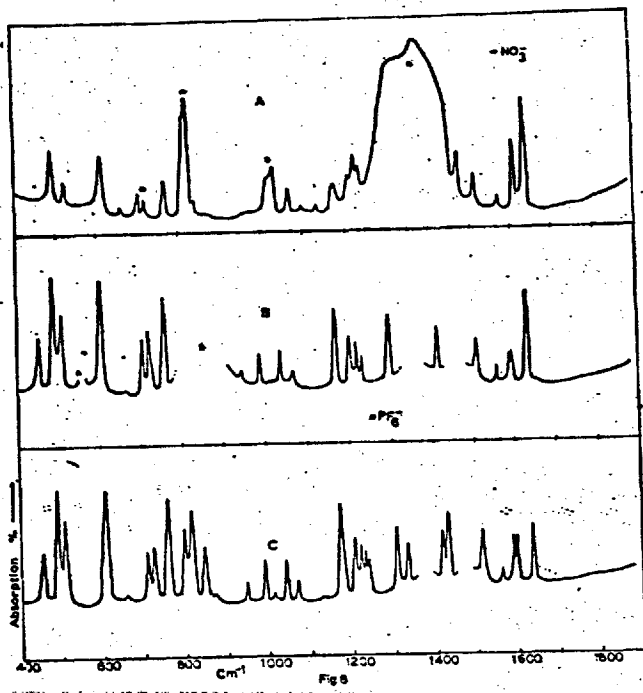
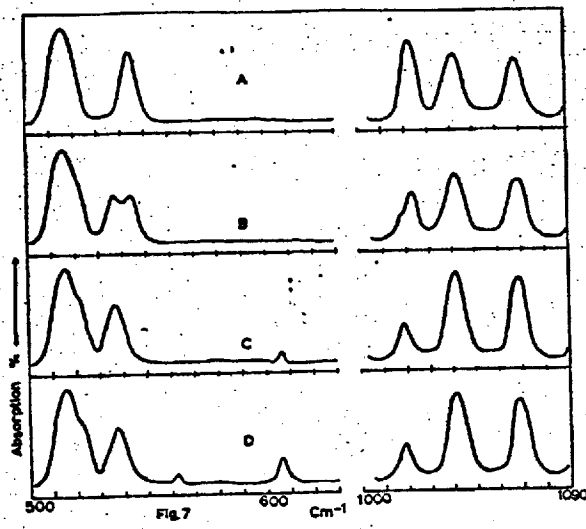
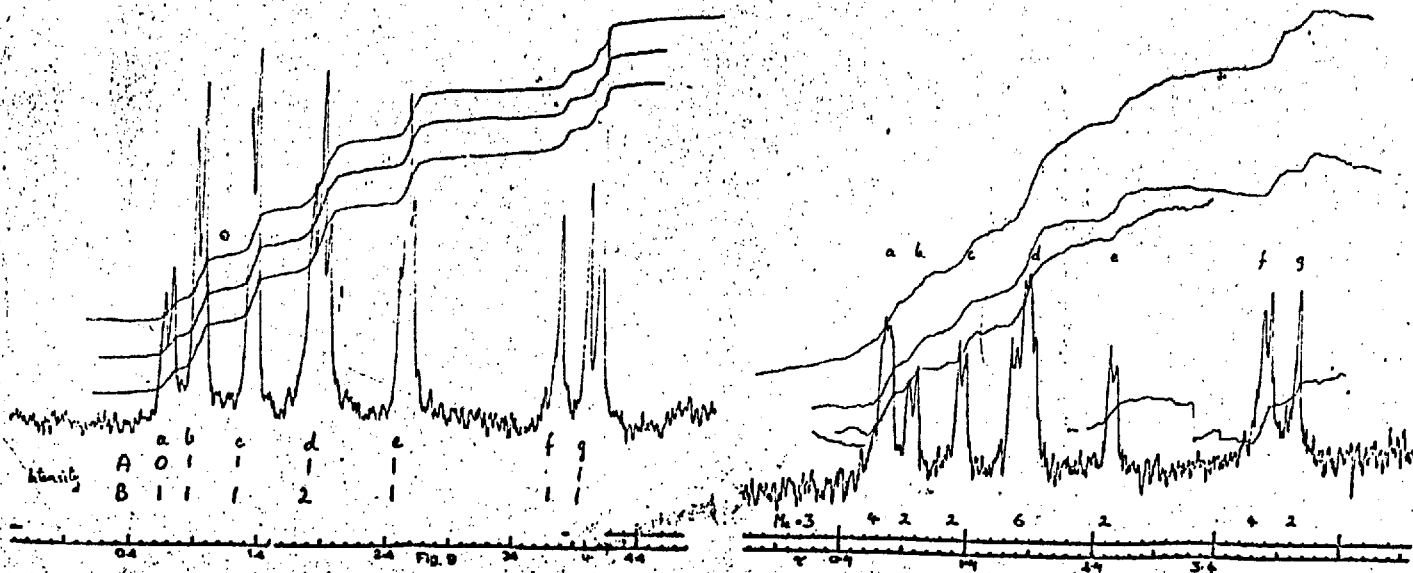
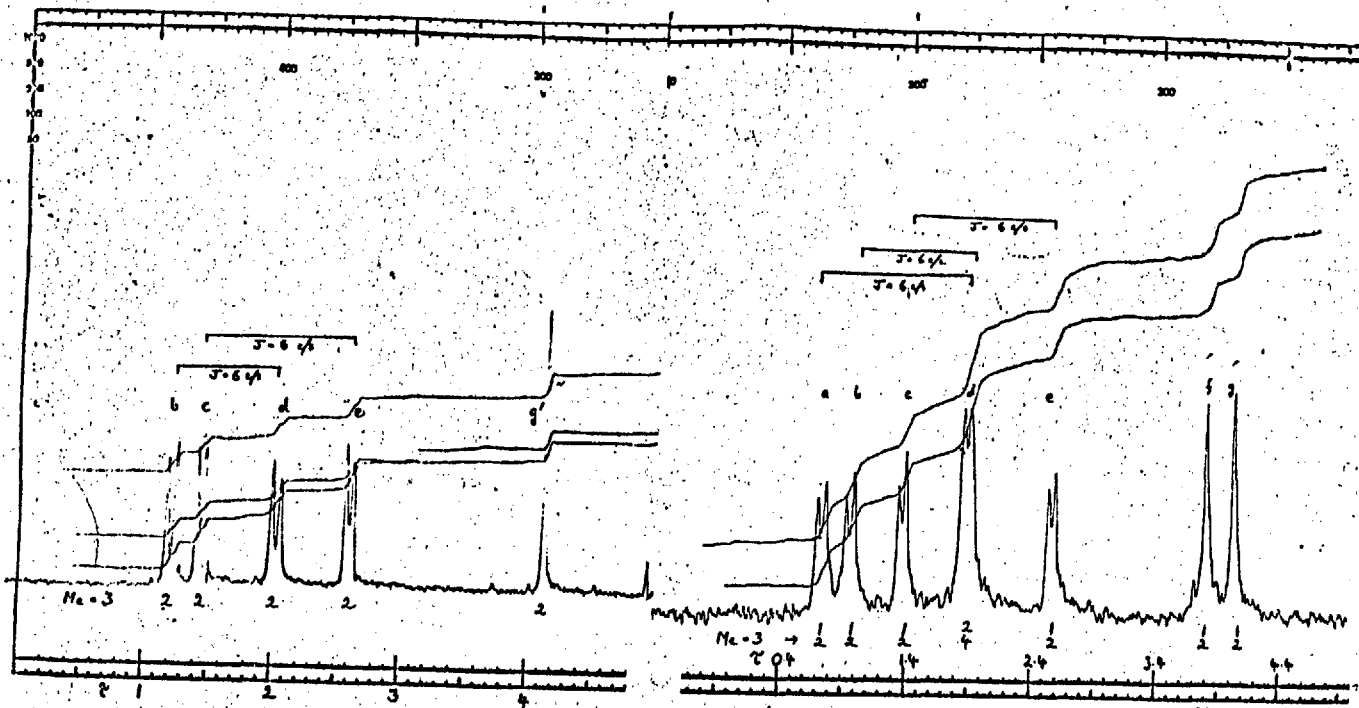


Fig. 3







APPENDIX

Table I.

Analyses %

	C	H	N	I	(PF <sub>6</sub> ) <sup>-</sup>
I <sub>A</sub> from YPic+I <sub>2</sub>	45.7	4.43	8.15	42.8	
C <sub>12</sub> H <sub>13</sub> N <sub>2</sub> I requires	46.1	4.16	8.97	40.7	
I <sub>A</sub> from (YPic <sub>2</sub> I) PF <sub>6</sub> <sup>-</sup> + Ypic	43.6	4.76	8.15	32.0	11.6
Empirical Formula	12	15.8	1.93	0.84	0.26
I <sub>B</sub>	38.5	3.53	7.38	46.9	
C <sub>18</sub> H <sub>19</sub> N <sub>3</sub> I <sub>2</sub> requires	40.67	3.57	7.9	47.8	
I <sub>C</sub>	37.79	3.26	7.52	47.6	
C <sub>24</sub> H <sub>25</sub> N <sub>4</sub> I <sub>3</sub> requires	38.4	3.30	7.46	50.8	

APPENDIX

Table 2.

I.R. Spectra of Solids I<sub>a</sub>, I<sub>b</sub> and I<sub>c</sub>

as the iodides

Solid I <sub>a</sub>	Solid I <sub>b</sub>	Solid I <sub>c</sub>
1639s	1631s	1633s
1600sh	1598ms	1597m
1592ms	-	-
1562w	1560m	1561m
1513ms	-	1513m
-	1504ms	1504ms
1428s	-	-
1416ms	1413s	1415ms
1333w		
1307m	1295s	1295w
1239w		
1231w	1233w	1233sh
1224w	1224m	1222w
1207m	1205w	1207m
		1190w
1172s	-	-
-	1162ms	1165ms
-	1148ms	1156ms
1131w	1131w	
		1093sh



APPENDIXTable 2 (contd.)

Solid I <sub>a</sub>	Solid I <sub>b</sub>	Solid I <sub>c</sub>
1070w	1073w	1071w
1044w	1048w	1050w
-	1031w	1034w
1015sh	-	-
-	1000m	-
-	-	996w
993m	-	991w
-	-	961(broad)m
947w	947sh	
-	-	884ms
869vw		
858sh		
847w		
-	838ms	838w
-	826s	824ms
816s	816sh	814sh
799ms	-	-
-	-	773n
758s	765s	759s
-	735ms	-
724s	721ms	724s
-	711ms	-
704m	704sh	705m

APPENDIS

Table 2 (contd.)

Solid I <sub>a</sub>	Solid I <sub>b</sub>	Solid I <sub>c</sub>
666w	668w	666w
663w	662w	
605s	608s	608s
-	582s	-
-	-	577s
-	521ms	-
-	-	514ms
509ms	500sh	-
490s	487ms	489s
454m	455m	
-	417m	

Table 3

Mass Spectra

Solid I<sub>a</sub> (as iodide)

Solid I<sub>b</sub> (as iodide)

Peaks with relative abundance less than 1% in both solids are omitted.



<u>Mass ratio <sup>m</sup>/e</u>	<u>Rel. Abund.</u>	<u>Rel. Abund.</u>	<u>Tentative Assignment</u>
38	6.0	7.5	
39	22.5	33.0	
40	8.6	12.5	
41	3.6	7.0	
50	5.0	6.0	Py ring fragments (9)
51	9.0	11.0	
52	5.8	7.0	
53	5.4	6.9	
54	7.1	8.1	
62	3.0	2.8	
63	8.3	6.3	
64	5.6	10.0	
65	30.8	26.5	
66	30.0	34.0	γ-Pic ring fragments
67	6.6	7.0	
78	4.8	6.1	C <sub>5</sub> H <sub>9</sub> N
91	1.9	2.1	CH 
92	8.4	55.0	CH <sub>2</sub> 

Table 3 (contd.)

<u>Mass ratio <sup>m</sup>/e.</u>	<u>Rel. Abund.</u>	<u>Rel. Abund.</u>	<u>Tentative Assignment.</u>
93	100	100	γ-picoline.
94	6.6	10.0	isotope.
127	10.9	35	I
128	15.5	60	HI
157	nil	2.8	64+93 or 65+92 fragment.
182	1.3	0.5	
184	3.7	0.7	<chem>CC1CCN(C1)CC2CCN(C2)</chem>
185	1.8	-	<chem>CN1CCN(C1)CC2CCN(C2)</chem>
219	15.3	6.5	<chem>CC1CCN(C1)</chem> -1
220	1.0	0.4	isotope
254	8.2	47.0	I <sub>2</sub>
275	1.0	-	